

46th GLOBAL MONITORING ANNUAL CONFERENCE 2018

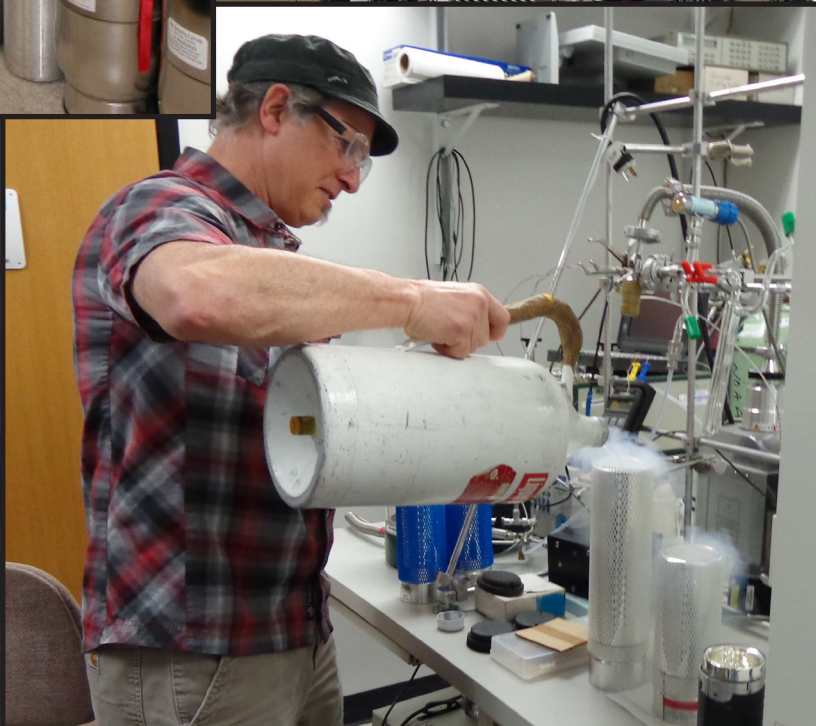
Boulder, Colorado

May 22 - 23, 2018

PROGRAM & ABSTRACTS



Taking the pulse of the planet



Mission of the Global Monitoring Division:

To acquire, evaluate, and make available accurate, long-term records of atmospheric gases, aerosol particles, clouds, and surface radiation in a manner that allows the causes and consequences of change to be understood.

Conference Website:

<http://www.esrl.noaa.gov/gmd/annualconference/>

Purpose of the Global Monitoring Annual Conference:

To bring together preeminent scientists to discuss the latest findings in climate research and how to integrate science, observations and services to better serve society.

Terms of use:

Material in this document may be copied without restraint for library, abstract service, educational, or personal research purposes. All other uses are prohibited without prior consent from authors.

This report may be cited as:

46th Global Monitoring Annual Conference, 2018 Program and Abstracts Booklet,
NOAA Earth System Research Laboratory, Global Monitoring Division

This report compiled and distributed by:

NOAA Earth System Research Laboratory
Global Monitoring Division
325 Broadway, R/GMD1
Boulder, CO 80305
<http://www.esrl.noaa.gov/gmd>



UNITED STATES DEPARTMENT OF COMMERCE
National Oceanic and Atmospheric Administration
Office of Oceanic and Atmospheric Research
Earth System Research Laboratory
325 Broadway – David Skaggs Research Center
Boulder, Colorado 80305-3337

NOAA Earth System Research Laboratory 46th Global Monitoring Annual Conference

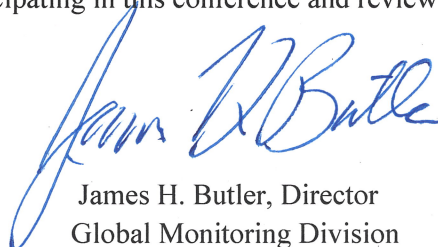
May 22-23, 2018
Boulder, Colorado

We in the Global Monitoring Division of NOAA's Earth System Research Laboratory welcome you to the 46th Global Monitoring Annual Conference (GMAC). Hosting this annual gathering is a hallmark of GMD and highlights our dedication to the global research community to collectively improve our knowledge and base practices. Throughout the years, the goal of this conference has remained steadfast – to create a forum for thoughtful and lively discussion on research from sustained measurement records and what it takes to understand them.

This year, we are trying something different by combining the Conference with our quinquennial laboratory review. Although this GMAC is structured identically to past conferences, you will see some differences, most notably the presence of a review panel, but also in some of the presentations by GMD scientists, as we in GMD are asked to speak directly to the relevance and quality of our work. Posters will be arranged a little differently, but in the same space as before. Rather than organize the conference around GMD's research groups, we have structured it this year around the three themes highlighted in our 2018-2022 scientific research plan – Greenhouse Gases and Carbon Cycle Feedbacks; Surface Radiation, Aerosols, and Clouds; and Recovery of Stratospheric Ozone. Finally, the review panel and NOAA's leadership at this conference want to hear from you, as stakeholders in a common effort, as to how our joint research advances the state of the science better than any of us could do alone.

The GMAC, as always, will focus on observations and their value for improving understanding of our ever-changing Earth system. We anticipate discussions highlighting long-term data sets, advances in technology, evolution of networks, observing gaps, and the immense possibilities achievable through our collaborations. The conference agenda and abstracts from all presentations and posters at the conference are available at <https://www.esrl.noaa.gov/gmd/annualconference/>.

Thank you all for coming and participating in this conference and review!



James H. Butler, Director
Global Monitoring Division



LIST OF ACRONYMS

Organizations and Networks

AERONET – NASA
AGAGE – Advanced Global Atmospheric Gases
Experiment network
ARM – Atmospheric Radiation Measurement
BSRN – Baseline Surface Radiation Network
GAW – Global Atmosphere Watch
GGGRN – Global Greenhouse Gas Reference
Network
HIPPO – HIAPER Pole-to-Pole Observations
IPCC – Intergovernmental Panel on Climate
Change
NASA - National Aeronautics and Space
Administration
NDAAC – Network for the Detection of
Atmospheric Composition Change
WMO – World Meteorological Organization

Chemical compounds

Br – Bromine
CCl₄ – Carbon tetrachloride
CFC – Chlorofluorocarbon
CH₄ – Methane
Cl – Chlorine
CO – Carbon monoxide
¹²C – Carbon-12
¹³C – Carbon-13
δ¹³C – ‘delta c thirteen’
¹⁴C – Carbon-14, or radiocarbon
¹⁴CO₂ – Carbon-14 CO₂
CO₂ – Carbon dioxide
H₂ – Hydrogen
H₂O – Water
HCFC – Hydrochlorofluorocarbon
HFC – Hydrofluorocarbon
O₃ – Ozone
OH – Hydroxyl (radical)
N₂O – Nitrous oxide
PM_{2.5} – Particulate Matter (≤ 2.5 microns width)
SF₆ – Sulfur hexafluoride
VOC – Volatile Organic Compound

Satellites and Satellite Sensors

CERES – Clouds and the Earth’s Radiant Energy
System satellite
GOSAT – Greenhouse gases Observing SATellite
ISS – International Space Station
JPSS – Joint Polar Satellite System
MLS – Microwave Limb Sounder
MODIS – MODerate resolution Imaging
Spectroradiometer satellite
OCO-2 – Orbiting Carbon Observatory-2
OMI – Ozone Monitoring Instrument

Other Acronyms and Terms

AAOD – Aerosol Absorption Optical Depth
AOD – Aerosol Optical Depth
CRDS - cavity ring down spectroscopy
FID - flame ionizing detector
GC - gas chromatograph/chromatography
GCMS - gas chromatograph mass spec
GCECD - gas chromatograph electron capture
detector
GHG – Greenhouse gas
HRRR – High-Resolution Rapid Refresh
HYSPLIT - Hybrid Single Particle Lagrangian
Integrated Trajectory Model
IR – Infrared
MFRSR – Multi-Filter Rotating Shadow-band
Radiometers
NWP – Numerical Weather Prediction
ODS – Ozone-depleting substance
ONG - Oil and natural gas
OSSEs – Observing System Simulation
Experiments
PgCyr⁻¹ – Petagrams of carbon per year, or
Billion Tonnes of Carbon per year
ppb – parts per billion; ppm – parts per million
RAP - Rapid Refresh model
UAS – Unmanned Aerial Systems
UTC - Universal Time Coordinated (also Zulu,
Greenwich Mean Time)
UTLS - upper troposphere lower stratosphere
UV – Ultraviolet; UVR – Ultraviolet Radiation
Wm⁻² – Watts per meter squared, unit of
radiative forcing

NOAA ESRL GLOBAL MONITORING ANNUAL CONFERENCE 2018

David Skaggs Research Center, Room GC-402
325 Broadway, Boulder, Colorado 80305 USA

Tuesday Morning, May 22, 2018 Agenda

(Only presenter's name is given; please refer to abstract for complete author listing.)

07:00 **Registration Opens in GC-402 - lunch orders and posters collected at registration table**

07:45 - 08:30 **Morning Snacks - coffee, tea, fruit, bagels and donuts served**

| | | Page No. |
|----------------------|--|----------|
| Session 1 | Welcome, Keynote Address & Highlights — Chaired by James H. Butler | |
| 08:30 - 08:45 | Welcome and Setting the Stage <i>James H. Butler (NOAA Earth System Research Laboratory, Global Monitoring Division (GMD))</i> | - |
| 08:45 - 09:00 | Where GMD Fits in the Big Picture <i>Ko Barrett (NOAA Office of Oceanic and Atmospheric Research (OAR))</i> | - |
| 09:00 - 09:45 | KEYNOTE ADDRESS - Science for Policy and Policy for Science in the Federal Government <i>John P. Holdren (Harvard University, John F. Kennedy School of Government)</i> | - |
| 9:45 - 10:15 | Morning Break & Group Photo on the Stage | |
| Session 2 | Tracking Greenhouse Gases and Understanding Carbon Cycle Feedbacks - Global Constraints on the Carbon Cycle — Chaired by Gabrielle Petron | |
| 10:15 - 10:30 | The Primacy of Observations in Climate Prediction <i>Pieter Tans (NOAA Earth System Research Laboratory, Global Monitoring Division (GMD))</i> | 1 |
| 10:30 - 10:45 | Constraints on Global Carbon and Heat Exchanges from Measurements of Atmospheric O ₂ and Related Tracers <i>Ralph Keeling (Scripps Institution of Oceanography, University of California at San Diego)</i> | 2 |
| 10:45 - 11:00 | Monitoring Trends and Spatial Distributions of Carbon Cycle Greenhouse Gases and Related Tracers <i>Edward J. Dlugokencky (NOAA Earth System Research Laboratory, Global Monitoring Division (GMD))</i> | 3 |
| 11:00 - 11:15 | The OCO-2 Model Intercomparison Project Reveals Systematic Transport Model Effects on Inverse Model CO ₂ Fluxes <i>Andrew R. Jacobson (Cooperative Institute for Research in Environmental Sciences (CIRES), University of Colorado)</i> | 4 |
| 11:15 - 11:30 | CarbonTracker Asia 2016: an Estimation of CO ₂ Fluxes Centering on Asia <i>Jae-Sang Rhee (National Institute of Meteorological Sciences, Seogwipo-si, South Korea)</i> | 5 |
| 11:30 - 11:45 | The Mysterious Global Methane Budget <i>Lori Bruhwiler (NOAA Earth System Research Laboratory, Global Monitoring Division (GMD))</i> | 6 |
| 11:45 - 13:00 | Catered Lunch - Outreach Classroom GB-124 (pre-payment of \$12.00 at registration) | |

NOAA ESRL GLOBAL MONITORING ANNUAL CONFERENCE 2018

David Skaggs Research Center, Room GC-402
325 Broadway, Boulder, Colorado 80305 USA

Tuesday Afternoon, May 22, 2018 Agenda

(Only presenter's name is given; please refer to abstract for complete author listing.)

| | Page No. |
|---|----------|
| Session 3 | |
| <i>Monitoring and Understanding Changes in Surface Radiation, Clouds, and Aerosol Distributions</i> — <i>Chaired by Allison McComiskey</i> | |
| 13:00 - 13:15 The Scientific Utility of GMD Surface Radiation Measurements <i>Chuck Long (Cooperative Institute for Research in Environmental Sciences (CIRES), University of Colorado)</i> | 7 |
| 13:15 - 13:30 Trends in U.S. Surface Radiation and Aerosol Optical Depth over the Past 20 Years <i>John A. Augustine (NOAA Earth System Research Laboratory, Global Monitoring Division (GMD))</i> | 8 |
| 13:30 - 13:45 Climatology of Aerosol Optical Properties from Storm Peak Laboratory <i>Gannet Hallar (University of Utah)</i> | 9 |
| 13:45 - 14:00 On Measurements and Spatial Distribution of Light Absorbing Aerosols in the Arctic <i>John Backman (Finnish Meteorological Institute, Helsinki, Finland)</i> | 10 |
| 14:00 - 14:15 Winter 2017-2018 Results from the De-Icing Comparison Experiment (D-ICE) at NOAA's Barrow Atmospheric Baseline Observatory, Utqiagvik, Alaska <i>Sara M. Morris (Cooperative Institute for Research in Environmental Sciences (CIRES), University of Colorado)</i> | 11 |
| 14:15 - 14:30 The Role of Atmospheric Circulation in the Seasonal Melt of Snow and Sea Ice in the Pacific Arctic <i>Christopher J. Cox (Cooperative Institute for Research in Environmental Sciences (CIRES), University of Colorado)</i> | 12 |
| 14:30 - 15:00 Afternoon Break | |
| Session 4 | |
| <i>Guiding Recovery of Stratospheric Ozone - Ozone and Ozone Depleting Gases in the Stratosphere</i> — <i>Chaired by Dale Hurst</i> | |
| 15:00 - 15:15 Increasing CFC-11 Emissions and other Unusual Atmospheric Changes: How Delayed Will Ozone Recovery Be? <i>Steve Montzka (NOAA Earth System Research Laboratory, Global Monitoring Division (GMD))</i> | 13 |
| 15:15 - 15:30 Diagnosing CFC-11's Emissions in a Chemistry-Climate Model <i>Pengfei Yu (Cooperative Institute for Research in Environmental Sciences (CIRES), University of Colorado)</i> | 14 |
| 15:30 - 15:45 Ozone and Chemical Composition in the Pacific Region Measured by IAGOS <i>Hannah Clark (IAGOS-AISBL, Brussels, Belgium)</i> | 15 |
| 15:45 - 16:00 Global Observations of Aerosol and Ozone from SAGE III ISS – A First Year Showcase <i>Kevin R. Leavor (Science Systems and Applications, Inc. (SSAI))</i> | 16 |
| 16:00 - 16:15 South Pole Ozonesondes in 2017 Continue to Show Less Severe Ozone Loss <i>Bryan Johnson (NOAA Earth System Research Laboratory, Global Monitoring Division (GMD))</i> | 17 |
| 16:15 - 16:30 Is Stratospheric Ozone Recovering as We Expect? Results of the SPARC LOTUS Analyses <i>Irina Petropavlovskikh (Cooperative Institute for Research in Environmental Sciences (CIRES), University of Colorado)</i> | 18 |
| 16:30 - 16:45 The Trials and Triumphs of SHADOZ: The Who's Who of Tropical Ozone Profiles <i>Jacquelyn C. Witte (Science Systems and Applications, Inc. (SSAI))</i> | 19 |
| 17:00 - 19:30 Poster Session (DSRC Cafeteria) with appetizers and refreshments | |

The Primacy of Observations in Climate Prediction

P. Tans

NOAA Earth System Research Laboratory, Global Monitoring Division (GMD), Boulder, CO 80305; 303-497-6678, E-mail: Pieter.Tans@noaa.gov

The first International Panel on Climate Change (IPCC) report in 1990 characterized the uncertainty of the equilibrium climate sensitivity to a doubling of carbon dioxide (CO_2) as being in the range 1.5-4.5 K. The fifth IPCC report in 2013 states the same range of 1.5-4.5 K, despite great progress in our understanding of many aspects of our contemporary climate and that of the ice ages. The difficulty lies in the magnitude of feedbacks and in the time scales over which they operate. Many feedbacks are still unknown. A few examples of carbon cycle - climate feedbacks will be presented. Climate predictions over several decades and longer can serve to show what is currently considered somewhat plausible. Our global civilization is carrying out multiple simultaneous experiments with our planet. Only high-quality observations of the changes as they unfold, and of human behavior, allow us to make discoveries about how the climate system really works. Not making these observations now will limit future generation's understanding of climate, and future models will be the worse for it.

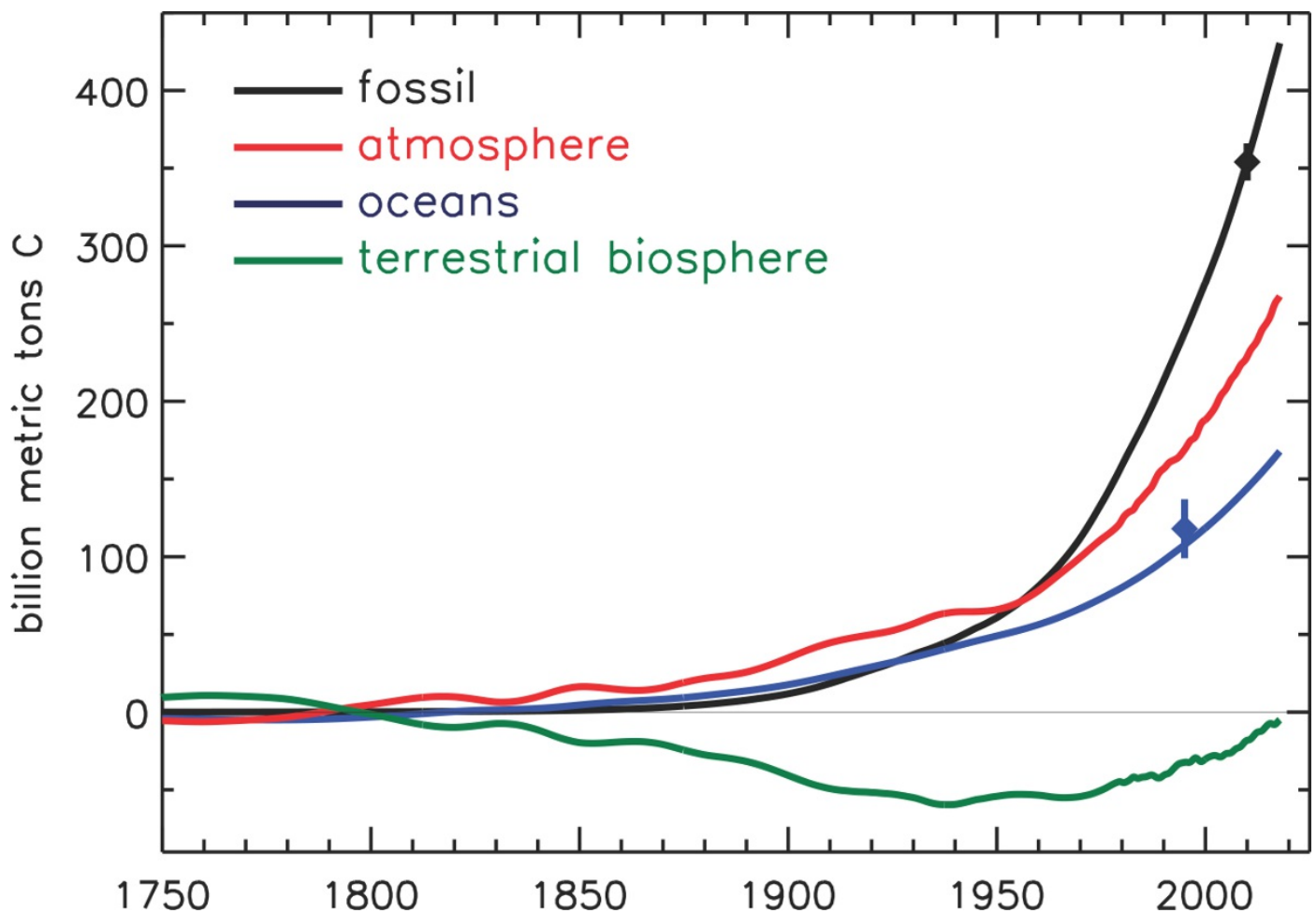


Figure 1. Known cumulative fossil fuel emissions and observed global atmospheric increase (zero corresponds to the pre-industrial value 280 ppm). An empirical model of air-sea CO_2 exchange calculates cumulative CO_2 uptake by the oceans, with parameters chosen to fit ocean observations (blue diamond in 1994) as well as the rate of uptake during the last two decades based on atmospheric oxygen/nitrogen observations. Net changes in global terrestrial biomass follow from the mass balance of the other three terms.

Constraints on Global Carbon and Heat Exchanges from Measurements of Atmospheric O₂ and Related Tracers

R. Keeling¹, E. Morgan¹, B. Paplawsky¹, A. Cox¹ and L. Resplandy²

¹Scripps Institution of Oceanography, University of California at San Diego, La Jolla, CA 92037; 858-534-7582, E-mail: rkeeling@ucsd.edu

²Princeton University, Princeton, NJ 08540

The Scripps O₂ program sustains measurements of changes in the O₂/N₂ ratio begun in 1990 using the interferometric method. The measurements track a long-term decrease in O₂/N₂ caused mostly by uptake of O₂ during fossil burning, but also strongly influenced by processes impacting the land sink carbon sink, such as photosynthesis and respiration. The O₂ measurements, in conjunction with measurements of atmospheric CO₂, continue to provide strong constraints on the global land and ocean carbon sinks. A principle limitation of the method involves the need to correct for long-term release of O₂ from the oceans associated with ocean warming and stratification. The method is nevertheless an important complement to other methods, which have similarly large limitations.

As alternate methods of resolving ocean carbon sinks have improved in parallel, an additional application for the O₂ measurements has emerged, involving tracking changes in ocean global heat uptake. The global heat uptake remains a primary measure of global warming, and quantifying the rate of heat uptake is critical to improving estimates Earth's climate sensitivity to excess CO₂, and thereby forecasts of future warming. Previous estimates of ocean heat uptake rely on thermometer measurements of ocean temperature in combination with data-filling methods for extrapolating the sparse temperature database to the entire ocean. By combining atmospheric O₂ and CO₂ to compute the tracer "atmospheric potential oxygen" (APO ~ O₂ + CO₂) an independent estimate of ocean heat uptake can be formulated. APO is decreasing over time as the O₂ decrease exceeds the CO₂ increase. This APO decrease is insensitive to land exchanges because impacts on O₂ and CO₂ cancel. It is sensitive mainly to fossil-fuel burning, ocean uptake of "anthropogenic CO₂", and climate driven exchanges of O₂ and CO₂. The latter influence can be isolated because the other influences are quite well known. The climate-driven exchanges of O₂ and CO₂ in principle include both physically (e.g. solubility) and biologically-driven exchanges, but it turns out that the solubility effects strongly dominate. This can be shown both from hydrographic data and across ocean climate models. The climate-driven APO trend thus directly constrains global ocean heat uptake, providing an alternate method that is completely independent of ocean hydrographic data and places estimates of ocean warming on a more secure footing.

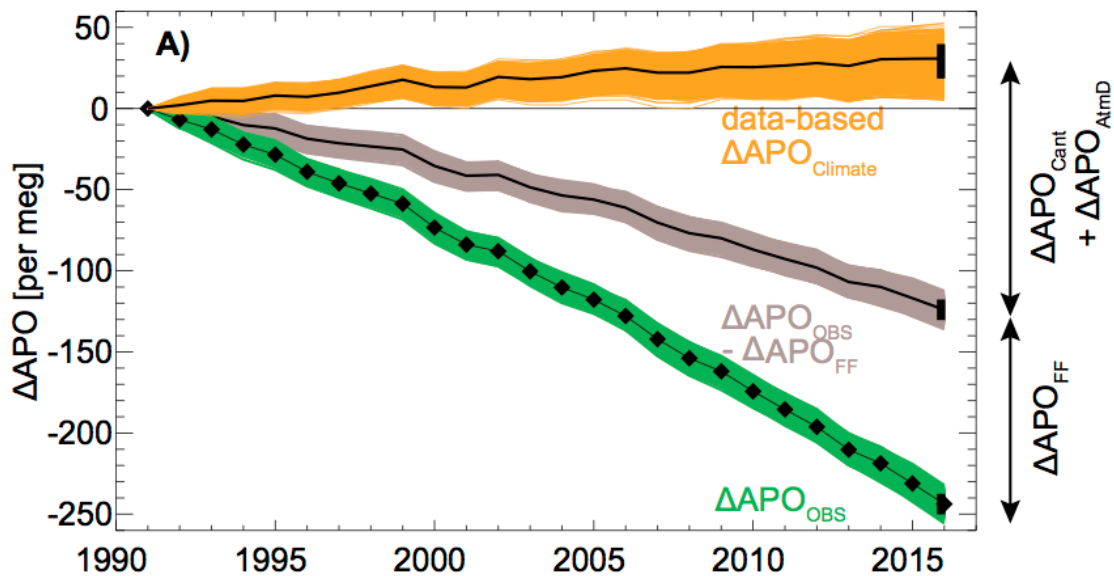


Figure 1. Residual change in APO (orange) after correcting raw signal (green) for fossil-fuel contribution (grey) and anthropogenic CO₂ uptake by the oceans. From Resplandy et al. (in prep, 2018).

Monitoring Trends and Spatial Distributions of Carbon Cycle Greenhouse Gases and Related Tracers

E.J. Dlugokencky¹, A. Crotwell^{2,1}, M.J. Crotwell^{2,1}, P.M. Lang¹, E. Moglia^{2,1}, J. Mund^{2,1}, D. Neff^{2,1}, G. Petron^{2,1}, P.P. Tans¹ and K. Thoning¹

¹NOAA Earth System Research Laboratory, Global Monitoring Division (GMD), Boulder, CO 80305; 303-497-6228, E-mail: ed.dlugokencky@noaa.gov

²Cooperative Institute for Research in Environmental Sciences (CIRES), University of Colorado, Boulder, CO 80309

ESRL/GMD's Carbon Cycle Group began monitoring carbon dioxide (CO₂) from weekly discrete air samples collected at Niwot Ridge, Colorado in 1968. Since then, the network of air sampling sites has grown, with 55 active sites in early-2018, and we now precisely measure CO₂, methane (CH₄), nitrous oxide (N₂O), sulfur hexafluoride (SF₆), carbon monoxide (CO), and hydrogen (H₂). Additional tracers (non methane hydrocarbons and isotopic composition of CO₂ and CH₄) are measured by our colleagues at the University of Colorado, Institute of Arctic and Alpine Research.

The original intent of this monitoring program was to document changes in atmospheric components that affect climate: in other words, trends. Since then, the scientific motivation has evolved; our primary goal is now quantifying greenhouse gas (GHG) budgets at large spatial scales. Success or failure at meeting this goal depends primarily on measurement quality, long-term continuity of measurements, and ensuring sufficient network sampling density.

These long-term, internally consistent measurements are at the core of understanding GHG budgets. When combined with other information, the observations tell us that ~45% of CO₂ emitted by fossil fuel combustion has been removed from the atmosphere by sinks, and that historically, most of that sink has been in the ocean, although the terrestrial biosphere has also been important in recent decades. While details of changes to the global CH₄ budget remain uncertain, our observations constrain total global emissions and yield insights into where emissions are changing, or not. For SF₆, the global distribution of our air sampling network provides important constraints on atmospheric transport models, so the measurements are vital to data assimilation systems. While we still have a great deal to learn about GHG budgets, particularly how processes that emit and remove GHGs from the atmosphere will respond to climate change, these observations remain fundamental to our scientific understanding.

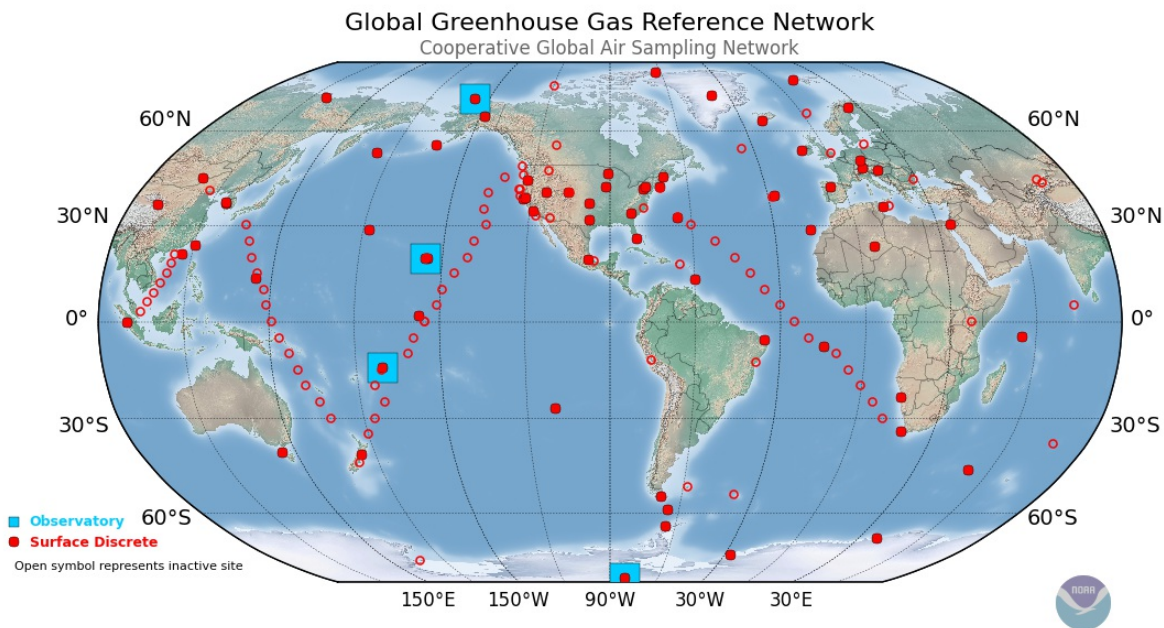


Figure 1. Carbon Cycle Group's Cooperative Global Air Sampling Network, a component of the Global Greenhouse Gas Reference Network.

The OCO-2 Model Intercomparison Project Reveals Systematic Transport Model Effects on Inverse Model CO₂ Fluxes

A.R. Jacobson^{1,2}, A. Schuh³, S. Basu^{1,2}, B. Weir⁴, D.F. Baker⁵, K. Bowman⁶, F. Chevallier⁷, S. Crowell⁸, K.J. Davis^{9,10}, F. Deng¹¹, S. Denning³, L. Feng¹², D. Jones¹¹, J. Liu⁶ and P. Palmer¹²

¹Cooperative Institute for Research in Environmental Sciences (CIRES), University of Colorado, Boulder, CO 80309; 303-497-4916, E-mail: andy.jacobson@noaa.gov

²NOAA Earth System Research Laboratory, Global Monitoring Division (GMD), Boulder, CO 80305

³Colorado State University, Fort Collins, CO 80523

⁴NASA Goddard Space Flight Center (GSFC), Greenbelt, MD 20771

⁵Cooperative Institute for Research in the Atmosphere (CIARA), Colorado State University, Fort Collins, CO 80521

⁶NASA Jet Propulsion Laboratory, California Institute of Technology, Pasadena, CA 91109

⁷Laboratoire des Sciences du Climat et de l'Environnement (LSCE), Institut Pierre-Simon Laplace, Orme des Merisiers, France

⁸University of Oklahoma, Norman, OK 73019

⁹Department of Meteorology and Atmospheric Science, The Pennsylvania State University, University Park, PA 16802

¹⁰Earth and Environmental Systems Institute, The Pennsylvania State University, University Park, PA 16802

¹¹University of Toronto, Toronto, Ontario, Canada

¹²University of Edinburgh, Edinburgh, United Kingdom

The NASA Orbiting Carbon Observatory-2 (OCO-2) program has organized an atmospheric inverse model intercomparison activity, in which modeling groups have performed experiments assimilating OCO-2 retrievals and traditional *in situ* carbon dioxide (CO₂) measurements. This collection of inverse models is dominated by atmospheric transport simulated by two models: three use the Tracer Model, Version 5 (TM5) and four use Goddard Earth Observing System-Chem (GEOS-Chem). Forward simulations of CO₂ and sulfur hexafluoride (SF₆) in these two models reveal systematic differences in vertical-meridional transport, suggesting that GEOS-Chem moves tracer mass out of northern midlatitudes more quickly than TM5. In an inverse model framework, the ensemble of GEOS-Chem models retrieves a larger annual cycle of surface CO₂ fluxes in the large zonal band from the equator to 45°N. Since inverse models frequently simulate a net land sink by amplifying the annual cycle of prior models, one might expect that GEOS-Chem would have a larger net sink in this latitude range, but we find the opposite. The differences between the two models in seasonality and long-term mean fluxes are reversed north of 45°N. We provide potential explanations for these flux differences, and link them to transport processes using SF₆ constraints.

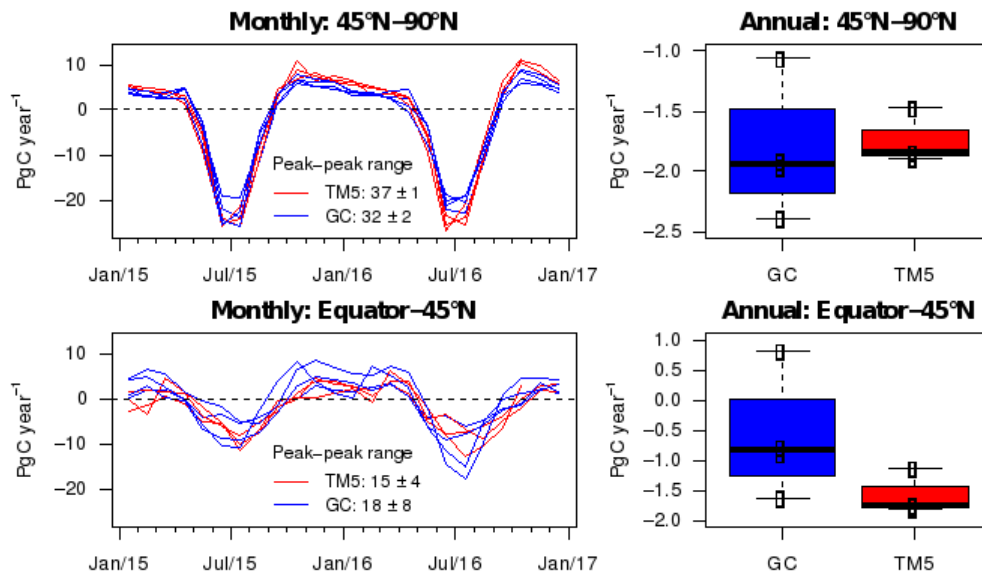


Figure 1. OCO-2 MIP fluxes estimated by GEOS-Chem ("GC", blue) and TM5 (red) transport in the latitude bands from the equator-45°N (bottom row) and from 45°N-90°N (top row). These optimized fluxes are derived by assimilation of traditional *in situ* measurements. Seasonality is revealed by monthly fluxes (left column) and the annual means are portrayed in the right column.

CarbonTracker Asia 2016: an Estimation of CO₂ Fluxes Centering on Asia

J. Rhee¹, A.R. Jacobson^{2,3}, H.M. Kim⁴, S.T. Kenea¹, Y. Oh¹, L. Labzovskii¹, S. Li¹, T. Goo¹ and Y. Byun¹

¹National Institute of Meteorological Sciences, Seogwipo-si, Jeju-do, South Korea; 820145627093, E-mail: jsrhee@snu.ac.kr

²Cooperative Institute for Research in Environmental Sciences (CIRES), University of Colorado, Boulder, CO 80309

³NOAA Earth System Research Laboratory, Global Monitoring Division (GMD), Boulder, CO 80305

⁴Yonsei University, Department of Atmospheric Sciences, Seoul, South Korea

CarbonTracker is the inverse modeling system developed by ESRL/GMD. The method estimates the surface CO₂ flux. In the Tracer Model, version 5 (TM5) which simulates carbon dioxide (CO₂) concentrations on the globe and ensemble, Kalman filters are employed. As part of carbon monitoring, National Institute of Meteorological Sciences (NIMS) in the Republic of Korea is now operating CarbonTracker Asia. CarbonTracker Asia adopts two-nested grids centered on East Asia (3°×2° global, 1°×1° Asia), and Ryori, Yonagunijima, and Minimitorishima (RYM) CO₂ observation data provided by Japan Meteorological Agency (JMA) are assimilated. Those three data fields have never been assimilated before in CarbonTracker in ESRL/GMD. Furthermore, an aircraft data assimilation module was implanted to our CarbonTracker. We use the data obtained from the Comprehensive Observation Network for Trace gases by AirLiner (CONTRAIL) project. In the meantime, CarbonTracker 2016 was released in Feb. 2017 by ESRL/GMD. That being said, studies on CarbonTracker Asia had been carried out based on 2013B. For this reason, we updated CarbonTracker Asia 2013B to 2016. In this study, we introduce CarbonTracker Asia 2016, which was newly updated in 2017. Then, the retrieved data for the period of 2000~2015 are presented. In addition, in order to verify the impact of the observation data, we also provide additional data as follows: (1) Difference before and after the aircraft data assimilation, (2) Difference in results on whether RYM observations are assimilated. Fig. 1. and Fig. 2. show the effect of the assimilation of RYM observations. Fig. 2. shows the uncertainty reduction which is calculated as $100 \times (\sigma_{\text{norym}} - \sigma_{\text{rym}}) / \sigma_{\text{rym}}$, the subscript ‘rym’ means RYM observations are assimilated, and ‘norym’ means the opposite.

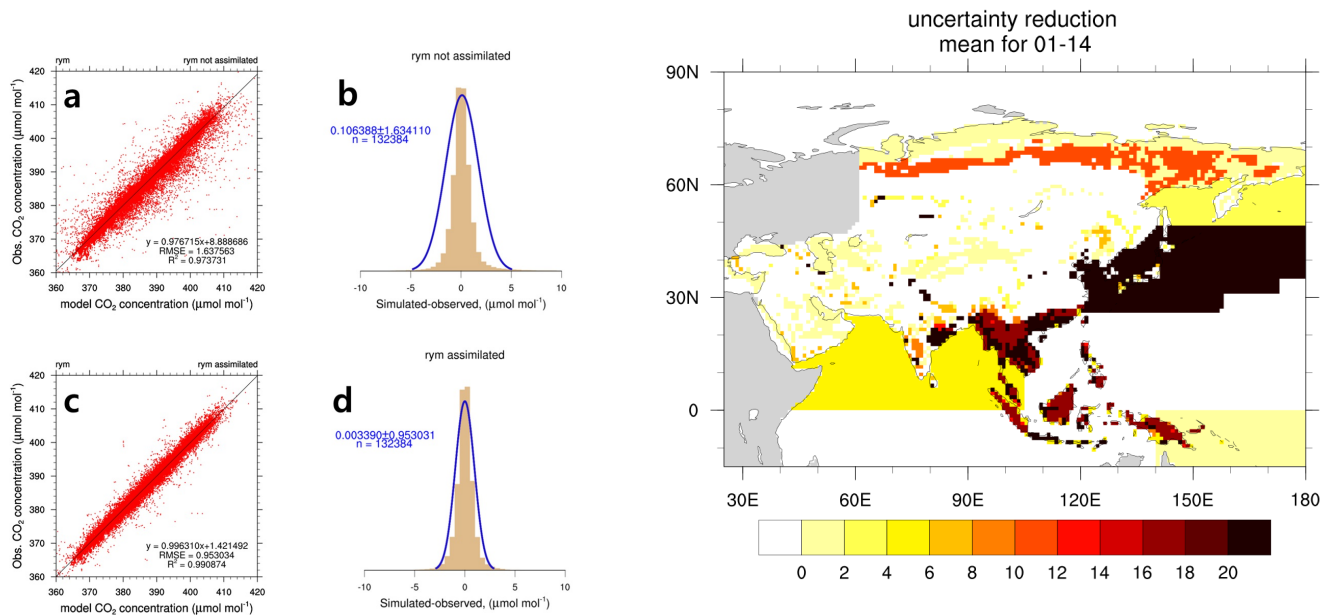


Figure 1. a), c) The scatter plots between measured and simulated CO₂ concentrations at RYM for 2000.01.01~2015.11.21, information at the right top tells whether RYM data assimilated or not. b), d) The histograms and its density function of the simulated minus measured CO₂ concentrations. Then, the number at the left middle show the average with standard deviations and ‘n’ denotes the number of data.

Figure 2. Average uncertainty reduction for 2001~2014 on Asia.

The Mysterious Global Methane Budget

L. Bruhwiler¹, E.J. Dlugokencky¹ and S.E. Michel²

¹NOAA Earth System Research Laboratory, Global Monitoring Division (GMD), Boulder, CO 80305; 303 497-6921, E-mail: lori.bruhwiler@noaa.gov

²Institute of Arctic and Alpine Research (INSTAAR), University of Colorado, Boulder, CO 80309

Atmospheric methane (CH_4) contributes 0.5 W m^{-2} to global radiative forcing, making it the second most important anthropogenic greenhouse gas after carbon dioxide. Over half of global CH_4 emissions are related to human activities that range from food and energy production to waste disposal. The largest natural source of atmospheric methane is microbial production in wetlands, and this source is difficult to quantify and potentially sensitive to changing climate. Understanding the global CH_4 budget is essential due to the large human influence on the global CH_4 budget and the potential for climate feedbacks, especially for formulation of climate mitigation policy. ESRL/GMD's global observations of CH_4 and related species are fundamental to understanding the CH_4 budget, and globally-distributed observations are essential for estimating regional emissions, such as for the U.S. and the Arctic where ESRL/GMD observations currently suggest no significant increase in emissions despite rapid Arctic warming.

CH_4 has an atmospheric chemical sink that approximately balances emissions globally, although the size and variability of the sink is uncertain. Until 2006 it seemed that atmospheric CH_4 had reached steady-state after a precipitous rise over the industrial period from pre-industrial levels of ~ 800 ppb to ~ 1770 ppb. Since 2006 the atmospheric growth of global CH_4 has increased, even accelerating to over 10 ppb/yr in recent years. Currently, global average CH_4 is about 1850 ppb. The reason for the recent increase is not currently well understood, although global measurements of CH_4 isotopes strongly suggest that the recent atmospheric growth is due mainly to microbial sources. Despite this, there remains considerable controversy about the causes of the period of stability in the late 1990s and early 2000s, and the recent growth. Various studies implicate wetlands, fossil fuels, biomass burning, and changes in the chemical sink. Why is it so difficult for scientific consensus on what drives variability in global atmospheric CH_4 , and what do we need to do to make progress?

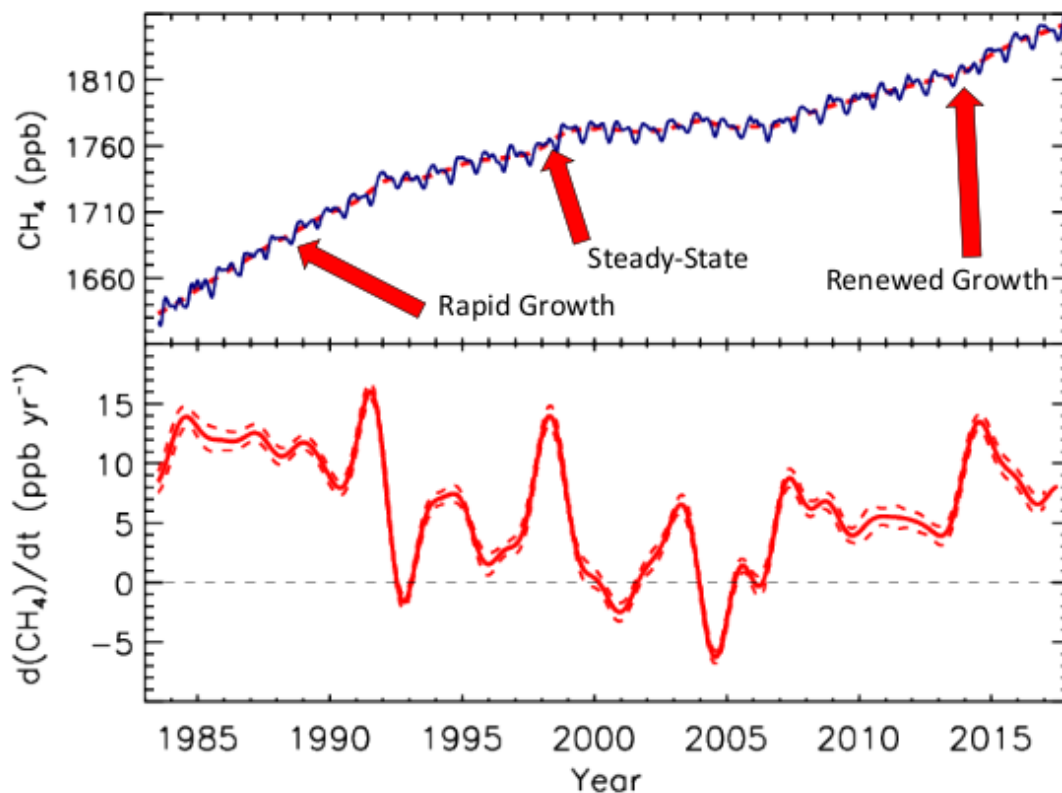


Figure 1. Global average CH_4 and its growth rate based on ESRL/GMD measurements.

The Scientific Utility of GMD Surface Radiation Measurements

C. Long^{1,2}, J.A. Augustine² and A. McComiskey²

¹Cooperative Institute for Research in Environmental Sciences (CIRES), University of Colorado, Boulder, CO 80309; 303-497-6056, E-mail: chuck.long@noaa.gov

²NOAA Earth System Research Laboratory, Global Monitoring Division (GMD), Boulder, CO 80305

The Earth system receives virtually all of its energy from the sun. Of the solar energy that reaches Earth orbit, about 30% is reflected away. Of the remaining absorbed energy, about 70% is absorbed at the surface and then balanced by net terrestrial infrared radiation and latent and sensible heat exchange. Thus the surface radiative energy budget is a fundamental energy driver of the earth-atmosphere-ocean system. These fundamental measurements made by the G-Rad group at various locations are used in many ways by the science community. A large contribution of ESRL/GMD Global Radiation (G-Rad) measurements has been the validation of satellite algorithms that attempt to estimate surface irradiance and the surface radiation budget. G-Rad measurements played an important role in NASA Earth Observing System and GOES validation, and algorithm development for GOES-R. This talk will present several examples of such use, including investigations of trends, cloud radiative effects, constraining global models for global energy budget estimations, and testing and development of models.

Hour average surface obs. versus the new CERES SYN 1-deg. product using the 7 U.S. SURFRAD sites (2003 – 2014)

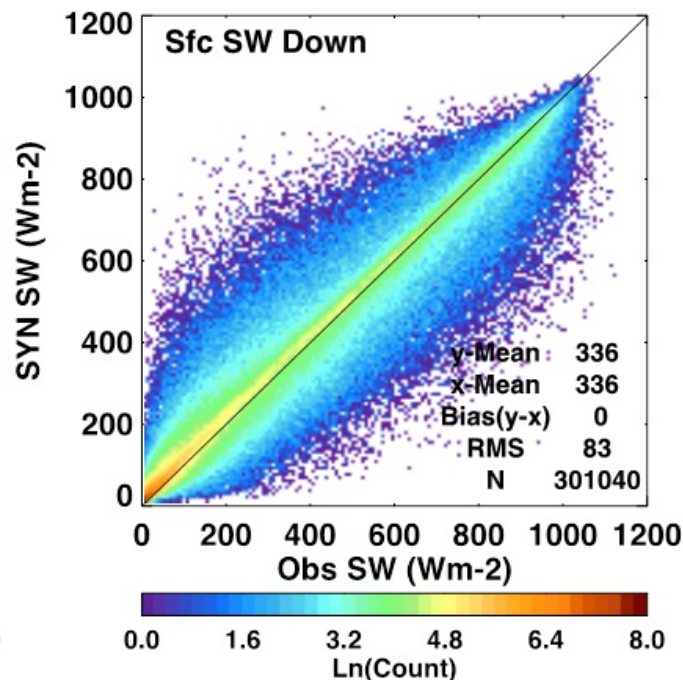


Figure 1. The SURFRAD sites have been used by many as ground truth in testing satellite retrievals and model calculations of surface radiation. This example shows a comparison between SURFRAD observed surface downwelling shortwave and CERES satellite-based retrievals from 2003 through 2014.

Trends in U.S. Surface Radiation and Aerosol Optical Depth over the Past 20 Years

J.A. Augustine¹, C. Long^{2,1} and A. McComiskey¹

¹NOAA Earth System Research Laboratory, Global Monitoring Division (GMD), Boulder, CO 80305; 303-497-6415, E-mail: john.a.augustine@noaa.gov

²Cooperative Institute for Research in Environmental Sciences (CIRES), University of Colorado, Boulder, CO 80309

Periods of solar dimming and brightening at the surface have been documented over the globe since the 1950s. In general, all-sky solar irradiance at the surface decreased (dimmed) from the 1950s to the 1980s and increased (brightened) from the 1990s through the first decade of the 21st century. According to Martin Wild's 2009 review, all continents experienced dimming and brightening except for parts of China and India, where dimming dominated. These trends have been linked to aerosol variability in Europe and Asia. For the U.S., high-quality measurements from the SURFRAD network document brightening of $+7.2 \text{ Wm}^{-2}/\text{decade}$ from 1995 to 2012, however, a quick retreat to normal levels has been observed from 2012 to 2017. Clear-sky short wave irradiance during the brightening period show an increase of $+4.6 \text{ Wm}^{-2}/\text{decade}$, but almost all of that is in the diffuse, leading to speculation that ice in the stratosphere from increased airline traffic may be the cause. Aerosol optical depth (AOD) over the U.S. has steadily decreased by $-0.023/\text{decade}$ over the past 22 years, in agreement with other inventories. The change in the direct effect of aerosols corresponding to that decrease would account for only $\sim 0.8 \text{ Wm}^{-2}/\text{decade}$ of the measured brightening. Furthermore, decreasing AOD over the past five years is not consistent with the observed dimming during that period. In contrast, sky cover variability over the U.S. is inverse to that of surface irradiance over the past 20 years, suggesting that systematic changes in cloud cover have been mostly responsible for the recent brightening and dimming trends. Coincident with the systematic decrease of AOD is an *increase* in the network-wide annual AOD minima from 1998 through 2012, followed by a sharp decrease to 2017. That variability has been linked to northern hemisphere volcanic activity by comparing SURFRAD average annual AOD minima to the zonal average (30° to 60°N) of stratospheric AOD from the Cloud-Aerosol Lidar and Infrared Pathfinder Satellite Observation (CALIPSO) space-lidar. The similarity in their variabilities demonstrates that area averaged surface-based annual AOD minima can be a proxy for stratospheric aerosol variability.

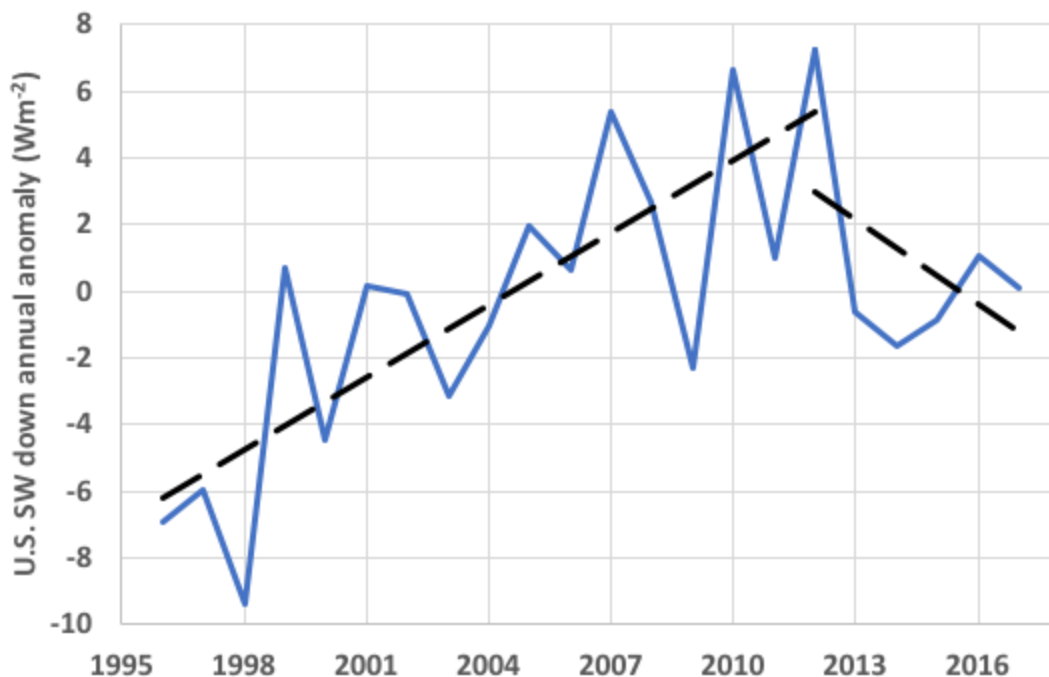


Figure 1. U.S. annual anomaly of downwelling short wave from the SURFRAD network. Dashed lines show trends for distinct periods of brightening and dimming.

Climatology of Aerosol Optical Properties from Storm Peak Laboratory

G. Hallar^{1,2}, C. Green-Japngie¹, E. Andrews^{3,4} and I. McCubbin²

¹University of Utah, Salt Lake City, UT 84112; 801-587-7238, E-mail: gannet.hallar@utah.edu

²Storm Peak Laboratory, Desert Research Institute, Steamboat Springs, CO 80488

³Cooperative Institute for Research in Environmental Sciences (CIRES), University of Colorado, Boulder, CO 80309

⁴NOAA Earth System Research Laboratory, Global Monitoring Division (GMD), Boulder, CO 80305

The effect of aerosol particles is critical in understanding Earth's radiation budget, yet significant uncertainties in the radiative properties of aerosols globally and on regional scales prevent the needed accuracy within numerical models to define future climate change.

Establishing aerosol climatology is important for identifying aerosol sources, distributions, and movements. Mountain regions create unique difficulties for numerical models due to representation of complex terrain and insufficient model resolution. Thus, long-term *in situ* data collected at high elevations is particularly useful. Data will be presented from Storm Peak Laboratory (SPL) mountain-top (3,220 m asl) site located near Steamboat Springs, CO, owned and operated by the Desert Research Institute. Aerosol optical measurements have been collected from 2011 – 2016. Using these data, seasonal and diurnal trends in aerosol type have been elucidated. Specifically, the seasonal impact of dust and biomass burning aerosols are considered. This data set highlights the wide-scale implications of a warmer, drier climate on visibility in the western U.S.A.

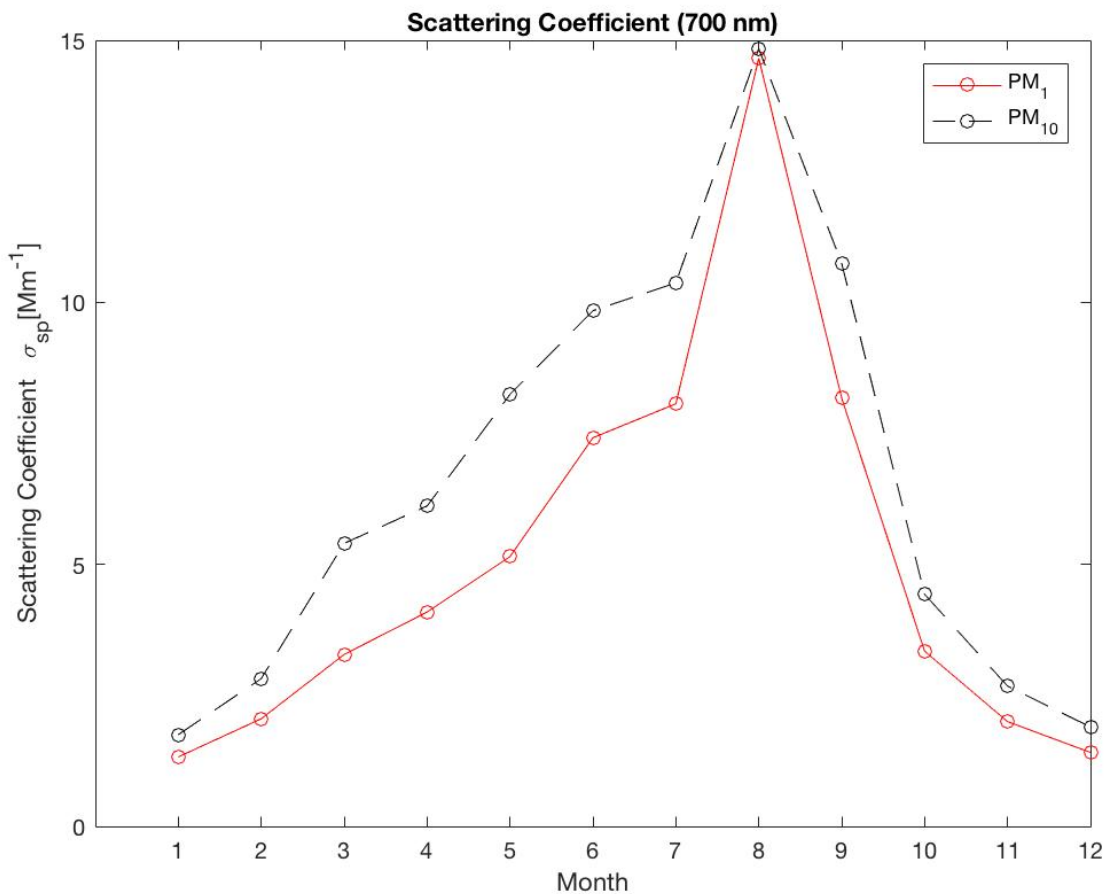


Figure 1. Monthly average of scattering coefficient (at 700 nm) from 2011-2016 measured at Storm Peak Laboratory in Steamboat Springs, CO using a TSI nephelometer. Particles were sampled behind an impactor, results are shown for particles smaller than 1 micron (PM₁) and smaller than 10 microns (PM₁₀) in red and black, respectively.

On Measurements and Spatial Distribution of Light Absorbing Aerosols in the Arctic

J. Backman¹, L. Schmeisser^{2,3}, A. Virkkula¹, J.A. Ogren^{2,3}, E. Asmi¹, S. Starkweather^{2,4}, S. Sharma⁵, K. Eleftheriadis⁶, T. Uttal⁴, A. Jefferson^{2,3}, M. Bergin⁷, A.P. Makshtas⁸ and H. Lihavainen¹

¹Finnish Meteorological Institute, Helsinki, Finland; +358-50-566-05-02, E-mail: john.backman@fmi.fi

²Cooperative Institute for Research in Environmental Sciences (CIRES), University of Colorado, Boulder, CO 80309

³NOAA Earth System Research Laboratory, Global Monitoring Division (GMD), Boulder, CO 80305

⁴NOAA Earth System Research Laboratory, Physical Sciences Division (PSD), Boulder, CO 80305

⁵Environment and Climate Change Canada, Toronto, Ontario, Canada

⁶Institute of Nuclear and Radiological Science & Technology, Energy & Safety, Environmental Radioactivity Laboratory, National Centre of Scientific Research "Demokritos", Athens, Greece

⁷Duke University, Civil and Environmental Engineering, Durham, NC 27708

⁸Arctic and Antarctic Research Institute, St.Petersburg, Russia

A widely-used means to measure the presence of black carbon (BC) in the Arctic is using filter-based instruments that measure light absorption coefficients. Several types of filter-based instruments are in use. Here, the focus is on the aethalometer which is well-suited for unattended measurements, as is often the case in the Arctic. Results are presented based on aethalometer measurements at six Arctic stations from 2012–2014. An alternative method of post-processing the aethalometer data is presented which reduces measurement noise and lowers the detection limit of the instrument more effectively than boxcar averaging. The biggest benefit of this approach can be achieved if instrument drift is minimized. Moreover, by using an attenuation threshold criterion for data post-processing, the relative uncertainty from the electronic noise the instrument is kept constant. This approach results in a time series with a variable collection time (Δt), but with a constant relative uncertainty with regard to electronic noise in the instrument. An additional advantage of this method is that the detection limit of the instrument will be lowered at small aerosol concentrations at the expense of temporal resolution, whereas there is little to no loss in temporal resolution at high aerosol concentrations. At high aerosol concentrations, minimizing the detection limit of the instrument is less critical. The time series obtained is put into use with the Hybrid Single-Particle Lagrangian Integrated Trajectory model (HYSPPLIT) version 4.9. The HYSPPLIT model was run 7 days back in time. The meteorological data used for the trajectories was the National Centers for Environmental Prediction Global Data Assimilation System dataset with a 1° horizontal resolution. The back-trajectory analysis was done by assigning the aerosol properties as measured at the arrival time and assigning those properties to the grid cell centers that the trajectory-path traversed. This allows for a footprint to be constructed using the measured aerosol properties at the different receptor sites shown in Figure 1. Due to multiple receptor locations, the weights used were inverse distance travelled from the receptor point. Thus, the receptor location closest to a grid cell will weigh the grid cell the most, which is justified since the trajectory path becomes more uncertain with greater distance travelled.

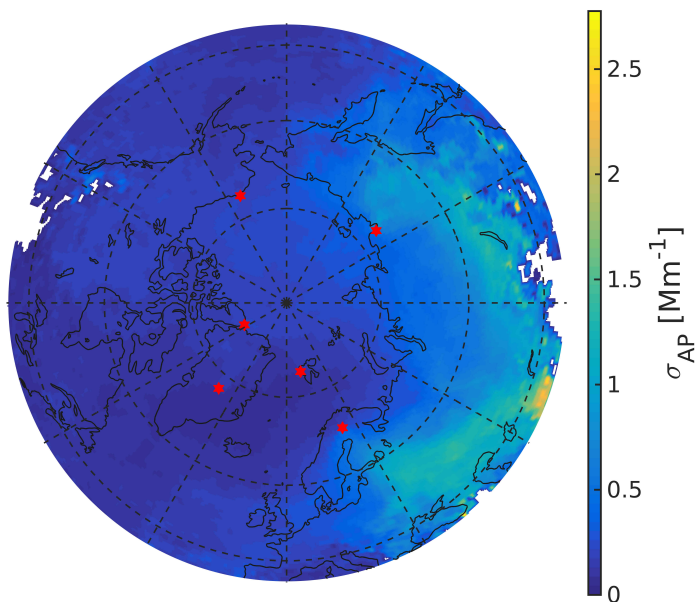


Figure 1. Footprint of light absorption coefficients using data from the six Arctic stations at a wavelength of 700 nm. The figure comprises back-trajectories where the trajectory altitude was less than 500 metres above ground level. Red stars mark the locations of the six Arctic stations.

Winter 2017-2018 Results from the De-Icing Comparison Experiment (D-ICE) at NOAA's Barrow Atmospheric Baseline Observatory, Utqiagvik, Alaska

S.M. Morris^{1,2}, C.J. Cox^{1,3}, C. Long^{1,2} and the D-ICE Team

¹Cooperative Institute for Research in Environmental Sciences (CIRES), University of Colorado, Boulder, CO 80309; 303-497-4453, E-mail: sara.morris@noaa.gov

²NOAA Earth System Research Laboratory, Global Monitoring Division (GMD), Boulder, CO 80305

³NOAA Earth System Research Laboratory, Physical Sciences Division (PSD), Boulder, CO 80305

In cold climates, ice in many forms including frost, rime, snow, etc. frequently obscures broadband longwave and shortwave sensors, contaminating measurements. Since icing occurs under particular meteorological conditions, associated data losses constitute a climatological bias. Furthermore, the signal is difficult to distinguish from that of clouds, hampering efforts to identify contamination in post-processing. The De-Icing Comparison Experiment (D-ICE) is evaluating systems designed to mitigate the formation of ice using various configurations of ventilation and heating within customized housings, and also aims to characterize any potentially adverse effects of the techniques themselves. Since August 2017, data from a suite of 25 systems has been collected alongside standard units operating with only regularly-scheduled manual cleaning by human operators at the ESRL/GMD Baseline Surface Radiation Network (BSRN) station in Utqiagvik (formerly Barrow), Alaska. Icing on the sensors is monitored visually using cameras recording images every 10-15 minutes at the ESRL/GMD observatory, as well as the operational stations at the nearby Department of Energy Atmospheric Radiation Measurement (ARM) Program North Slope Alaska site and the more distant ARM Oliktok Point mobile facility, 250 km east of Utqiagvik.

Previous experience within the BSRN community suggests that aspiration of ambient air alone may be sufficient to maintain ice-free radiometers. Initial results based on data collected from November 2017 through February 2018 support this assertion. Most tested systems are observed to significantly reduce icing with several showing markedly little vulnerability (90%+ reduction in the frequency of ice). However, we have also observed large variability in performance between systems, some of which differ in only very minor ways, implying the effectiveness of ventilation is highly sensitive to subtle variations in design. Generally, the systems are more effective at mitigating ice on pyrgeometers than pyranometers, possibly because the former have lower profile domes. For November-February, we compared the raw (pre-quality control) upward-facing BSRN pyrgeometer data to a best-estimate downwelling longwave (LWD) time series constructed from a combination of the data from the D-ICE pyrgeometers when the instruments were ice-free. During brief periods, icing was observed to enhance the BSRN LWD by up to 55 W m^{-2} . However, despite the fact that the ambient air on the D-ICE platform was saturated w.r.t. ice ~49% of the time, we estimate the operational BSRN data suffered only a small positive bias caused by icing when averaged over time ($+1.4 \text{ W m}^{-2}$).



Figure 1. The D-ICE platform at the ESRL/GMD observatory, Utqiagvik, Alaska, on 6 November 2017. Photo by Station Chief, Bryan Thomas.

The Role of Atmospheric Circulation in the Seasonal Melt of Snow and Sea Ice in the Pacific Arctic

C.J. Cox^{1,2}, R.S. Stone^{3,4}, D.C. Douglas⁵ and D. Stanitski⁴

¹Cooperative Institute for Research in Environmental Sciences (CIRES), University of Colorado, Boulder, CO 80309; 303-497-4518, E-mail: christopher.j.cox@noaa.gov

²NOAA Earth System Research Laboratory, Physical Sciences Division (PSD), Boulder, CO 80305

³Science and Technology Corporation, Boulder, CO 80305

⁴NOAA Earth System Research Laboratory, Global Monitoring Division (GMD), Boulder, CO 80305

⁵USGS Alaska Science Center, Juneau, AK 99801

Recent springtime climate extremes have been observed along the northern coast of Alaska. The dates when snow melted at Barrow in 2015 and 2016 were the 4th and 1st earliest recorded, respectively, since 1901. These early years were followed in 2017 by the latest date of snow melt since 1988, nearly seven weeks later than in 2016. However, unlike the previous anomalies, in 2017 the late melt was more confined to the western North Slope, whereas ~250 km to the east at Oliktok Point, the timing of the melt was about 25 days earlier than at Barrow. Previous work implicates the northward advection of warm air circulating around the Aleutian Low during years of early melt and blocking by the Beaufort High during years of later melt. The juxtaposition of the two pressure centers resulted in the late melt at Barrow in 2017, while favoring the advection of warmer air to Oliktok, which contributed to an earlier melt there. The existence and relative position of a high-pressure ridge to the east of the Aleutian Low appears to be a key factor in when snow melts along Alaska's northern coast. Spatial and temporal variability of snow melt is linked to subtle variations in the way air circulates around these dominant pressure centers. Here, we investigate these relationships using reanalysis, satellite retrievals, and surface-based data sets. Anomalies are further investigated by analysis of the resulting spatial patterns of the timing of snow melt over land areas and ice melt onset in the Chukchi and Beaufort seas that are affected by the same regional circulation patterns. We introduce a new climate index that explains some of the variance in those variables. This index is suitable for monitoring changes in regional circulation and may be useful for developing seasonal-scale predictive tools.

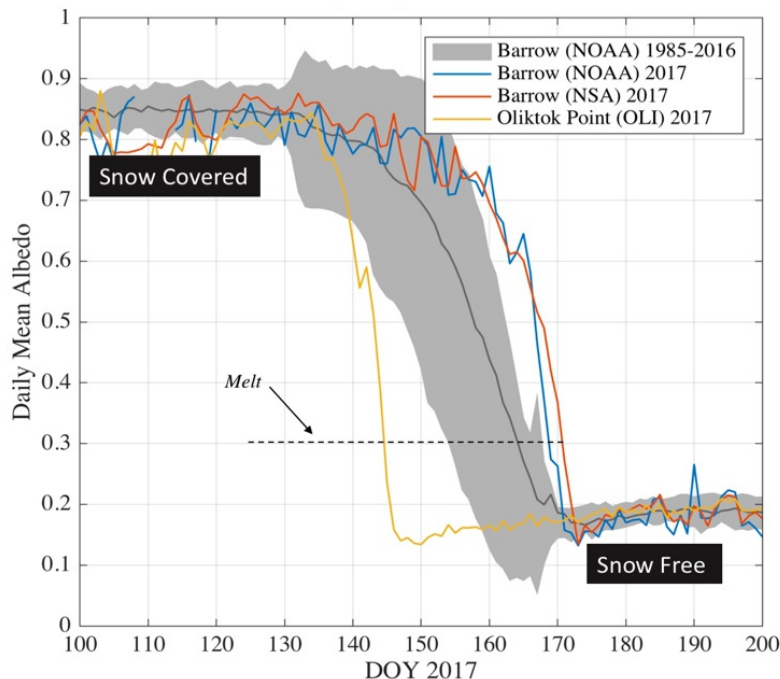


Figure 1. Daily mean albedo in 2017 from April 10 (Day of Year [DOY] 100) through July 19 (DOY 200) measured at the NOAA Atmospheric Baseline Observatory at Utqiagvik (Barrow), Alaska (blue); at the Department of Energy Atmospheric Radiation Measurement (ARM) North Slope Alaska observatory, also in Utqiagvik (red); and at the ARM mobile facility east at Oliktok Point (yellow). For reference, the gray line and shading are the mean and standard deviation of the daily albedo climatology from the ESRL/GMD station, 1985-2016. The date of melt is defined as the first date when the albedo falls below 0.3.

Increasing CFC-11 Emissions and other Unusual Atmospheric Changes: How Delayed Will Ozone Recovery Be?

S. Montzka¹, G.S. Dutton^{2,1}, P. Yu^{2,3}, E. Ray^{2,3}, R.W. Portmann³, J. Daniel³, L. Kuijpers⁴, B.D. Hall¹, D. Mondeel^{2,1}, C. Siso^{2,1}, D. Nance^{2,1}, M. Rigby⁵, A. Manning⁶, L. Hu^{2,1}, F.L. Moore^{2,1}, B.R. Miller^{2,1} and J.W. Elkins¹

¹NOAA Earth System Research Laboratory, Global Monitoring Division (GMD), Boulder, CO 80305; 303-497-6657, E-mail: stephen.a.montzka@noaa.gov

²Cooperative Institute for Research in Environmental Sciences (CIRES), University of Colorado, Boulder, CO 80309

³NOAA Earth System Research Laboratory, Chemical Sciences Division (CSD), Boulder, CO 80305

⁴Eindhoven Centre for Sustainability, Technical University Eindhoven, Eindhoven, Netherlands

⁵University of Bristol, School of Chemistry, Bristol, United Kingdom

⁶UK Meteorological Office, Exeter, United Kingdom

Surprising changes have been measured in our observational network for some ozone-depleting substances (ODSs) in recent years that are relevant for stratospheric ozone recovery. Concentrations of dichloromethane, an ODS not controlled by the Montreal Protocol, doubled over the past decade. Concentrations of methyl bromide, a controlled ODS, increased in 2016 for the first time in nearly two decades. Methyl chloride concentrations also increased in 2016, suggesting a natural cause for the methyl halide changes. Is this a trend in natural emissions responding to climate change, or something else?

The most surprising and concerning ODS trend in recent years, however, is the slowdown in the decline of atmospheric CFC-11 concentrations. The decline in CFC-11 concentrations was expected to gradually accelerate after production reported to the United Nations Environmental Programme for all uses became negligible in 2007, or three years before the phase-out required by the Montreal Protocol. Since 2012, however, CFC-11 concentrations have declined at a rate that is half as fast as was measured during the preceding decade. A large reservoir of CFC-11 still exists in foams and is slowly leaking to the atmosphere, but an increased emission from this reservoir or bank is unlikely. In this presentation, we will show the evidence indicating a significant increase in global CFC-11 emissions since 2012 (of up to 13 ± 5 Gg/yr or 25% of the 2002-2012 mean) and discuss evidence suggesting that this emission increase is more likely associated with new production inconsistent with Montreal Protocol controls as opposed to faster releases from the CFC-11 bank.

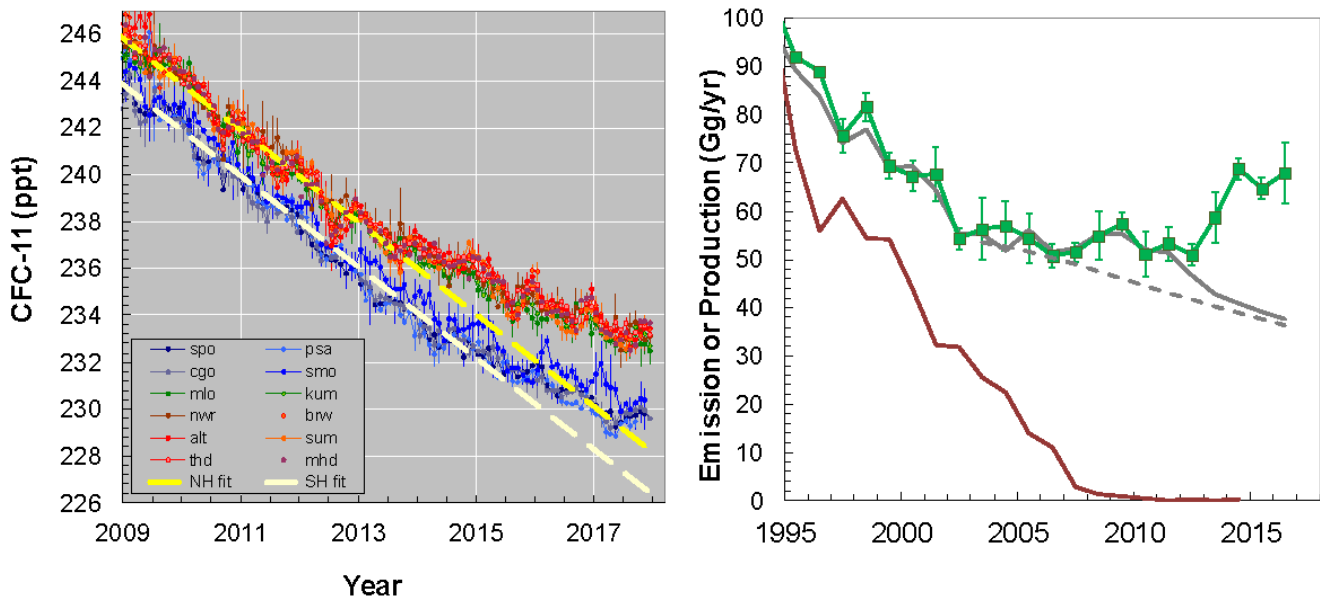


Figure 1. Left: CFC-11 atmospheric mole fraction over time measured at Northern Hemisphere sites (red and green points) and Southern Hemisphere sites (blue points). Fits to hemispheric mean data during 2002 to 2012 are extrapolated to 2018 (yellow- and white-dashed lines). **Right:** Reported production (brown line) and emission derived from atmospheric data (green points) along with emission projections based on WMO scenarios (grey solid line; Carpenter and Reimann et al. 2014) and a constant release rate of 3.3%/yr from the CFC-11 bank after 2002 (gray dashed line).

Diagnosing CFC-11's Emissions in a Chemistry-Climate Model

P. Yu^{1,2}, R.W. Portmann², E. Ray^{1,2}, J. Daniel², G. Dutton³, B. Hall³, D. Nance^{1,3}, S. Davis^{1,2}, N. Davis¹, J. Elkins³ and S. Montzka³

¹Cooperative Institute for Research in Environmental Sciences (CIRES), University of Colorado, Boulder, CO 80309; 303-497-4711, E-mail: pengfei.yu@noaa.gov

²NOAA Earth System Research Laboratory, Chemical Sciences Division (CSD), Boulder, CO 80305

³NOAA Earth System Research Laboratory, Global Monitoring Division (GMD), Boulder, CO 80305

Trichlorofluoromethane (CFC-11) is one of the major stratospheric ozone-depleting substances for which production has been strictly controlled by the Montreal Protocol. As demonstrated in a recent paper (Montzka et al. 2018), the decline of global CFC-11 concentration slowed by 50% after 2012, and the hemispheric difference of CFC-11 increased by 50% concurrently. Neither the observed global growth rate nor the hemispheric difference of CFC-11 after 2012 can be simulated in our Chemistry-Climate Model (CCM) simulations without an emission increase. However, large uncertainties still remain on how much and where the additional emissions occur. Much of this uncertainty comes from poor constraints on interannual variability in stratosphere-troposphere exchange of CFC-11. Thus, to quantify the emissions from global surface concentration changes we need a better understanding of the stratospheric influence on the global growth rate and hemispheric difference. We use a CCM to show that some of the seasonal and inter-annual variability observed by the ground-based measurements include stratospheric dynamical components. This dynamical variability is connected to changes in the Brewer-Dobson circulation and the quasi-biennial oscillation (QBO) in the stratosphere. We explore uncertainties in the modeled surface concentrations of CFC-11 and other trace gases induced by choices in the modeling configuration, such as the reanalysis input, model resolution, and nudging methods. We demonstrate that the ESRL/GMD measurements of long-lived gases provide an excellent observational constraint to diagnose and improve the CCM's capability to model dynamical variability. In addition, the surface measurements provide one of the few means by which interannual changes in stratosphere-troposphere exchange can be assessed.

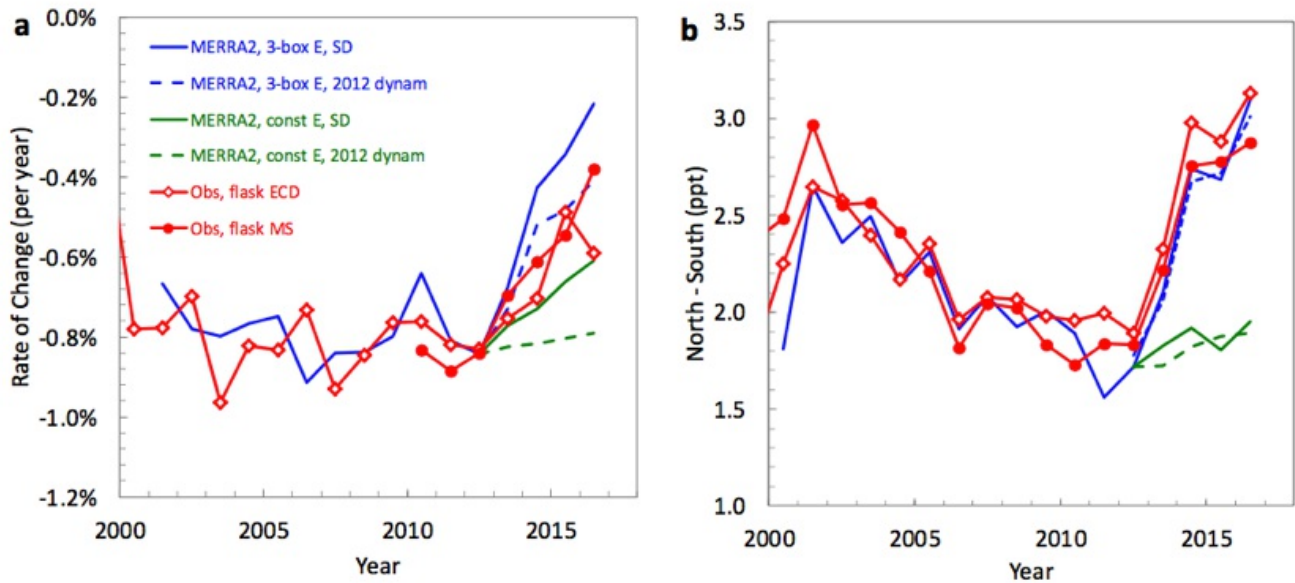


Figure 1. Global annual rates of change and hemispheric differences from 3-D simulations and observations. **a**, Global rates for CFC-11 mole fractions simulated in a 3-D model (CAM) with Modern-Era Retrospective analysis for Research and Applications, Version 2 (MERRA-2) reanalysis meteorology (SD) and emissions from 1) the 3-box model (blue lines), or 2) same as 1) but with constant emissions after 2012 at the 2012 rate (green lines). Simulations were also performed with 2012 dynamics for years after 2012 (dashed lines). **b**, simulated and observed hemispheric differences. In **a** and **b**, observed annual means are from flasks analyzed by GCECD and GCMS (red lines and symbols).

Ozone and Chemical Composition in the Pacific Region Measured by IAGOS

H. Clark and IAGOS-team

IAGOS-AISBL, Brussels, Belgium; +33-5-61-33-27-69, E-mail: hannah.clark@iagos.org

Since 1994, the program IAGOS (In-service Aircraft for a Global Observing System) has been equipping commercial aircraft with instruments to monitor the composition of the atmosphere on long-haul flights around the world. Time-series and climatologies of ozone and humidity at cruise altitude now span almost 25 years. With the participation of China Airlines in 2012, the first data over the northern Pacific UTLS were collected. The aircraft are based in Taipei and provide daily measurements of ozone, carbon monoxide, and humidity. We present time-series from the surface to the upper troposphere of ozone, carbon monoxide, and humidity at Taipei focusing on periods influenced by the passage of tropical cyclones. Downstream of the typhoons, high ozone mixing ratios are anti-correlated with relative humidity suggesting stratospheric air, with trajectories also indicating transport from the stratosphere to the troposphere. After the tropical cyclone, the tropospheric column is filled with very low ozone mixing ratios due to the rapid uplift of air from the marine boundary layer. Locally, the passage of typhoons has a positive effect on air quality at the surface, cleansing the atmosphere and reducing the mixing ratios of pollutants. Last year, Hawaiian Airlines joined IAGOS, greatly increasing coverage over the Central and Southern Pacific. We present the first few months of ozone and cloud data from the Hawaiian Airlines flights, relating the large increases in ozone to stratospheric intrusions and the position of the sub-tropical jet in the Southern Hemisphere.

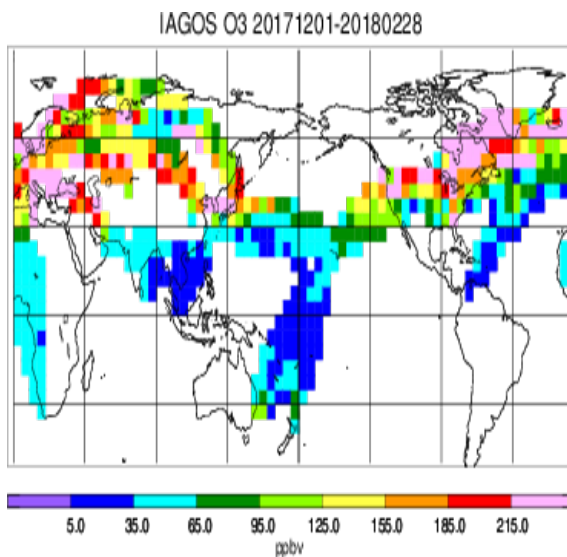


Figure 1. Ozone mixing ratios (ppbv) from IAGOS at 200 hPa during December 2017 - February 2018.

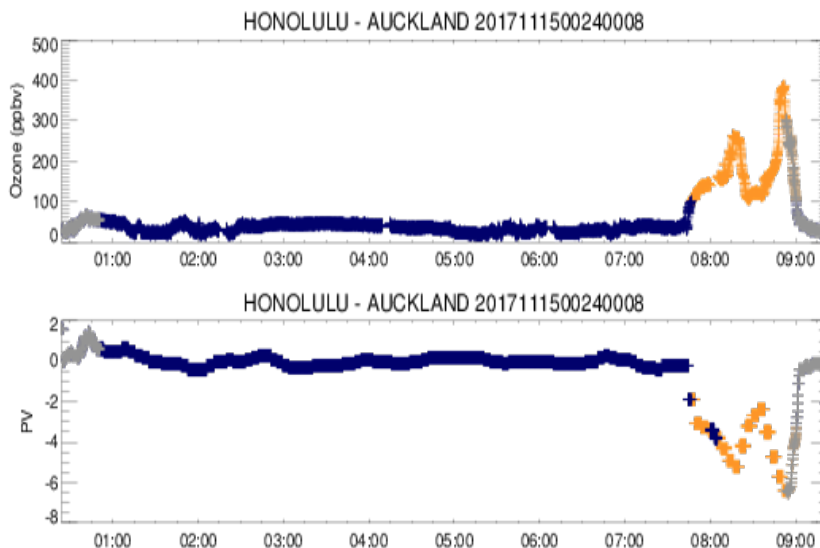


Figure 2. A flight from Honolulu to Auckland on 15 November 2017 showing ozone mixing ratios (top) and potential vorticity (bottom). Measurements during landing and take-off are in grey, measurements at cruise altitude in the troposphere are blue, and measurements which are in the lower stratosphere according to ozone mixing ratio > 100 ppbv or PV > 2PVU are colored in orange.

Global Observations of Aerosol and Ozone from SAGE III ISS – A First Year Showcase

K.R. Leavor¹, M. Roell² and D. Flittner²

¹Science Systems and Applications, Inc. (SSAI), Lanham, MD 20706; 757-864-3828, E-mail: kevin.r.leavor@nasa.gov

²NASA Langley Research Center, Hampton, VA 23681

The Stratospheric Aerosol and Gas Experiment III on the International Space Station (SAGE III ISS) achieved first light on 17 March 2017. Near-continuous observations of ozone, aerosol, and related species have been made covering altitudes from the upper troposphere to the mesosphere and latitudes from 67° S to 69° N. Historically, SAGE II's stable directly-measured profiles of atmospheric transmission have been used by the atmospheric science community as a standard in aerosol and ozone observations and trends. SAGE III ISS has made over one year of similar observations, beginning a new highly-anticipated record. Measurement capabilities and observations of aerosol and ozone spanning the first year of observation are presented, showcasing SAGE III ISS's first year in orbit. In that first year, SAGE III ISS has made observations of stratospheric pyrocumulus resulting from wildfires in the United States Pacific Northwest and British Columbia, Canada, validated unique measurements through an Antarctic polar vortex air mass, and compared well against other contemporary satellite observations. These early results are highly indicative of a mission with significant potential capable of adding to and renewing the existing SAGE record.

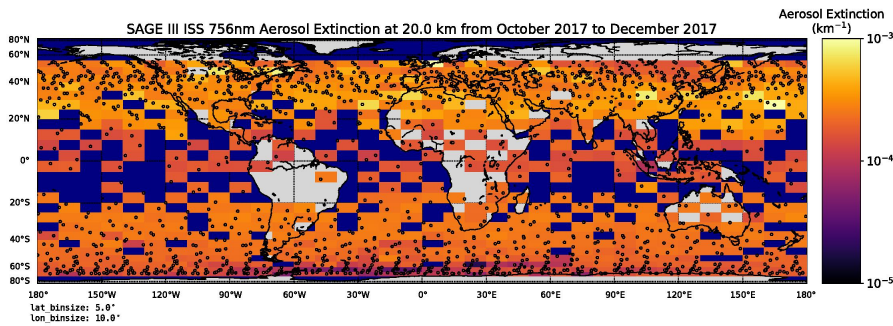


Figure 1. Geospatial averages of 756nm aerosol extinction coefficients retrieved at 20 km in the time period following the extinguishing of the 2017 North American summer wildfires. Enhanced extinction is observed at latitudes North of 20° N.

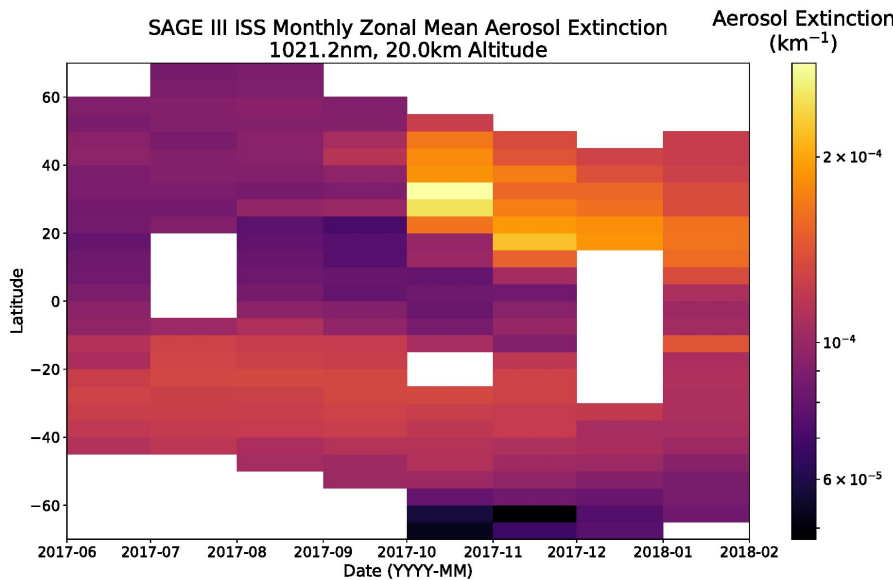


Figure 2. Monthly zonal means of 1021 nm aerosol extinction coefficient from the beginning of the SAGE III ISS public data release in June 2017 through January 2018. Significant enhancement is visible as early as September, with wide dispersion across latitudes observable from October onward.

South Pole Ozonesondes in 2017 Continue to Show Less Severe Ozone Loss

B. Johnson¹, P. Cullis^{2,1}, G. McConville^{2,1}, G. Chensue¹ and I. Petropavlovskikh^{2,1}

¹NOAA Earth System Research Laboratory, Global Monitoring Division (GMD), Boulder, CO 80305; 303-475-5816, E-mail: bryan.johnson@noaa.gov

²Cooperative Institute for Research in Environmental Sciences (CIRES), University of Colorado, Boulder, CO 80309

The 2017 minimum total column ozonesonde profile measured at South Pole station was 136 Dobson Units (DU) measured on September 25th. This was 24 DU above the average yearly minimum, placing 2017 as the 28th lowest ozone minimum profile observed in the 32-year South Pole record. Total column ozone and size (area < 220 DU) measured by satellites, ground-based instruments, and ozonesondes have provided the broad view of the yearly ozone hole. These observations have recently shown that the ozone hole is in recovery or healing stages. Another important indicator is the measured September loss rate measured by South Pole ozonesondes within the 14-21 km altitude range. The ozone loss rate, since 1991, has been on a slight upward trend and appears to be on the way to breaking out from the severe depletion range of 3 to 4 DU/day. A loss rate less than 3 DU/day will fall into the 2-3 DU/day range observed during the 1986-1990 period, just after the discovery of the ozone hole. Trends in ozone and temperature in 2 km layers will be highlighted to show where the greatest changes have occurred within the main depletion layer over South Pole.

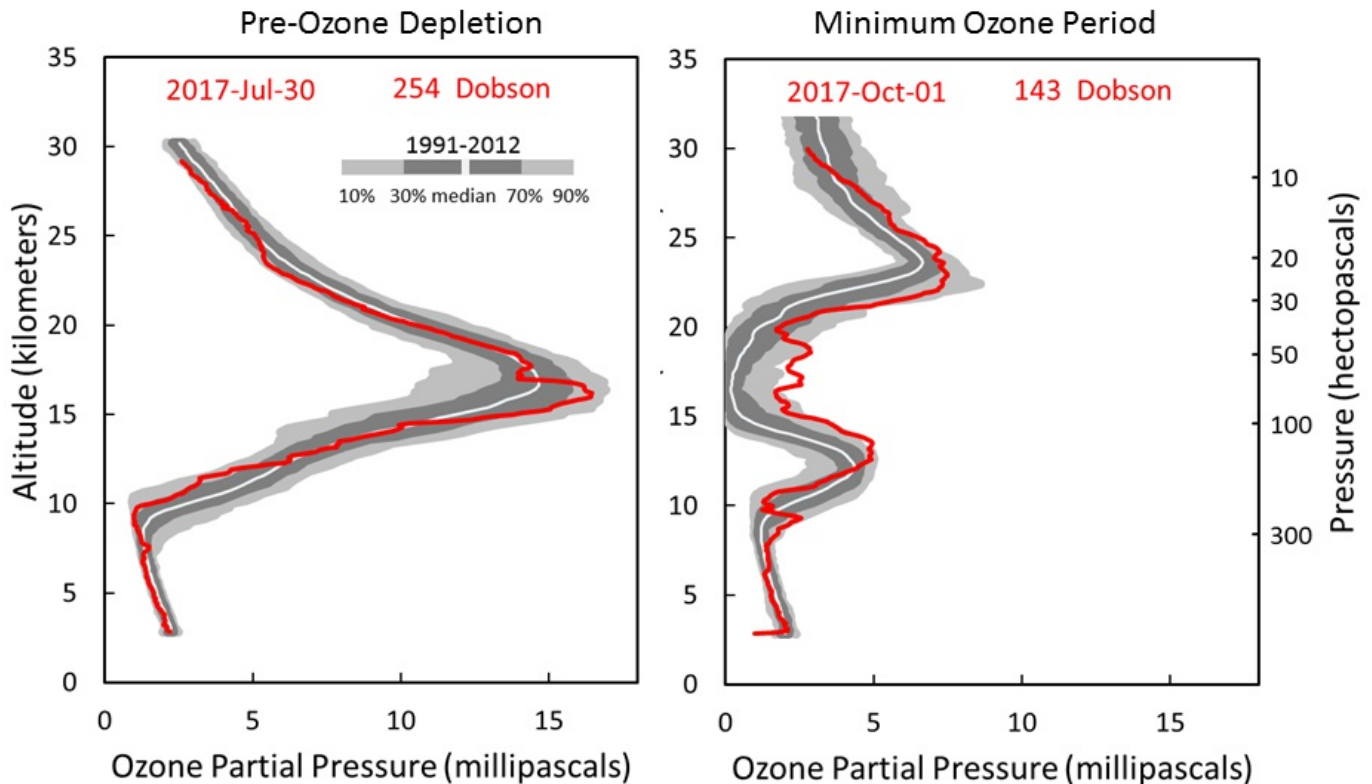


Figure 1. Selected ozonesonde profiles showing the normal ozone profile in July (before sunrise and rapid depletion begins) and the ozone profile in early October when the yearly minimum occurs. In 2017, the lowest total column ozone profile of 136 Dobson Units was observed earlier than normal on Sept 25 due to a weakened polar vortex.

Is Stratospheric Ozone Recovering as We Expect? Results of the SPARC LOTUS Analyses

I. Petropavlovskikh^{1,2}, S. Godin-Beekmann³, D. Hubert⁴, K. Chang^{5,2}, K. Tourpali^{6,7}, R. Damadeo⁶, V. Sofieva⁸ and B. Hassler^{9,10}

¹Cooperative Institute for Research in Environmental Sciences (CIRES), University of Colorado, Boulder, CO 80309; 303-497-6279, E-mail: irina.petro@noaa.gov

²NOAA Earth System Research Laboratory, Global Monitoring Division (GMD), Boulder, CO 80305

³Université de Versailles Saint-Quentin en Yvelines (UVSQ), Centre National de la Recherche Scientifique (CNRS), Guyancourt, France

⁴Royal Belgian Institute for Space Aeronomy, Brussels, Belgium

⁵National Research Council Post-Doc, Boulder, CO 80305

⁶NASA Langley Research Center, Hampton, VA 23681

⁷Laboratory of Atmospheric Physics, Aristotle University of Thessaloniki, Thessaloniki, Greece

⁸Finnish Meteorological Institute, Helsinki, Finland

⁹Bodeker Scientific, Alexandra, New Zealand

¹⁰Deutsches Zentrum für Luft- und Raumfahrt (DLR), Institut für Physik der Atmosphäre, Oberpfaffenhofen, Germany

The WMO United Nations Environment Programme Assessment 2018 on the state of the ozone layer (a.k.a. Ozone Assessment) requires an accurate evaluation of both total ozone and ozone profile long-term trends. These trend results are of utmost importance in order to evaluate the success of the Montreal Protocol with regards to the recovery of the ozone layer. A previous activity sponsored by Stratosphere-Troposphere Processes and their Role in Climate (SPARC), International Ozone Commission (IO3C), Integrated Global Atmospheric Chemistry Observations - O₃ (IGACO-O3), and NDACC (SI²N) successfully provided estimates of stratospheric ozone recovery trend in the period 1998 - 2012, from a variety of long-term records, however its results were different from those published in the WMO 2014 Ozone Assessment report. In the most recent years, new merged satellite data sets and several homogenized ozonesonde data series have been produced. Improved datasets feature correction of the drifts in satellite records (i.e. Origins, Spectral Interpretation, Resource Identification, and Security [OSIRIS], Global Ozone Chemistry And Related trace gas Data records for the Stratosphere [GOZCARDs], Michelson Interferometer for Passive Atmospheric Sounding [MIPAS]), reduction in the sampling biases, addition of four extra years in established satellite records (i.e. Aura Microwave Limb Sounder [MLS], Aura Ozone Monitoring Instrument [OMI], etc.), addition of new satellites (i.e. Joint Polar Satellite System Ozone Mapping Profiler Suite [JPSS OMPS]), and re-evaluation and re-processing of ground-based records. Initiation of the SPARC Long-term Ozone Trends and Uncertainties in the Stratosphere (LOTUS) activity in 2016 provided an opportunity for assessment of new and updated data records, comparisons of multiple regression models, assessment of stability in the combined satellite and ground-based records, evaluation of representativeness of the ground-based records in the broad-band trends, and determination of statistical methods for combining trends from different observational records. The LOTUS assessment of the stratospheric ozone recovery rates delivers high confidence in the results and creates a platform for understanding of limitations in determining significance of ozone recovery. This presentation will provide overview of the LOTUS results and discuss the way forward.

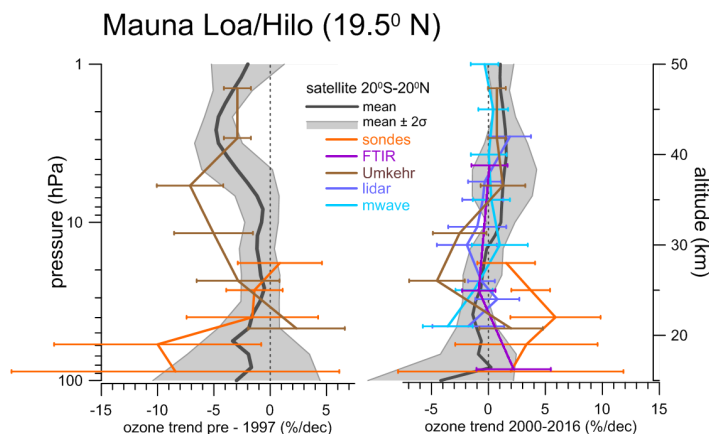


Figure 1. Ozone trends for the pre-1997 and post-2000 period from the satellites, averaged over 20°S-20°N, and ground-based stations, which includes ESRL/GMD Dobson Umkehr record from the Mauna Loa Atmospheric Baseline Observatory, and ozone-sondes records from multiple NOAA/Southern Hemisphere Additional OZonesonde (SHADOZ) stations.

The Trials and Triumphs of SHADOZ: The Who's Who of Tropical Ozone Profiles

J.C. Witte^{1,2}, B.J. Johnson³, H.G.J. Smit⁴, A. Jordan^{5,3}, C.W. Sterling^{5,3}, P. Cullis^{5,3} and S.J. Oltmans⁶

¹Science Systems and Applications, Inc. (SSAI), Lanham, MD 20706; 301-614-5991, E-mail: jacquelyn.witte@nasa.gov

²NASA Goddard Space Flight Center (GSFC), Atmospheric Chemistry and Dynamics Laboratory, Greenbelt, MD 20771

³NOAA Earth System Research Laboratory, Global Monitoring Division (GMD), Boulder, CO 80305

⁴Institute of Chemistry and Dynamics of the Geosphere: Troposphere, Research Centre Juelich, Germany

⁵Cooperative Institute for Research in Environmental Sciences (CIRES), University of Colorado, Boulder, CO 80309

⁶Retired from NOAA Earth System Research Laboratory, Global Monitoring Division (GMD), Boulder, CO 80305

SHADOZ (Southern Hemisphere Additional OZonesondes) is the premier archive for tropical and sub-tropical electrochemical concentration cell (ECC) ozonesonde data. Since 1998, vertical profiles of ozone and P-T-U (pressure - temperature - humidity) have been collected from 14 stations in close collaboration with ESRL/GMD and international partners. We summarize the collective efforts to homogenize datasets, assign uncertainty estimates, and converge towards optimizing standard operating procedures among SHADOZ stations. One major accomplishment of the past year has been the reprocessing of 13 stations ozonesonde datasets. The homogenization of SHADOZ datasets have led to improved agreements between sonde and independent instruments, both ground- and space-based to within 2%. Another milestone is deriving uncertainty estimates for ozone profiles and total column. The first approach shows overall uncertainties in total column ozone are 5-6% and are comparable to the variability found in satellite overpasses. Finally, the Juelich [Germany] Ozonesonde Intercomparison Experiment (JOSIE) (Oct-Nov 2017) invited SHADOZ representatives from eight stations to test operating procedures, new solutions, and instrument biases against the world standard ozone photometer. JOSIE underscores the importance of community-driven consensus in operating procedures and equipment, optimal solution/ECC combinations, and completeness of metadata reporting. We summarize our campaign activities and preliminary findings.



Figure 1. Map of SHADOZ stations. Data are publicly available at <https://tropo.gsfc.nasa.gov/shadoz>.

Notes:

NOAA ESRL GLOBAL MONITORING ANNUAL CONFERENCE 2018

David Skaggs Research Center, Room GC-402
325 Broadway, Boulder, Colorado 80305 USA

Wednesday Morning, May 23, 2018 Agenda

(Only presenter's name is given; please refer to abstract for complete author listing.)

07:00 **Registration Opens in GC-402 - lunch orders collected at registration table**

07:45 - 08:30 **Morning Snacks - coffee, tea, fruit, bagels and donuts served**

| | Page No. |
|--|----------|
| Session 5 | |
| Tracking Greenhouse Gases and Understanding Carbon Cycle Feedbacks - Regional Carbon Cycle Feedbacks and Observations — Chaired by Colm Sweeney | |
| 08:30 - 09:00 Response of North American Terrestrial CO ₂ Fluxes to Climate Variability | 20 |
| <i>Lei Hu (Cooperative Institute for Research in Environmental Sciences (CIRES), University of Colorado)</i> | |
| 09:00 - 09:15 Arctic-CAP: Northern High Latitude CO ₂ , CH ₄ , and CO Airborne Vertical Profile Surveys during the Arctic-Boreal Vulnerability Experiment (ABOVE) | 21 |
| <i>Charles Miller (NASA Jet Propulsion Laboratory, California Institute of Technology)</i> | |
| 09:15 - 09:30 ICOS Research Infrastructure, Progress in the European Carbon Cycle and Greenhouse Gas Observing Network | 22 |
| <i>Alex Vermeulen (Integrated Carbon Observation System (ICOS) European Research Infrastructure Consortium (ERIC), Carbon Portal, Lund, Sweden)</i> | |
| 09:30 - 09:45 Single-blind Testing of a Regional, Continuous Monitoring System for Finding Methane Leaks from Oil and Gas Operations | 23 |
| <i>Caroline Alden (Cooperative Institute for Research in Environmental Sciences (CIRES), University of Colorado)</i> | |
| 9:45 - 10:15 Morning Break | |
| Session 6 | |
| Tracking Greenhouse Gases and Understanding Carbon Cycle Feedbacks - Urban/Regional Emissions — Chaired by Arlyn Andrews | |
| 10:15 - 10:30 Unexpected and Significant Biospheric CO ₂ Fluxes in the Los Angeles Basin Indicated by Atmospheric Radiocarbon | 24 |
| <i>John B. Miller (NOAA Earth System Research Laboratory, Global Monitoring Division (GMD))</i> | |
| 10:30 - 10:45 Development of an Open-path, Laser Dispersion Spectroscopy (LDS) Analyzer for Methane Emissions Mapping and Quantification | 25 |
| <i>Graham Leggett (MIRICO Ltd., Chilton, United Kingdom)</i> | |
| 10:45 - 11:00 Little Evidence for Significant Increases in Total U.S. CH ₄ Emissions over the Past Decade | 26 |
| <i>Xin Lan (Cooperative Institute for Research in Environmental Sciences (CIRES), University of Colorado)</i> | |
| 11:00 - 11:15 A Multi-species Analysis of Carbon Enhancements during the ACT-America Campaign | 27 |
| <i>Bianca Baier (Cooperative Institute for Research in Environmental Sciences (CIRES), University of Colorado)</i> | |
| 11:15 - 11:30 How Much Can Atmospheric Data Tell Us About the North American Land Sink? | 28 |
| <i>Sha Feng (Department of Meteorology and Atmospheric Science, The Pennsylvania State University)</i> | |
| 11:30 - 11:45 Detecting Trends in Fossil Fuel CO ₂ Emissions from Atmospheric Measurements of CO ₂ and ¹⁴ CO ₂ | 29 |
| <i>Sourish Basu (Cooperative Institute for Research in Environmental Sciences (CIRES), University of Colorado)</i> | |
| 11:45 - 13:00 Catered Lunch - Outreach Classroom GB-124 (pre-payment of \$12.00 at registration) | |

NOAA ESRL GLOBAL MONITORING ANNUAL CONFERENCE 2018

David Skaggs Research Center, Room GC-402
325 Broadway, Boulder, Colorado 80305 USA

Wednesday Afternoon, May 23, 2018 Agenda

(Only presenter's name is given; please refer to abstract for complete author listing.)

| | | Page No. |
|----------------------|--|----------|
| Session 7 | <i>Monitoring and Understanding Changes in Surface Radiation, Clouds, and Aerosol Distributions</i> — <i>Chaired by Patrick Sheridan</i> | |
| 13:00 - 13:15 | Use of Radiation and Cloud Observations in Model Diagnosis/Development to Reduce Cloud-Radiation Model Errors from 4-hour to 4-week Forecasts <i>Stan Benjamin (NOAA Earth System Research Laboratory, Global Systems Division (GSD))</i> | 30 |
| 13:15 - 13:30 | Variability of Surface Radiation Observations and HRRR Forecasts at Sites across the Columbia River Basin as Part of the Wind Forecasting Improvement Project (WFIP-2) <i>Kathleen Lantz (Cooperative Institute for Research in Environmental Sciences (CIRES), University of Colorado)</i> | 31 |
| 13:30 - 13:45 | Comparison of Aerosol Optical Properties from <i>In Situ</i> Surface Measurements and Model Simulations <i>Elisabeth Andrews (Cooperative Institute for Research in Environmental Sciences (CIRES), University of Colorado)</i> | 32 |
| 13:45 - 14:00 | Synthesis of Aerosol Physical, Chemical, and Radiative Properties from Various Sources: Consistency and Closure <i>Hagen Telg (Cooperative Institute for Research in Environmental Sciences (CIRES), University of Colorado)</i> | 33 |
| 14:00 - 14:15 | Reducing Uncertainty in Aerosol Direct Radiative Effect Through Synergistic Use of Long-term Satellite and Ground-based Measurements <i>James Patrick Sherman (Appalachian State University, Department of Physics and Astronomy)</i> | 34 |
| 14:15 - 14:30 | Measurements of Aerosol Absorption during Ultra-light Global Circumnavigation, Arctic and Mediterranean Campaigns <i>Grisa Mocnik (Jozef Stefan Institute, Ljubljana, Slovenia)</i> | 35 |
| 14:30 - 15:00 | <i>Afternoon Break</i> | |
| Session 8 | <i>Cross-cutting Topics - Water Vapor, Tropospheric Ozone, and Other Measurements</i> — <i>Chaired by Irina Petropavlovskikh</i> | |
| 15:00 - 15:15 | An Overview of GMD's Water Vapor Research <i>Dale Hurst (Cooperative Institute for Research in Environmental Sciences (CIRES), University of Colorado)</i> | 36 |
| 15:15 - 15:30 | Local Measurements, Global Studies: The Utility of Balloon-borne Frost Point Hygrometer Measurements for Studying Global Stratospheric Water Vapor <i>Sean M. Davis (Cooperative Institute for Research in Environmental Sciences (CIRES), University of Colorado)</i> | 37 |
| 15:30 - 15:45 | Tropospheric Column Ozone Variability from Space: Results from the First Multi-instrument Intercomparison <i>Audrey Gaudel (Cooperative Institute for Research in Environmental Sciences (CIRES), University of Colorado)</i> | 38 |
| 15:45 - 16:00 | Tropospheric Ozone Assessment Report: Tropospheric Ozone Observations – How Well Do We Know Tropospheric Ozone Changes? <i>David W. Tarasick (Environment and Climate Change Canada, Toronto, Canada)</i> | 39 |
| 16:00 - 16:15 | An Overview of the Fires, Asian, and Stratospheric Transport-Las Vegas Ozone Study (FAST-LVOS) <i>Andrew O. Langford (NOAA Earth System Research Laboratory, Chemical Sciences Division (CSD))</i> | 40 |
| 16:15 - 16:30 | Preliminary Results from GMD's Halocarbons and other Trace Gases Measurements on ATom <i>James W. Elkins (NOAA Earth System Research Laboratory, Global Monitoring Division (GMD))</i> | 41 |
| 16:30 - 16:45 | Ambient Air Measurements of Formaldehyde by Near-infrared Cavity Ring-down Spectroscopy <i>David Kim-Hak (Picarro Inc.)</i> | 42 |
| 16:45 | <i>Closing Remarks - Dr. James Butler, Director (NOAA/ESRL Global Monitoring Division)</i> | |

Response of North American Terrestrial CO₂ Fluxes to Climate Variability

L. Hu^{1,2}, A.E. Andrews², K. Thoning², C. Sweeney², J.B. Miller², E.J. Dlugokencky², P.P. Tans², A. Michalak³, M. Mountain⁴, T. Nehrkorn⁴, S.A. Montzka², D. Worthy⁵, K. McKain^{1,2}, S.E. Michel⁶, B.H. Vaughn⁶, J. White⁶, M. Fischer⁷, S. Biraud⁷, S. Basu^{1,2} and I.R. van der Velde^{1,2}

¹Cooperative Institute for Research in Environmental Sciences (CIRES), University of Colorado, Boulder, CO 80309; 303-497-5238, E-mail: lei.hu@noaa.gov

²NOAA Earth System Research Laboratory, Global Monitoring Division (GMD), Boulder, CO 80305

³Carnegie Institution for Science, Department of Global Ecology, Stanford, CA 94305

⁴Atmospheric and Environmental Research (AER), Inc., Lexington, MA 02421

⁵Environment and Climate Change Canada, Toronto, Ontario, Canada

⁶Institute of Arctic and Alpine Research (INSTAAR), University of Colorado, Boulder, CO 80309

⁷Lawrence Berkeley National Laboratory (LBNL), Berkeley, CA 94720

North America is an important source and terrestrial sink for atmospheric carbon dioxide (CO₂). However, uncertainties on North American terrestrial CO₂ fluxes are large, including their magnitude, distribution, inter-annual variability, and trend. Given such large uncertainties, it has been extremely difficult to identify a coherent relationship between climate drivers and North American terrestrial CO₂ fluxes. Here, we analyzed atmospheric CO₂ and delta carbon-13 dioxide ($\delta^{13}\text{CO}_2$) data obtained from North America under the ESRL/GMD Greenhouse Gas Reference Network for the last two decades. Derived atmospheric CO₂ and $\delta^{13}\text{CO}_2$ anomalies indicate consistent responses of North American terrestrial CO₂ fluxes to large climate phenomena, such as El Niño and Southern Oscillation (ENSO) and the Arctic Oscillation (Figure 1). Such persistent responses, as we find, are primarily driven by the modulation of hydrological and temperature conditions associated with these large global climate phenomena. Inverse analyses of the same suite of atmospheric CO₂ observations over the last decade allowed us to further quantify the North American CO₂ flux anomalies corresponding to ENSO and the Arctic Oscillation. The derived annual anomalies of North American terrestrial CO₂ fluxes are substantial compared to the variability of anthropogenic greenhouse gas emissions over North America.

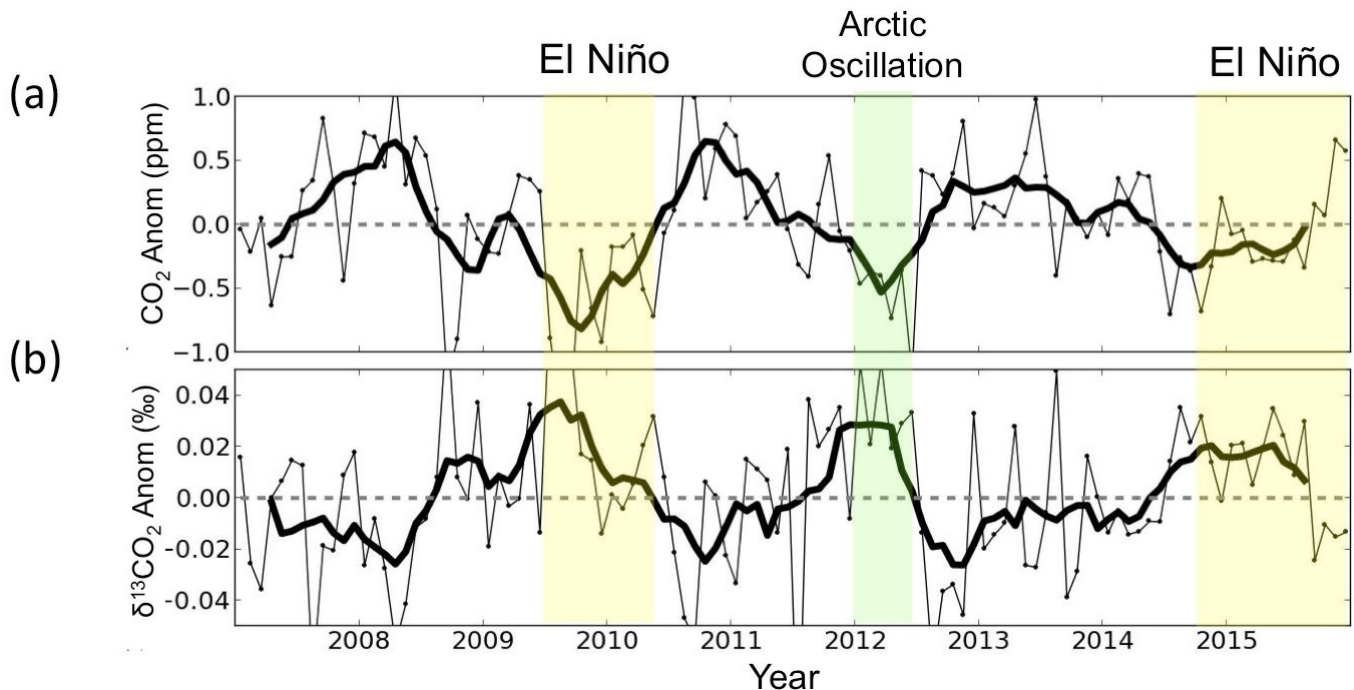


Figure 1. Monthly anomalies (thin lines) of atmospheric CO₂ and $\delta^{13}\text{CO}_2$ averaged across North American sampling sites under the ESRL/GMD Greenhouse Gas Reference Network. Thick lines indicate 6-month running averages on monthly anomalies. Yellow shading indicates El Niño periods whereas green shading indicates the period influenced by the Arctic Oscillation over the last decade.

ICOS Research Infrastructure, Progress in the European Carbon Cycle and Greenhouse Gas Observing Network

A. Vermeulen^{1,2}, M. Hellström², O. Mirzov², L. Rivier^{3,4} and W. Kutsch⁵

¹Integrated Carbon Observation System (ICOS) European Research Infrastructure Consortium (ERIC), Carbon Portal, Lund, Sweden; +46-722-494-214, E-mail: alex.vermeulen@icos-ri.eu

²Lund University, Lund, Sweden

³Integrated Carbon Observation System (ICOS) Atmosphere Thematic Centre (ATC), Gif-sur-Yvette, France

⁴Université de Versailles Saint-Quentin en Yvelines (UVSQ), Centre National de la Recherche Scientifique (CNRS), Guyancourt, France

⁵Integrated Carbon Observation System (ICOS) European Research Infrastructure Consortium (ERIC), Helsinki, Finland

Since the Integrated Carbon Observation System (ICOS) European Research Infrastructure Consortium (ERIC) was established in November 2015 as the legal framework for the European Integrated Carbon Observing Network, large progress has been made in making the *in situ* network operational. The main objective of ICOS is to provide long-term high quality multi-domain (atmosphere, ecosystem, and ocean) observations using highly-standardized operations using community-developed protocols. Currently ICOS has 12 member states that provide national networks with in total 126 stations. All stations, new and already established, currently go through the labeling process, to be certified as an ICOS station that complies with the ICOS standards for measurement and data quality. The first few stations have been certified at the end of 2017 and many more will follow in 2018. All ICOS data will be licensed using CC4BY through the ICOS data portal, called the Carbon Portal. In this talk we will concentrate on the setup and progress in the atmospheric network and the data portal. The Carbon Portal has been designed from the ground off as open source, open-linked data system, that allows for full transparency and reproducibility of the data, long-term persistent storage of all data levels, full and open discovery and access, while at the same time providing the checking of the data licence, usage tracking, and dynamic data citation for proper attribution to the data provider. The basis functionality for this portal is now operational and is serving a fast-growing amount of data objects (>10,000), including the first higher level datasets from the certified atmospheric network stations and higher levels elaborated products, and services, like atmospheric footprint calculations in the cloud, that build upon the data and metadata services.



Figure 1. Overview of the ICOS station network for all three domains. Overseas stations are not all shown here.

Single-blind Testing of a Regional, Continuous Monitoring System for Finding Methane Leaks from Oil and Gas Operations

C. Alden^{1,2}, S. Coburn³, R. Wright³, E. Baumann⁴, K. Cossel⁵, C. Sweeney², A. Karion⁴, K. Prasad⁴, I. Coddington⁵ and G.B. Rieker³

¹Cooperative Institute for Research in Environmental Sciences (CIRES), University of Colorado, Boulder, CO 80309; 719-930-5281, E-mail: caroline.alden@noaa.gov

²NOAA Earth System Research Laboratory, Global Monitoring Division (GMD), Boulder, CO 80305

³University of Colorado, Department of Mechanical Engineering, Boulder, CO 80309

⁴National Institute of Standards and Technology (NIST), Gaithersburg, MD 20880

⁵National Institute of Standards and Technology (NIST), Boulder, CO 80305

Advances in natural gas extraction technology have led to increased U.S. production and transport activity, and, as a consequence, an increased need for monitoring of methane leaks. Known intermittency in fugitive methane emissions means that continuous monitoring is critical for emissions quantification and mitigation. Here, we present the results of single-blind testing of a new leak detection method that employs dual frequency comb spectrometry coupled with atmospheric inversions to offer continuous, autonomous, leak detection and quantification over large (square-km) regions. In the tests described here, the dual frequency comb spectrometer is situated > 1 km away from a field of “Hollywood” natural gas pads (sets of decommissioned oil and gas facilities plumbed with known, controlled leaks) at the METEC test site in Fort Collins, CO. A series of retroreflectors around the field direct light back to a detector. The laser light spans 1620-1680 nm with 0.002 nm resolution, simultaneously measuring hundreds of individual absorption features from multiple species, and resulting in high-stability trace gas (here methane, carbon dioxide, and water vapor) measurements over long (1 km+) open paths through the atmosphere. Measurements are used in an atmospheric inversion to estimate the locations (at well pad, sub-pad, and component-level scales) and rates of emissions in 18 single-blind tests. The measurement framework and inversion solve explicitly for background concentrations, which vary through time due to changes in upwind sources. The frequency comb-inversion system successfully detects 18 of 18 leaks. The system also successfully quantifies most leaks, which range in size from < 1 g min⁻¹ to 11 g min⁻¹ (average reported emissions from pneumatic controllers found on well pads fall within this range), to within 20% of the actual rate. All leak locations are attributed to the correct well pad or sub-pad, and in many cases the system also correctly identifies which component (that is, wellhead, separator, or tank) is leaking. We present the methods and results of the METEC test site experiments, as well as results of experiments examining the effects of the choice of transport model on leak detection and quantification.

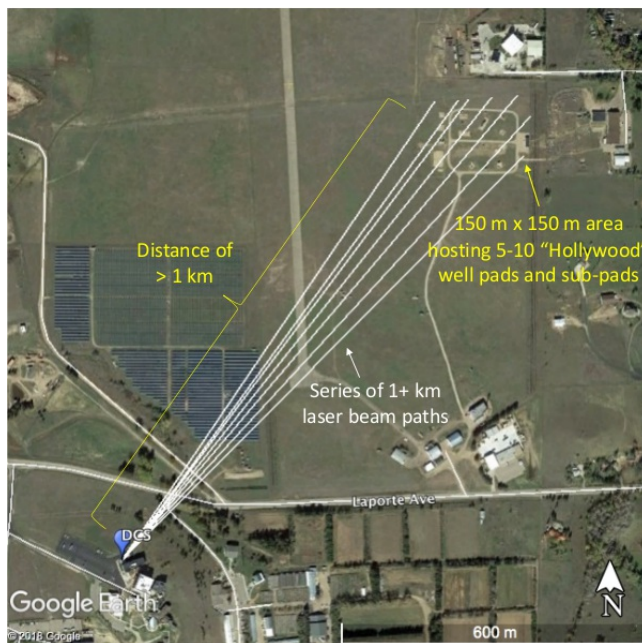


Figure 1. Map showing dual frequency comb spectrometer (labeled “DCS”) location and the location of the METEC test site. White lines show the paths of laser light beams measuring integrated open-atmosphere concentrations of methane gas.

Unexpected and Significant Biospheric CO₂ Fluxes in the Los Angeles Basin Indicated by Atmospheric Radiocarbon

J.B. Miller¹, S. Lehman², K.R. Verhulst³, V. Yadav³, C. Miller³, R. Duren³, S. Newman⁴ and C. Sloop⁵

¹NOAA Earth System Research Laboratory, Global Monitoring Division (GMD), Boulder, CO 80305; 303-497-7739, E-mail: john.b.miller@noaa.gov

²Institute of Arctic and Alpine Research (INSTAAR), University of Colorado, Boulder, CO 80309

³NASA Jet Propulsion Laboratory, California Institute of Technology, Pasadena, CA 91109

⁴California Institute of Technology, Pasadena, CA 91125

⁵Earth Networks, Inc., Germantown, MD 20876

It is normally assumed that emissions and concentrations of carbon dioxide (CO₂) in and around cities are dominated by fossil fuel-combustion. This is surprisingly not the case for Los Angeles, despite its naturally dry climate. Measurements of atmospheric carbon-14 dioxide (¹⁴CO₂), the gold standard for identifying fossil fuel emissions in the atmosphere, quantify not only the influence of fossil fuel combustion but, by residual, the biospheric contribution as well. Here we report results from an air sampling network for CO₂ and radiocarbon (¹⁴C) measurements within the Los Angeles monitoring network. Unexpectedly, mid-day CO₂ enhancements above background at our three sites in Los Angeles are very high, averaging 16 ppm. However, our analysis using radiocarbon reveals that only ~75% of the enhancement resulted from fossil fuel combustion. The remaining 25% comes from biospheric sources. We will quantify the contributions of possible sources to this unexpectedly large biospheric contribution. Moreover, the biospheric component of the Los Angeles CO₂ signal exhibits seasonal behavior with net uptake of carbon in mid-summer, suggesting a substantial role for managed urban ecosystems. Finally, we will discuss the implications of these results for urban fossil fuel emissions monitoring using surface and space-based approaches.

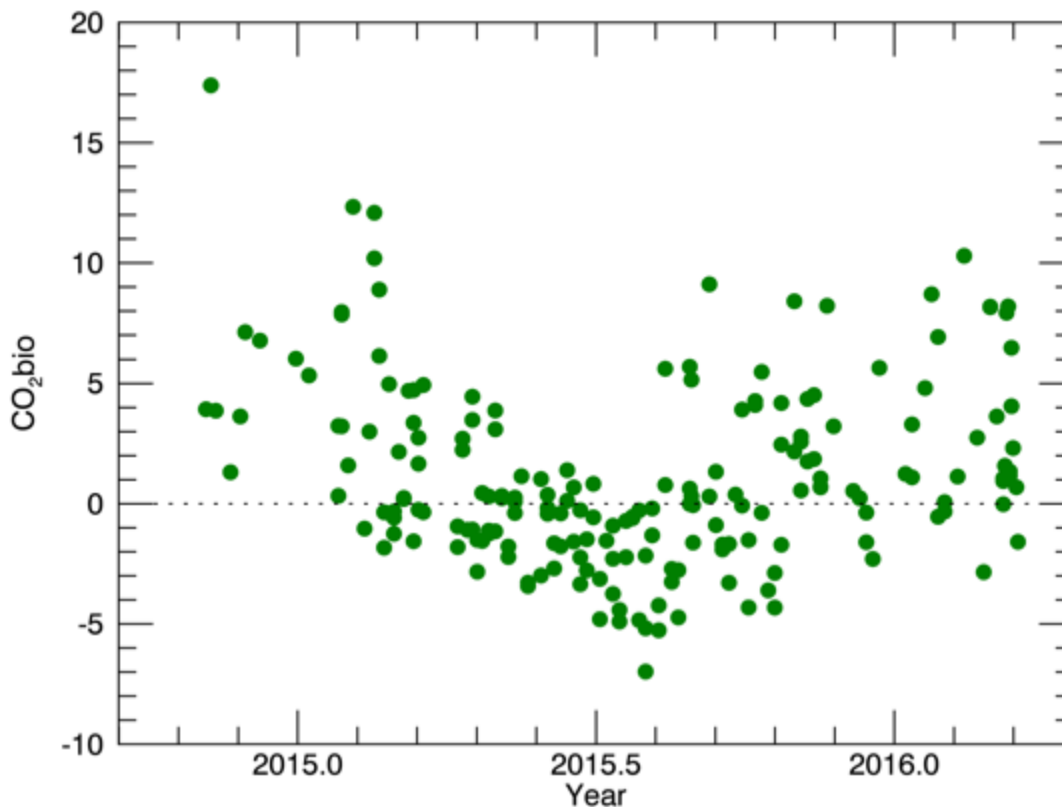


Figure 1. Time series of biospheric enhancements (or drawdown, negative) relative to background concentrations for three sites in the Los Angeles Basin: U. of Southern California, Granada Hills, and Cal. State Fullerton. Summertime CO₂ uptake and wintertime release are evident.

Development of an Open-path, Laser Dispersion Spectroscopy (LDS) Analyzer for Methane Emissions Mapping and Quantification

G. Leggett¹, D. Weidmann¹, J. Chu¹, A. Kannath¹ and B. Hirst²

¹MIRICO Ltd., Chilton, United Kingdom; +44-771-567-6751, E-mail: graham@mirico.co.uk

²Shell Global Solutions International BV, The Hague, The Netherlands

Laser Dispersion Spectroscopy (LDS) is a new gas sensing technique that applies a novel approach to tuneable diode laser spectroscopy. Established laser absorption techniques depend on measuring detected intensity to derive concentration. This significantly impacts measurements in “dirty” environments where detected intensity of the transmitted light is bound to fluctuate. MIRICO’s LDS-based instrument derives concentration using the phase of light. This makes it highly immune to intensity fluctuations received at the photodetector. The instrument enables precise, real-time measurements of trace gas molecules in demanding environments. Furthermore, compared to absorption techniques, the analyser can measure gas concentrations within a very wide dynamic range (typically about five to six orders of magnitude), meaning, for example, from parts per billion all the way to sub-percent concentrations without the requirement for dilution.

In a long open-path, multi-direction configuration, coupled with a retroreflector array, and anemometer, the LDS analyser is capable of measuring methane concentrations associated with large area sources, and locating and quantifying point source emissions within said area. Here we describe the principle of LDS, and the development of a field-deployable instrument. In addition, we introduce the basic configuration required for mapping applications.

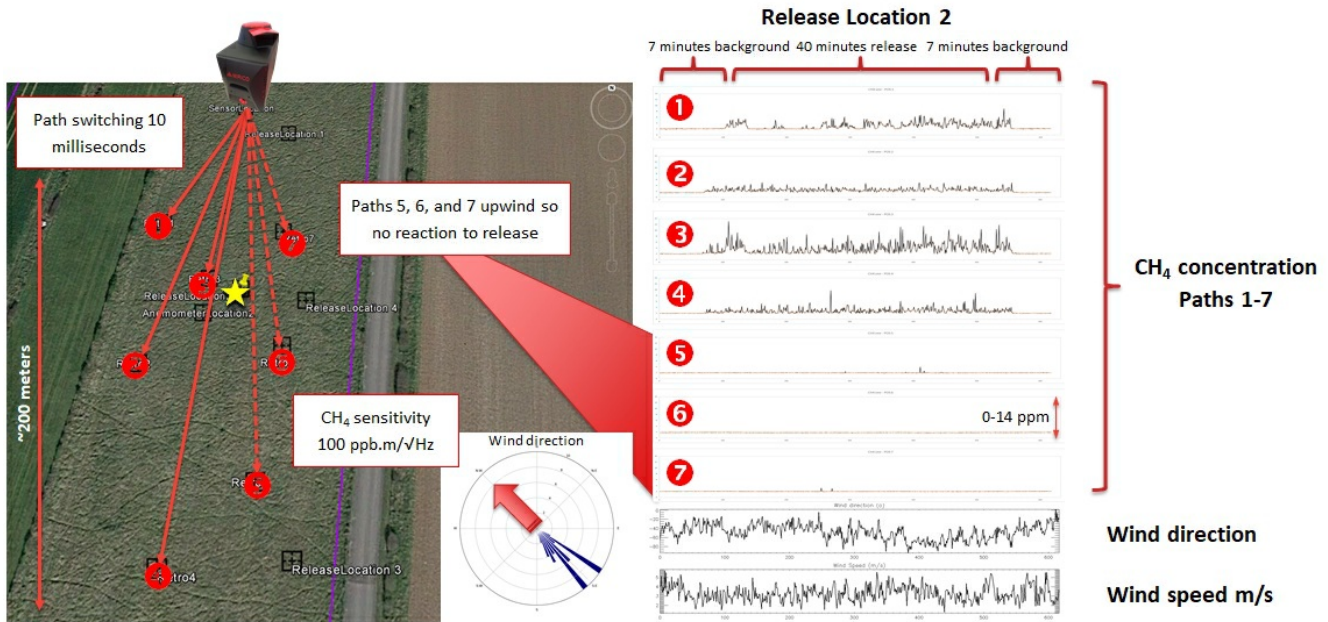


Figure 1. Mapping controlled methane release using MIRICO LDS spectrometer.

Little Evidence for Significant Increases in Total U.S. CH₄ Emissions over the Past Decade

X. Lan^{1,2}, P.P. Tans², C. Sweeney², A.E. Andrews², E.J. Dlugokencky², S. Schwietzke^{1,2}, P. Lang², K. Thoning², M.J. Crotwell^{1,2}, B.R. Miller^{1,2}, S. Montzka², D. Helmig³, S. Biraud⁴, J. Kofler^{1,2} and K. McKain^{1,2}

¹Cooperative Institute for Research in Environmental Sciences (CIRES), University of Colorado, Boulder, CO 80309; 303-497-3615, E-mail: xin.lan@noaa.gov

²NOAA Earth System Research Laboratory, Global Monitoring Division (GMD), Boulder, CO 80305

³Institute of Arctic and Alpine Research (INSTAAR), University of Colorado, Boulder, CO 80309

⁴Lawrence Berkeley National Laboratory (LBNL), Berkeley, CA 94720

Recent studies show conflicting estimates of trends in methane (CH₄) emissions from oil and natural gas (ONG) operations in the U.S. We analyze atmospheric CH₄ measurements from 20 North American air sampling sites in the ESRL/GMD Global Greenhouse Gas Reference Network (GGGRN) and determined trends for 2006-2015. Using CH₄ vertical gradients as an indicator of regional surface emissions, we find no significant trends at most GGGRN sites, but modest trends at three sites heavily influenced by oil and natural gas (ONG) activities. The suggested increases in ONG CH₄ emissions (on average $\sim 2.91 \pm 0.69 \text{ \% yr}^{-1}$) are much smaller than several studies, and below detection threshold for the east coast sites that capture the outflows of the U.S. We also find that when enhancements of ethane (C₂H₆) and propane (C₃H₈) are used to estimate trends in ONG CH₄ emissions, they significantly overestimate CH₄ trends.

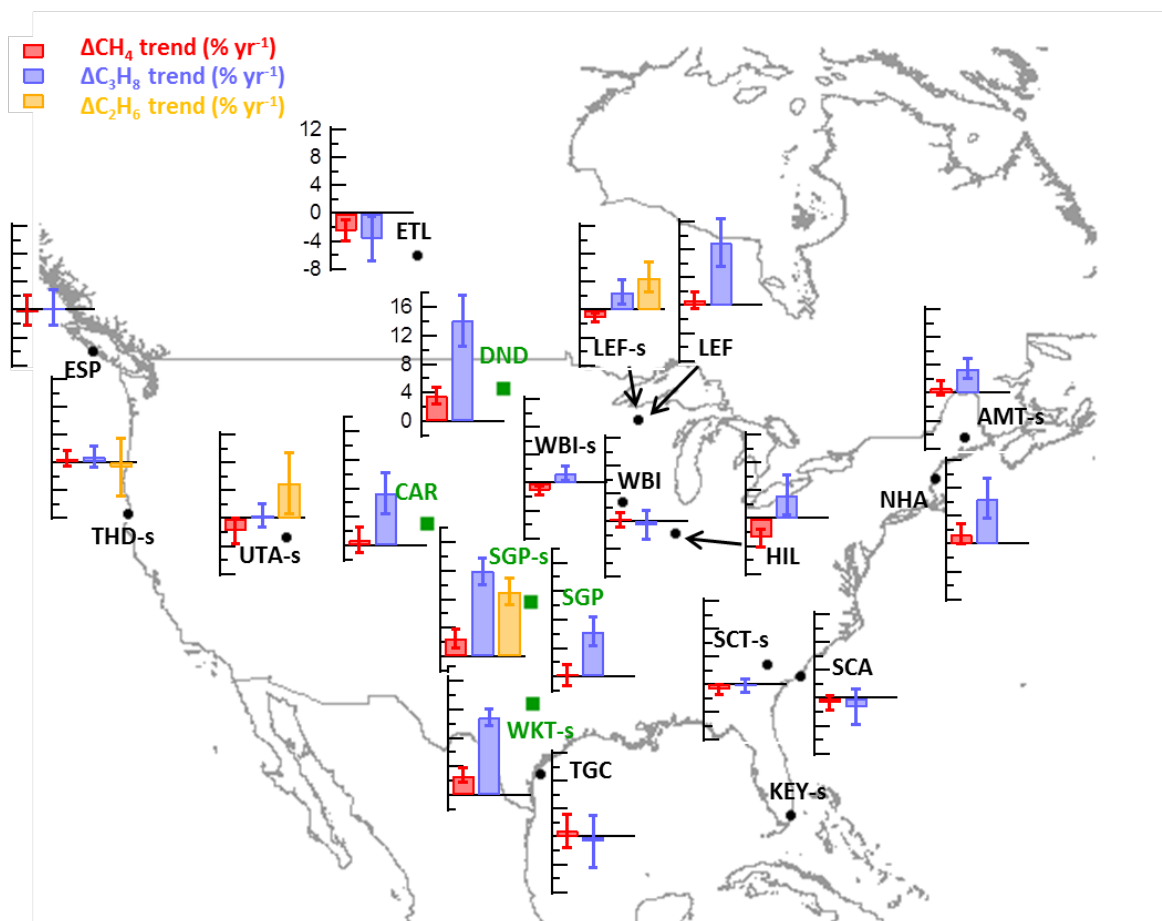


Figure 1. Trends in CH₄, C₃H₈ and C₂H₆ enhancements (Δ) over the North America in recent years (2006-2015 for CH₄, and 2008-2015 for C₂H₆ and C₃H₈ for most sites). Green squares and black dots show the geographic locations of ONG sites and non-ONG sites, respectively. Bar figures show trends in \% yr^{-1} increase of mole fraction relative to previous year. The left axes in the bar figures for ONG sites are the same as for DND (Site codes on map are defined in Table S1). For non-ONG sites, left axes are the same as for ETL, and the axis ranges are the same as those for ONG sites so that the size of the bars from all sites are comparable. Error bars show 1σ uncertainty.

A Multi-species Analysis of Carbon Enhancements during the ACT-America Campaign

B. Baier^{1,2}, C. Sweeney², A.E. Andrews², Y. Choi³, M.J. Crotwell^{1,2}, K.J. Davis^{4,5}, J. DiGangi³, S. Feng⁴, A. Fried⁶, J. Higgs², P. Lang², T. Lauvaux⁴, B.R. Miller^{1,2}, J.B. Miller², E. Moglia^{1,2}, T. Newberger^{1,2}, J. Nowak³, S. Lehman⁶ and S. Pal⁴

¹Cooperative Institute for Research in Environmental Sciences (CIRES), University of Colorado, Boulder, CO 80309; 303-497-5769, E-mail: bianca.baier@noaa.gov

²NOAA Earth System Research Laboratory, Global Monitoring Division (GMD), Boulder, CO 80305

³NASA Langley Research Center, Hampton, VA 23681

⁴Department of Meteorology and Atmospheric Science, The Pennsylvania State University, University Park, PA 16802

⁵Earth and Environmental Systems Institute, The Pennsylvania State University, University Park, PA 16802

⁶Institute of Arctic and Alpine Research (INSTAAR), University of Colorado, Boulder, CO 80309

While the global carbon cycle is relatively well-constrained, diagnosing carbon sources and sinks on regional scales is complicated by sparse atmospheric observations, uncertainties in regional transport, and uncertainties in upwind boundary conditions. The Atmospheric Carbon and Transport - America (ACT-America) campaign is focused on reducing these uncertainties in regional inversions through broadly surveying the emissions and transport of carbon dioxide (CO_2) and methane (CH_4) in three eastern U.S. regions. As part of ACT-America, ESRL/GMD flask samples are analyzed for greenhouse and trace gases, including isotopic ratios of CO_2 and CH_4 . These discrete flask measurements can approximate background greenhouse gas abundances and help to characterize sources of regional carbon enhancements above background levels when combined with back trajectory and footprint analyses. We present an overview on the use of flask sample species, including non-methane hydrocarbons, methyl halides, and delta carbon-14 dioxide ($\Delta^{14}\text{CO}_2$), for source characterization and background level determination during ACT-America, and comparisons to the ESRL/GMD Carbon Cycle and Greenhouse Gas aircraft network.

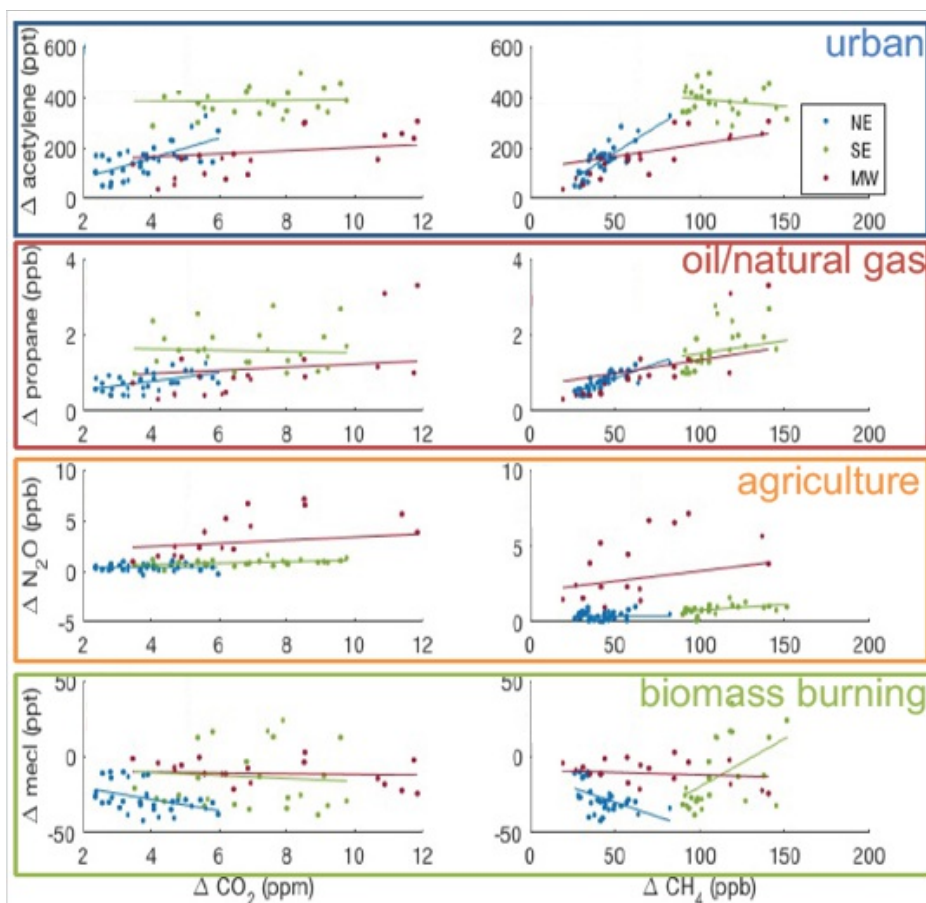


Figure 1. Multi-species correlations between flask tracer species and carbon enhancements in each of the three ACT-America regions, demonstrating the use of additional tracers for emissions characterization.

How Much Can Atmospheric Data Tell Us About the North American Land Sink?

S. Feng¹, T. Lauvaux¹, K. Keller^{2,3}, M. Butler¹, K.J. Davis^{1,3}, A.E. Schuh⁴, S. Basu^{5,6}, D.F. Baker⁴, J. Liu⁷, C. Williams⁸, Y. Zhou⁸, T. Oda⁹, K. Gurney¹⁰ and A.E. Andrews⁶

¹Department of Meteorology and Atmospheric Science, The Pennsylvania State University, University Park, PA 16802; 813-658-8196, E-mail: sfeng@psu.edu

²Department of Geosciences, The Pennsylvania State University, University Park, PA 16802

³Earth and Environmental Systems Institute, The Pennsylvania State University, University Park, PA 16802

⁴Cooperative Institute for Research in the Atmosphere (CIARA), Colorado State University, Fort Collins, CO 80521

⁵Cooperative Institute for Research in Environmental Sciences (CIRES), University of Colorado, Boulder, CO 80309

⁶NOAA Earth System Research Laboratory, Global Monitoring Division (GMD), Boulder, CO 80305

⁷NASA Jet Propulsion Laboratory, California Institute of Technology, Pasadena, CA 91109

⁸Clark University, Worcester, MA 01610

⁹NASA Goddard Space Flight Center (GSFC), Earth Science Technology and Research, Greenbelt, MD 20771

¹⁰Arizona State University, Tempe, AZ 85287

We use a newly-developed ensemble-based mesoscale modeling system to analyze the cause of the large uncertainties in atmospheric estimates of the terrestrial biospheric fluxes over North America. We first quantify the uncertainty from biospheric fluxes, transport, boundary conditions, and fossil fuel emissions on the simulated atmospheric carbon dioxide (CO₂) concentrations, based on the ESRL/GMD tall tower measurements of CO₂ concentration. We determine the optimal time scale for atmospheric inversions to inform terrestrial biospheric flux estimates. The monthly-to-seasonal scale maximizes the potential to detect and potentially improve flux estimates for the terrestrial biosphere contribution. We demonstrate the importance of fossil fuel emissions uncertainties. The fossil fuel emissions uncertainty may have been underestimated in past inversions, limiting the ability to isolate the biospheric contribution from total atmospheric CO₂. Our results demonstrate the potential of regional atmospheric modeling systems to improve the phenology and climate response of the terrestrial biosphere to climate anomalies and, in turn, provide more accurate estimates of carbon sinks at national to continental scales. Our finding can inform the design of sampling strategies for atmospheric CO₂ mixing ratios, specifically where and when to observe in order to optimally constrain the different contributors of the overall observation uncertainty.

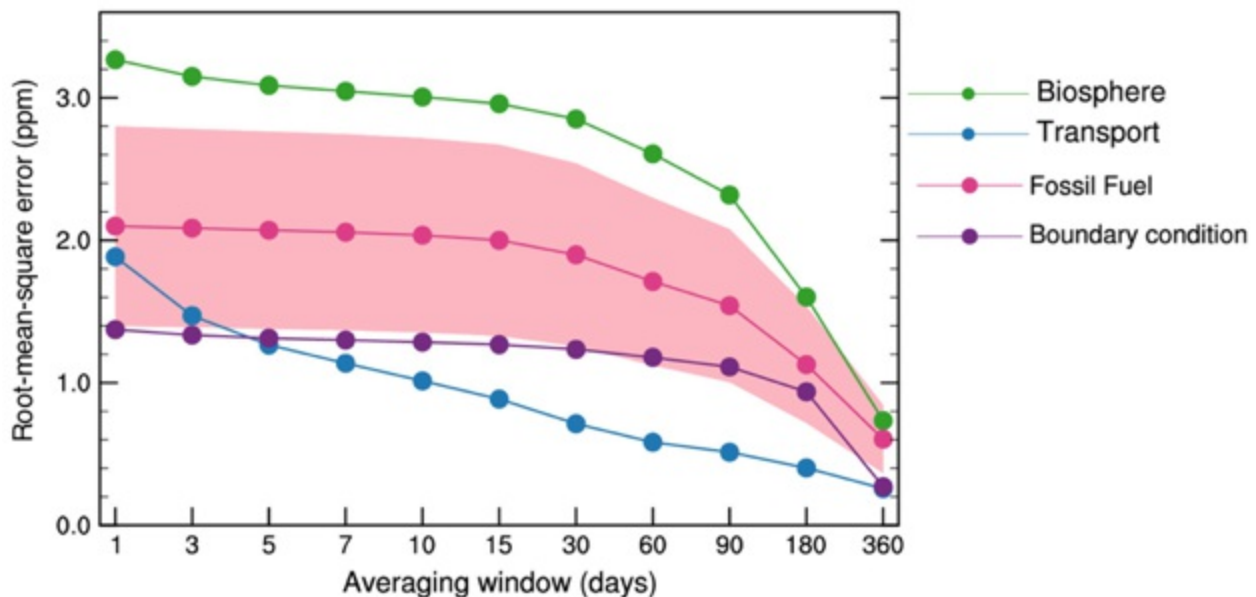


Figure 1. Root-mean-square errors of modeled atmospheric CO₂ mixing ratios varying with time scales against the ESRL/GMD tall tower CO₂ mixing ratio measurements, presented for four modeling components of the domain-limited simulations, i.e. uncertainties from transport model, biogenic fluxes, fossil fuel emissions, and the boundary conditions.

Detecting Trends in Fossil Fuel CO₂ Emissions from Atmospheric Measurements of CO₂ and ¹⁴CO₂

S. Basu^{1,2}, J.B. Miller² and S. Lehman³

¹Cooperative Institute for Research in Environmental Sciences (CIRES), University of Colorado, Boulder, CO 80309; 303-497-6650, E-mail: sourish.basu@noaa.gov

²NOAA Earth System Research Laboratory, Global Monitoring Division (GMD), Boulder, CO 80305

³Institute of Arctic and Alpine Research (INSTAAR), University of Colorado, Boulder, CO 80309

Carbon in fossil fuels is devoid of carbon-14 (¹⁴C), so burning them injects ¹⁴C-devoid carbon dioxide (CO₂) into the atmosphere, in contrast to the other surface fluxes of CO₂ such as wildfires and ecosystem exchange. Therefore, the depletion in atmospheric carbon-14 dioxide (¹⁴CO₂) relative to total CO₂ can serve as a proxy for recently emitted fossil fuel CO₂. Over the past several years, we have developed the capability to estimate fossil fuel emissions by assimilating atmospheric measurements of CO₂ and ¹⁴CO₂ simultaneously in a source-sink inversion. We have presented this capability previously, using Observing System Simulation Experiments (OSSEs) to demonstrate our ability to estimate monthly and annual fluxes from the continental U.S. (ConUS) as well as smaller regions therein. We have shown that with the current network of ¹⁴CO₂ measurements, we can estimate the U.S. national total emission to within a few percent, while with a proposed enhanced network of 5,000 observations per year we can estimate monthly totals from highly emissive regions to within 5% for most months. In this work, we present our ability to estimate decadal trends in emissions from those geographical areas, with quantified uncertainties, in the presence of realistic errors in the atmospheric transport model. We evaluate our trend detection capability with the existing observation network as well as the enhanced network of 5,000 observations per year. We show that with the enhanced network, we can robustly detect a national trend consistent with Nationally Determined Contributions (NDCs) of the COP21 Paris agreement, even when our system starts from prior emissions with zero trend. This ability to estimate and verify trends using independent data will become important in the future as more and more regions implement policies to reduce their own fossil fuel emissions. Finally, we will present some preliminary fossil fuel flux estimates over ConUS using real ¹⁴CO₂ data from our existing observation network.

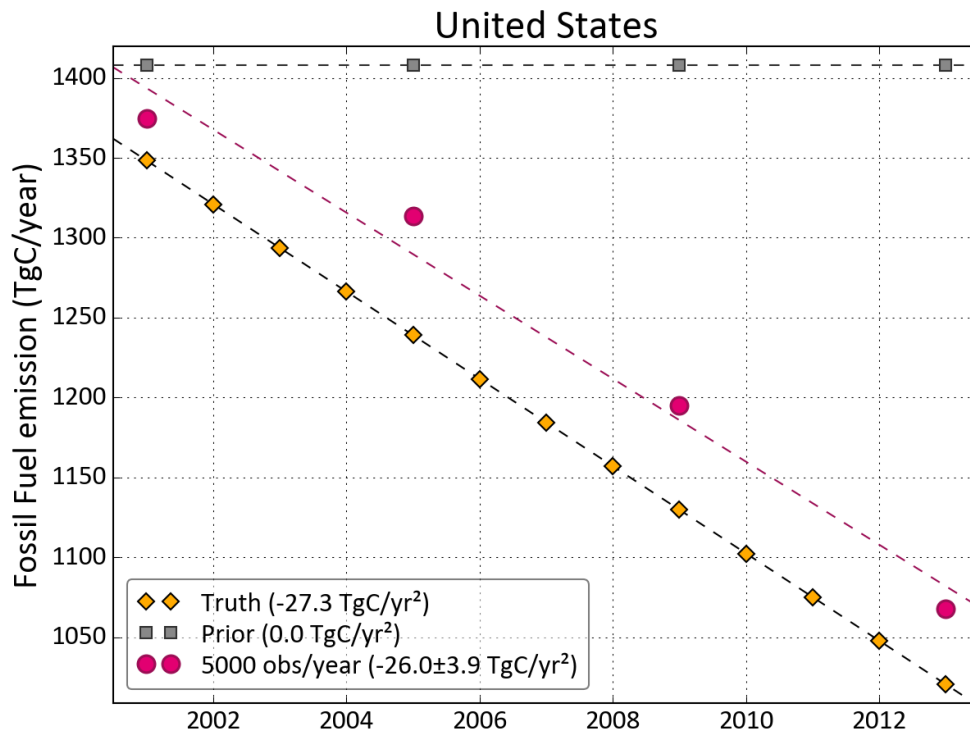


Figure 1. The performance of our inversion system in estimating fossil fuel trends over the U.S. yellow diamonds represent the “true” trend used to produce pseudo-observations, while gray squares represent the prior assumed in our inversions. Finally, pink circles are estimates from our inversion. The trend estimated by the circles is within 1 sigma of the true trend and statistically distinct from the prior trend. This performance is despite the prior being 40% off from the truth towards the end of the time period. In reality, we expect our system to perform even better, since fossil fuel inventories are typically within 10% of the true emissions for developed countries such as the U.S.

Use of Radiation and Cloud Observations in Model Diagnosis/Development to Reduce Cloud-Radiation Model Errors from 4-hour to 4-week Forecasts

S. Benjamin¹, J. Olson¹, T. Smirnova¹, S. Sun¹, A. McComiskey², K.O. Lantz^{3,2}, C. Long^{3,2}, C. Alexander¹ and G. Grell¹

¹NOAA Earth System Research Laboratory, Global Systems Division (GSD), Boulder, CO 80305; 303-497-6387, E-mail: stan.benjamin@noaa.gov

²NOAA Earth System Research Laboratory, Global Monitoring Division (GMD), Boulder, CO 80305

³Cooperative Institute for Research in Environmental Sciences (CIRES), University of Colorado, Boulder, CO 80309

ESRL/GSD develops advanced models and data assimilation, including the 3-km High-Resolution Rapid Refresh (HRRR) model and the 13km Rapid Refresh (RAP) model. It also develops advanced global models including coupled models to improve Week 3-4 subseasonal prediction for NOAA.

ESRL/GSD has developed a parameterization suite (turbulent mixing, deep/shallow convection, 9-layer land/snow/vegetation model) to improve planetary boundary layer biases (temperature and moisture) including better representation of clouds and precipitation. This parameterization suite development has been accompanied by an effort for improved data assimilation of clouds, near-surface observations, and radar for the atmosphere-land system. ESRL/GMD has worked with ESRL/GSD in evaluation of the HRRR and RAP models using SURFRAD and other radiation/flux measurements.

Cloud-radiation representation in models for subgrid-scale clouds is a known gap from subseasonal-to-seasonal models down to storm-scale models applied for forecast duration of only a few hours. NOAA/ESRL has been applying these common physical parameterizations for scale-aware deep/shallow convection and boundary-layer mixing over this wide range of time and spatial scales with some progress to be reported in this presentation. SURFRAD/SOLRAD observational data has been critical in evaluation of these models, along with other data from CERES, METAR ceilometer, aircraft, and rawinsondes.

The Grell-Freitas scheme (2014), MYNN boundary-layer Eddy-Diffusivity/ Mass-Flux (EDMF) scheme (Olson / Benjamin et al. 2016), and Rapid Update Cycle (RUC) land-surface model (Smirnova et al. 2016) have been applied and tested extensively for the NOAA hourly updated 3-km HRRR and 13-km RAP model/assimilation systems over the United States and North America, with targeting toward improvement to boundary-layer evolution and cloud-radiation representation in all seasons. This representation is critical for both warm-season severe convective storm forecasting and for winter-storm prediction of snow and mixed precipitation for aviation, severe-storm, hydrology, and energy applications. Improvement of cloud/radiation model representation has been achieved from this ongoing GSD-GMD collaboration.

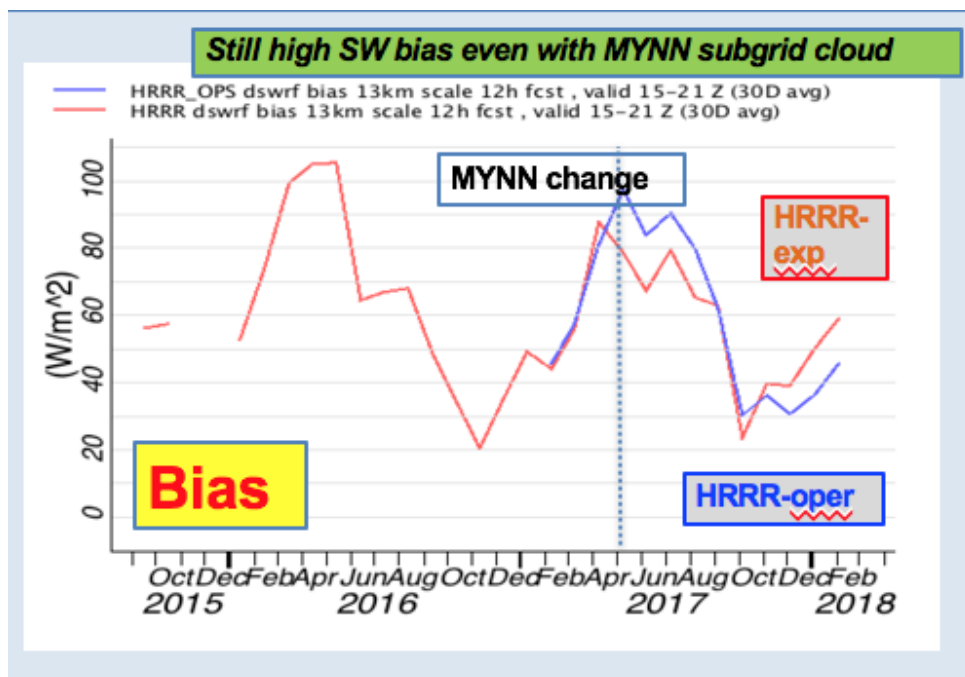


Figure 1. Downward short wave (SW) bias errors from HRRR model vs. SURFRAD observations.

Variability of Surface Radiation Observations and HRRR Forecasts at Sites across the Columbia River Basin as Part of the Wind Forecasting Improvement Project (WFIP-2)

K. Lantz¹, C.N. Long^{1,2}, A. McComiskey², M. Marquis³, J.B. Olson^{1,3}, J. Kenyon^{1,3}, E. Hall^{1,2}, G. Hodges^{1,2} and J. Wendell²

¹Cooperative Institute for Research in Environmental Sciences (CIRES), University of Colorado, Boulder, CO 80309; 303-497-7280, E-mail: kathy.o.lantz@noaa.gov

²NOAA Earth System Research Laboratory, Global Monitoring Division (GMD), Boulder, CO 80305

³NOAA Earth System Research Laboratory, Global Systems Division (GSD), Boulder, CO 80305

The second Wind Forecast Improvement Project's (WFIP-2) major goal is to improve atmospheric processes in numerical weather prediction models for more accurate wind forecasts in complex terrain. This effort involves multiple U.S. agencies, industry, and universities with a large suite of instrumentation including vertical profiling wind radars, sodars, lidars, shortwave and longwave radiation, sensible and latent heat for understanding the development of low-level winds. This suite of instrumentation was deployed across the Columbia River Basin from approximately October 2016 – March 2017 to capture meteorological regimes throughout the year, e.g. mountain gap events, cold pools. The sum of the incoming and outgoing radiative components at the surface is the bulk of the energy available for atmospheric dynamic processes that influence boundary layer height and low-level winds. In this presentation, surface radiation observations will be used to determine uncertainties (biases, root-mean-square error, mean absolute error) in the forecast of these variables from the NOAA 13-km Rapid Refresh (RAP), 3-km High Resolution Rapid Refresh (HRRR), as well as a high resolution (750-m) nest across four sites. This study will investigate whether the HRRR and RAP models capture the diurnal and seasonal variability in radiation quantities across the sites and within identified meteorological regimes. The HRRR has been targeted for specific improvements in model physics such as scale-aware aspects of turbulence parameterizations (planetary boundary layer + shallow cumulus scheme) and land-surface physics. This analysis will explore the improvements in the model physics on forecasts of surface longwave and shortwave radiation, and shortwave surface albedo.



Figure 1. Mobile SURFRAD deployment at Wasco, OR for WFIP-2 Field Study.

Comparison of Aerosol Optical Properties from *In Situ* Surface Measurements and Model Simulations

E. Andrews^{1,2}, M. Schulz³, M. Fiebig⁴, the AeroCom Modelling Community and the ACTRIS and NOAA Aerosol Monitoring Communities

¹Cooperative Institute for Research in Environmental Sciences (CIRES), University of Colorado, Boulder, CO 80309; 303-442-5142, E-mail: betsy.andrews@noaa.gov

²NOAA Earth System Research Laboratory, Global Monitoring Division (GMD), Boulder, CO 80305

³Norwegian Meteorological Institute, Oslo, Norway

⁴Norwegian Institute for Air Research (NILU), Oslo, Norway

AeroCom, an open international collaboration of scientists seeking to improve global aerosol models, recently initiated a project comparing model output to *in situ*, surface-based measurements of aerosol optical properties. The model/measurement comparison project, called INSITU, aims to evaluate the performance of a suite of AeroCom aerosol models with site-specific observational data in order to inform iterative improvements to model aerosol modules. Surface *in situ* data are directly traceable to physical standards, which is an asset in accomplishing the overall goal of bettering the overall accuracy of aerosols processes and predicative capability of global climate models. The INSITU project looks at how well models reproduce aerosol optical property climatologies on a variety of time scales, aerosol persistence, and the systematic relationships between aerosol optical properties, and aerosol trends.

Here we present comparisons from ~60 surface sites with model output from 12 global climate models. Our analysis shows substantial model biases in absorption and scattering coefficients compared to surface measurements, though the sign and magnitude of the bias varies with location. Our results also indicate that model-simulated values for single scattering albedo (SSA) and scattering Angstrom exponent tend to be lower (i.e., aerosol is darker and larger) than the *in situ* measurements. Spatial patterns in the biases highlight model weaknesses, e.g., the inability of models to properly simulate aerosol characteristics at sites with complex topography as well as predicting more absorbing aerosol over Asia than is observed. Additionally, differences in modeled and measured systematic variability of aerosol optical properties suggest that some models are not accurately capturing specific aerosol behaviors, for example, the tendency of *in situ* SSA to decrease with decreasing aerosol extinction coefficient.

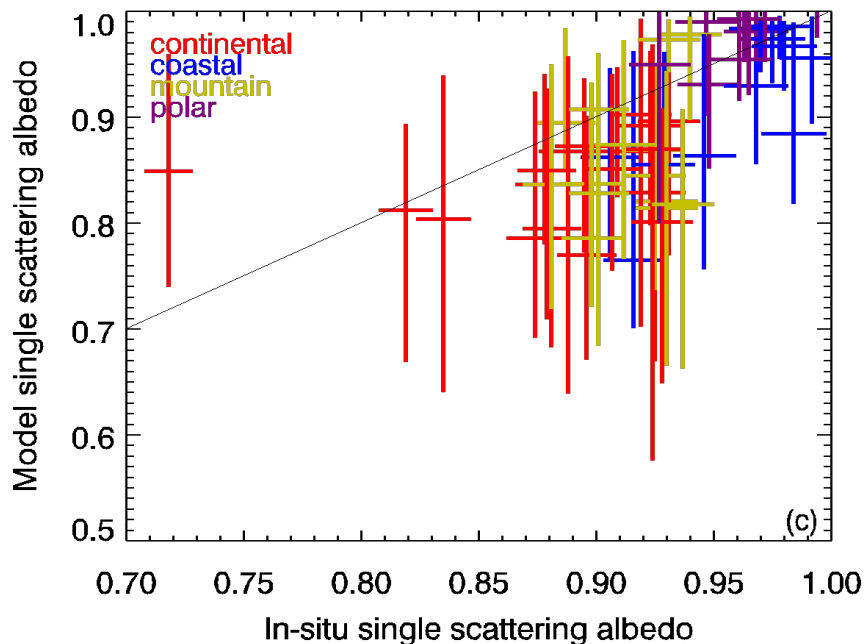


Figure 1. Comparison of observed and simulated aerosol SSA. Vertical bar shows range of model medians from 12 models, horizontal bar is measurement uncertainty. Bars cross at model and measurement median.

Synthesis of Aerosol Physical, Chemical, and Radiative Properties from Various Sources: Consistency and Closure

H. Telg^{1,2}, A. McComiskey², D. Collins³, E. Andrews^{1,2}, G. Hodges^{1,2} and T. Watson⁴

¹Cooperative Institute for Research in Environmental Sciences (CIRES), University of Colorado, Boulder, CO 80309; 505-205-5425, E-mail: hagen.telg@noaa.gov

²NOAA Earth System Research Laboratory, Global Monitoring Division (GMD), Boulder, CO 80305

³Texas A&M University, Department of Atmospheric Sciences, College Station, TX 77843

⁴Brookhaven National Laboratory, Environmental and Climate Sciences Department, Upton, NY 11973

Aerosol direct radiative forcing is determined from a set of optical properties - aerosol optical depth, single scattering albedo, and asymmetry parameter - which can be obtained from a range of different measurement techniques. Every technique has unique benefits and limitations, thus uncertainty and bias in radiative forcing estimates can vary depending on the measurement approach used. Given that a small fraction of these observations are most widely used for climate change studies, a comprehensive assessment of the interrelationship among all measurements would benefit uncertainty reduction. We present a closure study of aerosol products from ground-based *in situ* observations. Physical (size distribution) and chemical composition data are used to derive aerosol optical properties and results are compared to direct measurements of the aerosol light scattering. Since most *in situ* measurements are conducted under dry conditions, a further parameter - the aerosol hygroscopicity or the aerosol particle ability to take up water - needs to be measured to infer the optical parameters at ambient conditions. We use the results of this closure analysis including hygroscopic properties to inform the relationship between detailed *in situ* measurements and remote sensing of aerosol in the ambient column, the latter which are widely used for constraining aerosol radiative effects for climate change analysis.

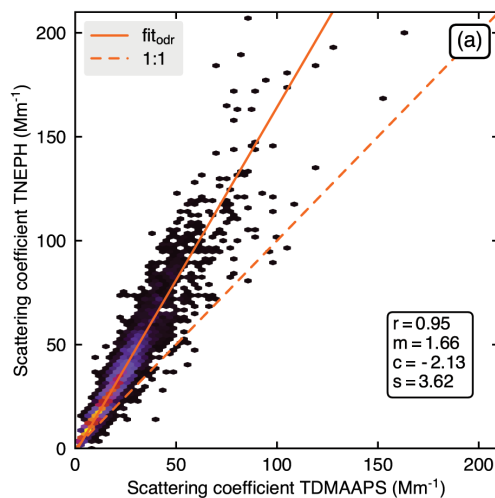


Figure 1. Correlation of measured aerosol light scattering and size distribution derived scattering coefficients for the year 2012 from dry *in situ* measurements at the surface.

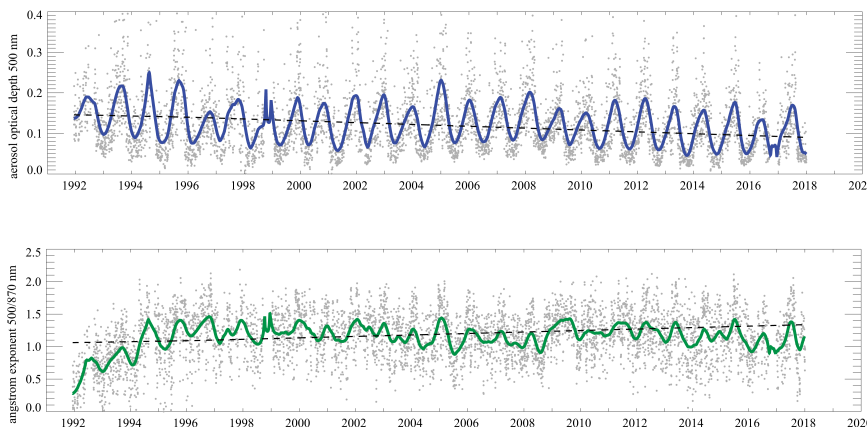


Figure 2. Long-term records of ambient, column aerosol optical depth (light scattering + absorption) and Angstrom exponent (a proxy for size) showing distinct annual cycles driven by relative humidity and longer-term variability that impacts size and scattering.

Reducing Uncertainty in Aerosol Direct Radiative Effect Through Synergistic Use of Long-term Satellite and Ground-based Measurements

J.P. Sherman, I. Krintz and H. Suthers

Appalachian State University, Department of Physics and Astronomy, Boone, NC 28608; 828-262-2438, E-mail: shermanjp@appstate.edu

Based on current uncertainties in satellite-retrieved aerosol optical depth (AOD) and especially the particle properties (i.e. single-scattering albedo and asymmetry parameter) used by radiative transfer models to calculate aerosol direct radiative effect (DRE), Kahn (2011) concluded that satellite data alone cannot provide enough quantitative detail to yield the required improvements in DRE estimates. Reducing the uncertainty in measurement-based DRE to $\sim 1 \text{ Wm}^{-2}$ necessitates uncertainties in AOD and single-scattering albedo (ω_0) of ≤ 0.02 (Sherman and McComiskey 2018). Ground-based Cimel sunphotometers (as part of NASA AERONET) and multi-filter rotating shadowband radiometers (MFRSRs) can measure AOD to within ~ 0.01 (Eck et al. 1999, Hallar-personal correspondence). *In situ* measurements of ω_0 at ESRL/GMD sites possess ambient relative humidity (RH) ω_0 uncertainties of ~ 0.02 (Sherman and McComiskey 2018), although humidified light scattering measurements are necessary to correct the dry aerosol optical properties to ambient RH at humid sites. Aerosol DRE calculated using the ground-based aerosol optical properties as inputs possess uncertainties of $\sim 1 \text{ Wm}^{-2}$ (Figure 1; Sherman and McComiskey 2018). However, there are currently only two co-located AERONET/ESRL sites in the U.S. possessing such measurement capabilities (Southern Great Plains [SGP] and Appalachian State [APP]), along with one co-located MFRSR/ESRL site (Storm Peak Lab). As part of a proposed strategy for reducing DRE uncertainty, Kahn et al. (2017) have the goal to acquire enough sub-orbital *in situ* measurements of aerosol optical and microphysical properties corresponding to major aerosol types to construct probability density functions (PDFs) of the key properties corresponding to each major aerosol air mass type. The PDFs can then be used to prescribe aerosol optical properties and calculate aerosol DRE at any location, using satellite-retrieved AOD and aerosol type (Kahn et al. 2017).

We will present a modified version of the strategy proposed by Kahn et al. (2017) to better constrain aerosol DRE, using (1) ground-based aerosol properties measured at APP's AERONET and ESRL/GMD sites; (2) AOD and surface albedo retrieved by Multi-angle Imaging SpectroRadiometer (MISR) and/or MODIS; (3) aerosol type retrieved by MISR; and (4) sub-pixel AOD measurements made by Citizen Scientists, using handheld sunphotometers developed and calibrated at APP. We also present a method for evaluating the strategy. While our focus is on evaluating and improving upon DRE estimates over mountainous sites (where satellite aerosol retrievals often perform poorly, if they are even attempted), the strategy can easily be extended to any ESRL/GMD aerosol monitoring site with a continuous, long-term record of particle property measurements (and their RH-dependence, for humid regions).

| | MAR | JUN | SEP | DEC |
|---|-------------|-------------|-------------|------------|
| $\Delta\text{DRE}_{\text{AOD}}$ | 0.47 (2.3) | 0.35 (1.8) | 0.34 (1.7) | 0.43 (2.1) |
| $\Delta\text{DRE}_{\omega_0}$ | 0.27 | 0.77 | 0.36 | 0.079 |
| ΔDRE_g | 0.059 | 0.18 | 0.12 | 0.018 |
| ΔDRE_R | 0.16 | 0.34 | 0.18 | 0.04 |
| DRE (Base case) | -2.4 | -5.7 | -3.6 | -0.91 |
| $\Delta\text{DRE} / \text{DRE (Base Case)}$ | 0.24 (0.97) | 0.20 (0.39) | 0.20 (0.56) | 0.49 (2.4) |

Figure 1. Calculated measurement uncertainties in DRE at the top of atmosphere above APP, including the contributions due to uncertainties in aerosol optical depth (AOD), single-scattering albedo (ω_0), scattering asymmetry parameter (g), and broadband surface reflectance (R). Units of ΔDRE are W m^{-2} . Uncertainties are also calculated as a fraction of DRE calculated using seasonal median aerosol optical properties (base-case values). The uncertainties associated with AOD are calculated twice; once using AERONET AOD uncertainties and once using the lower bound for MODIS AOD uncertainty (shown in parentheses).

Measurements of Aerosol Absorption during Ultra-light Global Circumnavigation, Arctic and Mediterranean Campaigns

G. Mocnik^{1,2}, L. Drinovec^{1,2}, G. Razoršek², P. Vidmar² and M. Lenarcic³

¹Jozef Stefan Institute, Ljubljana, Slovenia; +386-4-165-74-38, E-mail: grisa.mocnik@ijs.si

²Aerosol d.o.o., Ljubljana, Slovenia

³Aerovizija d.o.o., Ljubljana, Slovenia

We performed airborne measurements of aerosol light absorption with ultra-light aircraft during four flight campaigns: around the world (2012, 2016), over the Arctic (2013), and the Mediterranean (2017). A small ultra-light aircraft operated at altitudes around 3000m and up to 8900m ASL over all continents and oceans.

The aircraft carried specially-developed high-sensitivity multi-wavelength aethalometers, measuring aerosol absorption with high temporal resolution and sensitivity. We present examples from flights, and, using the aerosol absorption dependence on the wavelength, we show that aerosols produced during biomass combustion can be transported to high altitude in high concentrations. We show good agreement between models and measurements for long-range transport of pollution into the Arctic and the transport of mixtures of mineral dust and black carbon (BC) regionally. We show by measurements that the assumption of a simple linear relationship between BC concentration and forcing underestimates the direct forcing by about a quarter.

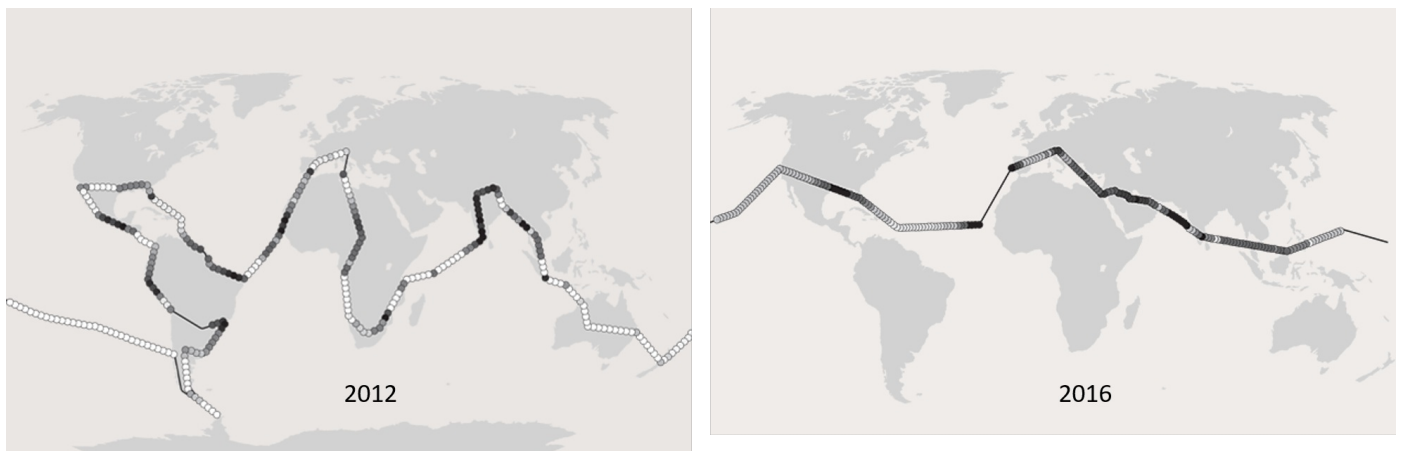


Figure 1. Flights around the world in 2012 and 2016.

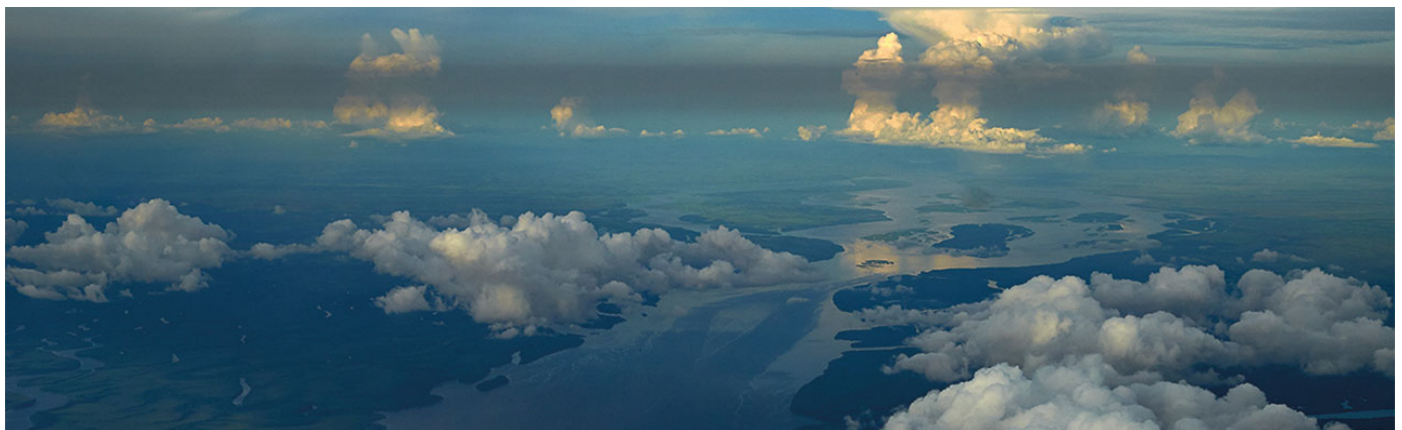


Figure 2. A layer of polluted air over the river Congo.

An Overview of GMD's Water Vapor Research

D. Hurst^{1,2}, E. Hall^{1,2} and A. Jordan^{1,2}

¹Cooperative Institute for Research in Environmental Sciences (CIRES), University of Colorado, Boulder, CO 80309; 303-497-7003, E-mail: Dale.Hurst@noaa.gov

²NOAA Earth System Research Laboratory, Global Monitoring Division (GMD), Boulder, CO 80305

Atmospheric water vapor is a strong infrared absorber and a potent greenhouse gas. It is also part of an ominous climate feedback loop: as the Earth's surface warms, the atmospheric burden of water vapor also increases, further warming the surface that responds by evaporating more water vapor into the atmosphere. ESRL/GMD's water vapor monitoring efforts focus on the upper troposphere and stratosphere, where even small abundance perturbations can drive significant changes in surface temperatures. ESRL/GMD's pioneering role in the monitoring of upper atmospheric water vapor with balloon-borne frost point hygrometers began in Boulder in 1980 and continues today at Boulder, Colorado; Hilo, Hawaii; and Lauder, New Zealand. Despite today's prevalence of satellite-based water vapor sensors with near-global coverage, ESRL/GMD's *in situ* measurements, with high vertical resolution and stable accuracy, prove extremely valuable for the analysis of seasonal and longer-term variability in upper atmospheric water vapor, and for ongoing evaluations of bias and drift in the measurement records of satellite-based water vapor sensors.

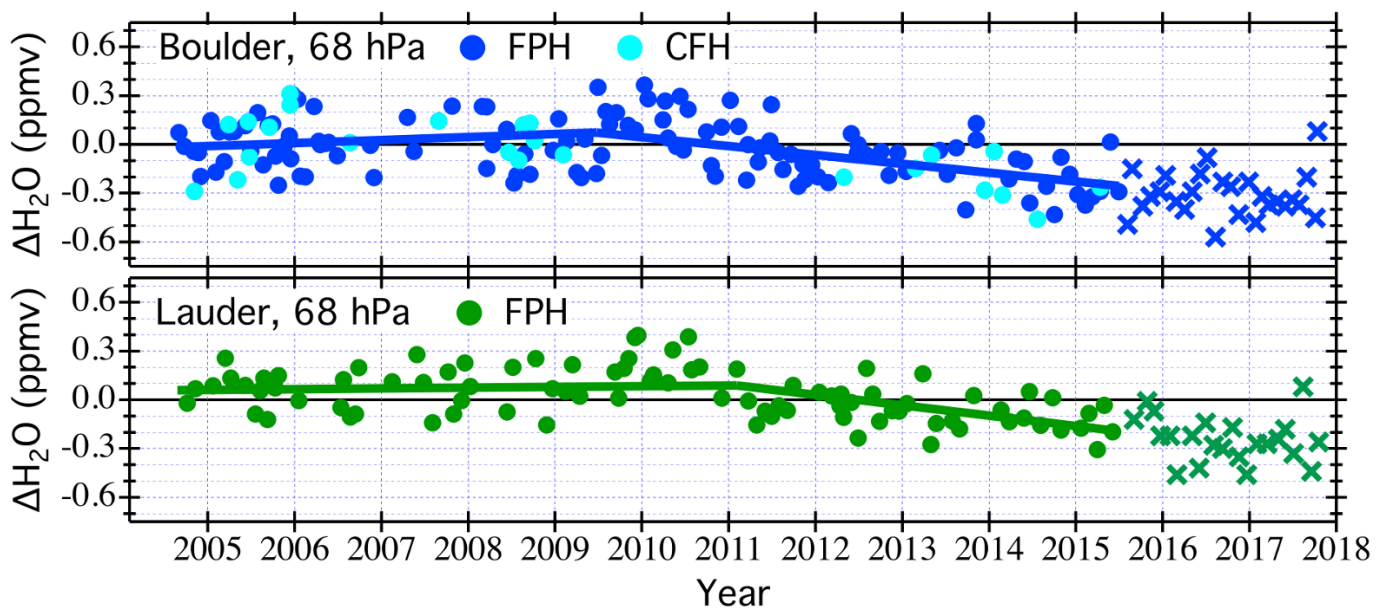


Figure 1. Trends in the differences between stratospheric water vapor measurements by frost point hygrometers and the Aura Microwave Limb Sounder (MLS) over Boulder, Colorado, and Lauder, New Zealand. Trend changes beginning in 2009-2011 indicate significant drifts in the MLS retrievals that persisted through 2017.

Local Measurements, Global Studies: The Utility of Balloon-borne Frost Point Hygrometer Measurements for Studying Global Stratospheric Water Vapor

S.M. Davis^{1,2}, K.H. Rosenlof², D.F. Hurst^{1,3}, E.G. Hall^{1,3}, A.F. Jordan^{1,3} and R.W. Portmann²

¹Cooperative Institute for Research in Environmental Sciences (CIRES), University of Colorado, Boulder, CO 80309; 303-497-4328, E-mail: sean.m.davis@noaa.gov

²NOAA Earth System Research Laboratory, Chemical Sciences Division (CSD), Boulder, CO 80305

³NOAA Earth System Research Laboratory, Global Monitoring Division (GMD), Boulder, CO 80305

Despite the number density of stratospheric water vapor (SWV) being 5 orders of magnitude less than at the surface, it has an inordinate influence on global energy balance and a significant impact on stratospheric ozone chemistry. Variations in SWV on monthly to decadal scales are predominantly controlled by variations of temperature in the tropical tropopause layer that are impacted by numerous potentially interrelated phenomena such as the El Niño Southern Oscillation (ENSO), the Quasi-Biennial Oscillation (QBO), variations in the lower branch of the Brewer-Dobson circulation, and increasing amounts of greenhouse gases.

In this presentation, I will argue that understanding variability and long-term changes in SWV requires a synergy of long-term measurements from both satellite sensors and balloon-based hygrometers. Although the global coverage provided by satellites is crucial, the high vertical resolution and inherent accuracy of “local-scale” balloon hygrometer measurements provide three important aspects of global monitoring: 1) confirming and quantifying short-term variability seen in satellite records, 2) detecting and potentially correcting biases and drifts in the satellite data, and 3) bridging potential gaps in the satellite data record. I will present examples of each of these, focusing on the recent near-record breaking swings in SWV, as well as how frost point hygrometer measurements inform the interpretation of global climate models and merged satellite data records such as the Stratospheric Water and OzOne Satellite Homogenized (SWOOSH) data set.

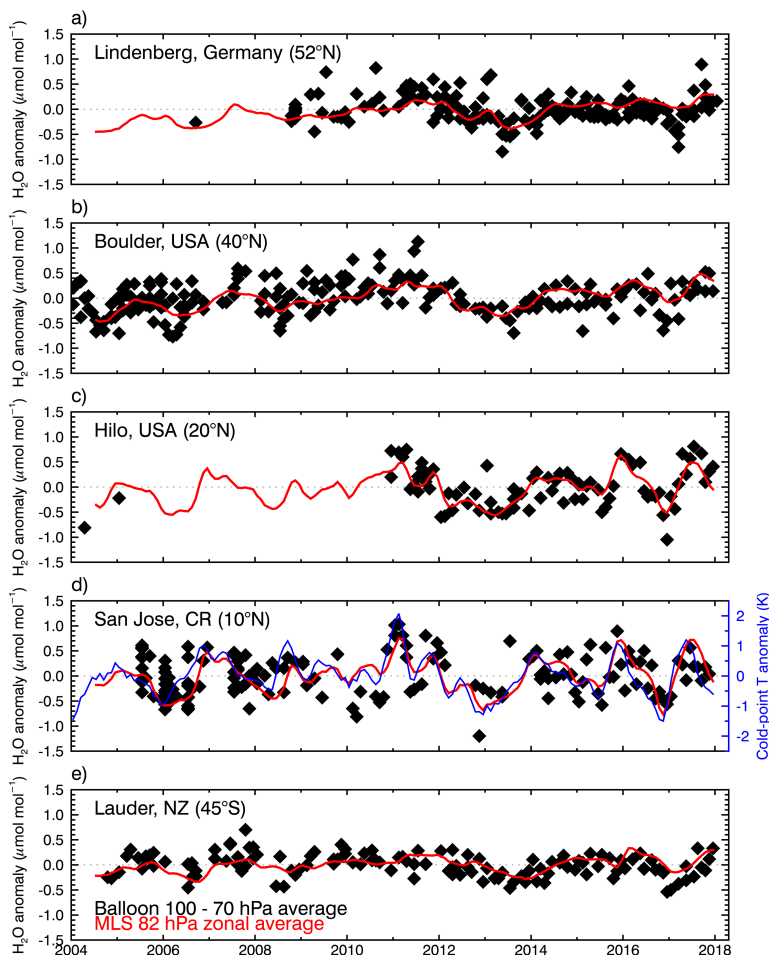


Figure 1. Lower stratospheric water vapor anomalies over five balloon-borne frost point (FP) hygrometer stations. Each panel shows the lower stratospheric anomalies of individual FP soundings (black) and of monthly zonal averages of Microwave Limb Sounder (MLS) retrievals at 82 hPa in the 5° latitude band containing the FP station (red). High-resolution FP vertical profile data were averaged between 70 and 100 hPa to emulate the MLS averaging kernel for 82 hPa. Each MLS monthly zonal mean was determined from 2,000–3,000 profiles. Anomalies for MLS and FP data are calculated relative to the 2004 – 2017 period for sites except for Lindenberg (2009 – 2017) and Hilo (2011 – 2017). Tropical cold-point tropopause anomalies based on the Modern-Era Retrospective analysis for Research and Applications, Version 2 (MERRA-2) reanalysis (d, blue curve).

Tropospheric Column Ozone Variability from Space: Results from the First Multi-instrument Intercomparison

A. Gaudel^{1,2}, O.R. Cooper^{1,2}, V. Thouret³, B. Barret³, A. Boynard^{4,5}, J.P. Burrows⁶, C. Clerbaux⁴, G. Huang⁷, B. Kerridge⁸, B. Latter⁸, X. Liu⁷, N. Rahn⁶, A. Rosanov⁶, C. Wespes⁹ and J.R. Ziemke¹⁰

¹Cooperative Institute for Research in Environmental Sciences (CIRES), University of Colorado, Boulder, CO 80309; 303-497-6563, E-mail: audrey.gaudel@noaa.gov

²NOAA Earth System Research Laboratory, Chemical Sciences Division (CSD), Boulder, CO 80305

³Laboratoire d'Aérodynamique, The National Center for Scientific Research (CNRS), and Université Paul Sabatier Toulouse III, Toulouse, France

⁴Laboratoire Atmosphères, Milieux, Observations Spatiales-Institute Pierre Simon Laplace (LATMOS-IPSL), Université Pierre et Marie Curie (UPMC) Univ. Paris 06 Sorbonne Universités, UVSQ, CNRS, Paris, France

⁵SPASCI, Ramonville Saint-Agne, France

⁶Institute of Environmental Physics, University of Bremen, Bremen, Germany

⁷Harvard-Smithsonian Center for Astrophysics, Cambridge, MA 02138

⁸Rutherford Appleton Laboratory, Chilton, United Kingdom

⁹Université libre de Bruxelles (ULB), Service de Chimie Quantique et Photophysique, Brussels, Belgium

¹⁰Morgan State University, Baltimore, MD 21251

Tropospheric ozone is a pollutant detrimental to human health, and crop and ecosystem productivity. Tropospheric ozone is also the third most important greenhouse gas (after carbon dioxide and methane), responsible for approximately 17% of global radiative forcing since 1750. However, the lack of a comprehensive global ozone monitoring network means that ozone's radiative forcing must be estimated by chemistry-climate models. As a result, the most recent estimate of ozone's radiative forcing has large error bars of plus or minus 50% due to model uncertainties ($0.40 \pm 0.20 \text{ W m}^{-2}$, according to the fifth Intergovernmental Panel on Climate Change [IPCC] assessment report). Improvements to this estimate require an accurate observation-based quantification of the present-day tropospheric ozone burden (TOB), and greater confidence in chemistry-climate model estimates of TOB in pre-industrial times. In its most simple form, TOB is the total mass of ozone in the troposphere (expressed in units of Tg), calculated by summing all of the tropospheric column ozone (TCO) values at every point on Earth. Presently there is only one published observation-based estimate of TOB, which comes from the Ozone Monitoring Instrument/Microwave Limb Sounder (OMI/MLS) satellite instruments on NASA's Aura satellite. Recently, four new satellite products have been developed for measuring TCO and TOB, with two based on the OMI satellite instrument and two based on the Infrared Atmospheric Sounding Interferometer (IASI) satellite instrument. The first intercomparison of these products will soon be published as a component of the Tropospheric Ozone Assessment Report (TOAR). While all five products show the same general tropospheric ozone features across the globe, they differ in absolute TCO quantities and they also differ in terms of decadal trends. The next step is to evaluate all products against the exact same set of *in situ* ozone observations to gauge the performance of each product in different regions of the world. We will present preliminary results from this evaluation which relies on daily In-service Aircraft for a Global Observing System (IAGOS) commercial aircraft profiles above Frankfurt, Germany and weekly ESRL/GMD ozonesonde profiles above Hilo, Hawaii; Trinidad Head, California; and Boulder, Colorado.

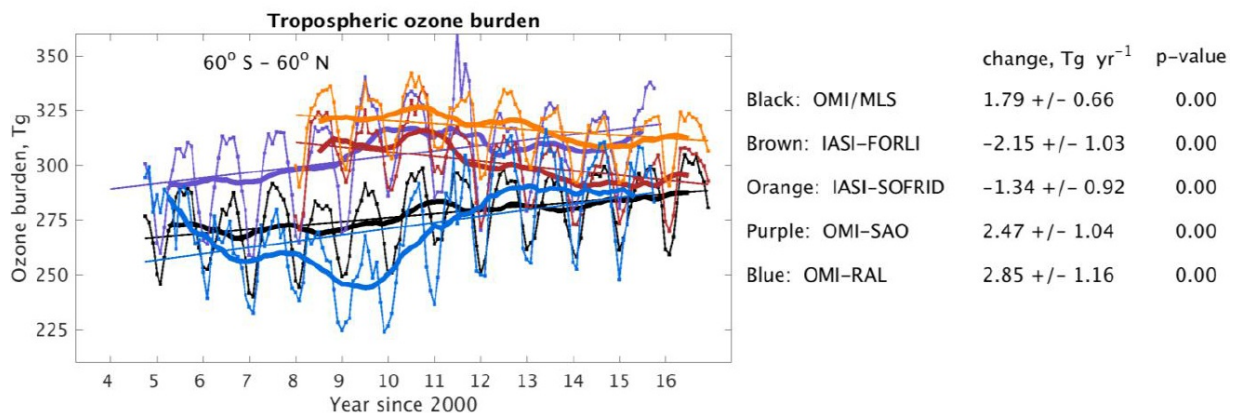


Figure 1. Monthly tropospheric ozone burden (thin curves) for 60° S - 60° N for 5 different satellite products. Thick curves are the 12-month running means and the thin straight lines are the least square linear fits.

Tropospheric Ozone Assessment Report: Tropospheric Ozone Observations – How Well Do We Know Tropospheric Ozone Changes?

D.W. Tarasick

Environment and Climate Change Canada, Toronto, Ontario, Canada; 416-739-4623, E-mail: david.tarasick@canada.ca

From the earliest observations of ozone in the 19th century, both measurement methods and the portion of the globe observed by them have evolved and changed significantly. These methods have different uncertainties and biases, and the data records differ with respect to coverage (space and time), information content, and representativeness. These records are reviewed and compared, based on validation and intercomparison experiments, and related to the modern ultraviolet (UV) standard. There are significant uncertainties with the 19th and early 20th century measurements by potassium iodide methods in urban areas that are related to interference of other gases. Sulfur dioxide (SO₂) levels in particular appear to have been quite high in urban areas, and may have negatively biased ozone measurements. There is no firm evidence of very low ozone values in the 19th century, although there is evidence of a modest increase in the 20th century, primarily in the Northern Hemisphere. Spectroscopic methods are not subject to SO₂ interference, but differing values of ozone absorption coefficients used before 1960 may have caused ozone to be underestimated by 11% at the surface and by about 24% in the free troposphere.

The great majority of validation and intercomparison studies of free tropospheric ozone measurement methods are undertaken with electrochemical-concentration (ECC) ozonesondes. ECC sondes have been compared to UV-absorption measurements in a number of intercomparison studies. They show a modest (~1-5%) high bias in the troposphere, with an uncertainty of 5%, but no evidence of a change with time. Other methods – Umkehr, lidar, FTIR, and commercial aircraft – all show modest low biases relative to the ECCs, and so, using ECC sondes as a transfer standard, all appear to agree to within 1 σ with the modern UV-absorption standard. Relative to the UV standard, Brewer-Mast sondes show a 20% increase in sensitivity to tropospheric ozone from 1970-1995. In combination with the gradual shift of the global network to ECC sondes, this will, if uncorrected, induce a false positive trend in the free troposphere, in analyses based on sonde data.

Satellite biases are often larger than those of other free tropospheric measurement systems, ranging between -10% and +20%, and standard deviations are large: about 10-30%, versus 5-10% for sondes, aircraft, lidar, and ground-based Fourier-transform infrared spectroscopy. There is currently little information on temporal changes of bias for satellite measurements of tropospheric ozone. This is an evident area of concern if satellite retrievals are used for trend studies. The importance of ECC sondes as a transfer standard for satellite validation means that effort should be put into reducing their uncertainties.

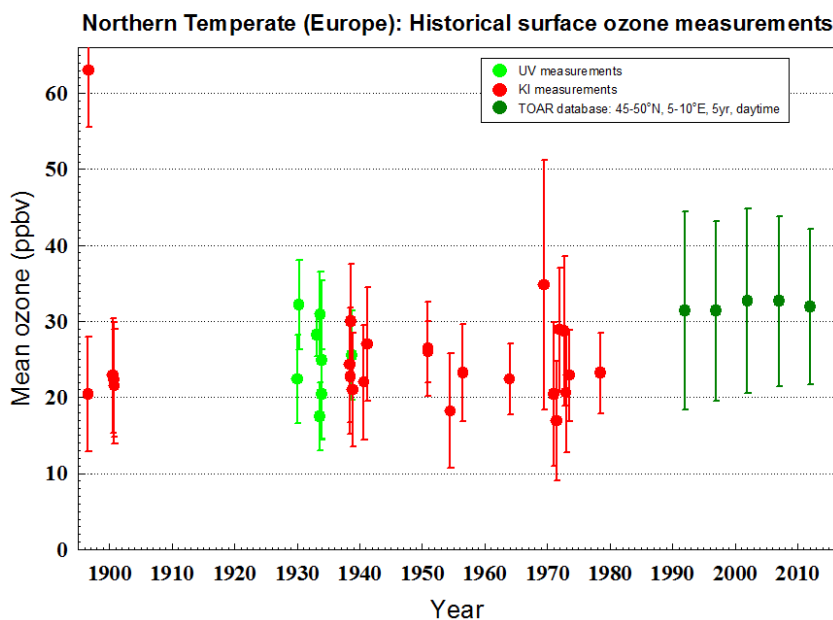


Figure 1. Historical measurements of surface ozone in northern temperate regions (almost exclusively Europe). Error bars represent standard deviations of the measurement averages (atmospheric variability), not uncertainty of the measurement. Five-year averages of modern UV measurements at sites classified as “rural” in the Tropospheric Ozone Assessment Report (TOAR) database are also shown (Schultz et al. 2017).

An Overview of the Fires, Asian, and Stratospheric Transport-Las Vegas Ozone Study (FAST-LVOS)

A.O. Langford¹, R.J.A. II¹, T.A. Bonin², A. Brewer¹, G. Kirgis², S.P. Sandberg¹, C.J. Senff², A.M. Weickmann², S.S. Brown¹, Z. Decker², B. Dubé², D.L. Fibiger^{2,1}, J. Peischl^{2,1}, T. Ryerson¹, D.J. Caputi³, S. Conley^{4,3}, P. Cullis^{2,5}, I. Petropavlovskikh^{2,5} and C.W. Sterling^{2,5}

¹NOAA Earth System Research Laboratory, Chemical Sciences Division (CSD), Boulder, CO 80305; 303-497-3115, E-mail: andrew.o.langford@noaa.gov

²Cooperative Institute for Research in Environmental Sciences (CIRES), University of Colorado, Boulder, CO 80309

³University of California at Davis, Davis, CA 95616

⁴Scientific Aviation, Roseville, CA 95661

⁵NOAA Earth System Research Laboratory, Global Monitoring Division (GMD), Boulder, CO 80305

The Fires, Asian, and Stratospheric Transport-Las Vegas Ozone Study (FAST-LVOS) was conducted in Southern Nevada and California over a 6-week period from May 17 to June 30, 2017. The primary goal of the study was to assess the impact of transport from outside sources including wildfires, Asian pollution, and stratospheric intrusions on surface ozone (O_3) in Clark County, NV during late spring and early summer. The study combined ground-based lidar, aircraft, ozonesonde, and *in situ* measurements, and was funded by the Clark County (NV) Department of Air Quality with additional support from NOAA and the NASA-sponsored Tropospheric Ozone Lidar Network. The 45-day field campaign produced more than 500 hours of O_3 and aerosol backscatter lidar profiles and continuous Doppler lidar measurements of mixed layer heights and vertical velocities at the North Las Vegas Airport, with nearly-continuous *in situ* sampling of O_3 , carbon monoxide (CO), carbon dioxide (CO_2), methane (CH_4), nitrous oxide (N_2O), nitric oxide (NO), nitrogen dioxide (NO_2), and total reactive nitrogen (NOy) at the summit of Angel Peak in the nearby Spring Mountains. These measurements were augmented by ozonesonde launches on 12 days, and by aircraft profiles of O_3 , NO_2 , CH_4 , and CO_2 above southern Nevada and California on 16 days. In this talk, I will describe the FAST-LVOS campaign and present a summary of the measurements and preliminary findings.

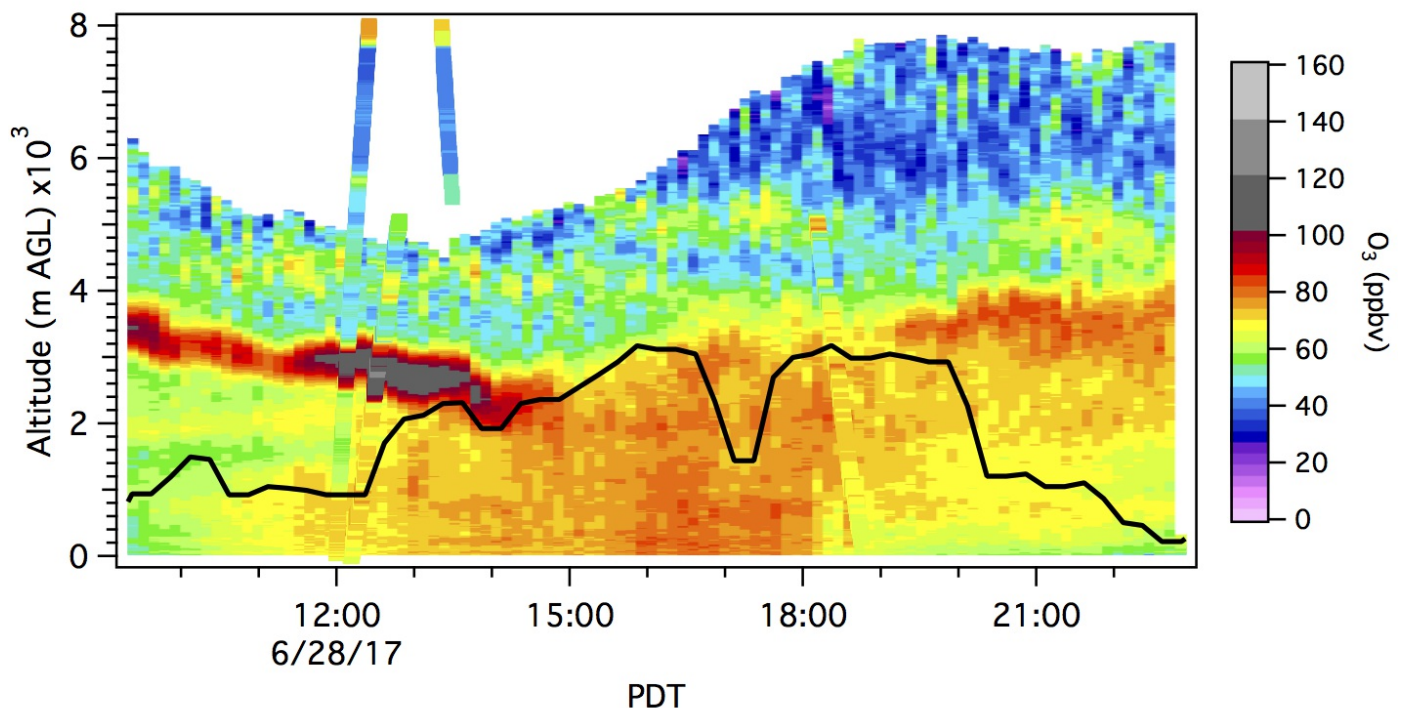


Figure 1. Time-height curtain plot of ozone concentrations measured by the Tunable Optical Profiler for Aerosol and oZone (TOPAZ) lidar during the FAST-LVOS field campaign showing the entrainment of an Asian pollution plume on June 28, 2017. Note the ozonesonde and aircraft measurements superimposed on the plot.

Preliminary Results from GMD's Halocarbons and other Trace Gases Measurements on ATom

J.W. Elkins¹, F.L. Moore^{2,1}, E.J. Hints^{2,1}, E. Ray^{2,3}, G.S. Dutton^{2,1}, J.D. Nance^{2,1}, B.D. Hall¹, S.A. Montzka¹, C. Sweeney¹, B.R. Miller^{2,1}, E.J. Dlugokencky¹, P.A. Newman⁴ and S.C. Wofsy⁵

¹NOAA Earth System Research Laboratory, Global Monitoring Division (GMD), Boulder, CO 80305; 303-497-6224, E-mail: james.w.elkins@noaa.gov

²Cooperative Institute for Research in Environmental Sciences (CIRES), University of Colorado, Boulder, CO 80309

³NOAA Earth System Research Laboratory, Chemical Sciences Division (CSD), Boulder, CO 80305

⁴NASA Goddard Space Flight Center (GSFC), Greenbelt, MD 20771

⁵Harvard University, School of Engineering and Applied Sciences, Cambridge, MA 02138

We have learned a great deal about our atmosphere from the 25 years plus of airborne observations of the halocarbons and other trace atmospheric species on both a regional and global scale. We will have completed four seasonal circuits of the NASA Atmospheric Tomography Mission (ATom). One of the primary purposes of ATom is to study the influence of air quality on climate during all seasons over the Atlantic and Pacific Oceans.

Two ESRL/GMD airborne *in situ* gas chromatographs (GCs), the peroxyacyl nitrates (PAN) and other Trace Hydrohalocarbons Experiment (PANTHER) and UAS (Unmanned Aerial System) Chromatograph for Atmospheric Trace Species (UCATS), and one flask collection sampling system, Programmable Flask Package (PFP), operated on ATom. Data from the first two circuits of over 450 atmospheric parameters are publically available from

<https://espoarchive.nasa.gov/archive/browse/atom>.

As an example, from ATom-2 (Feb. 2017), the altitude-latitude cross sections of sulfur hexafluoride (SF_6) mixing ratios from the (a) GCs and (b) PFPs are in good agreement. Sources are mostly located in the Northern Hemisphere (NH) (~95%). The upper troposphere indicates inter-hemispheric mixing. At high altitudes in polar regions, older air mixes in from the stratosphere. Using the procedure described by Waugh et al. (2013) and a recent growth rate of 0.32 ppt yr^{-1} , we have calculated the mean age of each SF_6 measurement from its source at ground level in the NH, (lat. range of $30\text{-}50^\circ\text{N}$). The contours of age (c) are in agreement with the mean inter-hemispheric exchange time (τ_{NH}) of ~1.2 yr. and higher ages in the polar stratosphere (2-3 yr.).

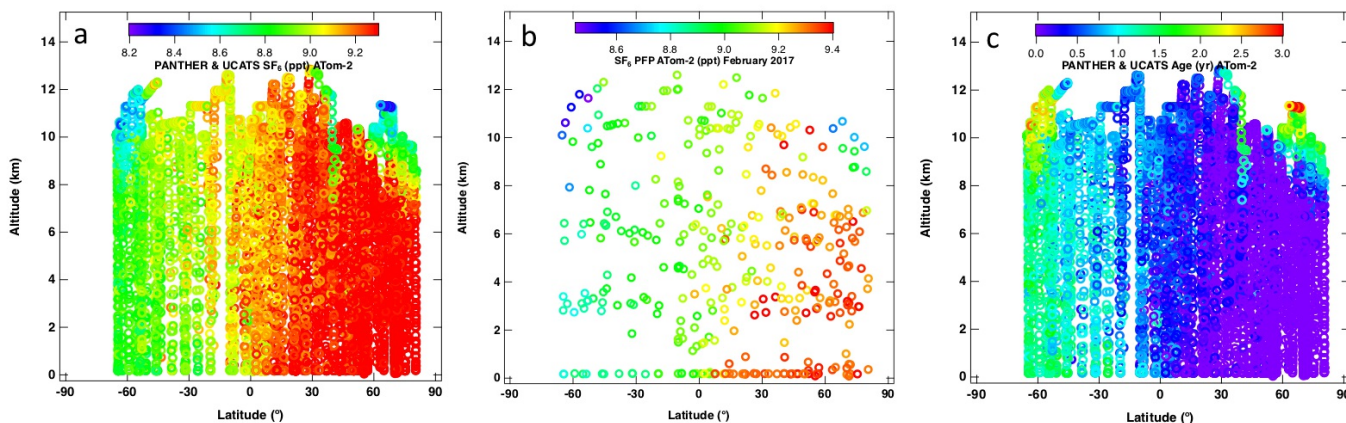


Figure 1. The altitude-latitude cross sections of SF_6 mixing ratios from the (a) higher sampling frequency GCs and (b) PFPs, and (c) calculated tropospheric age of the air mass from NH sources are shown for ATom-2.

Ambient Air Measurements of Formaldehyde by Near-infrared Cavity Ring-down Spectroscopy

C. Rella, M. Markovic, D. Kim-Hak and J. Hoffnagle

Picarro Inc., Santa Clara, CA 94054; 408-656-6741, E-mail: rella@picarro.com

Formaldehyde (HCHO or H₂CO) is an important species in atmospheric chemistry. There are multiple direct emission sources of HCHO and it is the photochemically-driven decay product of volatile organic compounds from both natural and anthropogenic sources. For this reason, real-time HCHO measurements provide critical insights into the mechanisms of tropospheric ozone formation. Formaldehyde has a clearly resolved ro-vibrational absorption spectrum that is well-suited to optical analysis of formaldehyde concentration. We describe a commercial instrument based on cavity ring-down spectroscopy for the real-time quantitative analysis of HCHO concentration in ambient air. The instrument has a precision (1-sigma) of about 1 ppb at a measurement rate of 1-second, and provides measurements of less than 100 ppt with minutes of averaging. Long-term laboratory measurements of a gas standard demonstrate that the instrument provides stable measurements (drift <1 ppb) over long periods of time (days). Given the difficulty of preparing known concentrations of HCHO, the stability of the instrument often exceeds the stability of prepared standards. Because it is based upon high resolution optical absorption spectroscopy, it does not suffer from cross-talk with other aldehydes or other carbonyl containing compounds. The instrument has been ruggedized for both mobile (ground and flight) applications or for unattended operation at ground monitoring stations, and with a fast response time of a couple of seconds, it is suitable for ground-based vehicle deployments for fenceline monitoring of HCHO emissions. In addition to the laboratory testing described above, we report on ambient atmospheric measurements at a 10 m urban tower, which demonstrate the suitability of the instrument for applications in atmospheric chemistry and outdoor air quality.

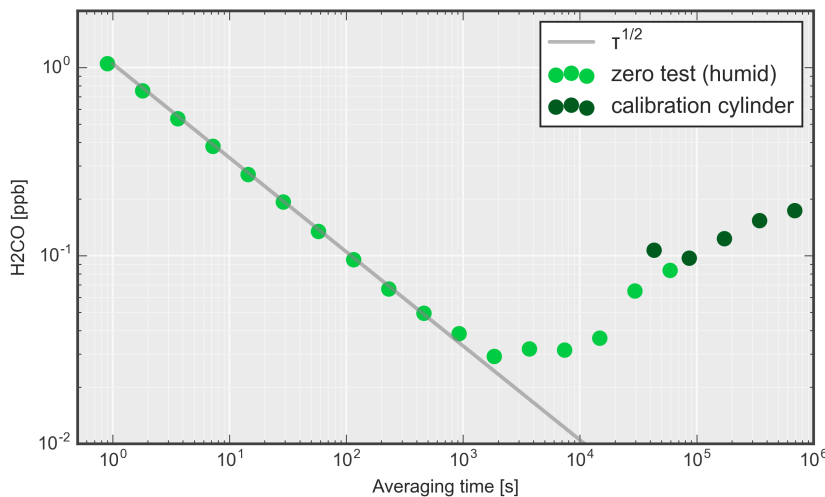


Figure 1. Measured Allan standard deviation indicating precision of 1 ppb in 1 second, 0.1 ppb with 100 seconds of averaging, and stability of about 0.2 ppb (1-sigma) over several days.

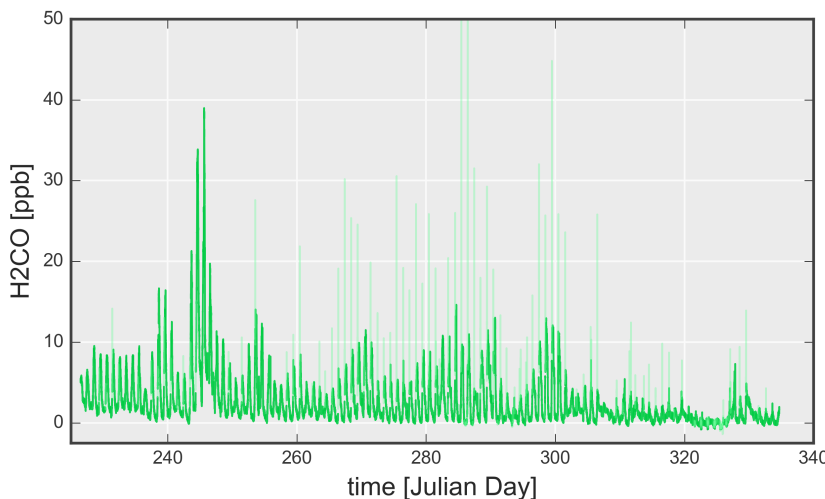


Figure 2. Outdoor ambient air measurements in Santa Clara, CA, from August to December 2017, indicating a strong diurnal cycle and large synoptic scale variability of the peak HCHO concentration.

Notes:

NOAA ESRL GLOBAL MONITORING ANNUAL CONFERENCE 2018

David Skaggs Research Center, Cafeteria
325 Broadway, Boulder, Colorado 80305 USA

Tuesday, May 22, 2018 Poster Session Agenda

(Only presenter's name is given; please refer to abstract for complete author listing.)

2018 GMAC and GMD Review Joint Session

- P-0 Evaluating the Impact of Baseline Ozone in California using Ozone-Sonde Measurements at Trinidad Head, CA (THD): Overview
Toshihiro Kuwayama (California Air Resources Board)
- P-1 Global Atmosphere Watch Programme: the Role of the National Programmes in Supporting the Global Value Chain
Oksana Tarasova (World Meteorological Organisation, Geneva, Switzerland)
- P-2 The Radon Measurement Programs at Cape Grim, Mauna Loa, and other Global Atmospheric Monitoring Sites
Alastair G. Williams (Australian Nuclear Science and Technology Organisation (ANSTO), Lucas Heights, Australia)
- P-3 NOAA and U.S. Department of Energy/Office of Science Cooperative Efforts in Barrow (Utqiagvik), Alaska
Mark Ivey (Sandia National Laboratories)
- P-4 Ozone, Aerosols and Carbon Gases at the Mt. Bachelor Observatory
James Laing (University of Washington)
- P-5 Black Carbon Mass Observations across Canada (2006-2015): Constraining on Regional Emissions in North America
Lin Huang (Environment and Climate Change Canada, Toronto, Canada)
- P-6 Aerosol Hygroscopicity during the Haze Red Alert Period in Winter 2016 at a Rural Site of the North China
Junying Sun (Chinese Academy of Meteorological Sciences, Key Laboratory of Atmospheric Chemistry of CMA, Beijing, China)
- P-7 Using SURFRAD Aerosol Optical Depth Measurements for Model Evaluation. A Study with FV3-GOCART and WRF-Chem and Their Assimilation Systems
Mariusz Pagowski (NOAA Earth System Research Laboratory, Global Systems Division (GSD))
- P-8 Ratios of Greenhouse Gas Emissions Observed over the Yellow Sea and the East China Sea
Lingxi Zhou (China Meteorological Administration, Chinese Academy of Meteorological Sciences, Beijing, China)
- P-9 TCCON Updates and Improvements to Precision Requirements
Coleen Roehl (California Institute of Technology)
- P-10 Engaging Agencies and the Public in Atmospheric Monitoring Observations Through Real-time Data Posting
Detlev Helmig (Institute of Arctic and Alpine Research (INSTAAR), University of Colorado)
- P-11 The Importance of Ozone-sonde Quality Assurance and JOSIE-SHADOZ (2017)
Jacquelyn C. Witte (Science Systems and Applications, Inc. (SSAI))
- P-12 The Evolving Role of Space-based Measurements in a Global Carbon Monitoring System
Charles Miller (NASA Jet Propulsion Laboratory, California Institute of Technology)

Tracking Greenhouse Gases and Understanding Carbon Cycle Feedbacks

- P-13 AirCore: The Gold Standard for Comparing Remote Sensing Observations to the Ground Network and the Capturing Changes in Stratospheric Circulation Changes
Colm Sweeney (NOAA Earth System Research Laboratory, Global Monitoring Division (GMD))
- P-14 Monitoring of Atmospheric Acetylene in the NOAA Global Greenhouse Gas Reference Network
Jacques Hueber (Institute of Arctic and Alpine Research (INSTAAR), University of Colorado)
- P-15 Atmospheric Isoprene in the NOAA/INSTAAR Global Greenhouse Gas Reference Network
Jacques Hueber (Institute of Arctic and Alpine Research (INSTAAR), University of Colorado)
- P-16 Spatial and Temporal Gradients in Atmospheric CO₂ and CO in the Los Angeles Megacity
Kristal R. Verhulst (NASA Jet Propulsion Laboratory, California Institute of Technology)
- P-17 Investigating Hydrocarbon Tracers for Anthropogenic CO₂ at Indianapolis, IN
Isaac Vimont (National Research Council Post-Doc)
- P-18 Estimating Uncertainties of GC/MS Analyses of Programmable Flask Package (PFP) Atmospheric Samples from the GGGRN North American Tower and Aircraft Programs
Benjamin R. Miller (Cooperative Institute for Research in Environmental Sciences (CIRES), University of Colorado)

NOAA ESRL GLOBAL MONITORING ANNUAL CONFERENCE 2018

David Skaggs Research Center, Cafeteria
325 Broadway, Boulder, Colorado 80305 USA

Tuesday, May 22, 2018 Poster Session Agenda

(Only presenter's name is given; please refer to abstract for complete author listing.)

Tracking Greenhouse Gases and Understanding Carbon Cycle Feedbacks (continued)

- P-19 Untangling Greenhouse Gas Fluxes and Transport using ACT-America Observations
Sha Feng (Department of Meteorology and Atmospheric Science, The Pennsylvania State University)
- P-20 Recent Developments in Using Isotopic Measurements for Constraining Methane Sources and Sinks
Xin Lan (Cooperative Institute for Research in Environmental Sciences (CIRES), University of Colorado)
- P-21 Recent GAW Activities of KMA
Yuwon Kim (Korea Meteorological Administration, Daebang-dong, Dongjak District, Republic of Korea)
- P-22 Systematic Differences in Global CO₂ Inverse Model Results
Benjamin Gaubert (National Center for Atmospheric Research (NCAR), Atmospheric Chemistry Observations and Modeling Laboratory)
- P-23 Methane Leak Detection and Sizing using Large Eddy Simulations (LES)
Kuldeep Prasad (National Institute of Standards and Technology (NIST))
- P-24 Development of ECCO's Regional Transport Model for Simulation of Atmospheric Greenhouse Gases at High Spatial and Temporal Resolution
Jinwoong Kim (Environment and Climate Change Canada, Toronto, Canada)
- P-25 Constraining Carbon Exchange Processes over North America by Joint Assimilation of Atmospheric CO₂ and δ¹³C
Ivar R. van der Velde (Cooperative Institute for Research in Environmental Sciences (CIRES), University of Colorado)
- P-26 A Reanalysis of Inter-laboratory Comparisons as the Stable Isotope Lab at INSTAAR Switches to the JRAS-06 Realization of the VPDB Scale
Sylvia Englund Michel (Institute of Arctic and Alpine Research (INSTAAR), University of Colorado)
- P-27 An Update on the WMO CO X2014A Scale
Andrew Croftwell (Cooperative Institute for Research in Environmental Sciences (CIRES), University of Colorado)
- P-28 Successes and Challenges of Spectroscopic Based Techniques in Enteric Methane Measurements
Wilson Gichuhi (Department of Chemistry, Tennessee Tech University)
- P-29 Open-path Spectroscopy to an Airborne Retroreflector on a Quadcopter
Kevin Cossel (National Institute of Standards and Technology (NIST))
- P-30 Performance Validation of New High-precision CH₄ and CO₂ Analyzers Based on Optical Feedback Cavity Enhanced Absorption Spectroscopy
Israel Begashaw (LI-COR Biosciences)
- P-31 Estimation of Enteric Methane Emissions in Ruminants Using CO₂:CH₄ Ratio Obtained with a Wavelength-scanned Cavity Ring-down Spectrometer
Lahiru P Gamage (School of Environmental Studies, Tennessee Technological University)
- P-32 ¹³C and ¹⁸O Isotope Effects Resulting from High Pressure Regulation and CO₂ Cylinder Depletion
Matt C. Matthew (Airgas Specialty Gases)
- P-33 CO₂ Urban Synthesis and Analysis ("CO₂-USA") Network
Logan Mitchell (University of Utah)
- P-34 Investigating Methane Trends and Variability Using the GFDL-AM4 Model and NOAA GMD Observations
Jian He (Program in Atmospheric and Oceanic Sciences, Princeton University)
- P-36 Characterizing and Comparing Anthropogenic CH₄ Sources in the DJ Basin using Mobile Surveys
Chelsea Fougere (St. Francis Xavier University, Antigonish, Canada)
- P-37 Effects of Drought Conditions on CO₂ Flux in Semi-arid Chaparral Ecosystems.
Andrea Fenner (San Diego State University, Global Change Research Group)
- P-38 Sources and Variability of Air Toxics Downwind of an Oil and Natural Gas-producing Well Pad in a Residential Community
Ingrid Mielke-Maday (Cooperative Institute for Research in Environmental Sciences (CIRES), University of Colorado)

NOAA ESRL GLOBAL MONITORING ANNUAL CONFERENCE 2018

David Skaggs Research Center, Cafeteria
325 Broadway, Boulder, Colorado 80305 USA

Tuesday, May 22, 2018 Poster Session Agenda

(Only presenter's name is given; please refer to abstract for complete author listing.)

Tracking Greenhouse Gases and Understanding Carbon Cycle Feedbacks (continued)

- P-39 Ground-truth Calibration for the VIIRS Nightfire Detector of Gas Flares
Mikhail Zhizhin (Cooperative Institute for Research in Environmental Sciences (CIRES), University of Colorado)

Monitoring and Understanding Changes in Surface Radiation, Clouds, and Aerosol Distributions

- P-40 Volcanic Aerosol Optical Depths during the Post-Pinatubo Era, 1996-2018
Richard A Keen (University of Colorado, Department of Atmospheric and Oceanic Sciences)
- P-41 Use of Ground- and Space-based Visible Imagery with other Data for Model Evaluation and Assimilation
Steve Albers (Cooperative Institute for Research in the Atmosphere (CIRA), Colorado State University)
- P-42 Constraining Aerosol Properties with Ground-based Lidar and other Remote Sensing Techniques
John E. Barnes (Cooperative Institute for Research in Environmental Sciences (CIRES), University of Colorado)
- P-43 Cloud Measurements with an All-sky Camera System for Investigating Long-term Variability of Cloud Properties at South Pole
Masataka Shiobara (National Institute of Polar Research (NIPR), Tokyo, Japan)
- P-44 Mutual Information Analysis of Aerosol-cloud interactions by Meteorological State over Oklahoma, U.S.
Ian Glenn (Cooperative Institute for Research in Environmental Sciences (CIRES), University of Colorado)
- P-45 Black Carbon's Contribution to Aerosol Absorption Optical Depth in South Korea
Kara Lamb (Cooperative Institute for Research in Environmental Sciences (CIRES), University of Colorado)
- P-46 NOAA Global Radiation Group Participation in International Comparisons Offering Traceable Calibration to World Solar Radiation Standards
Emiel Hall (Cooperative Institute for Research in Environmental Sciences (CIRES), University of Colorado)
- P-47 Variability of UV at Sites Equipped with NIWA Spectrometer Systems for 20 Years or More
Patrick Disterhoft (Cooperative Institute for Research in Environmental Sciences (CIRES), University of Colorado)
- P-48 Improvements in the Brewer Mark IV Spectrophotometer Ultraviolet AOD Retrievals
Scott Stierle (Cooperative Institute for Research in Environmental Sciences (CIRES), University of Colorado)
- P-49 Shipboard Tilt Corrections for More Accurate Broadband Radiation Data
Chuck Long (Cooperative Institute for Research in Environmental Sciences (CIRES), University of Colorado)
- P-50 Validation of the Stratospheric Aerosol and Gas Experiment-III (SAGE-III) Aerosol Data Product
Travis N. Knepp (Science Systems and Applications, Inc. (SSAI))
- P-51 Validation of the Stratospheric Aerosol and Gas Experiment III on the International Space Station (SAGE III/ISS) Science Data Ozone Product: Preliminary Results
Susan Kizer (Science Systems and Applications, Inc. (SSAI))
- P-52 Overview and Selected Results from the NOAA Federated Aerosol Network
Patrick Sheridan (NOAA Earth System Research Laboratory, Global Monitoring Division (GMD))
- P-53 Relating Chemical and Optical Aerosol Properties at Mauna Loa Observatory
Katy Sun (Science and Technology Corporation)
- P-54 Reconciling Evapotranspiration Partitioning Models with Evidence of Anomalously Low Isotopic Fractionation during Evaporation in Semi-arid Landscapes
Aleya Kaushik (Cooperative Institute for Research in Environmental Sciences (CIRES), University of Colorado)
- P-55 Spatial Variations of Soil Temperature and its Environmental Controls across Eurasian Continent
Kang Wang (Institute of Arctic and Alpine Research (INSTAAR), University of Colorado)

Guiding Recovery of Stratospheric Ozone and Other Topics

- P-56 A Lamina-based Approach for Interpreting Variability in Ozonesonde Vertical Profiles
Ken Minschwaner (New Mexico Institute of Mining and Technology)
- P-57 Analysis of Ozone Trends from NOAA's Newly Homogenized Ozonesonde Data Record
Patrick Cullis (Cooperative Institute for Research in Environmental Sciences (CIRES), University of Colorado)

NOAA ESRL GLOBAL MONITORING ANNUAL CONFERENCE 2018

David Skaggs Research Center, Cafeteria
325 Broadway, Boulder, Colorado 80305 USA

Tuesday, May 22, 2018 Poster Session Agenda

(Only presenter's name is given; please refer to abstract for complete author listing.)

Guiding Recovery of Stratospheric Ozone and Other Topics (continued)

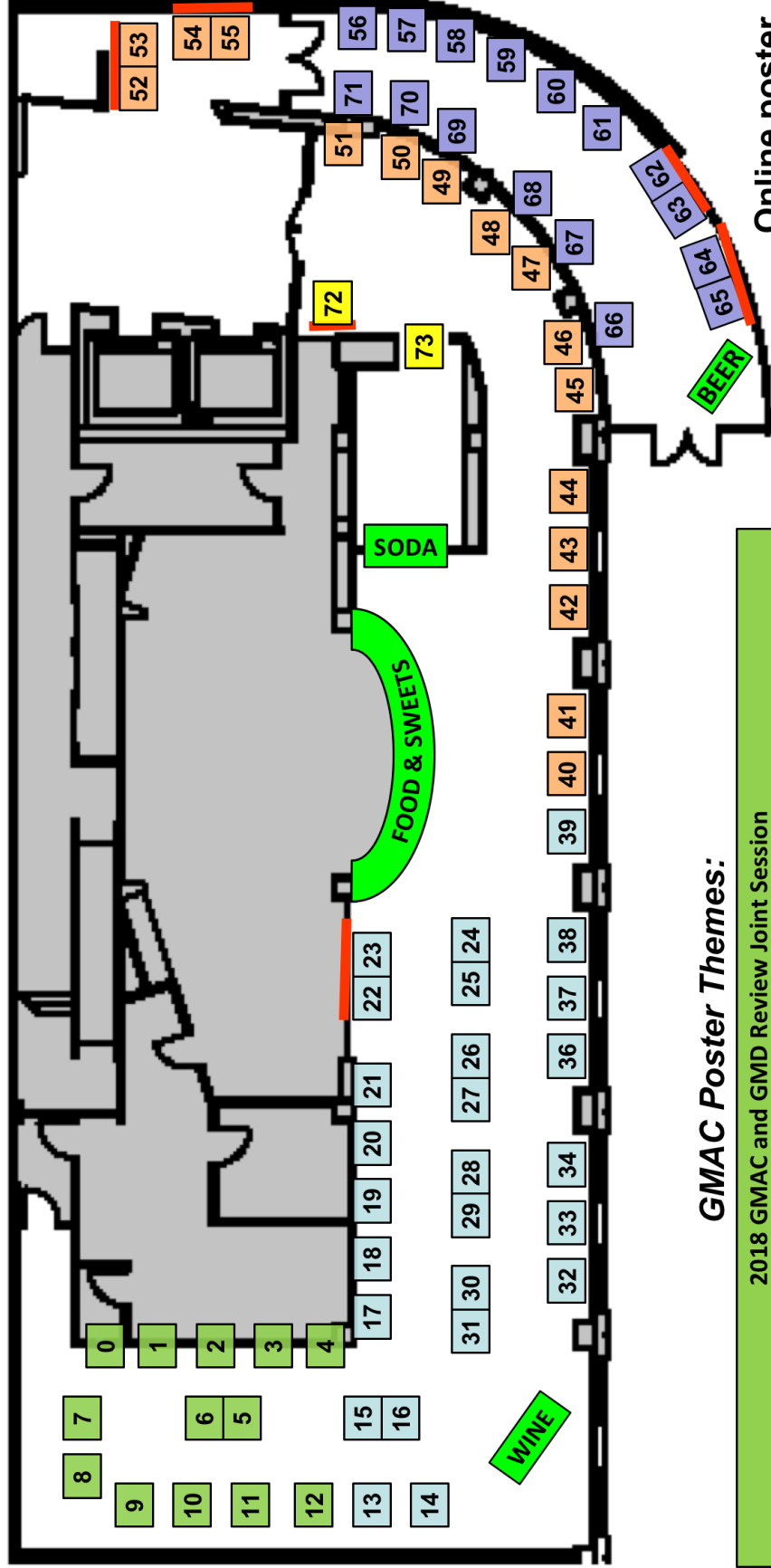
- P-58 Stratospheric Temperature Corrections and Improvement of Total Column Ozone Records in the NOAA Dobson Ozone Spectrophotometer Network
Glen McConville (Cooperative Institute for Research in Environmental Sciences (CIRES), University of Colorado)
- P-59 Uncertainty Improvement Optimized using the GMI Model for Umkehr Ozone Profile Retrieval
Koji Miyagawa (Guest Scientist at NOAA Earth System Research Laboratory, Global Monitoring Division (GMD))
- P-60 An Evaluation of C₁-C₃ Hydrochlorofluorocarbon (HCFC) Metrics: Lifetimes, Ozone Depletion Potentials, Radiative Efficiencies, Global Warming and Global Temperature Potentials
James Burkholder (NOAA Earth System Research Laboratory, Chemical Sciences Division (CSD))
- P-61 Chloroform Emissions Estimated with the CarbonTracker-Lagrange North American Regional Inversion Framework
Geoff Dutton (NOAA Earth System Research Laboratory, Global Monitoring Division (GMD))
- P-62 Using Observations of SF₆ to Examine Inter-annual Variations in Inter-hemispheric Exchange
Brad D. Hall (NOAA Earth System Research Laboratory, Global Monitoring Division (GMD))
- P-63 Increased Propane Emissions from the United States over the Last Decade
Lei Hu (Cooperative Institute for Research in Environmental Sciences (CIRES), University of Colorado)
- P-64 Using Carbonyl Sulfide to Explore Coastal Fog and Coast Redwood Interdependence
Timothy W. Hilton (University of California at Merced)
- P-65 NO_x Emissions from Switch Yard Locomotives Observed with the TRAX Air Quality Platform
Logan Mitchell (University of Utah)
- P-66 Advantages and Limitations of Measuring BTEX with a Commercial GC-PID System *In Situ*
Monica Madronich (Cooperative Institute for Research in Environmental Sciences (CIRES), University of Colorado)
- P-67 One Year of AOD, Halogen Radicals, OVOCs, H₂O and NO₂ Measurements at Mauna Loa Observatory
Barbara Dix (University of Colorado, Department of Chemistry and Biochemistry)
- P-68 Toward a High Degree of Freedom Full Atmosphere Retrieval of BrO Profiles from MAX-DOAS Instruments on Remote Tropical Marine Mountaintops
Theodore Koenig (University of Colorado, Department of Chemistry and Biochemistry)
- P-69 Contrasting Behavior of Inert and Photochemically Reactive Gases during the August 21, 2017, Solar Eclipse at the Boulder Reservoir
Detlev Helmig (Institute of Arctic and Alpine Research (INSTAAR), University of Colorado)
- P-70 Combining Observations and Multiple Models for an Improved Estimate of the Global Surface Ozone Distribution
Kai-Lan Chang (National Research Council Post-Doc)
- P-71 Changing Conditions in the Arctic: An Analysis of Trends in Observed Surface Ozone Conditions
Audra McClure-Begley (Cooperative Institute for Research in Environmental Sciences (CIRES), University of Colorado)

Technology

- P-72 Online Inclusion of Chemical Modules Into NOAA's Next Generation Global Prediction System (NGGPS)
Li Zhang (Cooperative Institute for Research in Environmental Sciences (CIRES), University of Colorado)
- P-73 SOS ExplorerTM: Interactive Visualizations for Museums and Classrooms
Eric Hackathorn (NOAA Earth System Research Laboratory, Global Systems Division (GSD))

2018 GMAC Poster Session

May 22nd, 5:00 – 7:30pm



GMAC Poster Themes:

| |
|--|
| 2018 GMAC and GMD Review Joint Session |
| Tracking Greenhouse Gases and Understanding Carbon Cycle Feedbacks |
| Monitoring and Understanding Changes in Surface Radiation, Clouds, and Aerosol Distributions |
| Guiding Recovery of Stratospheric Ozone and Other Topics |
| Technology |
| Food and Drink |

Online poster agenda available:



Evaluating the Impact of Baseline Ozone in California using Ozone-Sonde Measurements at Trinidad Head, CA (THD): Overview

T. Kuwayama¹, J. Xu¹, J.C. Borgeld², M. Ives², I. Petropavlovskikh^{3,4}, J.H. Butler⁴ and B. Croes¹

¹California Air Resources Board, Sacramento, CA 95812; 916-324-9287, E-mail: toshihiro.kuwayama@arb.ca.gov

²Humboldt State University, Department of Oceanography, Arcata, CA 95521

³Cooperative Institute for Research in Environmental Sciences (CIRES), University of Colorado, Boulder, CO 80309

⁴NOAA Earth System Research Laboratory, Global Monitoring Division (GMD), Boulder, CO 80305

In 2015, the Environmental Protection Agency (EPA) revised the 8-hour ozone (O₃) National Ambient Air Quality Standard (NAAQS) to 70 parts-per-billion (ppb). Previous studies in California have documented instances in which downward mixing of baseline O₃ aloft contributed to surface O₃ levels that exceeded this new O₃ threshold. In many cases, baseline O₃ entering California can frequently exceed 60 ppb. Since baseline O₃ is not governed by O₃ precursor emissions within the State, attainment of 8-hour O₃ NAAQS in environmentally sensitive areas can become even more challenging under certain meteorological and environmental conditions that allow surface O₃ levels to be influenced by long-range transported O₃. Information on baseline O₃ is becoming more important as the gap between O₃ standard and baseline O₃ levels diminish. The Ozone-Sonde dataset at Trinidad Head, CA (THD) contains the most temporally comprehensive vertical O₃ profile measurements in California and provides extensive information on the baseline O₃ that travel into the west coast. In order to determine the potential impact of baseline O₃ on surface air quality, the California Air Resources Board (CARB), air quality management districts (AQMD), and atmospheric sciences community are evaluating the magnitude and the temporal variation of baseline O₃ using the THD data. The information is also being used to improve regional air quality and global transport models. This poster presentation highlights the criticality of continued Ozone-Sonde measurements at THD and how the information is currently being used to support the State's air quality research and the development of future State Implementation Plans.



Figure 1. Trinidad Head and the town of Trinidad, CA from Luffenholz Beach.

Global Atmosphere Watch Programme: the Role of the National Programmes in Supporting the Global Value Chain

O. Tarasova

World Meteorological Organisation, Geneva, Switzerland; +41-22-730-8169, E-mail: otarasova@wmo.int

The Global Atmosphere Watch Programme (GAW) is the research programme of the World Meteorological Organisation (WMO) that provides a long-term international framework for integrated observations, analysis, and assessment of atmospheric chemical composition. The programme is a collaboration of more than 100 countries and it relies fundamentally on the contributions of its Members to help build a single, coordinated global understanding of atmospheric composition and its change. The mission of GAW and the key implementation principles are described in the “WMO Global Atmosphere Watch (GAW) Implementation Plan: 2016 – 2023”. The vision for the next decade of GAW is to grow the international network of high-quality atmospheric observations across local to global scales to drive high quality and impact science while co-producing a new generation of research-enabled products and services.

The research activities of GAW are supported by a dedicated infrastructure, which includes observing systems supplemented by a set of Central Facilities supporting the quality assurance system, a data management system, advisory groups, expert teams, and a steering committee (Fig.1). To address the needs of the countries related to diverse environmental issues, GAW currently focuses on six groups of variables (also called focal areas): greenhouse gases, ozone, aerosol, selected reactive gases, total atmospheric deposition, and solar ultraviolet (UV) radiation. Cross-cutting activities related to the development of regional and global scale atmospheric composition forecasting are addressed by the dedicated Scientific Advisory Group (SAG) on Applications, while similar activities on the urban scale are addressed by the SAG of the GAW Urban Research Meteorology and Environment (GURME) project.

National programmes, like the one operated by the ESRL/GMD, provide an essential contribution to the success of GAW at all steps of the value chain from observations through quality assurance to the delivery of integrated products and capacity development. In recognition of the highest measurement quality of the NOAA-operated observational networks, several of them are recognized as baseline networks of the Global Climate Observing System. ESRL/GMD operates a number of the global central facilities that allow having globally compatible observations. GMD supports global research related to the evaluation of sources and sinks as well as trends and global distributions of a number of atmospheric constituents relevant to climate and regional air quality. The value of the different ESRL/GMD contributions in the GAW Programme will be described in the presentation.

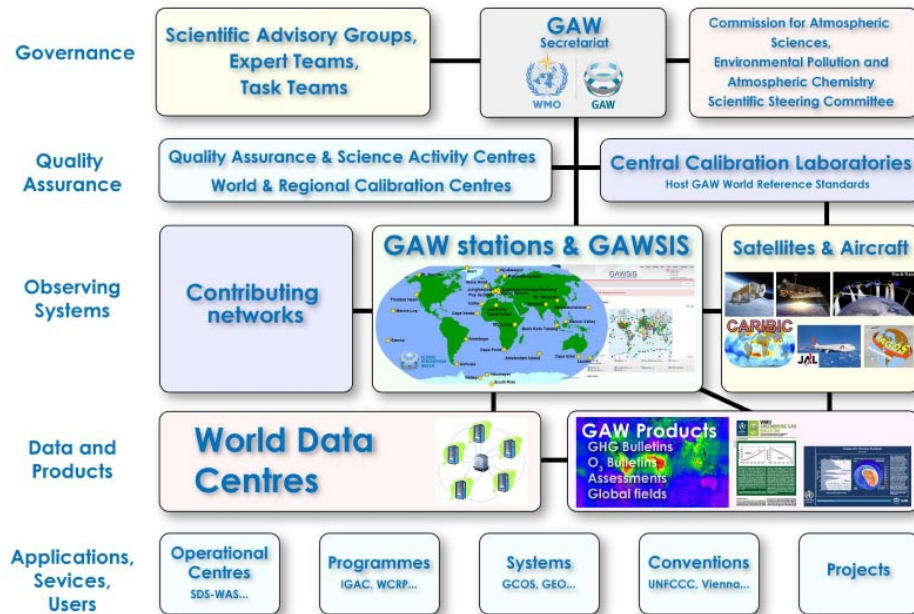


Figure 1. Components of the WMO/GAW Programme.

The Radon Measurement Programs at Cape Grim, Mauna Loa, and other Global Atmospheric Monitoring Sites

A.G. Williams, S.D. Chambers, O. Sisoutham, S. Werczynski and A.D. Griffiths

Australian Nuclear Science and Technology Organisation (ANSTO), Lucas Heights, Australia; +61-2-9717-3694, E-mail: agw@ansto.gov.au

Measurement of radon-222 at international monitoring sites aids in the interpretation of changes in atmospheric composition, tracking of movements in greenhouse gases and other trace species, and the evaluation of regional and global transport models. As radon provides an unambiguous indication of the degree of recent terrestrial influences on an air mass, it is an ideal tracer for a range of applications at baseline, high-elevation, and remote stations such as the Cape Grim Baseline Air Pollution Station (CGBAPS) in Tasmania. The Cape Grim Radon Program, operated jointly by the Australian Nuclear Science and Technology Organisation (ANSTO) and the Australian Bureau of Meteorology, is one of the premier atmospheric radon monitoring programs worldwide. The dual-flow-loop, two-filter detector design pioneered by ANSTO scientists is recognized within the WMO Global Atmosphere Watch (WMO-GAW) community as providing the international benchmark in radon monitoring for global and regional atmospheric composition studies, and the detectors used at CGBAPS are specifically designed to meet stringent requirements for accuracy and reliability at this demanding location.

ANSTO's radon group extends its contribution to WMO-GAW science by participating in other GAW-related observational programs. By forming and maintaining partnerships with leading international players such as Earth System Research Laboratory Global Monitoring Division (ESRL/GMD), we have been able to collaboratively operate a number of long-term radon measurement programs at other major stations in the WMO-GAW network. As a result of such arrangements, multi-year radon data sets are available from the Mauna Loa Observatory in Hawaii (ESRL/GMD), Cape Point in South Africa (SAWS), Gosan in Korea (Jeju Uni), and Jungfraujoch in the Swiss Alps (Uni Basel). In recent years, there has also been an effort to "fill gaps" in the coverage of radon observations in data-poor regions of the Southern Hemisphere, by establishing new measurement programs at existing and newly-established GAW stations. Collaborations with the Australian Antarctic Division, Commonwealth Scientific and Industrial Research Organisation (CSIRO), and the Korean Polar Research Institute have led to the establishment of radon programs at Macquarie Island, aboard the *RV Investigator*, and two sites on the Antarctic coastline.

The ongoing fruitful relationships between ANSTO and its many partners within the WMO-GAW community have enabled the development of new applications for radon in the atmospheric sciences, and allowed participation in a large number of productive collaborative research studies using radon data from Cape Grim, Mauna Loa, and other GAW-related stations.

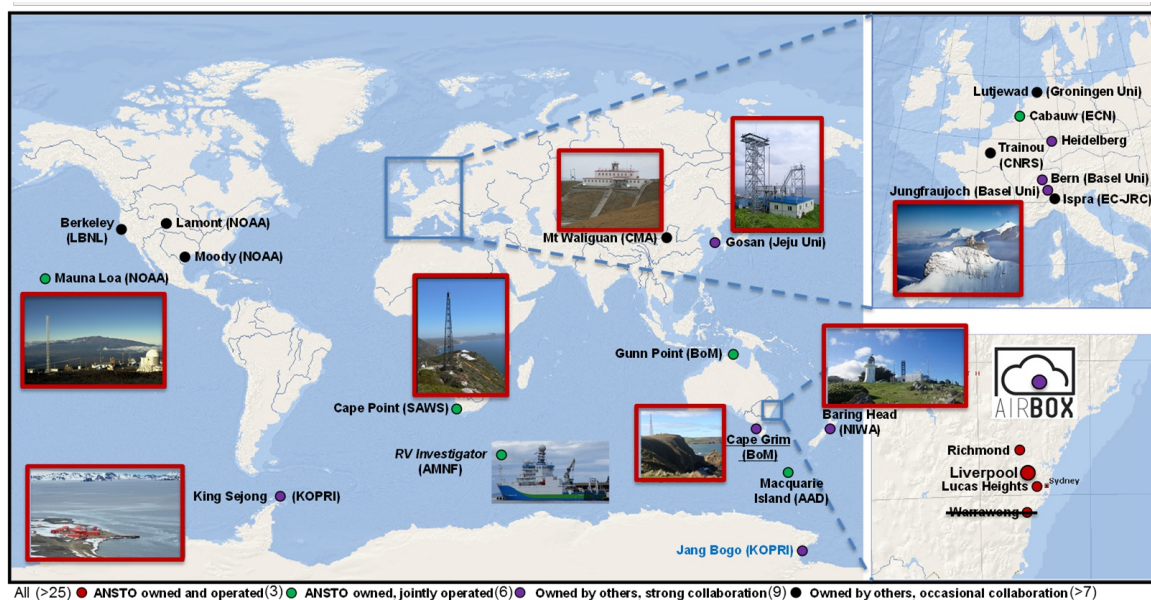


Figure 1. Global network of ANSTO-built dual-flow-loop two-filter radon detectors. WMO-GAW baseline stations are indicated by photos with red borders.

NOAA and U.S. Department of Energy/Office of Science Cooperative Efforts in Barrow (Utqiagvik), Alaska

M. Ivey

Sandia National Laboratories, Albuquerque, NM 87185; 505-284-9092, E-mail: mdivey@sandia.gov

ESRL/GMD and the U.S. Department of Energy (DOE) have collaborated at the Barrow Atmospheric Baseline Observatory (BRW) (Utqiagvik), Alaska research site for almost two decades. Our collaborative partnership with the Earth System Research Laboratory (ESRL) Global Monitoring Division (GMD) at Barrow is critical to the mission success of the DOE Atmospheric Radiation Measurement (ARM) facility located just a few hundred meters from the ESRL/GMD/BRW Observatory. The DOE/ARM program relies on BRW for many observational data sets, for operational assistance, for shelter for instruments including aerosol instruments, and for a close partnership on logistics in Utqiagvik. During this current winter (2017), that partnership included a combined effort to deal with record snows at the joint facilities. NOAA and DOE have many active and formal partnerships, including those roles described in the Interagency Arctic Research Policy Committee (IARPC) 2017-2021 Five-Year Research Plan.



Figure 1. Clearing snow from outside the DOE/ARM facility.



Figure 2. Snow drift heights winter 2017.

Ozone, Aerosols and Carbon Gases at the Mt. Bachelor Observatory

D. Jaffe¹, J. Laing¹, P. Sheridan², A.E. Andrews², B. Andrews^{3,2}, I. Petropavlovskikh^{3,2}, A. McClure^{3,2} and J. Kofler^{3,2}

¹University of Washington, Seattle, WA 98105; 425-352-5357, E-mail: djaffe@uw.edu

²NOAA Earth System Research Laboratory, Global Monitoring Division (GMD), Boulder, CO 80305

³Cooperative Institute for Research in Environmental Sciences (CIRES), University of Colorado, Boulder, CO 80309

The Mt. Bachelor Observatory is a high elevation (2.8 km asl) research site located on the summit of Mt. Bachelor in Central Oregon and is an ideal location to capture background/baseline air entering North America. The site was started by the University of Washington in 2004, with a focus on ozone (O_3), aerosols, mercury (Hg), and related trace species. The figure below shows an aerial view of Mt Bachelor. Over the past 15 years our research has focused on sources, chemistry, and transport associated with O_3 , aerosols, carbon gases, Hg, and related trace species. In 2011, we started a collaboration with the ESRL/GMD Carbon Cycle and Greenhouse Gas group and in 2018, we began collaborations with the GMD Aerosol and Ozone and Water Vapor groups. With these collaborations, we hope to ensure the site is available for long-term data collection.

In this presentation I will focus on some of our newest results including:

1. Relationship between carbon cycle gases, O_3 , aerosols, and transport patterns.
2. Aerosol size distributions in biomass burning plumes.
3. Observations of aerosol absorption and black carbon in biomass burning plumes.
4. New statistical approach to understand O_3 in the free troposphere.



Figure 1. Mt. Bachelor located in Central Oregon (2.8 km asl). Photo by Randy Hopfer.

Black Carbon Mass Observations across Canada (2006-2015): Constraining on Regional Emissions in North America

L. Huang, T. Chan, K. VonSalzen., R. Leitch, S. Sharma, W. Zhang, D. Ernst, J. Zhang, M. Moran, J. Brook, A.M. Macdonald and M. Wheeler

Environment and Climate Change Canada, Toronto, Ontario, Canada; 416-739-5821, E-mail: lin.huang@canada.ca

Black carbon (BC) plays an important role in Earth’s climate system from regional to global scales. To contribute to the evaluation of models, which may help constrain regional and global emissions, an observation network of aerosol elemental carbon (EC) as BC mass has been strategically established across Canada since 2006. The sites represent different geographic regions with various continental source influences, including: urban (Toronto, ON), rural (Egbert, ON), boreal forest (Fraserdale, ON, East Trout Lake, SK), high elevation (Whistler Mt., BC), and a remote Arctic region (Alert, NU). Because of its short atmospheric lifetime, changes in atmospheric EC concentration (specifically those observed in seasonal and inter-annual variability) largely reflect the changes of emission source influences at regional scales; although, the impacts of long-range transport should not be underestimated.

Weekly integrated quartz filter samples collected at these sites have been analyzed for EC concentrations over the period of 2006 to 2015. Seasonal patterns and inter-annual variability of BC mass have been observed. In comparison with several recently-published emission inventories, including the historic Intergovernmental Panel on Climate Change (IPCC) emissions of BC for Coupled Model Intercomparison Project 6th phase (CMIP6) and Canada /U.S. particulate matter 2.5 (PM2.5) emissions, it is shown that the trends observed at the sites in eastern Canada (e.g., Toronto, and Egbert, ON) are dominated by anthropogenic emission changes and the influence of U.S. emissions on the trends may be more significant than Canadian emissions. Whereas that the seasonal pattern and inter-annual variability observed at the sites in western Canada have been influenced much more by biomass burning events. The decreasing trends (2006-2015) in eastern Canada would imply beneficial effects from clean air policies both in the U.S. (Clean Air Act) and Canada (Clean Air Regulatory Agenda). However, there are inconsistencies in seasonal patterns between the observations in eastern Canada and the regional emissions inventories in North America. That raises questions and may suggest a possible pathway on constraining the seasonal profile of BC emissions in North America via observations.

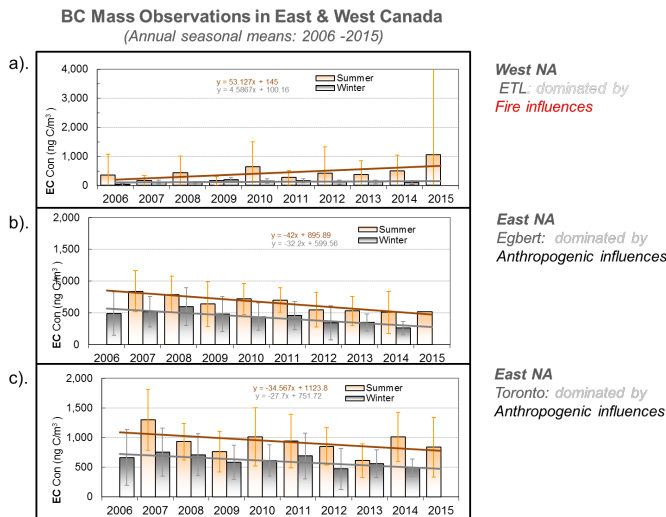


Figure 1. BC mass observations at representative sites in East and West Canada (2005-2016). Orange bars: warm seasons (May-Oct); Gray bars: cold seasons (Nov-Apr).
 a) East Trout Lake (ETL), SK; b) Egbert, ON;
 c) Toronto, ON

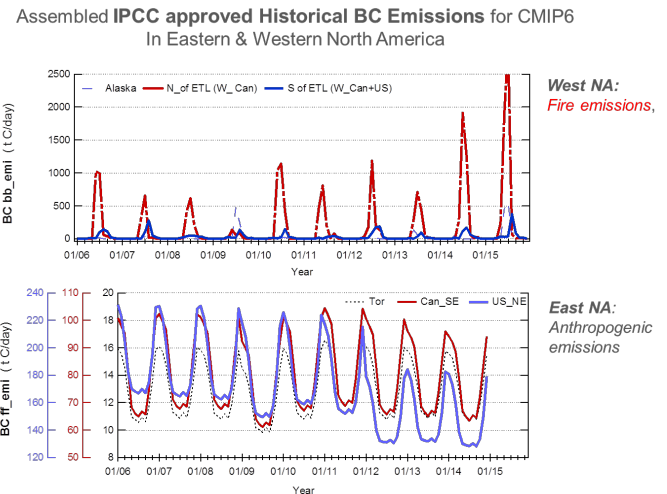


Figure 2. Regional assembled BC emissions (IPCC approved for CMIP6) in Eastern & Western North America (NA). Top panel: BC emissions from fires in Western NA; bottom panel: BC emission from anthropogenic emission in Eastern NA.

Aerosol Hygroscopicity during the Haze Red Alert Period in Winter 2016 at a Rural Site of the North China

X. Qi¹, J. Sun¹, L. Zhang¹, X. Shen¹, X. Zhang¹, Y. Zhang¹, Y. Wang¹, H. Che¹, Z. Zhang¹, J. Zhong¹, K. Tan², H. Zhao² and S. Ren²

¹Chinese Academy of Meteorological Sciences, Key Laboratory of Atmospheric Chemistry of CMA, Beijing, China; 86-10-6840-7943, E-mail: jysun@cma.gov.cn

²Integrated Ecological–Meteorological Observation and Experimental Station, Chinese Academy of Meteorological Sciences, Beijing 100081

Aerosol hygroscopic growth reflects the effect of relative humidity (RH) on the physical and chemical properties of the particles, which is one of the important properties of aerosols. A humidification system was deployed to measure aerosol hygroscopicity at a rural site of the North China Plain during the haze red-alert period 17–22 December 2016. The aerosol scattering coefficients under dry (RH<30%) and wet (RH in the range of 40%–85%) conditions were simultaneously measured at wavelengths of 450, 550, and 700 nm. Scattering enhancement factor $f(80\%)$ and backscattering enhancement factor $f_b(80\%)$ showed a negative correlation with the percentage of organics and a positive correlation with that of inorganics. There are similar trends for $f(80\%)$ and $f_b(80\%)$ but with different magnitudes. The $f(80\%)$ ranged from 1.12 to 1.62 with an average of 1.29, while $f_b(80\%)$ varied from 1.02 to 1.24, with an average of 1.10. Both $f(80\%)$ and $f_b(80\%)$ showed a diurnal pattern that peaked in the late afternoon (approximately 1400 LT), especially during the first 3 days. Aerosol hygroscopicity is highly dependent on the aerosol chemical composition. The fraction of nitrate was strongly correlated with the aerosol scattering coefficient at RH = 80%, which suggests that nitrate played an important role in aerosol hygroscopic growth during the heavy pollution period. The scattering enhancement factors do not show significant differences at the three wavelengths. Only an approximate 2% shift to higher $f(80\%)$ values with a larger standard deviation was observed as the wavelength increased, which is similar for the backscatter enhancement factors. Therefore, only slight spectral dependency of $f(\text{RH})$ was observed during the red-alert period.

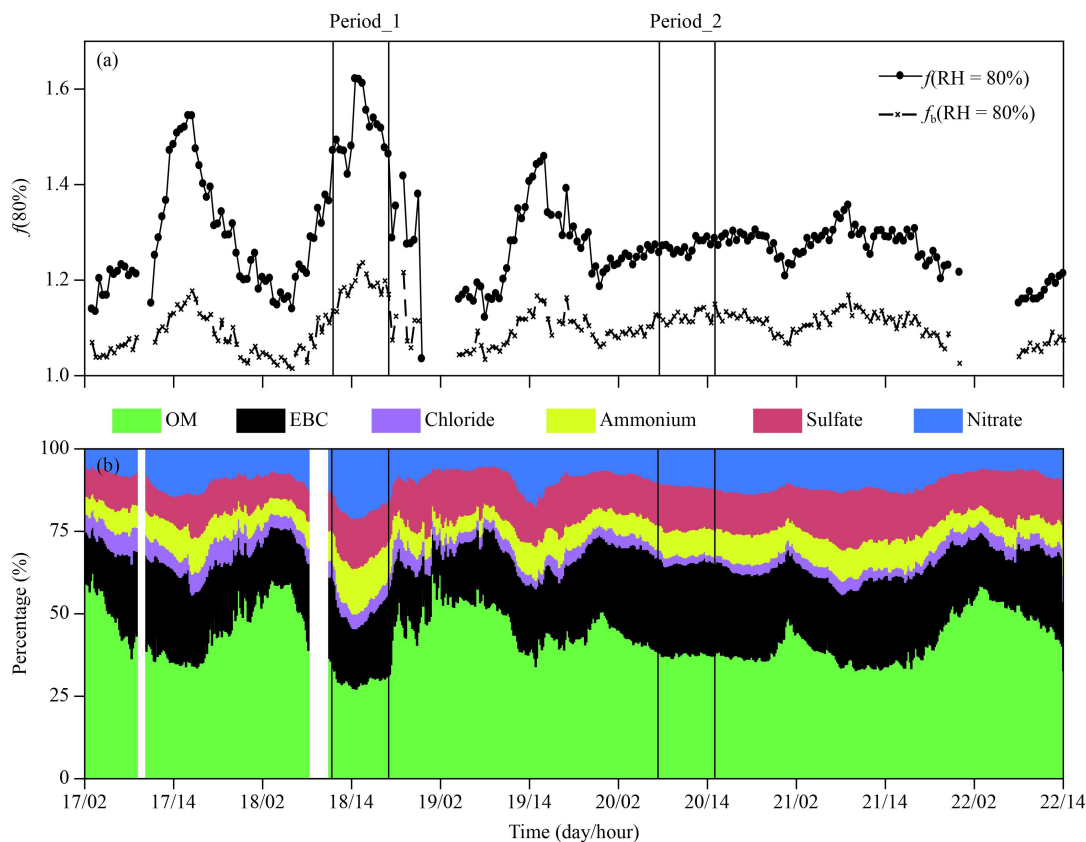


Figure 1. Time series of the (a) scattering enhancement factor $f(80\%)$ and backscattering enhancement factor $f_b(80\%)$, and (b) percentage of mass concentration of aerosol chemical composition. Two periods are defined: period_1 from 11:00 to 19:00 (Beijing Time) 18 December and period_2 from 07:00 to 15:00 20 December 2016.

Using SURFRAD Aerosol Optical Depth Measurements for Model Evaluation. A Study with FV3-GOCART and WRF-Chem and Their Assimilation Systems

M. Pagowski^{1,2}, A. McComiskey³ and J. Augustine³

¹NOAA Earth System Research Laboratory, Global Systems Division (GSD), Boulder, CO 80305; 303-497-6443, E-mail: mariusz.pagowski@noaa.gov

²Cooperative Institute for Research in Environmental Sciences (CIRES), University of Colorado, Boulder, CO 80309

³NOAA Earth System Research Laboratory, Global Monitoring Division (GMD), Boulder, CO 80305

In 2016 NOAA chose the FV3 dynamical core as a basis for its future global modeling system. First, we present the implementation of the aerosol module in the FV3 model and its assimilation framework. The parameterization of aerosols is based on the GOCART scheme. The assimilation methodology relies on the Ensemble Kalman Filter (EnKF) approach. Aerosol observations include de-biased aerosol optical depth at 550 nm from MODIS satellite and AERONET. The simulations are performed at C192 resolution (approx. 50 km) for August 2015 when significant wildfires over North America occurred. In parallel, simulations for that period are performed using the WRF-Chem model with 3D-Var based 550 nm aerosol optical depth (AOD) assimilation at 20 km resolution.

Results and evaluation of the systems against SURFRAD AOD measurements at different wavelengths as well as Visible Infrared Imaging Radiometer Suite (VIIRS) AOD retrievals are shown.

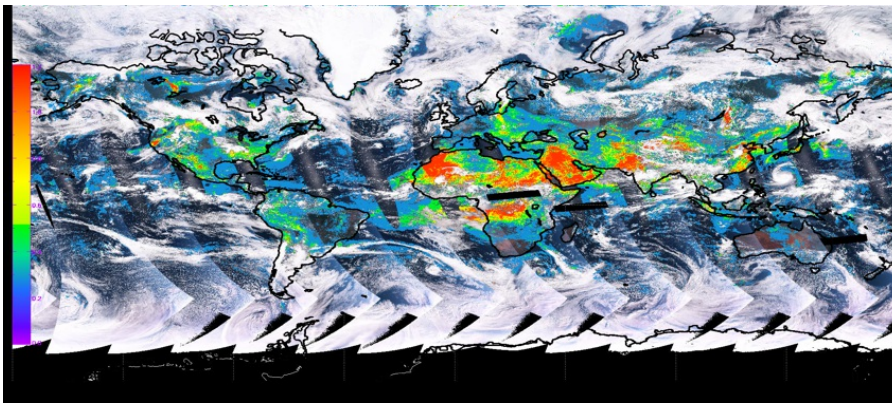


Figure 1. AOD 550 nm from VIIRS retrievals on 20150805.

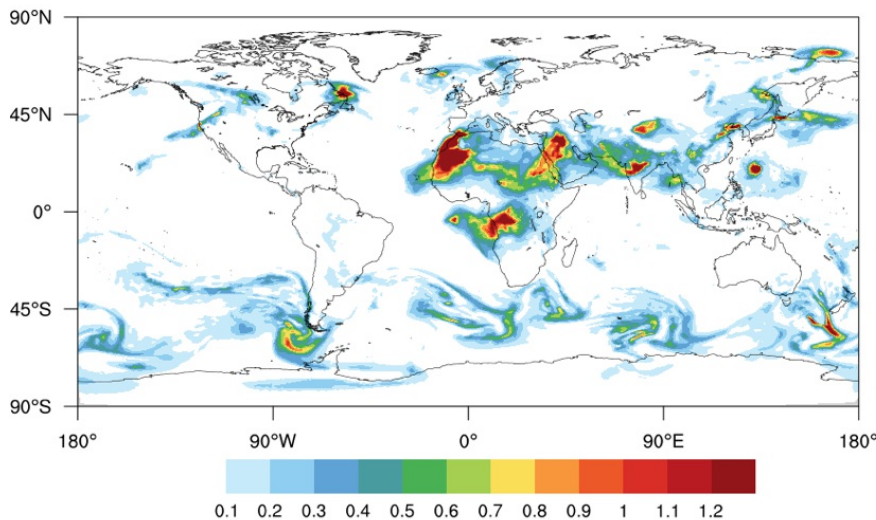


Figure 2. FV3/EnKF assimilation of de-biased MODIS retrievals at 2015080512.

TCCON Updates and Improvements to Precision Requirements

C. Roehl¹, M. Kiel¹, P. Wennberg¹, D. Wunch¹, J. Mendonca² and S. Roche²

¹California Institute of Technology, Pasadena, CA 91125; 626-395-2472, E-mail: coleen@gps.caltech.edu

²University of Toronto, Toronto, Ontario, Canada

The Total Carbon Column Observing Network (TCCON), which is currently made up of 26 sites, internationally, is a well-established network of ground-based Fourier Transform Spectrometers that record direct solar spectra in the near-infrared. Accurate and precise column-averaged abundances of carbon dioxide (CO₂) (as well as of other atmospheric constituents - methane [CH₄], nitrous oxide [N₂O], hydrogen fluoride [HF], carbon monoxide [CO], water [H₂O], and semi-heavy water [HDO]) are retrieved from these spectra. Dating back to 2004, TCCON data have already proven to be valuable in providing ground truth for satellite measurements of CO₂ and CH₄ column abundances and in evaluating large-scale carbon models and improving global estimates of the sources and sinks of CO₂ and CH₄. In this work, we will briefly describe developments to the TCCON network over the past year, including the most up to date CO₂ and CH₄ time series, the introduction of new network sites, and the extended measurement capabilities into the mid-IR at several sites. In addition, we will highlight ongoing efforts to reduce errors / improve precision of the TCCON results through a number of changes to the GGG retrieval software.



Figure 1. Since the installation of the first station in Park Falls, WI in May, 2004, the Total Carbon Column Observing Network (TCCON) has grown to over 26 sites worldwide with 4 future sites in the planning.

Engaging Agencies and the Public in Atmospheric Monitoring Observations Through Real-time Data Posting

D. Helmig¹, B. Blanchard¹, J. Hueber¹, P. Milmo² and C. Copeland²

¹Institute of Arctic and Alpine Research (INSTAAR), University of Colorado, Boulder, CO 80309; 303-492-2509, E-mail: detlev.helmig@colorado.edu

²Boulder County Public Health Department, Boulder, CO 80304

The influx of oil and natural gas development into densely-populated areas has raised citizens' concerns about air quality and resulting health impacts of emissions from these operations. This has prompted local governments to seek help in monitoring oil and gas pollutants for assessing citizens' exposures and associated risks. Sponsored by Boulder County Public Health, we developed and installed high time resolution monitoring of methane, volatile organic compounds (VOCs), and nitrogen oxides at the Boulder Reservoir. Automated chromatograms integration, calibration, and data processing routines were implemented, and data are posted in near real-time on a public website (http://instaar.colorado.edu/arl/boulder_reservoir.html), with additional educational information on the monitored gases and interpretation of results. Methane and light alkane VOC show a strong influence from oil and natural gas sources in the north to southeast of the site. Transport events with elevated levels of VOC, exceeding background levels by 20-100 times, are frequently observed. Mean annual concentrations for many VOCs exceed those of large U.S. urban areas. This monitoring and sharing of real-time results has been instrumental in raising the interest of citizens, and making this monitoring a viable source of information for use by agencies, citizen groups, and the media. This is further evidenced by the close to 10,000 visits to the public website during the first year of operation.

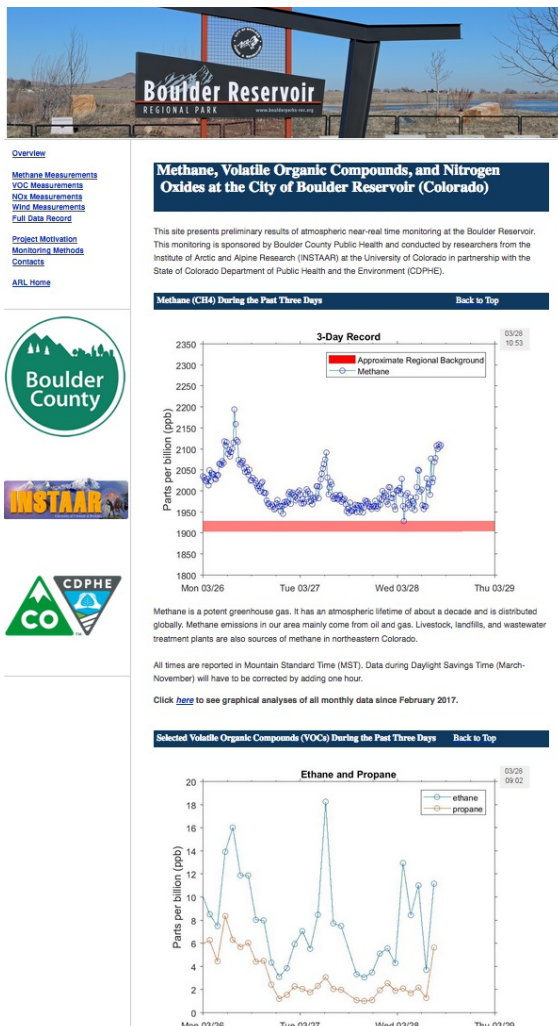


Figure 1. Data available in near real-time at http://instaar.colorado.edu/arl/boulder_reservoir.html.

The Importance of Ozonesonde Quality Assurance and JOSIE-SHADOZ (2017)

J.C. Witte^{1,2}, H.G.J. Smit³, R.M. Stauffer^{4,2}, B.J. Johnson⁵ and P. Cullis^{6,5}

¹Science Systems and Applications, Inc. (SSAI), Lanham, MD 20706; 301-614-5991, E-mail: jacquelyn.witte@nasa.gov

²NASA Goddard Space Flight Center (GSFC), Atmospheric Chemistry and Dynamics Laboratory, Greenbelt, MD 20771

³Institute of Chemistry and Dynamics of the Geosphere: Troposphere, Research Centre Juelich, Germany

⁴Universities Space Research Association (USRA) - NASA Postdoctoral Program (NPP), Columbia, MD 21046

⁵NOAA Earth System Research Laboratory, Global Monitoring Division (GMD), Boulder, CO 80305

⁶Cooperative Institute for Research in Environmental Sciences (CIRES), University of Colorado, Boulder, CO 80309

The ozonesonde is a small balloon-borne instrument that is attached to a standard radiosonde to measure profiles of ozone from the surface to 35 km with 100-m vertical resolution. Ozonesonde data constitute a mainstay of satellite calibration and model climatologies. Sonde profiles have been used for analysis of trends in the lower stratosphere where satellites can be problematic. The electrochemical-concentration cell ozonesonde has been used at ~100 stations worldwide for about 50 years. Because the instrument has undergone changes in manufacture and operating procedures over that time, there can be biases at different stations and discontinuities in profile time-series from individual site records. For 20 years the Juelich [Germany] Ozonesonde Intercomparison Experiment (JOSIE) has periodically tested ozonesondes in a simulation chamber designed as the World Calibration Centre for Ozonesondes by the World Meteorological Organization. In October-November 2017 NASA and ESRL/GMD sonde researchers helped lead a special JOSIE campaign to evaluate the sondes and procedures used in Southern Hemisphere Additional Ozonesondes (SHADOZ), a 14-station sonde network operating in the tropics and subtropics. Experimental protocol for the SHADOZ sonde configurations, which represent most of those in use today, are described, along with preliminary results. In terms of total column ozone, all SHADOZ stations, four of which follow the ESRL/GMD protocol, fall within 3-4% of the reference instrument in JOSIE.

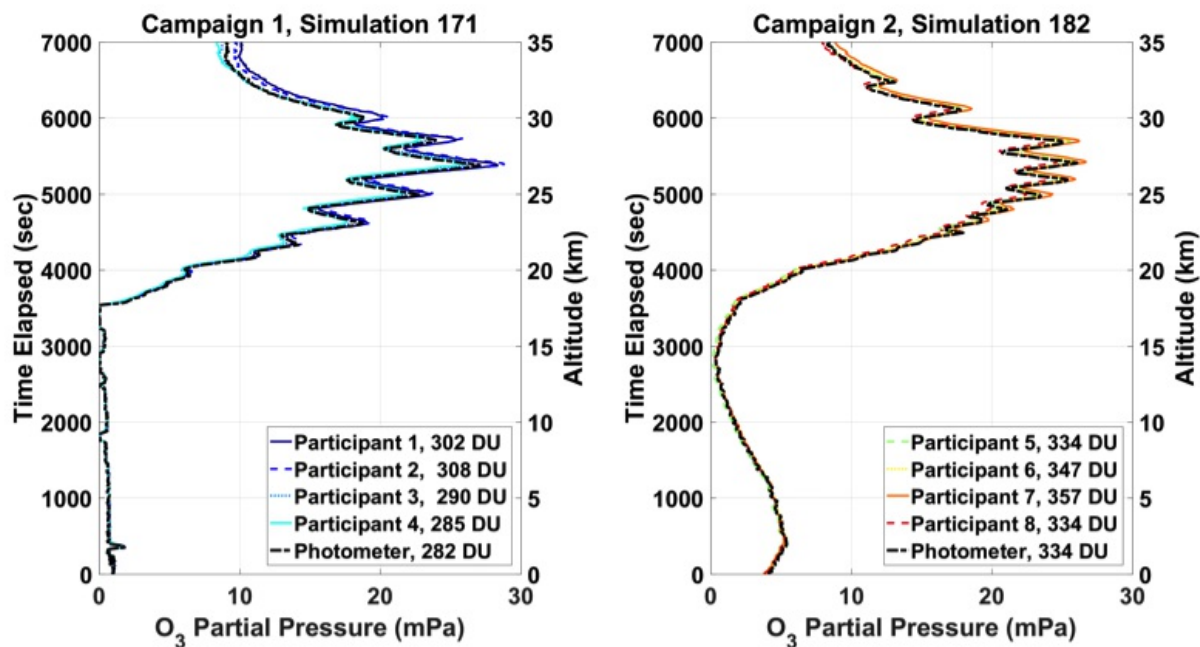


Figure 1. An example of two chamber simulations of ozone profiles representing the eight SHADOZ stations versus the world standard ozone photometer (black dashed).

The Evolving Role of Space-based Measurements in a Global Carbon Monitoring System

D. Crisp and C. Miller

NASA Jet Propulsion Laboratory, California Institute of Technology, Pasadena, CA 91109; 818-687-9939, E-mail: david.crisp@jpl.nasa.gov

Early flux inversion studies indicated that space-based observations of column-averaged dry-air mole fractions of carbon dioxide (X_{CO_2}) with accuracies of 1 ppm on regional scales at monthly intervals could substantially improve our understanding of carbon dioxide (CO_2) sources and sinks. Recent products from the OCO-2 mission are meeting or exceeding this target. In spite of this progress, and that anticipated from the growing fleet of greenhouse gas (GHG) missions, improvements in measurement accuracy, precision, resolution, and coverage are still needed to deliver timely information about CO_2 sources and sinks on the scale of individual nations or to track subtle trends in the natural carbon cycle resulting from climate change. Spatially- and temporally-correlated X_{CO_2} biases must be reduced to vanishingly-small values ($\ll 1$ ppm) to enable accurate local to regional scale CO_2 flux inversions. Greater single-sounding precision is needed to quantify trends in emissions from localized sources such as mega cities and power plants. Higher spatial and temporal resolution is needed to isolate discrete sources and sinks and to track their variations over diurnal to seasonal time scales. Improved coverage is needed, especially at high northern latitudes of the winter hemisphere and in tropical regions covered by persistent, optically-thick clouds. Some of these needs will require improved space-based instruments, calibration techniques, X_{CO_2} retrieval algorithms, validation capabilities, and flux inversion strategies. Others must be addressed by carefully coordinating the available space-based, aircraft, and ground-based sensors to produce a more effective GHG monitoring system. This presentation will summarize the progress and plans in these areas.



Figure 1. Currently operating GHG satellites: Greenhouse Gases Observing Satellite (GOSAT), OCO-2, TanSat, Sentinel-5p, FengYun 3D, and Gaofen-5.

| Mission (Agency) | CO ₂ | CH ₄ | FOV | Orbit | 2012 | 2013 | 2014 | 2015 | 2016 | 2017 | 2018 | 2019 | 2020 | 2021 | 2022 | 2023 | 2024 | 2025 | 2026 |
|---------------------------------|-----------------|-----------------|-------------------------|----------------------|------|------|------|------|------|------|------|------|------|------|------|------|------|------|------|
| ENVISAT SCIAMACHY (ESA) | • | • | 30x60 km ² | SS LEO (10:30) | | | | | | | | | | | | | | | |
| GOSAT TANSO-FTS (JAXA-NIES-MO) | • | • | 10km (d) | SS LEO (13:00) | | | | | | | | | | | | | | | |
| OCO-2 (NASA) | • | | 1.25x2.25 km | SS LEO (13:00) | | | | | | | | | | | | | | | |
| TanSat CDS (CAS-MOST-CMA) | • | | 2x2 km ² | SS LEO (13:30) | | | | | | | | | | | | | | | |
| Sentinel 5P TROPOMI (ESA) | | • | 7x7 km ² | SS LEO (13:30) | | | | | | | | | | | | | | | |
| Feng Yun 3D GAMI (CMA, NRSCC) | • | • | 10 km (d) | SS LEO (14:00) | | | | | | | | | | | | | | | |
| Gaofen 5 GMI (CNSA) | • | • | 10.5 km (d) | SS LEO (10:30) | | | | | | | | | | | | | | | |
| GOSAT-2 TANSO FTS (JAXA-NIES-M) | • | • | 9.7 (d) | SS LEO (13:00) | | | | | | | | | | | | | | | |
| OCO-3 (NASA) | • | | 0.7x2.6 km ² | LEO (51.6° incl.) | | | | | | | | | | | | | | | |
| MicroCarb (CNES) | • | | 4.5x9 km ² | SS LEO (13:30) | | | | | | | | | | | | | | | |
| MERLIN (DLR-CNES) | | • | 0.135 km (w) | SS LEO (06:00/18:00) | | | | | | | | | | | | | | | |
| GeoCarb (NASA) | • | • | 3x6 km ² | GEO (85° West) | | | | | | | | | | | | | | | |
| MetOp-SG Sentinel 5 (ESA) | | • | 7x7 km ² | SS LEO (09:30) | | | | | | | | | | | | | | | |

Legend: in orbit (dark blue), extension (light blue), planned (green)

Figure 2. Past, present, and planned GHG satellites.

AirCore: The Gold Standard for Comparing Remote Sensing Observations to the Ground Network and the Capturing Changes in Stratospheric Circulation Changes

C. Sweeney¹, J. Higgs¹, T. Newberger^{2,1}, S. Wolter^{2,1}, P. Tans¹ and B. Baier^{2,1}

¹NOAA Earth System Research Laboratory, Global Monitoring Division (GMD), Boulder, CO 80305; 303-497-4771, E-mail: colm.sweeney@noaa.gov

²Cooperative Institute for Research in Environmental Sciences (CIRES), University of Colorado, Boulder, CO 80309

After a decade of development at the ESRL/GMD, the balloon-borne AirCore sampling system is now being used by several groups around the world as a relatively cost-efficient way to capture and subsequently measure more than 95% of the atmospheric column. The AirCore, which is essentially a long tube with one end open and one end closed that is lifted by balloon to altitudes as high as 30 km and returned to the ground by parachute. It takes advantage of the fact that molecular diffusion length scales in a few hours to a day are small relative to its length (>50 m). By analyzing the air captured on descent with a high precision calibrated analyzer it is possible to get a detailed profile of the atmospheric carbon dioxide (CO₂), methane (CH₄), and carbon monoxide (CO). The resulting dataset of measurements has provided us with critical constraints for remote measurements of the total column and upper free troposphere/stratospheric CO₂, CH₄, and CO.

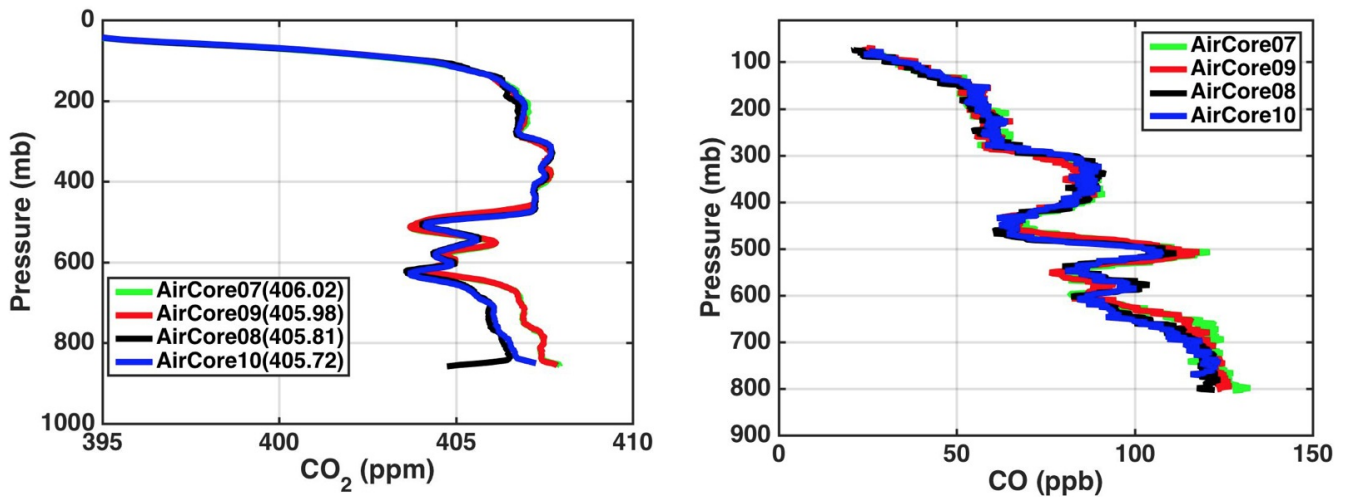


Figure 1. AirCore flight up to 27 km on July 14, 2017 showing CO₂ and CO profiles of 4 different AirCores. For each balloon launch two AirCores were flown together (AirCore 07 together with AirCore 09, and AirCore 08 together with AirCore 10). Balloon launches were 15 minutes apart. The comparability of the AirCores flown in pairs indicates only small differences in the profiles (<0.03 ppm for CO₂ and <5 ppb for CO) while larger difference are shown between the two balloon launch indicating large spatial variability in the free troposphere CO₂ profile in particular.

Monitoring of Atmospheric Acetylene in the NOAA Global Greenhouse Gas Reference Network

J. Hueber¹, D. Helmig¹, B. Blanchard¹, P.P. Tans², R. Steinbrecher³, A. Claude⁴ and C. Plass-Duelmer⁴

¹Institute of Arctic and Alpine Research (INSTAAR), University of Colorado, Boulder, CO 80309; 303-492-5059, E-mail: jhueber@colorado.edu

²NOAA Earth System Research Laboratory, Global Monitoring Division (GMD), Boulder, CO 80305

³Institute for Meteorology and Climate Research, Karlsruhe Institute of Technology, Campus Alpin, Karlsruhe, Germany

⁴Meteorological Observatory Hohenpeissenberg, German Meteorological Service, Hohenpeissenberg, Germany

Flask samples collected within the ESRL/GMD Global Greenhouse Gas Reference Network (GGGRN) have been routinely analyzed for a suite of hydrocarbons by INSTAAR's Atmospheric Research Lab (ARL) since 2005, using a custom-built Peltier-cooled microadsorbent trap pre-concentration system coupled with a GC-FID. Over the past three years, the feasibility of quantification of acetylene on this analytical system has been investigated. The main challenges encountered include a low available sample volume (about 500 mL), analyte break-through in the pre-concentration system, chromatography issues (co-elution with other compounds), and lack of a consistent calibration scale, leading to larger uncertainties than for alkane hydrocarbons. Breakthrough issues have been resolved by a redesign of the adsorbent trap assembly to reach a -40°C sample focusing temperature compared to -20°C in the previous design. The choice of an HP Al/KCL PLOT column and carefully chosen GC oven temperature parameters have allowed sufficient separation of acetylene from other compounds. As for the calibration scale, the acquisition in 2015 of two consistent reference standards from the National Physics Laboratory, UK, has allowed the alignment of the ARL standards with the Global Atmospheric Watch (GAW) scale. After adjustment of the ARL scale and reprocessing of the whole flask network dataset, a comparison has been conducted between flask results and *in situ* measurements at Hohenpeissenberg, Germany, resulting in an agreement within the 15% measurement uncertainty goal of GAW for acetylene. Time series data were calculated for network sites and synthesized to create the first carpet plot showing the global distribution of acetylene. The reproducibility of the acetylene determination is on the order of 2-5%. Detection limits in the 500 ml sample volumes are $\sim 20 \text{ pmol mol}^{-1}$, and the drift in the response factor from 2011- 2016 was on the order of 16%.

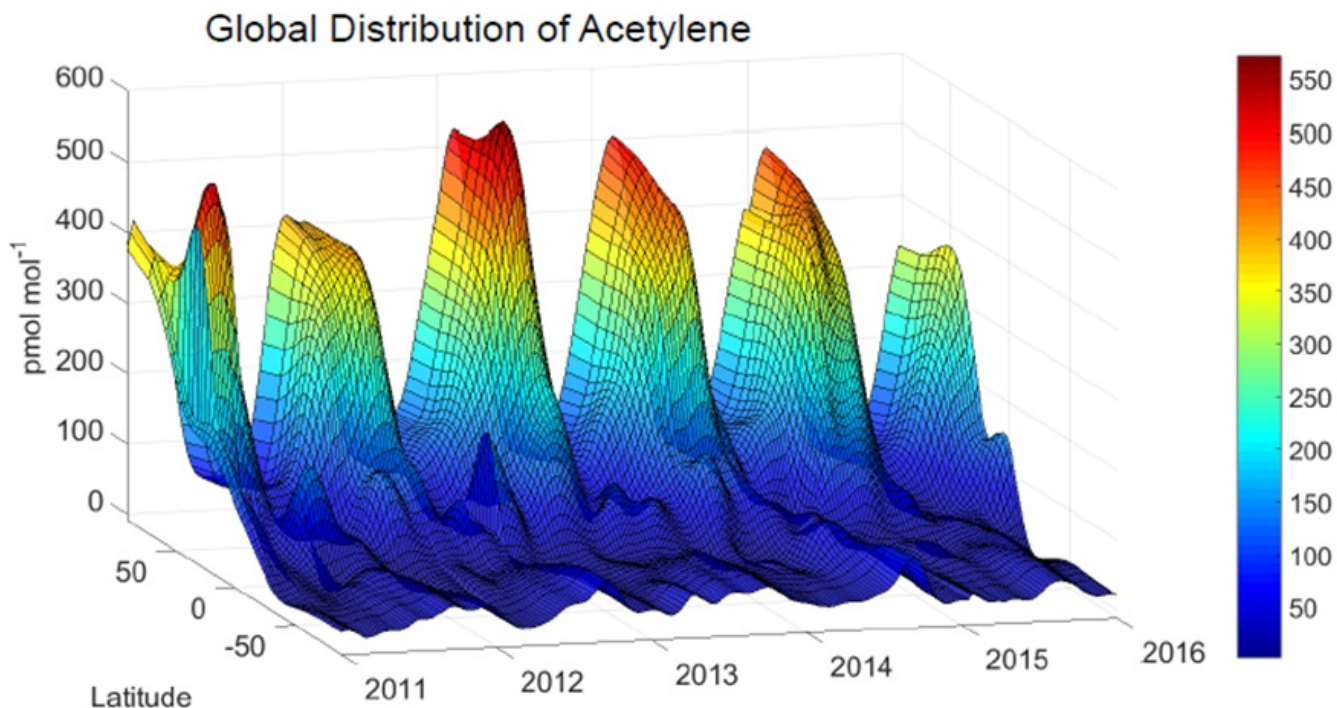


Figure 1. Carpet plot showing the global distribution of acetylene at GGGRN background sites from 2011-2016. This analysis illustrates the striking difference in atmospheric acetylene mole fractions between the Northern and Southern Hemisphere.

Atmospheric Isoprene in the NOAA/INSTAAR Global Greenhouse Gas Reference Network

J. Hueber¹, D. Helmig¹, B. Blanchard¹, K. Panwell¹, P. Tans², A. Claude³ and C. Plass-Duelmer³

¹Institute of Arctic and Alpine Research (INSTAAR), University of Colorado, Boulder, CO 80309; 303-492-5059, E-mail: jhueber@colorado.edu

²NOAA Earth System Research Laboratory, Global Monitoring Division (GMD), Boulder, CO 80305

³Meteorological Observatory Hohenpeissenberg, German Meteorological Service, Hohenpeissenberg, Germany

Two different methods of isoprene monitoring were evaluated from co-collected measurements at the Deutscher Wetterdienst Global Atmospheric Watch (GAW) site, Hohenpeissenberg, Germany. *In situ* sampling followed by gas chromatography analysis performed at the site was compared with whole air sampling within ESRL/GMD's Global Greenhouse Gas Reference Network (GGGRN). For the whole air sampling, air was collected in 2.5-liter glass flasks that were filled within 15 minutes of the *in situ* measurements, and later analyzed by gas chromatography at INSTAAR in Boulder, Colorado. Influences from sample storage time of the flasks, as well as ozone concentration, and humidity during sampling were investigated. None of these appear to have an influence on the isoprene recovery from the flasks. A ~10% systematic disagreement was seen between flask and *in situ* methods in calibration scales. A polynomial fit of the compared data was used to correct for this error, scaling flask measurements to the *in situ* observations. The detection limit for the flask analysis was determined to be 8 pmol mol⁻¹. This allowed quantification of isoprene in GGGRN network flasks at ~50% of the 44 sites included in the network. We present the global and seasonal distribution of isoprene from these data, where sites were classified as being subjected to year-round, seasonal, occasional, or no isoprene occurrence in the network samples.

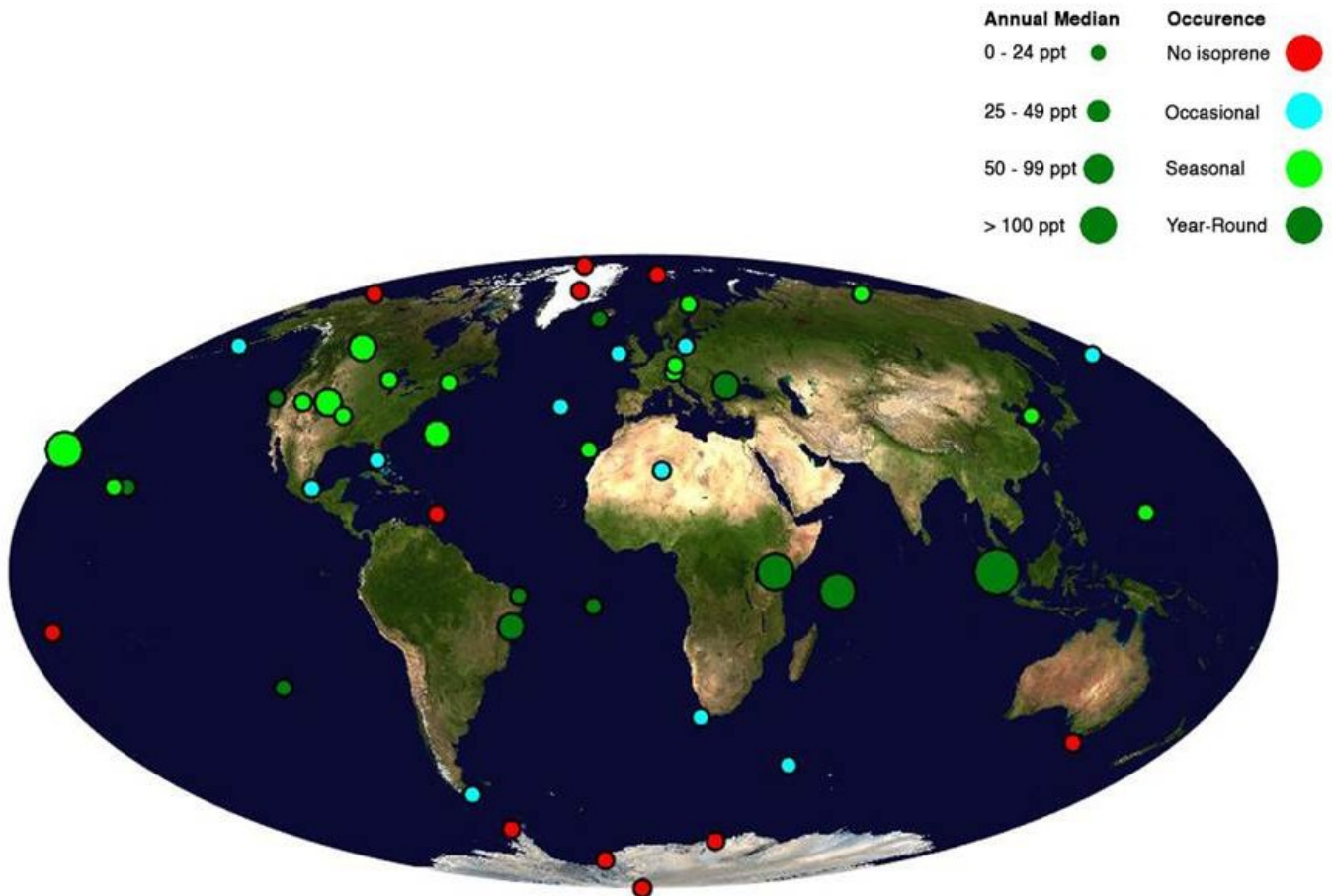


Figure 1. Map showing the global distribution of isoprene at GGGRN network sites. Sites were classified as having no, occasional, seasonal, or year-round isoprene. Point size corresponds to median mixing ratio and categorization (color) to the frequency of isoprene detection at each site.

Spatial and Temporal Gradients in Atmospheric CO₂ and CO in the Los Angeles Megacity

K.R. Verhulst¹, J.B. Miller², V. Yadav¹, S. Lehman³, K. Gurney⁴, C. Miller¹, R. Duren¹, S. Newman⁵, M. Fischer⁶, J. Kim⁷, P.K. Salameh⁷, R.F. Weiss⁷, R. Keeling⁷, T. Pongetti¹ and C. Sloop⁸

¹NASA Jet Propulsion Laboratory, California Institute of Technology, Pasadena, CA 91109; 818-393-5817, E-mail: Kristal.R.Verhulst@jpl.nasa.gov

²NOAA Earth System Research Laboratory, Global Monitoring Division (GMD), Boulder, CO 80305

³Institute of Arctic and Alpine Research (INSTAAR), University of Colorado, Boulder, CO 80309

⁴Arizona State University, Tempe, AZ 85287

⁵California Institute of Technology, Pasadena, CA 91125

⁶Lawrence Berkeley National Laboratory (LBNL), Berkeley, CA 94720

⁷Scripps Institution of Oceanography, University of California at San Diego, La Jolla, CA 92037

⁸Earth Networks, Inc., Germantown, MD 20876

Global atmospheric observations show an unprecedented rise in atmospheric carbon dioxide (CO₂) levels since the pre-industrial era. This trend correlates with estimates of CO₂ emissions from global fossil fuel consumption during the same period. Globally, urban regions account for ~70% of fossil carbon emissions; however, there are gaps in our understanding of the urban processes that influence carbon emissions. Measurements in urban areas are critical for linking atmospheric observations with fine-scale emissions data to understand the drivers of carbon emissions. The Los Angeles (LA) Megacities Carbon Project was established to develop and test robust techniques for monitoring distributions and trends of fossil carbon emissions in large cities (megacities.jpl.nasa.gov). The project includes a fifteen-node *in situ* greenhouse gas monitoring network spanning the LA metropolitan area and surrounding regions (Verhulst et al. 2017). We estimate "excess" CO₂ and carbon monoxide (CO) levels relative to nearby background mole fractions, which result from changes in local emissions and meteorology. CO is commonly used as a tracer for anthropogenic fossil fuel carbon dioxide (CO₂fos), the mole fraction of CO₂ in dry air resulting from fossil fuel combustion relative to background, because it is co-emitted during the incomplete combustion of fossil fuels. Atmospheric CO measurements alone do not give a quantitative estimate of atmospheric CO₂fos and require calibration using radiocarbon (¹⁴CO₂) observations. During the course of this study, ¹⁴CO₂ flask-sampling was conducted by NOAA/INSTAAR at 3 sites every ~3-4 days to derive atmospheric CO₂fos. CO₂fos signals derived from ¹⁴CO₂ suggest that ~75% of the midday CO₂ enhancements are explained by variability in CO₂fos, while the remainder may be attributed to biospheric fluxes. Utilizing the robust CO/CO₂ ratios and CO₂fos estimates derived from ¹⁴CO₂ allows approximation of a synthetic, continuous CO₂fos time series, CO₂fos_syn. CO₂fos_syn will be tested in our atmospheric modeling framework and compared with Hestia-LA, a bottom-up dataset quantifying anthropogenic CO₂fos emissions that relies on a mixture of activity data, fuel statistics, direct flux measurement, and modeling algorithms. The ¹⁴CO₂ record in LA also allows us to assess uncertainties in CO₂fos fluxes determined using methods that rely on total CO₂ observations.

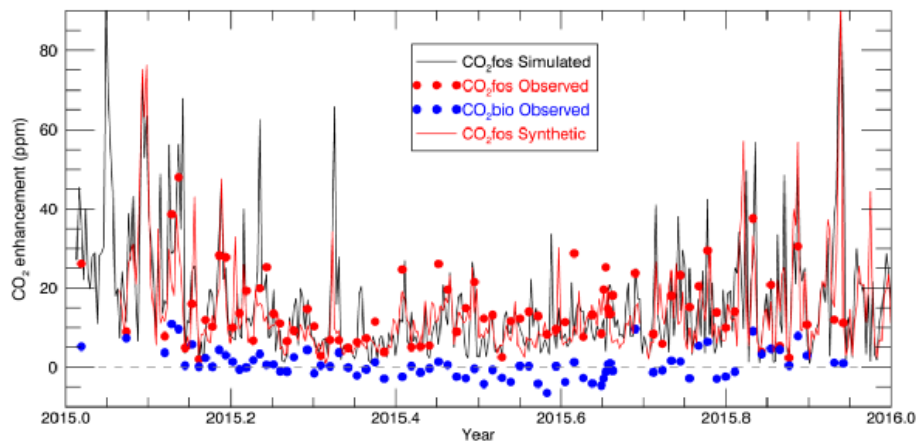


Figure 1. Time series of CO₂fos simulated using the Hestia emissions (Gurney et al. 2012) and the WRF-STILT footprint model (black), daily CO₂fos_syn (red) derived from 21:00 UTC *in situ* CO data, and observed CO₂fos and CO₂bio at a measurement site near Downtown LA (University of Southern California).

Investigating Hydrocarbon Tracers for Anthropogenic CO₂ at Indianapolis, IN

I. Vimont^{1,2}, J. Turnbull^{3,2}, T. Lauvaux⁴, K. Gurney⁵, B.R. Miller^{6,2} and S. Montzka²

¹National Research Council Post-Doc, Boulder, CO 80305; 303-497-6044, E-mail: isaac.vimont@noaa.gov

²NOAA Earth System Research Laboratory, Global Monitoring Division (GMD), Boulder, CO 80305

³GNS Science, National Isotope Centre, Lower Hutt, New Zealand

⁴Department of Meteorology and Atmospheric Science, The Pennsylvania State University, University Park, PA 16802

⁵Arizona State University, Tempe, AZ 85287

⁶Cooperative Institute for Research in Environmental Sciences (CIRES), University of Colorado, Boulder, CO 80309

Anthropogenic emissions of hydrocarbon compounds may provide information about carbon dioxide (CO₂) emissions in an urban environment. The Indianapolis FLUX experiment (INFLUX) has produced an eight-year time series of urban CO₂, methane (CH₄), carbon monoxide (CO), and several hydrocarbon species. We combine these measurements with the Hestia data product for Indianapolis, as well as footprints for each tower to learn about emissions of benzene (C₆H₆) as they relate to fossil fuel produced CO₂.

Using carbon-14 dioxide (¹⁴CO₂) measurements to quantify the urban enhancement of fossil CO₂ (CO_{2ff}), we calculate the ratio of benzene to CO_{2ff} observed for 5 years at Indianapolis. We then use benzene data from the Environmental Protection Agency (EPA) National Emissions Inventory 2014, and estimates of fossil fuel produced CO₂ from the Hestia data product for Marion County, Indiana to calculate ratios for eight distinct sectors represented by Hestia (Airport, Commercial, Industrial, Mobile, Non-road, Residential, Utility, and Rail).

Using these ratios, we calculate a “Hestia Benzene” product for a twelve-month period in 2012-2013. This is then multiplied by model footprints for each of the tower sites at Indianapolis. This produces modeled tower data, which we compare to the real measurements. This gives us two pieces of information. First, it provides a metric to determine how well the reported EPA emissions of benzene are represented by the measurements at Indianapolis. Second, we can begin to assess if benzene is a unique tracer for any of the sectors within Hestia. If a tracer is unique to a single sector, it becomes a very powerful tool for troubleshooting the Hestia and tower footprint models.

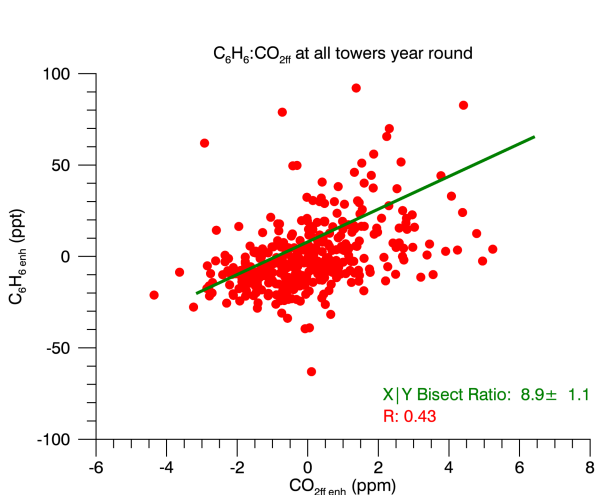


Figure 1. Benzene vs Fossil Fuel CO₂ (CO_{2ff}) enhancements at Indianapolis. Regression was done using an XIY Bisector approach. Data was filtered for desirable atmospheric conditions. R represents the Pearson correlation coefficient for the benzene vs CO_{2ff} data, not the r² of the linear model.

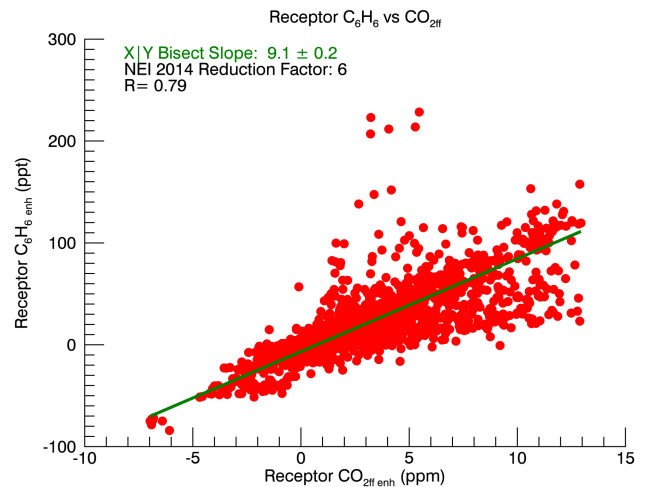


Figure 2. "Hestia Benzene" vs Hestia Fossil Fuel CO₂ (CO_{2ff}) enhancements at Indianapolis. Regression was done using an XIY Bisector approach. Data represents 12 months of receptor data from November 1, 2012 - October 31, 2013. R represents the Pearson correlation coefficient for the hestia benzene vs hestia CO_{2ff} data, not the r² of the linear model.

Estimating Uncertainties of GC/MS Analyses of Programmable Flask Package (PFP) Atmospheric Samples from the GGGRN North American Tower and Aircraft Programs

B.R. Miller^{1,2}, B.D. Hall², D. Neff^{1,2}, T. Legard^{1,2}, J. Higgs², M.J. Crotwell^{1,2}, C. Siso^{1,2}, A.E. Andrews², C. Sweeney² and P. Tans²

¹Cooperative Institute for Research in Environmental Sciences (CIRES), University of Colorado, Boulder, CO 80309; 303 497 6624, E-mail: ben.r.miller@noaa.gov

²NOAA Earth System Research Laboratory, Global Monitoring Division (GMD), Boulder, CO 80305

Estimates of measurement uncertainty are one component often considered when interpreting atmospheric trace gas observations with the aim of estimating emissions. Uncertainty estimates are also critical in the evaluation of spatial and temporal trends from discrete measurements at different times, locations, and/or instruments.

The “Guide to the expression of uncertainty in measurement” (GUM 1995, 2008) defines uncertainty of a measurement as a “parameter, associated with the result of a measurement, that characterizes the dispersion of the values that could reasonably be attributed to the measurand.” In general, uncertainty is comprised of many components, some of which may be evaluated as statistical distributions and characterized by standard deviations.

The Global Greenhouse Gas Reference Network (GGGRN) collects more than 8,000 flask samples of ambient air annually using Programmable Flask Packages (PFP) which are pressurized using Programmable Compressor Packages (PCP). Samples are acquired at a rate of approximately daily at 18 tower locations and approximately twice monthly aboard 15 small aircraft sites throughout North America. We have developed routine laboratory experiments that separate out the most relevant aspects of PFP/PCP sample collection and instrument processes so that their respective contributions to dispersion of the measurements or uncertainties may be elucidated.

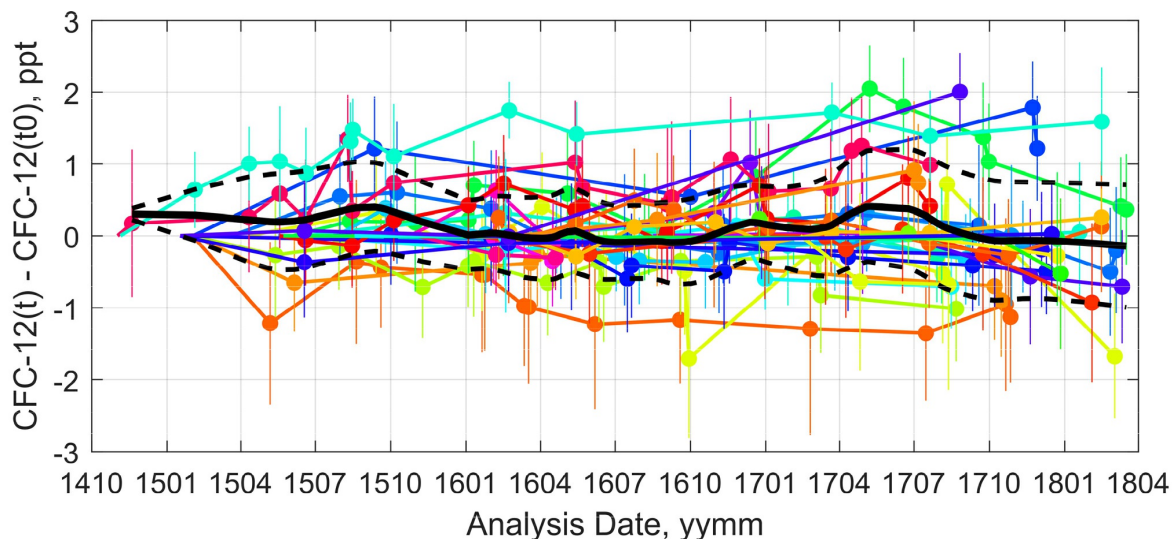


Figure 1. Long-term reproducibility of the PERSEUS GC/MS for CFC-12 (CCl_2F_2). More than 50 archived tanks of whole ambient air (Niwot Ridge, CO) were analyzed periodically over the past three years. Each color represents a different tank. Following the initial analysis of each tank, the change in assigned mole fraction over time can be calculated as the difference between the result at time t minus the initial (t_0) result (dots, with 1-sigma errorbars). A running mean (Lowess smoothed) of all these differences is shown as a black solid line, with ± 1 -sigma standard deviation (black dashed line). The overall long-term reproducibility of CFC-12 is ± 0.68 ppt, which represents the dispersion of the measurement from the combination of tank plus instrument.

Untangling Greenhouse Gas Fluxes and Transport using ACT-America Observations

B.J. Gaudet¹, D.F. Baker², Z. Barkley¹, S. Basu^{3,4}, K. Bowman⁵, E.V. Browell⁶, Y. Choi⁶, S. Crowell⁷, K.J. Davis^{1,8}, J. DiGangi⁶, F. Deng⁹, L. Feng¹⁰, S. Feng¹, A.R. Jacobson^{3,4}, D. Jones⁹, T. Lauvaux¹, J. Liu⁵, S. Pal¹, P. Palmer¹⁰, A.E. Schuh² and B. Weir¹¹

¹Department of Meteorology and Atmospheric Science, The Pennsylvania State University, University Park, PA 16802; 814-867-2110, E-mail: bjg20@psu.edu

²Cooperative Institute for Research in the Atmosphere (CIARA), Colorado State University, Fort Collins, CO 80521

³Cooperative Institute for Research in Environmental Sciences (CIRES), University of Colorado, Boulder, CO 80309

⁴NOAA Earth System Research Laboratory, Global Monitoring Division (GMD), Boulder, CO 80305

⁵NASA Jet Propulsion Laboratory, California Institute of Technology, Pasadena, CA 91109

⁶NASA Langley Research Center, Hampton, VA 23681

⁷University of Oklahoma, Norman, OK 73019

⁸Earth and Environmental Systems Institute, The Pennsylvania State University, University Park, PA 16802

⁹University of Toronto, Toronto, Ontario, Canada

¹⁰University of Edinburgh, Edinburgh, United Kingdom

¹¹NASA Goddard Space Flight Center (GSFC), Greenbelt, MD 20771

The Atmospheric Carbon and Transport (ACT) - America mission aims to improve our understanding of transport and fluxes of greenhouse gases (GHGs) via aircraft campaigns that cover three regions of the U.S. and four seasons, include frontal and fair-weather conditions, and span the boundary layer to the upper troposphere and horizontal transects of several hundred kilometers. Observations include GHG mole fractions and meteorological properties. Observations have shown large, spatially-coherent differences in GHGs that extend throughout the depth of the troposphere across fronts in summer and winter, large horizontal variability in GHGs in the atmospheric boundary layer (ABL) in fair weather conditions, and GHG “rivers” associated with cold frontal boundaries. A broad effort to compare these observations with a variety of atmospheric GHG numerical reanalyses is underway. An evaluation of the posterior carbon dioxide (CO₂) fields from the OCO-2 inverse MIP using summer 2016 campaign data reveals patterns of model-data differences. Inversions based on *in situ* data tend to be negatively biased in the lower troposphere, while land-nadir OCO-2 inversions tend to be positively biased. In the Mid-Atlantic, TM5-based inversions show more negative biases in lower tropospheric CO₂ than Goddard Earth Observing System-Chem (GEOS-Chem) -based inversions. Mid-Atlantic biases are largest, and Gulf biases are the smallest. WRF-Chem simulations that use CarbonTracker boundary conditions and surface fluxes are being used to isolate the impact of transport, and evaluation of the relative mix of CO₂ continental fluxes vs. boundary inflow are being examined to lend more insight into the causes of documented biases, and to inform how to improve atmospheric inversion systems.

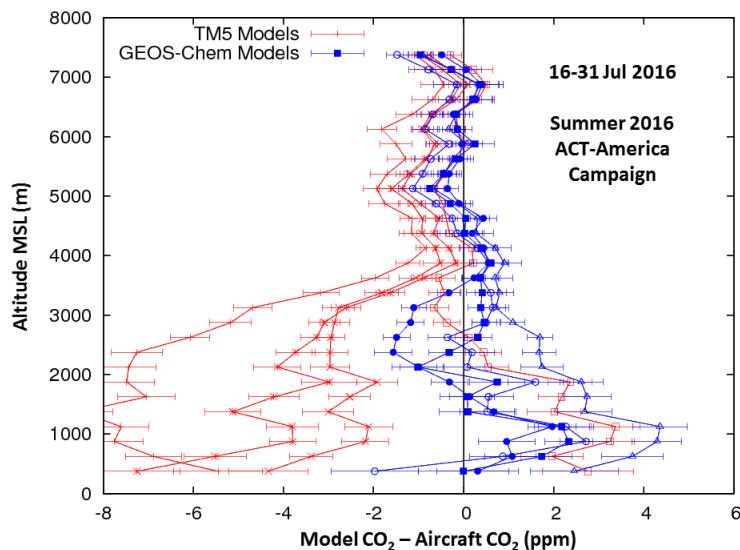


Figure 1. Model-data CO₂ differences from summer 2016 ACT-America vertical profiles in the Mid-Atlantic region. Models use *in situ* data in their inversions. Red indicates TM5 inversions, while blue indicates GEOS-Chem inversions.

Recent Developments in Using Isotopic Measurements for Constraining Methane Sources and Sinks

S. Schwietzke^{1,2}, S.E. Michel³, E.J. Dlugokencky², O.A. Sherwood³, L. Bruhwiler², S. Basu^{1,2}, X. Lan^{1,2}, G. Petron^{1,2}, J.B. Miller², B.H. Vaughn³ and P.P. Tans²

¹Cooperative Institute for Research in Environmental Sciences (CIRES), University of Colorado, Boulder, CO 80309; 303-497-5073, E-mail: stefan.schwietzke@noaa.gov

²NOAA Earth System Research Laboratory, Global Monitoring Division (GMD), Boulder, CO 80305

³Institute of Arctic and Alpine Research (INSTAAR), University of Colorado, Boulder, CO 80309

Several recent studies have led to different conclusions regarding the utility of measurements of the isotopic composition of methane (CH_4) on diagnosing its budget and trends of sources and sinks. Some studies have found isotopic evidence of a largely microbial source causing the renewed growth in global atmospheric methane since 2007, and underestimated global fossil fuel methane emissions compared to most previous studies. However, other studies have challenged these conclusions by pointing out the substantial range in isotopic source signatures as well as open questions in atmospheric sinks and biomass burning trends. These differing interpretations and conclusions come despite substantial recent scientific contributions to this field including (i) careful comparisons and merging of atmospheric isotope measurement datasets to increase spatial coverage, (ii) in-depth analyses of observed isotopic spatial gradients and seasonal patterns, and (iii) improved datasets of isotopic source signatures. This presentation will provide an overview of the contrasting arguments by distinguishing among the different research objectives including (i) global methane budget source attribution in steady-state, (ii) source attribution of recent global methane trends, and (iii) identifying specific methane sources in individual plumes during field campaigns. We will also present preliminary results from a current modeling project that will combine and incorporate the most recent available global methane isotopic data (source signatures and atmospheric measurements).

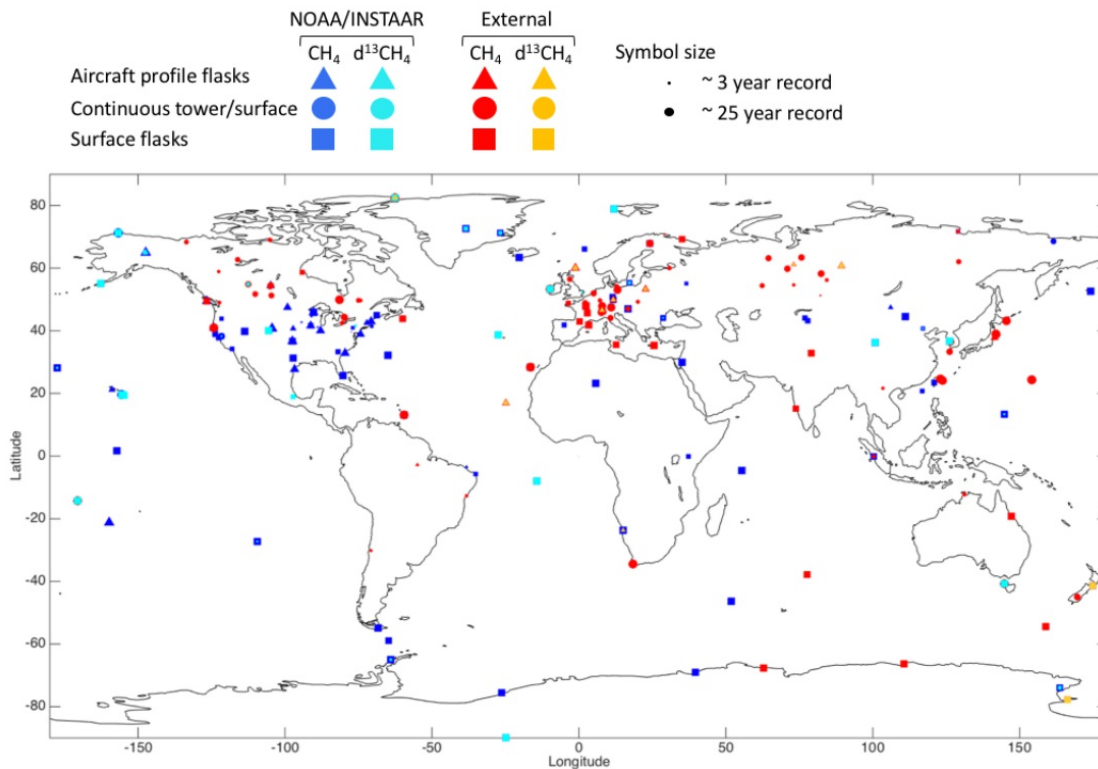


Figure 1. Overview of preliminary combined NOAA/INSTAAR (blue/cyan) and external (red/yellow) atmospheric CH_4 and delta carbon-13 ($\delta^{13}\text{C}$)- CH_4 dataset compiled for this study. Only “fixed” sites are shown, and additional data include horizontally “moving” sites such as container ships and aircraft routes. Note that not all sites have simultaneous records, and some entries overlap visually.

Recent GAW Activities of KMA

Y. Kim and S. Noh

Korea Meteorological Administration, Daebang-dong, Dongjak District, Seoul, Republic of Korea; +82-2-2181-0635, E-mail: yuwon@korea.kr

The Korea Meteorological Administration (KMA) has been maintaining observations for atmosphere monitoring stably and systematically since 1998. The monitoring factors include seven greenhouse gases (carbon dioxide [CO₂], methane [CH₄], nitrous oxide [N₂O], CFC_{-11,12,113}, and sulfur hexafluoride [SF₆]), four reactive gases (carbon monoxide [CO], ozone [O₃], nitrogen oxides [NO_x], and sulfur dioxide), several aerosols properties, atmospheric radiation, stratospheric ozone, and Ultra-A, B. The Anmyeondo site, designated as a regional WMO GAW site in 1998, has the longest history of atmosphere watch in Korea. The observation outcomes including trends of diverse species in the global and national level can be found on the website below.

(The website address is www.climate.go.kr/home/09_monitoring/index.php/main. English version of this website will be launched soon.)

Recognizing the importance of monitoring SF₆, the KMA began its observation of SF₆ at Anmyeondo in 2007, and accordingly hosted the WMO GAW World Calibration Center for SF₆ (hereinafter “WCC- SF₆”) in 2011, concluding a Memorandum of Understanding with the WMO in October 2012. As of 2016, 53 observatories in 19 countries are monitoring SF₆. The WCC- SF₆ maintains observation standards, regularly hosts international experiments for comparisons and analyses, and provides trainings on the analysis technology with the aim of disseminating SF₆ observation technology to the GAW stations around the world. The KMA, as the WCC- SF₆, published "Analytical Methods for Atmospheric SF₆ Using GC-μECD" and "Calibration Methods of GC-μECD for Atmospheric SF₆ Measurements", registered as WMO publications, WMO GAW Report No. 222 and No. 239, respectively. In line with these activities, the 8th Asia-Pacific GAW Workshop and training course on SF₆ will be held this year in Korea following previous ones every two years. Currently the KMA is planning to participate in the pilot project of WMO “Integrated Global Greenhouse Gases Information System (IG³IS)”. IG³IS is expected to serve as an international coordinating mechanism to guide greenhouse gas emission-reduction actions on the basis of sound scientific evidence. In accordance with the plan of WMO IG³IS Draft paper, KMA’s implementation plan is going to be developed in due course. For the first three years (2018~2020), we’re going to design our own project, benchmarking leading practices by the English and Swiss. We, consequently, will be able to produce new information on CO₂ emission from the inverse-modelling system using our present technology. During the second (2021~2023) and third (2024~2026) phase, we expect to develop and advance our inverse methodology for the national scale to gain information available.

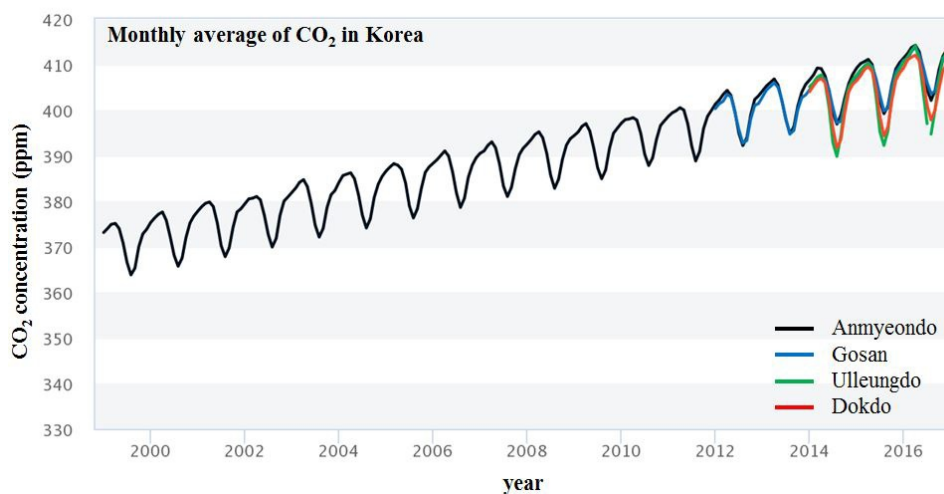


Figure 1. Monthly average of CO₂ over Korea. Black line is for Anmyeondo (1998~2016), blue line is for Gosan (2012~2016), green line is for Ulleungdo (2014~2016) and red line is for Dokdo (2014~2016).

Systematic Differences in Global CO₂ Inverse Model Results

B. Gaubert¹, B.B. Stephens², A.R. Jacobson^{3,4}, S. Basu^{3,4}, F. Chevallier⁵, C. Roedenbeck⁶, P.K. Patra⁷, T. Saeki⁸, I. van der Laan-Luijkx⁹, W. Peters⁹, D. Schimel¹⁰ and F. Deng¹¹

¹National Center for Atmospheric Research (NCAR), Atmospheric Chemistry Observations and Modeling Laboratory, Boulder, CO 80307; 303-497-1488, E-mail: gaubert@ucar.edu

²National Center for Atmospheric Research (NCAR), Earth Observing Laboratory, Boulder, CO 80307

³Cooperative Institute for Research in Environmental Sciences (CIRES), University of Colorado, Boulder, CO 80309

⁴NOAA Earth System Research Laboratory, Global Monitoring Division (GMD), Boulder, CO 80305

⁵Laboratoire des Sciences du Climat et de l'Environnement (LSCE), Institut Pierre-Simon Laplace, Orme des Merisiers, France

⁶Max Planck Institute (MPI) for Biogeochemistry, Jena, Germany

⁷Japan Agency for Marine-Earth Science and Technology (JAMSTEC), Department of Environmental Geochemical Cycle Research, Yokohama, Japan

⁸Center for Global Environmental Research, National Institute for Environmental Studies, Tsukuba, Japan

⁹Wageningen University, Department of Meteorology and Air Quality, Wageningen, The Netherlands

¹⁰NASA Jet Propulsion Laboratory, California Institute of Technology, Pasadena, CA 91109

¹¹University of Toronto, Department of Physics, Toronto, Ontario, Canada

We compared a suite of state-of-the-art global carbon dioxide (CO₂) inverse models to observations to assess the dependence on differences in northern extratropical vertical transport and to identify other drivers of the modelled spread. The posterior CO₂ concentration profiles have been evaluated against the High-Performance Instrumented Airborne Platform for Environmental Research (HIAPER) Pole-to-Pole Observations (HIPPO) aircraft campaign over the mid pacific in 2009-2011. The modelled CO₂ fields agree reasonably well with the HIPPO observations, in particular for the annual mean vertical gradients in the northern hemisphere. The latitudinal distributions of land fluxes have converged significantly since the Atmospheric Carbon Cycle Inversion Intercomparison (TransCom3) and the Regional Carbon Cycle Assessment and Processes (RECCAP) and they are now in close agreement. The results from these models for other time periods (2004-2014, 2001-2004, 1992-1996) confirm that the tropics have been almost neutral for several decades. However, models do still disagree on the ocean-land partitioning, and this is driven by differences in fossil fuel emissions associated with differences in retrieved atmospheric growth rates. The uncertainty on prescribed fossil fuel emissions is large relative to the natural fluxes of interest; the model range is 0.94 PgC/yr in global fossil fuel emissions. The models also retrieve surprisingly different three-year atmospheric growth rates, the model range is 0.65 ppm, or 1.38 PgC over 3 years.

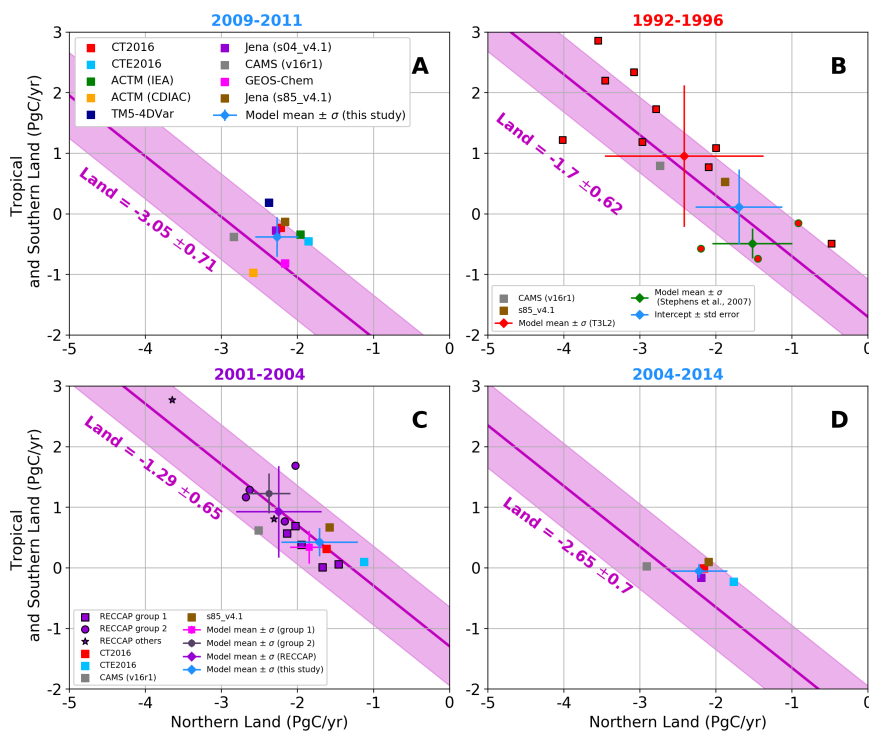


Figure 1. Tropical and Southern versus Northern Extratropical land fluxes for the periods **A)** 1992-1996, **B)** 2001-2004, **C)** 2009-2011 and **D)** 2004-2014. The average of the available simulation with uncertainty (1 standard deviation) is shown in blue with associated error bars. The TransCom Level 3 outputs (Gurney et al. 2004) are shown in red and transport corrected models from (Stephens et al., 2007) in green on panel B (1992-1996). Inversions from the RECCAP period (2001-2004) are also shown on panel C.

Methane Leak Detection and Sizing using Large Eddy Simulations (LES)

K. Prasad¹, S. Coburn², C. Alden^{3,4} and G.B. Rieker²

¹National Institute of Standards and Technology (NIST), Gaithersburg, MD 20880; 301-975-3968, E-mail: kprasad@nist.gov

²University of Colorado, Department of Mechanical Engineering, Boulder, CO 80309

³Cooperative Institute for Research in Environmental Sciences (CIRES), University of Colorado, Boulder, CO 80309

⁴NOAA Earth System Research Laboratory, Global Monitoring Division (GMD), Boulder, CO 80305

The NIST Large Eddy Simulation (LES) software is a computational fluid dynamics model that can resolve the turbulent flow field at length scales much smaller than is practical with mesoscale atmospheric transport models. High resolution LES models were used to simulate methane leak tests conducted at the Methane Emissions Testing and Evaluation Center (METEC) at spatial resolution of 2 m. LES simulations have the potential to evaluate the impact of complex urban topography on near-field dispersion and mixing of methane.

Simulations were combined with line integrated measurement data from a dual frequency comb laser spectrometer in an inversion framework to estimate methane leak size and location. Results demonstrate the capability of the LES model to accurately simulate transport and dispersion of methane plumes. The presentation will describe new developments in LES modeling including assimilation of meteorological observation data as well as coupling of lagrangian massless particles to model the sub-grid scale methane leaks and measurements.

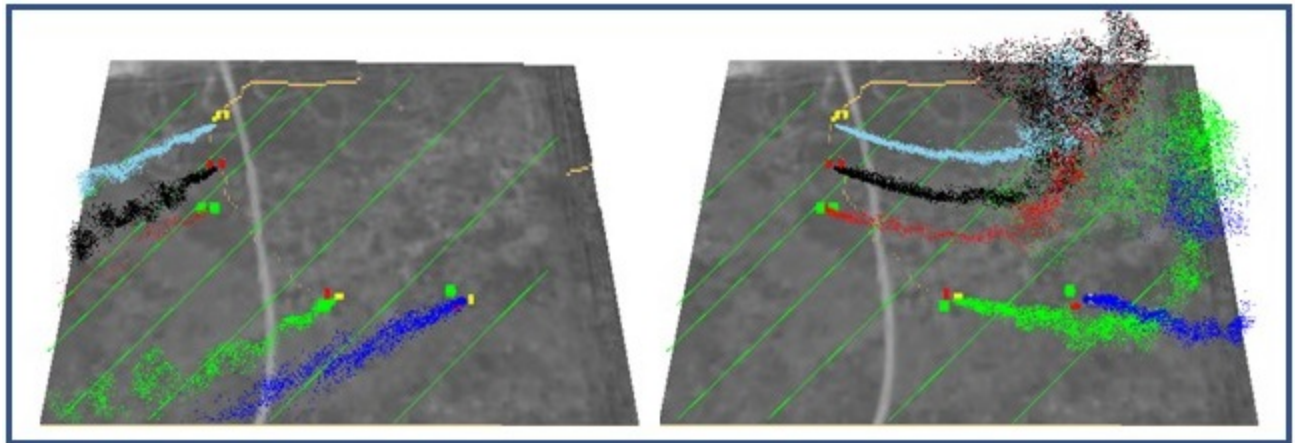


Figure 1. Large Eddy Simulations (LES) of the R1 methane leak tests performed at the METEC test facility. Images show the transport and dispersion of methane plumes from 5 leaks (color coded) located on various well-pads. Topographical data and obstructions such as separator tanks and wells were included in the simulation. The green lines indicate the location of the beams where path integrated measurement data was collected. The domain size was 200 m x 200 m and the spatial resolution of the simulations was set at 2 m.

Development of ECCC’s Regional Transport Model for Simulation of Atmospheric Greenhouse Gases at High Spatial and Temporal Resolution

J. Kim, S. Polavarapu, D. Chan and M. Neish

Environment and Climate Change Canada, Toronto, Ontario, Canada; 416-739-4929, E-mail: jinwoong.kim@canada.ca

With the advent of space-based observations of greenhouse gases (GHG) such as carbon dioxide (CO_2) and methane (CH_4) at high spatial resolution, as well as the expanding surface networks of GHG measurements, it may now be possible to constrain surface GHG fluxes at regional scale by atmospheric inverse modeling. However, this requires the high-resolution transport model to be able to accurately simulate GHG variability on synoptic and mesoscales captured in the measurements. Also, high-resolution anthropogenic and biospheric prior fluxes are required to provide detailed information associated with high-resolution topography and surface geophysical characteristics.

Here we present the development of a regional transport model for GHG, aiming at understanding the high spatio-temporal resolution interaction of the atmosphere and surface GHG fluxes, mainly focusing on Canada and the United States as shown in Fig. 1. This is an extension of the development of Environment and Climate Change Canada’s (ECCC) Carbon Assimilation System (EC-CAS) that is based on a global version of operational ECCC weather forecast and environmental prediction model. Our regional model is run at a 10 km horizontal grid spacing with 80 vertical levels spanning the ground to 0.1 hPa. The added benefit of the regional model over our low resolution global model (0.9° horizontal grid spacing) is assessed in terms of modeled tracer concentration and meteorological forecast quality. We find that our regional model has the capability to simulate high spatial and temporal scales of atmospheric GHG concentrations both horizontally- and vertically-based on comparisons to observations from various GHG observing systems including surface network, aircraft, and OCO-2 satellite. In addition, several sensitivity tests are conducted to investigate the impact of different lateral boundary conditions on modeled concentrations.

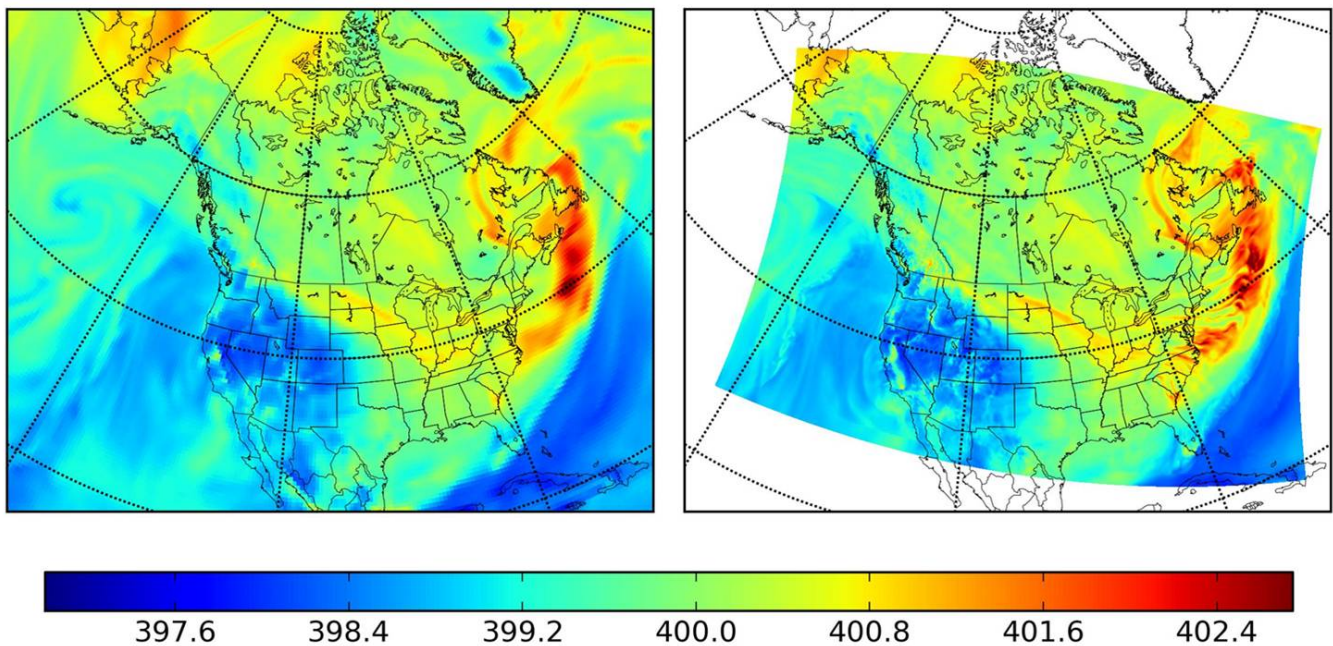


Figure 1. An example of modeled column mean CO_2 (ppm) weighted by air mass from global (**left panel**) and regional model (**right panel**) on 5 January 2015 22:00 UTC.

Constraining Carbon Exchange Processes over North America by Joint Assimilation of Atmospheric CO₂ and δ¹³C

I.R. van der Velde^{1,2}, J.B. Miller², W. Peters³, A.E. Andrews² and P.P. Tans²

¹Cooperative Institute for Research in Environmental Sciences (CIRES), University of Colorado, Boulder, CO 80309; 303-497-5591, E-mail: ivar.vandervelde@noaa.gov

²NOAA Earth System Research Laboratory, Global Monitoring Division (GMD), Boulder, CO 80305

³Wageningen University, Department of Meteorology and Air Quality, Wageningen, The Netherlands

Given the complex feedbacks that exist between the terrestrial biosphere and climate, the future of the terrestrial carbon sink remains uncertain in a world where droughts may be more extreme and more frequent. The ratio of carbon-13 (¹³C)/carbon-12 (¹²C) in atmospheric carbon dioxide (CO₂) (reported as delta carbon-13 [δ¹³C] in ‰ relative to the Vienna Pee Dee Belemnite [VPDB] reference ratio), which we measure, provides insight into climate-carbon coupling. Photosynthesis imposes distinctive isotopic fractionation (also known as discrimination depicted as Δ) patterns upon atmospheric δ¹³C. Variations of δ¹³C in the atmosphere reflect spatially coherent changes in stomatal and mesophyll conductance, and in the relative contributions from C3 (e.g. forests) and C4 (e.g. maize) plant growth. However, these biogeochemical interactions are often poorly represented in climate land surface models. In an effort to diagnose and improve such models, we have developed an inverse model capable of assimilating δ¹³C and CO₂ data. So far, δ¹³C in inversion experiments was mainly used to distinguish the global land carbon sink from the ocean carbon sink. Now we take this one step further by estimating the magnitude of Δ during photosynthesis. This could help us better understand the biogeochemical interactions between the atmosphere and vegetation, and help us to improve parameterizations of carbon exchange in land surface models. Starting with synthetic datasets of CO₂ and δ¹³C of North America, we present and discuss the performance of different inversion techniques. One complicating aspect is the nonlinearity of the δ¹³C budget as net carbon exchange (NEE) and Δ are multiplicative terms. Our findings confirm we can only retrieve meaningful signals in isotopic Δ if the total CO₂ budget is correctly estimated. We find noticeable improvements of the inverted NEE and Δ primarily over the aggregated boreal and temperate forests, and cultivated land of the U.S. Potential atmospheric transport errors may leave δ¹³C and estimates of Δ unaffected as biases are cancelled out in the isotope ratio carbon-13 dioxide (¹³CO₂)/carbon-12 dioxide (¹²CO₂) (example shown in figure below). Real data inversions furthermore reveal potential problems in land surface models, such as oversimplified description of biological processes (e.g. stomatal and mesophyll conductance) and land use.

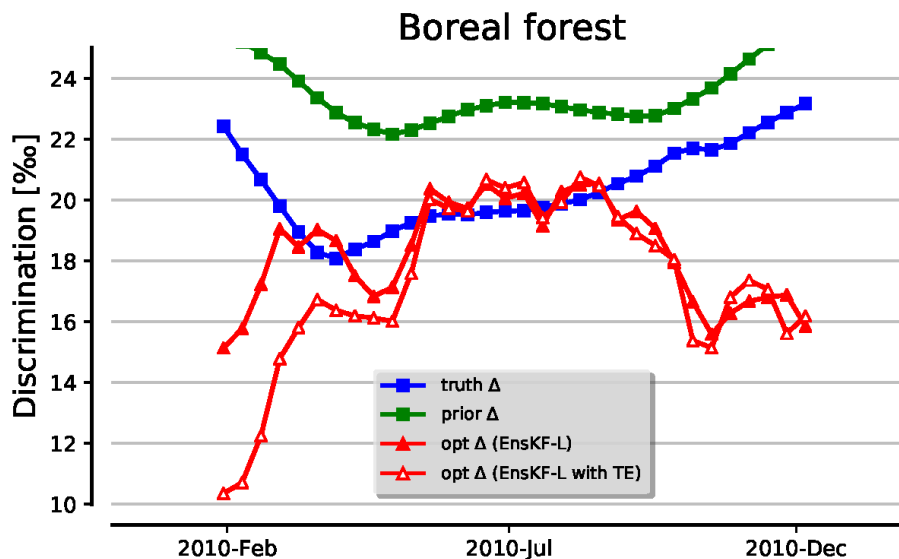


Figure 1. Synthetic data experiment showing aggregated 10-day mean Δ estimates (red) for boreal forest along with prior (green) and true (blue) Δ estimates. During summer, we are able to recover the true discrimination. The estimates with the open red symbols come from an inversion with an intentionally created atmospheric transport error (TE). These transport errors produced different CO₂ and ¹³CO₂ mole fractions over North America, but left δ¹³C ratios and Δ unaffected as biases cancel out when we take ratio of ¹³CO₂/¹²CO₂.

A Reanalysis of Inter-laboratory Comparisons as the Stable Isotope Lab at INSTAAR Switches to the JRAS-06 Realization of the VPDB Scale

S.E. Michel¹, K. Rozmiarek¹, B.H. Vaughn¹, I. Vimont^{2,3} and J. White¹

¹Institute of Arctic and Alpine Research (INSTAAR), University of Colorado, Boulder, CO 80309; 303-492-5495, E-mail: sylvia.michel@colorado.edu

²National Research Council Post-Doc, Boulder, CO 80305

³NOAA Earth System Research Laboratory, Global Monitoring Division (GMD), Boulder, CO 80305

The INSTAAR Stable Isotope Lab has a twenty-eight year record of measurements of stable isotopes of carbon dioxide (CO₂) from the ESRL/GMD Global Greenhouse Gas Reference Network. Until now we have been tied to the Vienna Pee Dee Belemnite (VPDB) scale by measurements of the primary reference material NBS19 done in the early 1990's and then carried forward by bootstrapping of working references. Following the recommendations of the Greenhouse Gas Measurement Techniques stable isotopes community, we are moving to the Jena Reference Air Set-06 (JRAS-06) tie to VPDB, produced by the Central Calibration Laboratory (CCL) for delta carbon-13 ($\delta^{13}\text{C}$) and delta oxygen-18 ($\delta^{18}\text{O}$) of CO₂ at The Max Planck Institute for Biogeochemistry (MPI-BGC), in Jena, Germany. We can now re-examine our suite of comparisons with other laboratories to see if our compatibility has improved.

Our offsets from the CCL decreased significantly: in a comparison of flasks filled with air and measured by both labs, the agreement in ambient delta carbon-13 dioxide ($\delta^{13}\text{CO}_2$) improves from -0.05 to -0.01 ‰ (Jena-INSTAAR). Our $\delta^{13}\text{C}$ agreement in the last round robin improved from -0.04 ‰ to -0.02 ‰. INSTAAR calibrates cylinders for many other laboratories, so our move to JRAS-06 will greatly improve inter-laboratory compatibility. However, many laboratories still use locally-produced realizations of JRAS-06, and discrepancies persist in correction algorithms, especially for oxygen-17 (¹⁷O). INSTAAR is making a major step toward implementing WMO-GAW recommendations, and other laboratories will need to do the same in order to achieve the data quality objectives of 0.01 ‰ and 0.05 ‰ for $\delta^{13}\text{C}$ and $\delta^{18}\text{O}$ respectively.

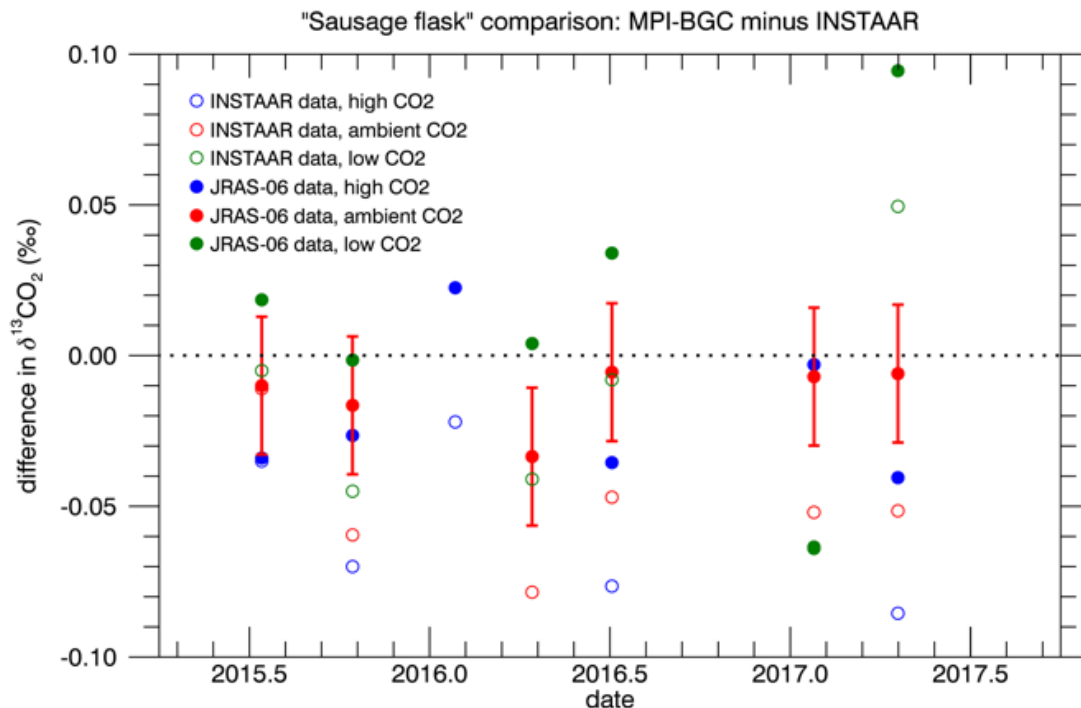


Figure 1. Offsets between MPI-BGC and INSTAAR measurements of flasks filled from high pressure cylinders. Open circles are on the old "INSTAAR" scale; closed circles are on the JRAS-06 scale. Colors represent low, ambient, and high CO₂ mole fraction of the fill gas.

An Update on the WMO CO X2014A Scale

A. Crotwell^{1,2}, B.D. Hall², M. Madronich^{1,2}, G. Petron^{1,2} and P. Novelli²

¹Cooperative Institute for Research in Environmental Sciences (CIRES), University of Colorado, Boulder, CO 80309; 303-497-6494, E-mail: andy.crotwell@noaa.gov

²NOAA Earth System Research Laboratory, Global Monitoring Division (GMD), Boulder, CO 80305

With the release of the WMO carbon monoxide (CO) X2014A scale revision in 2015, ESRL/GMD changed the method of maintaining the WMO CO in air scale. Previous scales were defined by repeated gravimetric sets made every 4 - 6 years. With X2014A, we maintain a single set of primary standards and all calibrations since January 2011 are traceable to this single set. This is more consistent with how other calibration scales are maintained by ESRL/GMD. However, the lack of stability of CO mixing ratio in high pressure aluminium cylinders (cylinders typically show CO growth rates of less than one ppb per year) means we had to develop a method for periodically evaluating drift in the CO primary standards.

We use an internal tracer technique to monitor the slow growth of CO in the primary standards. Percent-level gravimetric mixtures of CO and methane (CH₄) in air are used as “parent” tanks. We assume growth of CO has no significant impact on the gravimetrically determined CO: CH₄ ratio. Static dilutions from these parent tanks were made to create suits of standards with CO covering the range of interest (30 – 1000 nmol mol⁻¹). CH₄ in these daughter products is measured and CO is calculated using the known CO: CH₄ ratio of the parent. The parents are considered stable and by making fresh daughter standards twice a year, we determine the growth rate of CO in the primary standards.

Here we present results from the internal tracer method and the latest update on the most recent determinations of the drift rates in the CO primary standards, implications for the WMO CO scale, and future plans to ensure scale stability.

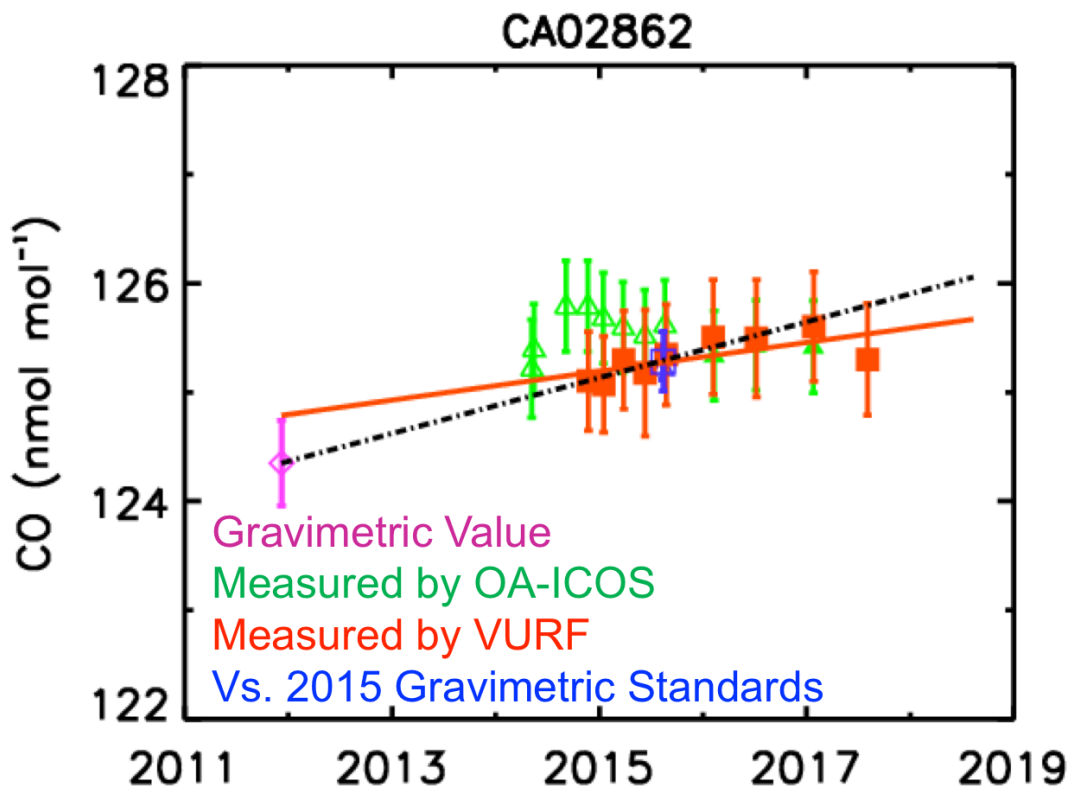


Figure 1. Example of results for one of the CO primary standards. The initial gravimetric assigned value (pink symbols), the measurement results using the internal tracer method on two different instruments (green and red symbols) and 2015 gravimetric standards (blue symbol) are plotted vs. time.

W. Gichuhi¹ and L. Gamage²

¹Department of Chemistry, Tennessee Tech University, Cookeville, TN 38505; 931-372-3499, E-mail: wgichuhi@tntech.edu

²School of Environmental Studies, Tennessee Technological University, Cookeville, TN 38505

Whereas livestock methane (CH₄) emissions are not the dominant overall source for the observed sharp rises in global CH₄ levels, the occurrence of significant uncertainties in the magnitude of the existing livestock CH₄ emission inventories calls for more experimental measurements of enteric CH₄. One major challenge associated with accurate experimental measurements of CH₄ production from livestock is the fact that the grazing animals are a representation of mobile emission sources with activity-related emission patterns. In this presentation, we assess the application of spectroscopic-based techniques in measuring enteric methane. The efficacy of a portable wavelength-scanned CRDS (Picarro G2401) in estimating CH₄ production from ruminants in a feedlot, based on the measured CH₄:carbon dioxide (CO₂) ratio from exhaled breath and the amount of CO₂ produced per Heat Producing Unit (HPU) is examined and compared with other spectroscopic techniques that are based on natural grazing conditions such as the open-path laser technique. Our measurements shows daily linear regression fits of the CH₄ to CO₂ concentration that have high correlation (R²=0.91), allowing for direct estimation of enteric CH₄ emission factors

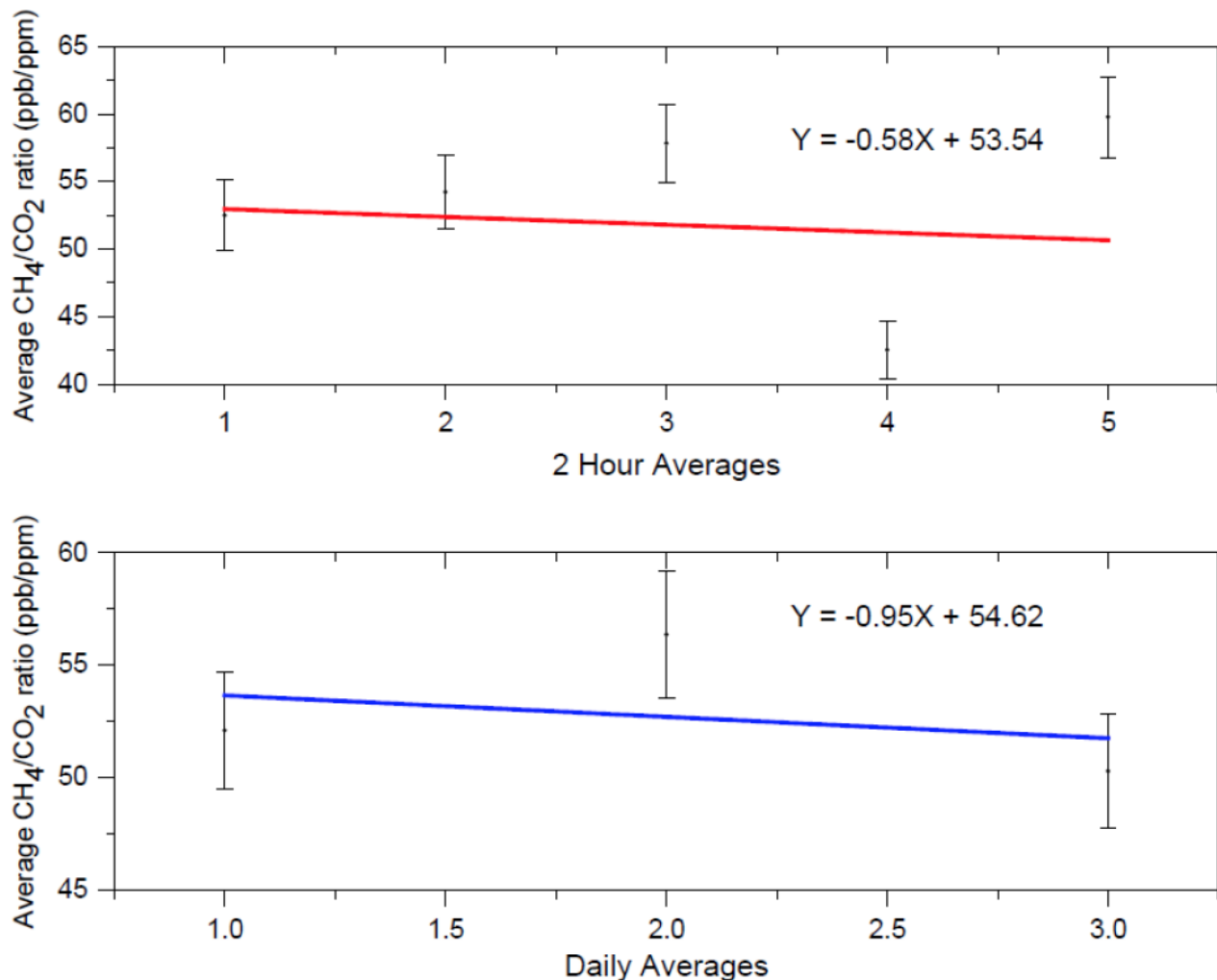


Figure 1. Daily and hourly averages of the linear regression ratios of CH₄:CO₂ (ppb/ppm).

Open-path Spectroscopy to an Airborne Retroreflector on a Quadcopter

K. Cossel¹, E. Waxman¹, E. Hoenig¹, M. Cermak¹, C. Choate², D. Hesselius², I. Coddington¹ and N. Newbury¹

¹National Institute of Standards and Technology (NIST), Boulder, CO 80305; 303-497-4115, E-mail: kevin.cossel@nist.gov

²University of Colorado, Integrated Remote and In Situ Sensing (IRISS), Boulder, CO 80309

Measuring trace gas emissions from spatially complex and temporally variable sources, such as leaking natural gas infrastructure, is challenging with existing measurement systems due to the associated variability. Small unmanned aerial systems (sUAS) could solve this challenge because of their ability to provide both horizontal and vertical spatial resolution. However, the payload restrictions of sUASs limit the available instrumentation. In particular, high-sensitivity trace gas measurement systems are currently too heavy and large to fly with most sUASs. Here, we present a new measurement system, based on the technique of dual frequency comb spectroscopy, that addresses this difficulty by simultaneously measuring the path-integrated concentration of multiple gases with high precision between a ground station and a retroreflector mounted on a small quadcopter. Currently, the frequency comb operates in the near-infrared spectral region from around 5900 to 6700 cm^{-1} , which allows rapid (~ 10 -second) measurements of acetylene (C_2H_2), carbon dioxide (CO_2), methane (CH_4), water (H_2O), and hydrogen-deuterium oxide (HDO). The eye-safe frequency comb light is launched from a telescope on a fast azimuth/elevation gimbal to a lightweight retroreflector mounted on a small quadcopter, which also carries a GPS receiver and pressure, temperature, and humidity sensors. The motion of the quadcopter is tracked by the ground station using an image-processing-based feedback system. We will show results from field tests of this system for emissions quantification using simultaneous controlled releases of CH_4 and C_2H_2 in an approximately $200 \times 200 \text{ m}^2$ area. Using a micro-meteorological mass-balance approach, we find good agreement with the known emissions rate with a scatter of $\pm 20\%$ for a single, ~ 10 -min-long measurement.

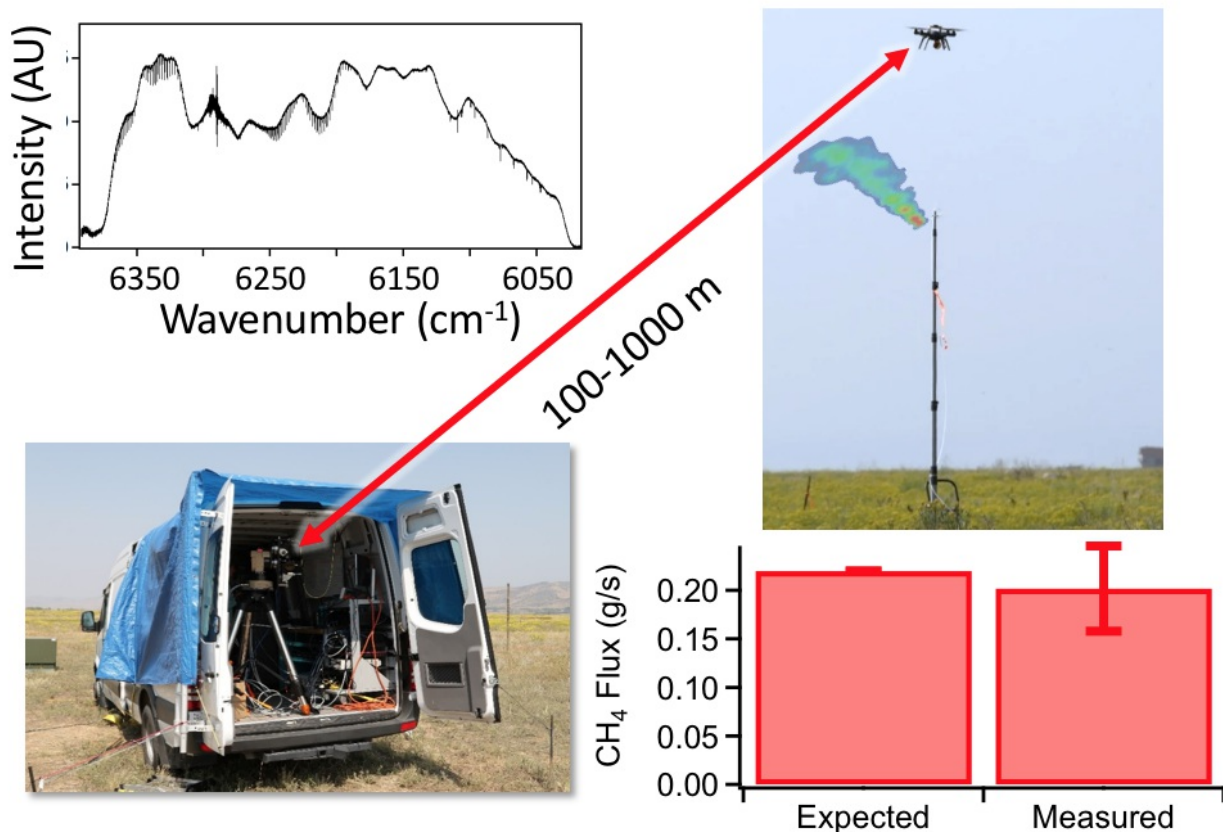


Figure 1. Mobile dual-comb spectroscopy for emissions quantification of controlled CH_4 releases. The frequency comb light is launched from a telescope in a van to a retroreflector on a quadcopter, which is flown downwind of a controlled CH_4 and C_2H_2 release. The returned spectrum (**upper left**) is processed to obtain the path-integrated gas concentration. By measuring a vertical profile downwind, the emissions rate can be determined (**lower right**).

Performance Validation of New High-precision CH₄ and CO₂ Analyzers Based on Optical Feedback Cavity Enhanced Absorption Spectroscopy

I. Begashaw, M. Johnson, A. Komissarov, B. Miller, D. Trutna, R. Walbridge, J. Welles and G. Burba

LI-COR Biosciences, Lincoln, NE 68504; 402-467-0907, E-mail: israel.begashaw@licor.com

Atmospheric carbon dioxide (CO₂) and methane (CH₄) measurements require instruments that are accurate, precise, and stable. Often these measurements are conducted in remote locations and require instrumentation that are robust, low power, and with minimal maintenance. In this presentation we report on progress towards the development of two instruments based on optical feedback cavity enhanced absorption spectroscopy that provide high-precision measurements of CH₄ ($1\sigma=0.25$ ppb, at 2 ppm CH₄ in dry air, 5-second averaging) and CO₂ ($1\sigma=25$ ppb, at 400 ppm CO₂ in dry air, 5-second averaging). We present results that show very low drift with temperature across the range from -20 to 45° C. In addition, both instruments measure the water vapor (H₂O) mole fraction in the sample and use that to perform the necessary correction for dilution and line broadening such that the reported CO₂ and CH₄ dry mole fractions are accurate from 0-4% H₂O.

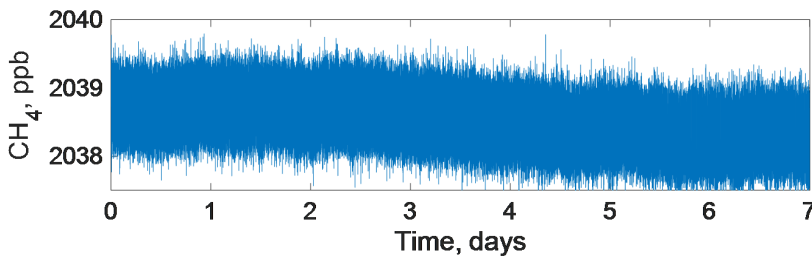


Figure 1. Continuous 1Hz measurements of cylinder air for 7 days.

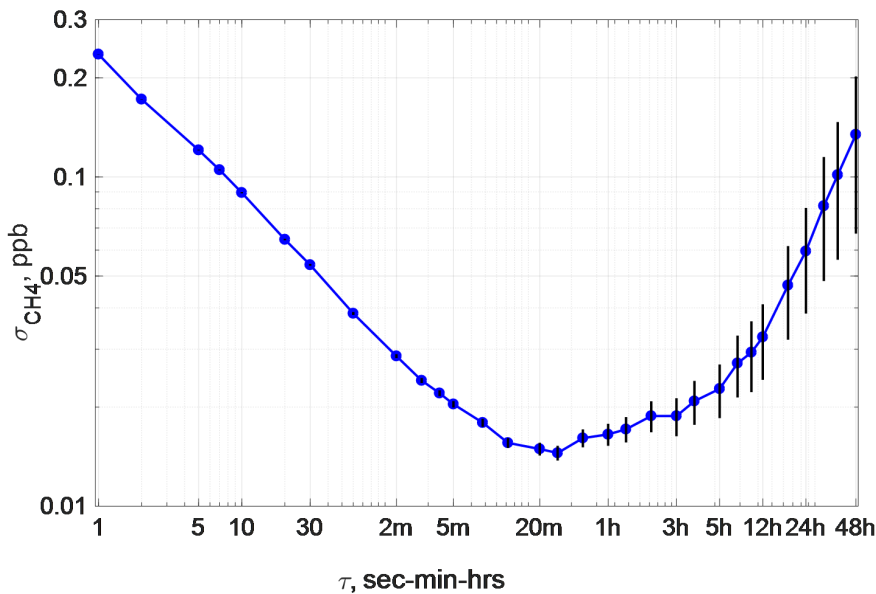


Figure 2. Allan deviation plot from 7 days of CH₄ measurement.

Estimation of Enteric Methane Emissions in Ruminants Using CO₂:CH₄ Ratio Obtained with a Wavelength-scanned Cavity Ring-down Spectrometer

L.P. Gamage¹ and W. Gichuhi²

¹School of Environmental Studies, Tennessee Technological University, Cookeville, TN 38505; 931-539-2363, E-mail: lpgamage42@students.tntech.edu

²Department of Chemistry, Tennessee Tech University, Cookeville, TN 38505

Experimental measurements of enteric methane (CH₄) involving either individual animals or a group of animals are usually complex and expensive. As a result, models are heavily relied upon when it comes to predicting enteric CH₄ emissions at global, regional, or even local levels. In this work, results on enteric methane measurements based on a direct experiment strategy that uses carbon dioxide (CO₂) as a tracer gas are presented. A calibrated, wavelength-scanned cavity ring down spectrometer (Picarro G2401) is utilized to make simultaneous measurements of dry mole fractions of CH₄ and CO₂ from a beef cattle feedlot located at the Hyder-Burks Agricultural Pavilion farm in Cookeville, Tennessee (36°11'53" N, 85°32'19" W). Heat production unit (HPU) is determined using the animal body weights, milk production, and days of pregnancy to yield CO₂ production (L/day) from ruminants. The value for the total CO₂ production is then combined with the experimentally calculated CH₄:CO₂ ratio to estimate CH₄ emission factors in Putnam County and Tennessee. Using a CH₄:CO₂ ratio of 52.90 ± 3.00 ppb/ppm and the respective livestock populations, we estimate an annual enteric CH₄ emission of 117 ± 7 Gg yr⁻¹ and 1.43 ± 0.08 Gg yr⁻¹ for Tennessee and Putnam county, respectively. The values obtained from this study are in close agreement to the ones reported by the Environmental Protection Agency's inventory on enteric methane in the United States obtained using the metabolizable energy intake data of nutrients fed to ruminants.

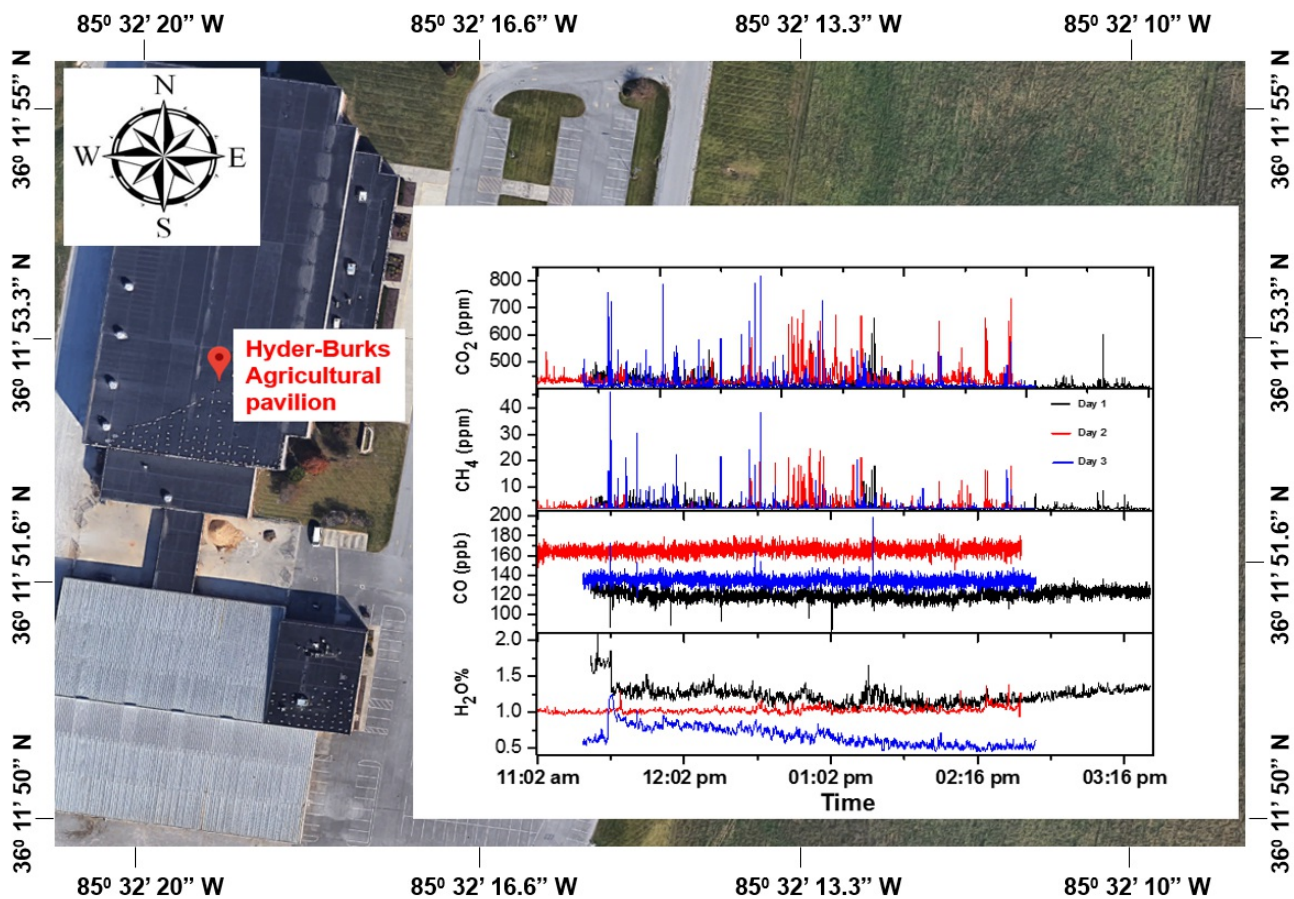


Figure 1. Location of the Hyder-Burks Agricultural Pavilion farm in Cookeville, TN (36°11' 53" N, 85°32' 19" W) where concentration measurements from the breath of animals were taken using a Picarro G2401 cavity ring down spectrometer. A daily average CH₄: CO₂ ratio of 0.053 ± 0.003 was obtained on 03/30/2017, 03/31/2017, and 04/07/2017.

¹³C and ¹⁸O Isotope Effects Resulting from High Pressure Regulation and CO₂ Cylinder Depletion

R.A. Socki¹, A. Kumar¹, T. Jacksier¹ and M.C. Matthew²

¹Air Liquide, Delaware Research & Technology Center, Newark, DE 19702

²Airgas Specialty Gases, Plumsteadville, PA 18949; 908-397-7371, E-mail: matt.matthew@airgas.com

Global observatories and research stations measure atmospheric gases, such as carbon dioxide (CO₂), to provide critical data for global climate change models. The models rely on precise and accurate isotopic measurements to help differentiate the various CO₂ sources and sinks. These measurements are typically made with an Isotope Ratio Mass Spectrometer (IRMS) which requires stable isotopic standards of CO₂.

An equilibrium isotope fractionation within the liquid-vapor system of carbon dioxide as a function of temperature for both carbon and oxygen isotopes is well established and has been for many years (Grootes et. al. 1969). Carbon isotopes tend to be enriched in carbon-13 (¹³C) in the vapor phase while oxygen isotopes tend to be depleted in oxygen-18 (¹⁸O) in the vapor phase. This observation has particular relevance in contemporary stable isotope laboratory practices mainly due to the advent of Continuous Flow-Isotope Ratio Mass Spectrometry (CF-IRMS) techniques. For ¹³C and ¹⁸O measurements, CF-IRMS relies almost exclusively on incorporating a high pressure cylinder of CO₂ as a calibrated internal reference gas. If reference gas contains a liquid phase, the laboratory's ability to produce reliable isotope data will be dependent on whether the isotopic composition of the CO₂ vapor phase will change during depletion of that CO₂. Intuitively, one may presume that as the liquid CO₂ within that cylinder decreases, the vapor produced from that liquid will change isotopically to reflect known isotopic fractionation between those phases.

This presentation will quantify isotopic fractionations for both ¹³C and ¹⁸O as a function of CO₂ cylinder depletion. CO₂ vapor samples from the cylinder that contains both liquid and vapor phases will be taken regularly and measured for both ¹³C and ¹⁸O via Dual Inlet-Isotope Ratio Mass Spectrometry. The carbon dioxide will be depleted during sequential sampling and resulting cylinder contents monitored gravimetrically. Observed isotopic effects (fractionation) of the vapor from the depleted CO₂ cylinder will be reflected in the ¹³C and ¹⁸O composition of that vapor. Thus the last remaining liquid within the cylinder, as confirmed gravimetrically, will likely show the largest isotope effect. Additionally, data will be presented to illustrate with selection of the appropriate regulator, pressure reduction can be achieved without fractionation.

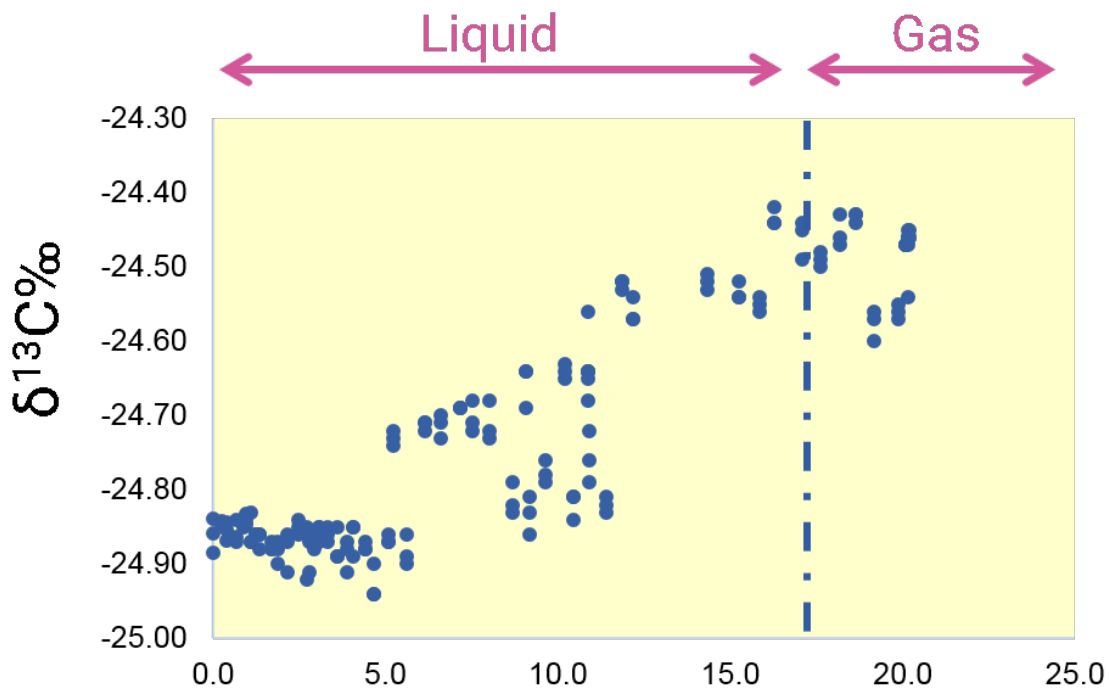


Figure 1. Effect of gas phase withdrawal from a LCO₂ cylinder on the carbon isotope ratio.

CO₂ Urban Synthesis and Analysis ("CO₂-USA") Network

J. Lin¹, L. Hutyra², C. Loughner³, A. Stein⁴, K. Lusk², L. Mitchell¹, C. Gately² and S. Wofsy⁵

¹University of Utah, Salt Lake City, UT 84112; 801-581-7530, E-mail: John.Lin@utah.edu

²Boston University, Department of Earth & Environment, Boston, MA 02215

³University of Maryland, College Park, MD 20742

⁴NOAA Air Resources Laboratory (ARL), Silver Spring, MD 20910

⁵Harvard University, Cambridge, MA 02138

Emissions of carbon associated with cities comprise a large component of the anthropogenic source. A number of cities have announced plans to reduce greenhouse gas emissions, but the scientific knowledge to quantitatively track emissions and assess the efficacy of mitigation is lacking. As the global population increasingly resides in urban regions, scientific knowledge about how much, where, and why a particular city emits carbon becomes increasingly important. To address this gap, researchers have initiated studies of carbon emissions and cycling in several U.S. cities, making it timely to develop a collaborative network to exchange information on community standards and common measurements, facilitate data sharing, and create analysis frameworks and cross-city syntheses to catalyze a new generation of researchers and enable new collaborations tackling important objectives that are difficult to address in isolation.

We describe initial results from an incipient network focusing initially on cities in the U.S. with low barriers of entry that entrains a cross-section of U.S. urban centers with varying characteristics: size, population density, vegetation, urban form, infrastructure, development rates, climate, and meteorological patterns. Results will be reported that emerged from the initial workshop covering data harmonization & integration, inventory comparison, stakeholder outreach, network design, inverse modeling, and collaboration. More information can be found on the project web site: <http://sites.bu.edu/co2usa/>

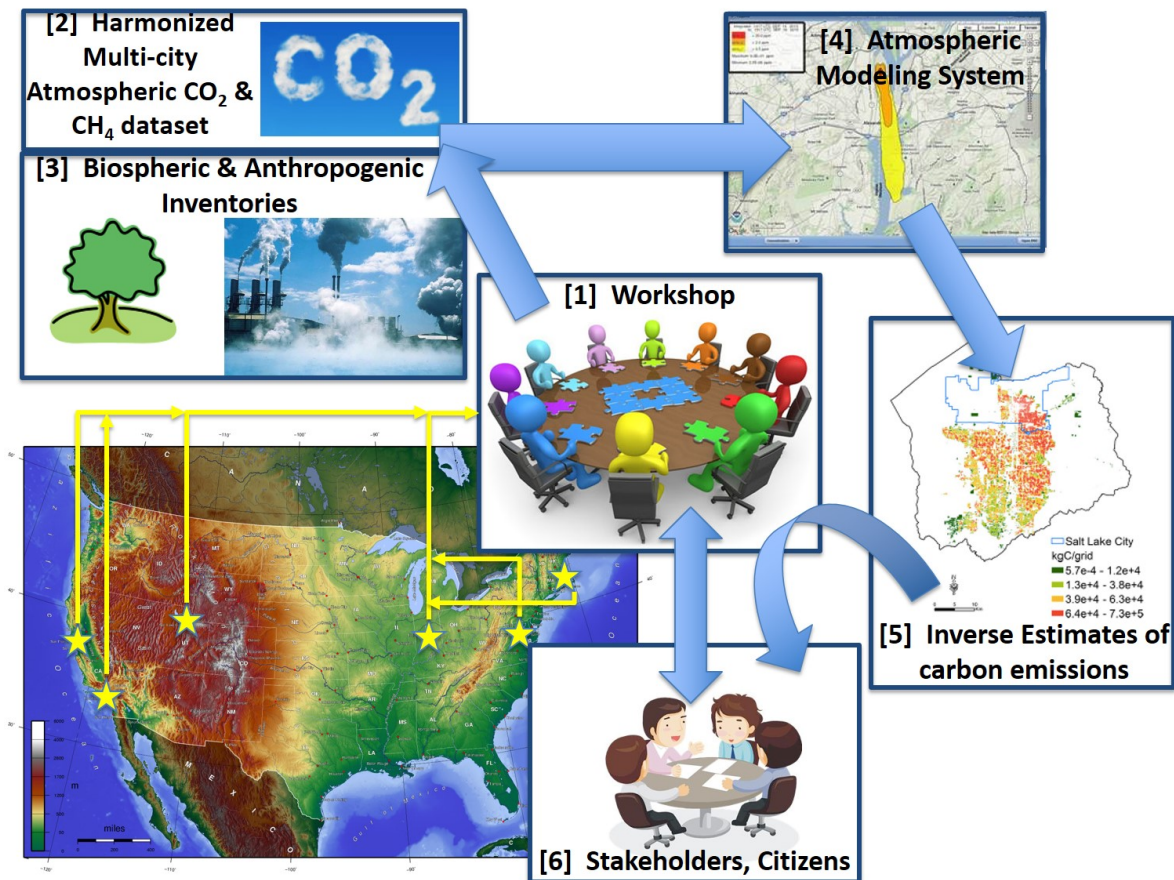


Figure 1. CO₂-USA project overview.

Investigating Methane Trends and Variability Using the GFDL-AM4 Model and NOAA GMD Observations

J. He^{1,2}, V. Naik² and L. Horowitz²

¹Program in Atmospheric and Oceanic Sciences, Princeton University, Princeton, NJ 08540; 609-452-5851, E-mail: Jian.He@noaa.gov

²NOAA Geophysical Fluid Dynamics Laboratory (GFDL), Princeton, NJ 08540

Large uncertainties persist in our understanding of the trends and variability in atmospheric methane (CH_4) over the past few decades. Bottom-up global Earth System Models (ESMs) that realistically simulate the physical, chemical, and biogeochemical processes characterizing the global methane cycle, and interactions and feedbacks between these processes are powerful tools for quantifying the global methane budget, its time evolution, and impacts on composition and climate. In this work, the representation of methane in the atmospheric chemistry model of ESM4 (AM4) has been improved with prescribed anthropogenic and natural emissions (Emis) and compared to that forced by methane concentrations as lower boundary conditions (Conc). We force the emission-driven simulation with anthropogenic methane emissions over the 1980-2014 from the Community Emissions Database System (CEDS) inventory developed in support of the Intergovernmental Panel on Climate Change (IPCC) - 6th Assessment Report. Our simulation with anthropogenic methane emissions increased by 30% is able to best capture the observed surface methane trend and variability (Figure 1) although there are moderate overpredictions, possibly indicating a problem in the emissions. Future work will focus on correcting these biases by optimizing the emissions and will explore the role of individual sources and sinks in driving methane variability by including a representation of methane isotopes in the model.

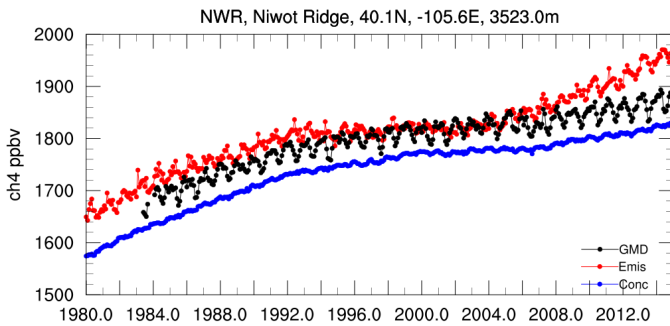


Figure 1. Comparison of surface methane dry mole fractions from GFDL-AM4 against ESRL/GMD surface observations at Niwot Ridge site. Black lines represent ESRL/GMD surface observations, blue lines represent simulated methane concentrations forced by prescribed concentrations as lower boundary condition (Conc), and red lines represent simulated methane forced by emissions (Emis).

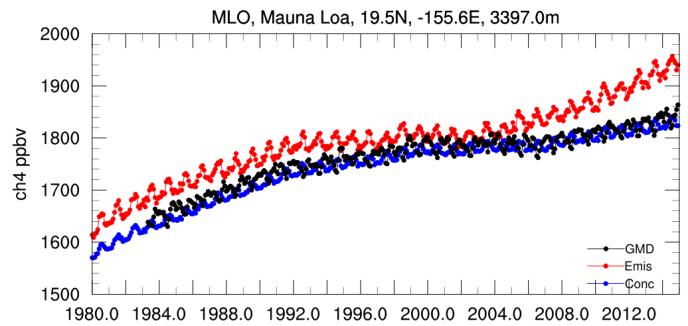


Figure 2. Comparison of surface methane dry mole fractions from GFDL-AM4 against ESRL/GMD surface observations at Mauna Loa site. Black lines represent ESRL/GMD surface observations, blue lines represent simulated methane concentrations forced by prescribed concentrations as lower boundary condition (Conc), and red lines represent simulated methane forced by emissions (Emis).

Characterizing and Comparing Anthropogenic CH₄ Sources in the DJ Basin using Mobile Surveys

C. Fougere¹, E. Atherton¹, E. Bourlon¹, D. Risk¹, O.A. Sherwood² and B.H. Vaughn²

¹St. Francis Xavier University, Antigonish, Nova Scotia, Canada; 902-521-0189, E-mail: cfougere@stfx.ca

²Institute of Arctic and Alpine Research (INSTAAR), University of Colorado, Boulder, CO 80309

Vehicle-based atmospheric surveys must be able to distinguish between source types in complex multi-use landscapes, and must also be sensitive to spatiotemporal changes in the ambient concentrations of naturally occurring gases. We performed 3,700 km of vehicle-based surveys with a Picarro Surveyor CRDS in the Denver-Julesburg (DJ) Basin during the summer of 2014 to compare emissions from different methane sources. During these surveys, we collected more than 500,000 geo-located multi-gas (carbon dioxide [CO₂], methane [CH₄], water vapor [H₂O], delta 13-methane [$\delta^{13}\text{CH}_4$]) measurements. We used super-ambient ratios of CO₂:CH₄ to detect CH₄ plumes and geospatial analysis to attribute the emissions to potential known sources. Based on wind direction and a threshold distance of 300 m, a total of 784 known infrastructure units were sampled on more than one occasion. Of the 2,524 CH₄-rich plumes (eCO₂:eCH₄ < 100), 954 (38%) were attributed to known local sources within 300 m of roadside. Though composting facilities and gas processing plants had the highest emission frequencies (25% and 20%, respectively), concentrated animal feeding operations and oil and gas wells accounted for 95% of emission sources (2% and 93%, respectively). These data are used to characterize the geochemical signature associated with each source type, as well as to compare emission rates to existing inventories. These data can ideally be used to inform policy and practice aimed at curbing greenhouse gas emissions and improving local air quality.

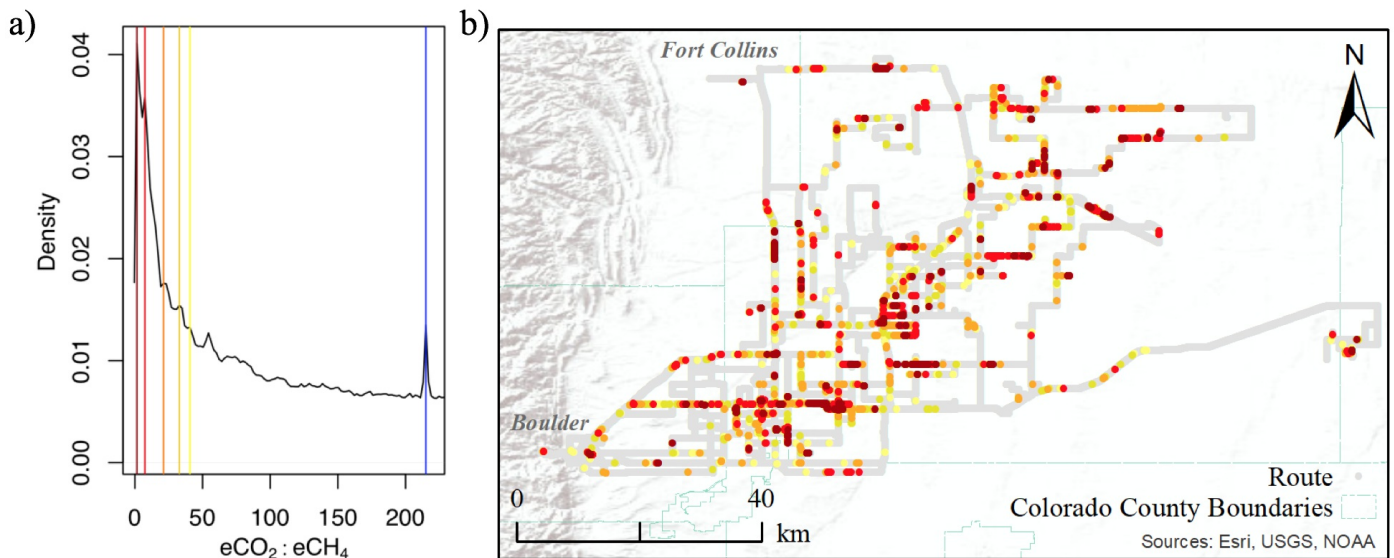


Figure 1. a) A density plot of the ratio of excess CO₂ to excess CH₄ reveals the most common CH₄-rich geochemical signatures observed during the survey campaign. The ambient ratio of excess CO₂ to excess CH₄ is marked by the minor isolated peak and blue line at 215. b) Locations of the CH₄-rich geochemical ratios marked on the previous plot are layered to form a heat map of CH₄ emissions.

Effects of Drought Conditions on CO₂ Flux in Semi-arid Chaparral Ecosystems.

A. Fenner

San Diego State University, Global Change Research Group, San Diego, CA 92182; 858-405-0473, E-mail: anfenner@sdsu.edu

As global atmospheric carbon dioxide (CO₂) increases due to human activity, it is vital that we create measures to reduce levels of CO₂ in the atmosphere. Carbon flux in semi-arid shrublands has rarely been studied using eddy covariance techniques. Semi-arid shrublands, especially old-growth shrub ecosystems, could mitigate the rising levels of CO₂ in the atmosphere. Under normal weather conditions, such ecosystems can become carbon sinks, ultimately absorbing the excess levels of carbon in the atmosphere. However, as global temperatures change due to human activity, precipitation patterns are likely to change resulting in an increase in drought events. As the prevalence of drought events increase in semi-arid shrubland ecosystems, gaining a better understanding of how these ecosystems act under non-normal weather conditions is key. In this study, eddy covariance measurements of the net ecosystem exchange (NEE) of CO₂ over a 14 to 20-year period were analyzed for three Mediterranean-type chamise (*Adenostoma fasciculatum*)-dominated chaparral ecosystems in Southern California. Findings from this study may suggest a shift in the carbon source-sink dynamics of these semi-arid chaparral ecosystems.

Keywords: carbon flux, eddy covariance, semi-arid shrublands, chaparral ecosystems, net ecosystem exchange (NEE)

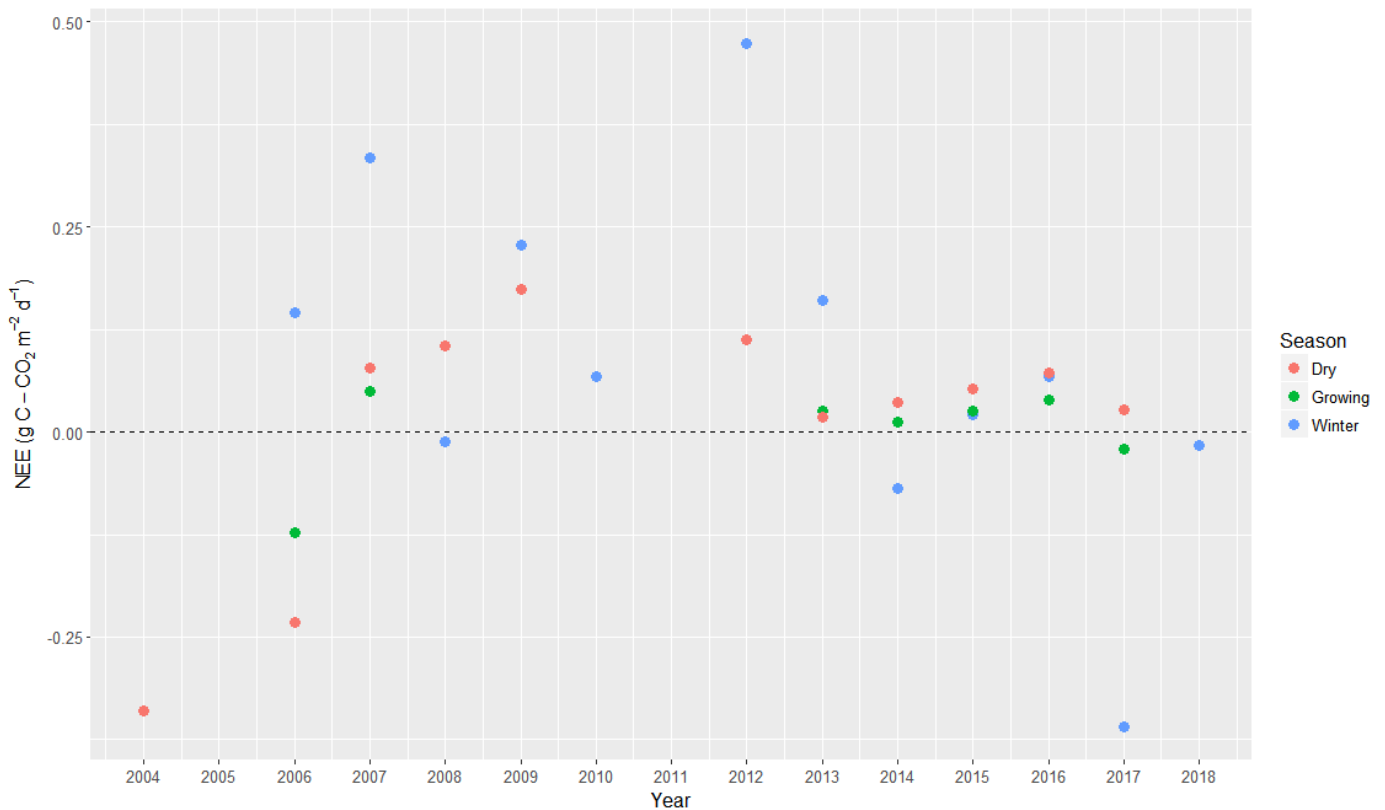


Figure 1. Average seasonal net ecosystem exchange (NEE) during the years of 2004 to 2018 collected by the New Stand eddy covariance tower. Winter season (November 1st to February 28th), growing season (March 1st to June 30th), dry season (July 1st to October 31st).

Sources and Variability of Air Toxics Downwind of an Oil and Natural Gas-producing Well Pad in a Residential Community

I. Mielke-Maday^{1,2}, M. Madronich^{1,2}, P. Handley^{1,2}, J. Kofler^{1,2}, B. Hall², D. Kitzis^{1,2}, B.R. Miller^{1,2}, P.M. Lang², E. Moglia^{1,2}, M.J. Crotwell^{1,2}, M. Rhodes^{1,2}, T.K. Mefford^{1,2}, E.J. Dlugokencky², K. Thoning², B.H. Vaughn³, L.M. McKenzie⁴, R.C. Schnell² and G. Petron^{1,2}

¹Cooperative Institute for Research in Environmental Sciences (CIRES), University of Colorado, Boulder, CO 80309; 303-497-5456, E-mail: ingrid.mielke-maday@noaa.gov

²NOAA Earth System Research Laboratory, Global Monitoring Division (GMD), Boulder, CO 80305

³Institute of Arctic and Alpine Research (INSTAAR), University of Colorado, Boulder, CO 80309

⁴Colorado School of Public Health, University of Colorado, Anschutz Medical Campus, Aurora, CO 80045

As population growth in the Colorado Front Range continues, local oil and natural gas (O&NG) production operations and communities are becoming closer in proximity, raising concern about potential exposure of residents to air pollutants from these operations. Operators can now drill over 20 wells from one pad and horizontally for two to three miles. These large multi-well pads are industrial sites that are rapidly transforming the northeastern Colorado rural and suburban landscape. Of particular concern is benzene, a carcinogen linked to leukemia that can be released from a number of O&NG sources. Here we present results from five weeks of continuous, calibrated *in situ* measurements at a residence downwind of a new 22-well oil and gas-producing pad in Greeley, CO with a focus on benzene, toluene, ethylbenzene and xylene (BTEX) and O&NG and combustion markers. The day-to-day and diurnal variability of ambient trace gas mixing ratios downwind of the well pad is presented and the role of meteorology in the observed variability evaluated. An analysis using O&NG and combustion tracers and wind data is used to identify different emission sources (well pad, nearby road traffic) and their contributions to the observed variability. This work is funded by the National Science Foundation AirWaterGas (AWG) Sustainability Research Network and is a collaboration with the Colorado School of Public Health.



Figure 1. The mobile laboratory, an instrumented van, was parked at a residence ~260 m downwind of a well pad.

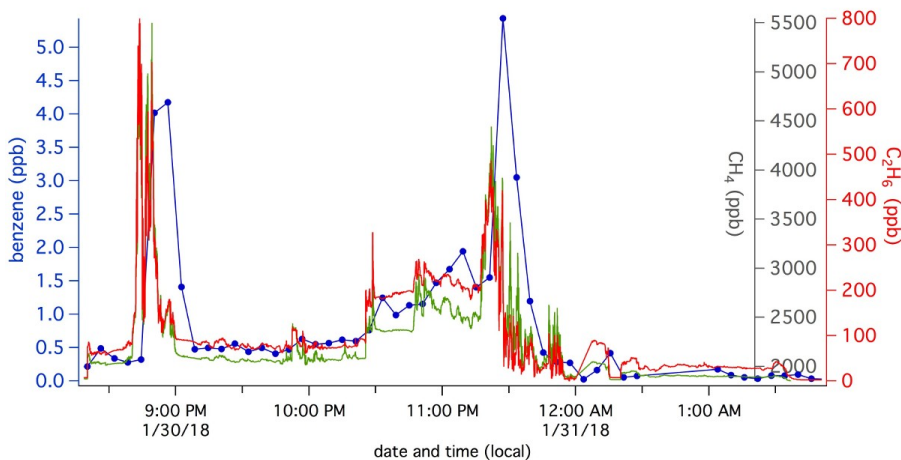


Figure 2. This period of elevated benzene is likely due to emissions from the well pad, indicated by elevated and correlated methane (CH_4) and ethane (C_2H_6).

Ground-truth Calibration for the VIIRS Nightfire Detector of Gas Flares

M. Zhizhin^{1,2}, C. Elvidge², E. Kihn² and Z. Kodesh³

¹Cooperative Institute for Research in Environmental Sciences (CIRES), University of Colorado, Boulder, CO 80309; 303-497-6385, E-mail: mikhail.zhizhin@noaa.gov

²NOAA National Environmental Satellite, Data, and Information Service (NESDIS), National Centers for Environmental Information (NCEI), Boulder, CO 80305

³John Zink LLC, Tulsa, OK 74116

A series of 12 nighttime gas flares were run at the John Zink LLC test facility in Tulsa, Oklahoma, in January and February 2018. The flares were lit at the time of the Soumi National Polar-orbiting Partnership (NPP) satellite overpass, so they could be detected by Visible Infrared Imaging Radiometer (VIIRS) with clear sky and wind speed < 20 mph local weather. The test plan includes 3 sizes of low pressure natural gas flares with flowrates of 750, 7,500 and 75,000 lb/hour observed by satellite from nadir, medium angle, and side view. During the calibration experiment the flares were filmed from 2 near-field sites. Total radiative heat from the flare and its short-wave infrared spectra were sampled exactly at the time of the satellite overpass. This is the first ground truth validation for the relation between the flared volume (BCM) and the Planck curve fitted to flare infrared signature detected by VIIRS (Nightfire). The experiment has confirmed the correlation between flow rate and satellite derived radiative heat with 0.99 R².



Figure 1. Large flowrate flare test at the moment of VIIRS overpass on January 12, 2018.

Volcanic Aerosol Optical Depths during the Post-Pinatubo Era, 1996-2018

R.A. Keen

University of Colorado, Department of Atmospheric and Oceanic Sciences, Boulder, CO 80309; 303-642-7721, E-mail: richard.keen@colorado.edu

About once per year, on average, the moon is totally eclipsed; the moon is then illuminated by sunlight refracted into the umbra, primarily by the stratosphere. Stratospheric aerosols can affect the brightness of the eclipsed moon, and climatically significant, visible-band, global aerosol optical depth (AOD) can be directly measured from the difference between observed and predicted brightness.

Successful observations of the total lunar eclipse of 31 January 2018 (the first eclipse in over two years) by the author and others reveal that the global volcanic AOD remains at very low levels. A 22+ year period of a relatively clear stratosphere therefore continues, and is the longest such stretch since 1837-1862. The stratospheric impacts of several climatically-insignificant volcanoes during 1996-2018 are identified. There is no trend in AOD over this period, ruling out volcanoes as a contributor to the stable global temperatures during 1998-2015. Compared to the volcanically active period 1980-1995 (el Chichon and Pinatubo), the clear stratosphere since 1995 has contributed an increase of radiative climate forcing equal to that due to increasing greenhouse gases.

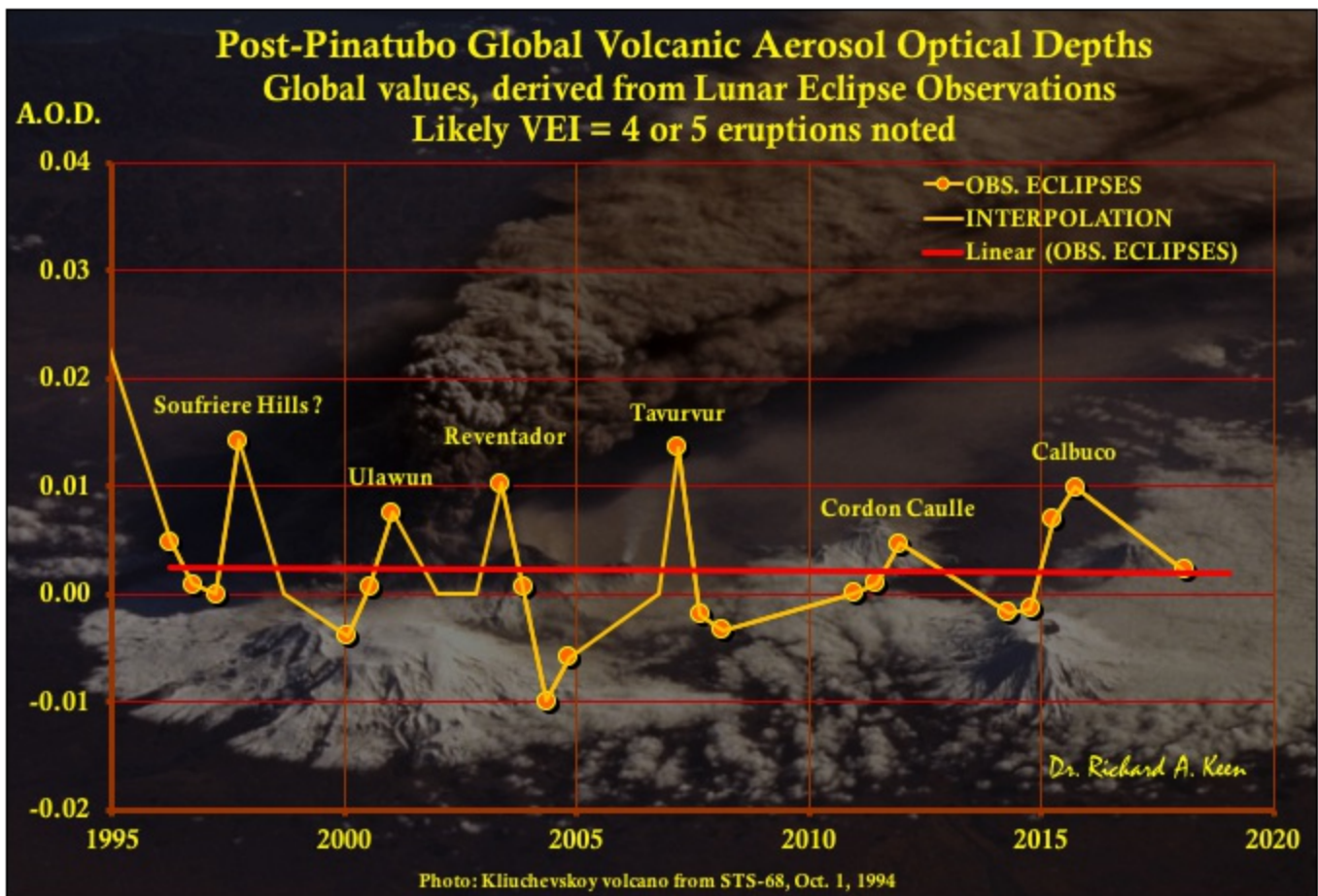


Figure 1. Global Volcanic Aerosol climate forcing during the post-Pinatubo era, 1996-2018.

Use of Ground- and Space-based Visible Imagery with other Data for Model Evaluation and Assimilation

S. Albers^{1,2} and Z. Toth²

¹Cooperative Institute for Research in the Atmosphere (CIRA), Colorado State University, Fort Collins, CO 80521; 303-497-6057, E-mail: steve.albers@noaa.gov

²NOAA Earth System Research Laboratory, Global Systems Division (GSD), Boulder, CO 80305

Simulated visually realistic camera-like images of the sky can provide informative displays of 3-D model fields. Comparisons of simulated and actual camera images can help with model evaluation. The image simulation software can also act as a forward model for coupling cameras with visible/infrared (VIS/IR) satellite and radar data for improved sub-hourly and sub-km cloud analysis.

Thus based on Numerical Weather Prediction (NWP) analysis of model conditions and the quantitative use of 3-D radiative transfer, color images of the current or future weather and land surface conditions can be rendered from any vantage point in a visually realistic manner. A comparison of these simulated images with space-, air-, and ground-based camera images offers powerful tools for subjective NWP interpretation and objective evaluation of NWP performance.

The simulated and actual images and related observations (e.g. VIS/IR satellite, radar, METARs) can be used in a 3- and 4-D variational tomographic data assimilation scheme. Here the differences between the observed and simulated images offer valuable information for constraining the model hydrometeor, aerosol, land surface, and other fields. The tomographic analysis entails having multiple viewing angles from available satellites, radars, and cameras. This along with 3-D radiative transfer that includes multiple scattering allows us to look inside of both precipitating and non-precipitating clouds. Other physical, dynamical, and statistical constraints help to round out the analysis.

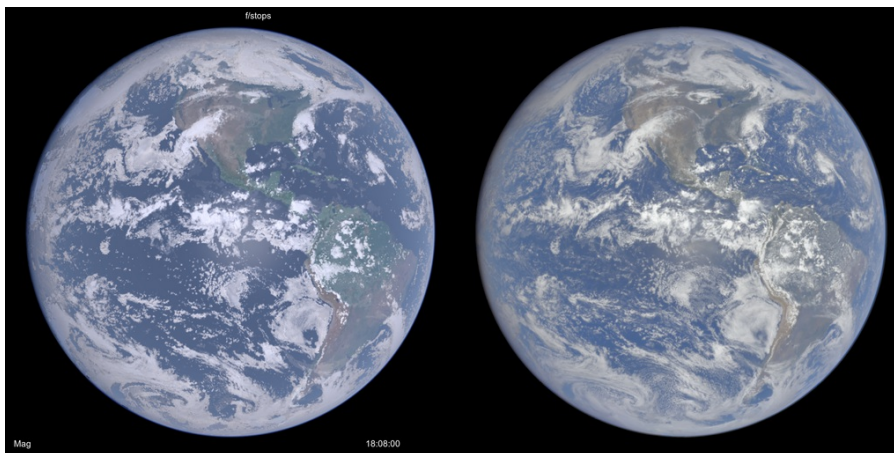


Figure 1. Comparison of simulated color image (left) with actual image taken by the Earth Polychromatic Imaging Camera (EPIC) aboard the Deep Space Climate Observatory (DSCOVR) satellite. Model fields (from Local Analysis and Prediction System [LAPS] analysis) of hydrometeors are used along with a default value for aerosols. Land surface data comes from the Next Generation Blue Marble imagery. The EPIC data are independent of the analyzed fields.

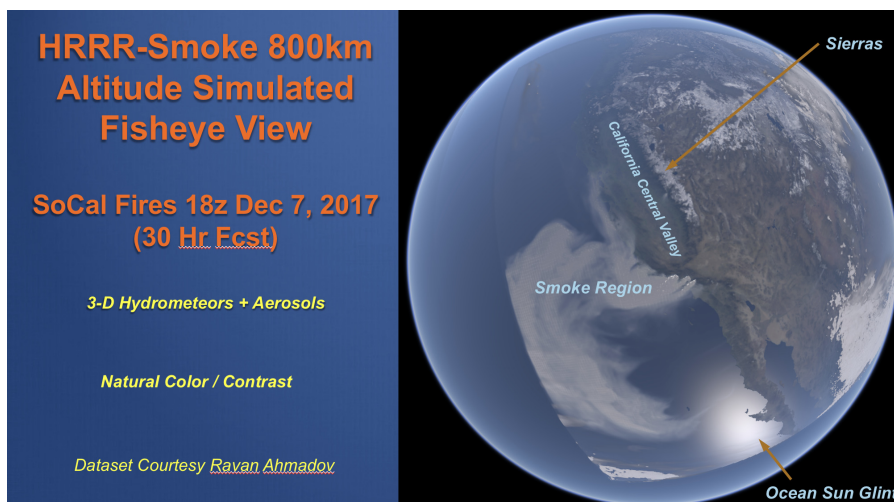


Figure 2. Simulated view from space of wildfires in California. Model fields are from the HRRR-Smoke developed at ESRL.

Constraining Aerosol Properties with Ground-based Lidar and other Remote Sensing Techniques

J.E. Barnes^{1,2}

¹Cooperative Institute for Research in Environmental Sciences (CIRES), University of Colorado, Boulder, CO 80309; 720-684-9143, E-mail: John.E.Barnes@noaa.gov

²NOAA Earth System Research Laboratory, Global Monitoring Division (GMD), Boulder, CO 80305

Lidars are versatile instruments for measuring aerosols but are limited by only measuring light scattered from a single angle for a given altitude, which is usually 180° backscattered light. Because the amount of backscattered light compared to the total scattered and absorbed light varies greatly with particle size, shape, and composition, the retrieval of aerosol properties is usually underdetermined by the data. Multiple wavelengths, polarizations, and Raman channels can be used to reduce the problem but there are still limitations. Conversion of lidar backscatter to more useful quantities like extinction often relies on the assumption of an extinction to backscatter ratio known as the “Lidar Ratio”. This assumption is especially necessary under the low background stratospheric conditions where direct measurement of extinction by Raman lidar is not possible. Examples of three volcanic eruptions, Kasatochi, Sarychev, and Nabro, are shown using backscatter profiles with two laser wavelengths as an example. Evolution of the plumes can be seen as the plumes diffuse with time. Added constraints of the aerosol properties can be achieved with the addition of a bistatic receiver located at some distance from the lidar. The second receiver measures scattered light at angles less than 180°. The improvement of the aerosol property retrieval errors with this additional data are examined.

Averages of lidar aerosol profiles heavily weight the profiles to any clouds that are present during the observations. Simply using the median instead of the average gives a much better representation of the aerosols. The median profile fits an exponential function remarkably well over two or three scale heights with a value of 2.5 km. The water vapor scale height is 2.1 km and the molecular scale height is 9.1 km over Mauna Loa Observatory (MLO).

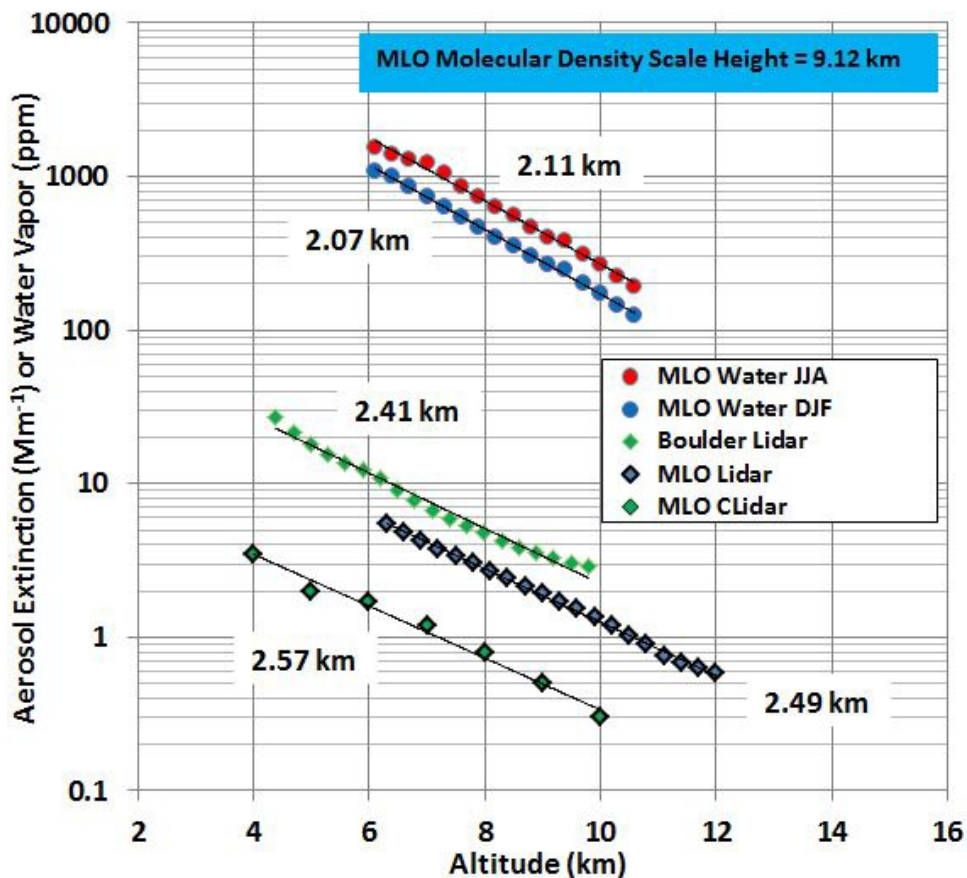


Figure 1. Scale heights for aerosols, water vapor, and molecular density are shown for MLO. The aerosol scale height for Boulder, CO is also shown. At MLO aerosol profiles were measured independently by the lidar and CLidar.

Cloud Measurements with an All-sky Camera System for Investigating Long-term Variability of Cloud Properties at South Pole

M. Shiobara¹, M. Yabuki², M. Kuji³, E.G. Dutton⁴, R.S. Stone^{5,4}, D. Longenecker⁶, B. Vasel⁴, J.J. Michalsky^{6,4}, A. McComiskey⁴ and R.C. Schnell⁴

¹National Institute of Polar Research (NIPR), Tokyo, Japan; +81 42-512-0678, E-mail: shio@nipr.ac.jp

²Kyoto University, Kyoto, Japan

³Nara Women's University, Nara, Japan

⁴NOAA Earth System Research Laboratory, Global Monitoring Division (GMD), Boulder, CO 80305

⁵Science and Technology Corporation, Boulder, CO 80305

⁶Cooperative Institute for Research in Environmental Sciences (CIRES), University of Colorado, Boulder, CO 80309

Since December 2005, an all-sky camera system has been used to acquire images for monitoring cloud conditions at the Amundsen-Scott South Pole Station. The project has been conducted in collaboration with the ESRL/GMD. The system is comprised of a Prede Model PSV-100 that includes a 3-color CCD camera with a fish-eye lens and a laptop computer for acquiring JPEG images. The camera was placed on the roof-top of the Atmospheric Research Observatory and programmed to collect images at 10-minute intervals continuously each year during the sunlit period from October into March. Measurements were made from 18 December, 2005 until 24 March, 2017. For the purpose of this study, only the data collected during November through February were analyzed to avoid issues related to low sun angles and very cold temperatures. An analysis method proposed by Yabuki et al. (2014) was applied to obtain the cloud fraction from the all-sky images. In this paper, variability of the South Pole cloud fraction will be shown for the Antarctic summer season for the last decade. Figure 1 depicts monthly mean cloud fraction at South Pole derived from the all-sky camera measurements made from December 2005 to February 2017. The result shows large variation of cloud fractions for both month-to-month and from year-to-year. Consequently, no clear trend is manifested in the decade-long time series.

*The project was initiated in 2004 with the advice and support of E. G. Dutton (1949-2012).

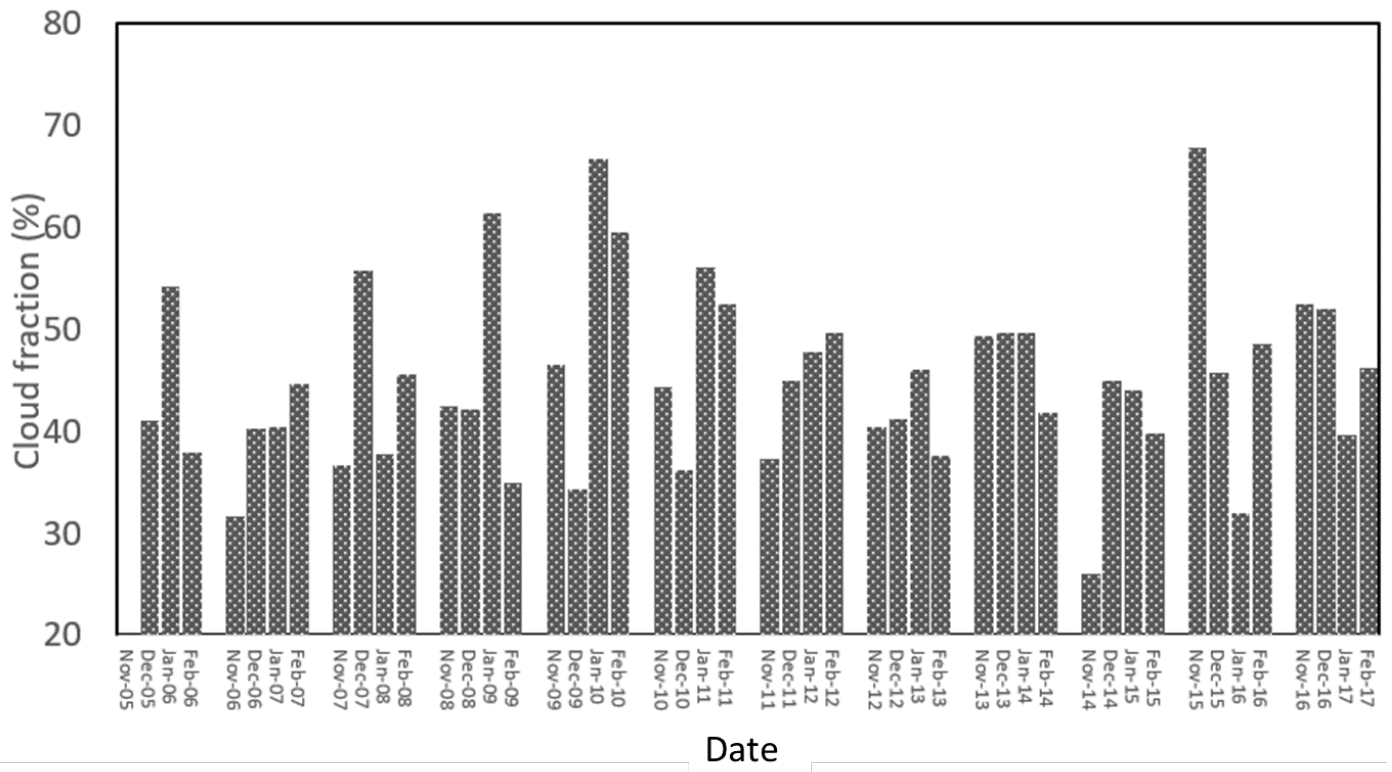


Figure 1. Monthly mean cloud fraction at South Pole for December 2005 - February 2017.

Mutual Information Analysis of Aerosol-cloud interactions by Meteorological State over Oklahoma, U.S.

I. Glenn^{1,2}, G. Feingold², T. Yamaguchi^{1,2} and E.T. Sena³

¹Cooperative Institute for Research in Environmental Sciences (CIRES), University of Colorado, Boulder, CO 80309; 303-497-5642, E-mail: ian.b.glenn@noaa.gov

²NOAA Earth System Research Laboratory, Chemical Sciences Division (CSD), Boulder, CO 80305

³Institute of Physics, University of São Paulo, São Paulo, Brazil

The aerosol indirect effect on cloud brightness has previously been measured over the Atmospheric Radiation Measurement (ARM) central continental U.S. Southern Great Plains (SGP) site in Lamont, Oklahoma for a handful of specially-selected cases. But an analysis of a 14-year dataset at the same location showed that the correlation between aerosol concentration and cloud radiative effect is negative as often as it is positive. Does co-variability with meteorological state sometimes mask the indirect effect of increasing aerosol concentration? Or instead, do feedbacks act to reduce or reverse an expected increase in cloud brightness due to increasing aerosol concentration?

To answer this question we use a scene albedo vs. cloud fraction framework to illustrate the co-variability between cloud brightness, cloud amount, diurnal variability, and variability due to meteorological state. We use a 14-year dataset as well as observations and Large Eddy Simulations (LES) from the current LES ARM Symbiotic Simulation and Observation (LASSO) campaign. We perform our own simulations with LASSO-processed initialization and ad-hoc perturbations of aerosol concentration, as well as adding measurements of natural aerosol concentration variability from SGP to perform high-resolution simulations of 18 different days with shallow cumulus of similar cloud fractions. A simulation keeping all else constant but doubling aerosol concentration shows the variability in the cloud fraction to albedo relationship illustrating the aerosol indirect effect (Figure 1). We have also performed and analyzed simulations based on days with similar doubling of aerosol concentration according to observations, but also including the observed difference in meteorological state between such days.

We calculate the information content, or Shannon entropy, of relevant variables, and then compare their mutual information. This is similar to an analysis of covariance, but has the advantage of not needing to assume a functional form (linear or otherwise) for any relationship. We then calculate the conditional mutual information to show which variables (and meteorological state) lead to a loss in mutual information between aerosol loading and cloud radiative effect. The conditional mutual information analysis allows us to quantify how much each variable leads to a loss of detectability of the aerosol indirect effect. Using multiple LES, a long-term observational dataset, and the mutual information analysis allows us to tease apart the interplay of convective dynamics, micro-physics, and meteorological state to quantify the detectability of cloud-aerosol interactions in shallow cumulus at SGP.

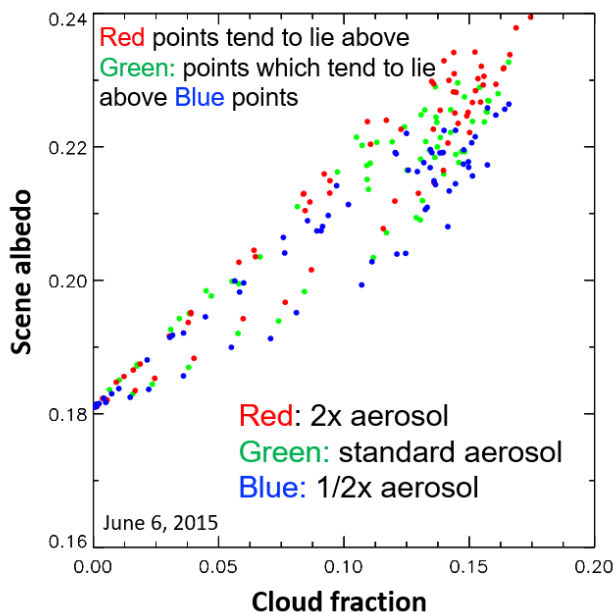


Figure 1. The scene albedo vs. cloud fraction for a simulation of the evolution of shallow cumulus over Lamont, Oklahoma on June 6th, 2015. Keeping all else constant, we perturb the aerosol concentration to illustrate the similar magnitude of brightening due to the aerosol indirect effect of a large aerosol concentration perturbation relative to the variability of scene albedo vs. cloud fraction over the course of the diurnal cycle.

Black Carbon's Contribution to Aerosol Absorption Optical Depth in South Korea

K. Lamb^{1,2}, A. Perring^{1,2}, A. Beyersdorf^{3,4}, B. Anderson⁴, C. Flynn⁵, M. Segal-Rozenhaimer^{6,7}, J. Redemann⁶, B. Samset⁸, B. Holben⁹ and J. Schwarz²

¹Cooperative Institute for Research in Environmental Sciences (CIRES), University of Colorado, Boulder, CO 80309; 303-497-5256, E-mail: kara.lamb@noaa.gov

²NOAA Earth System Research Laboratory, Chemical Sciences Division (CSD), Boulder, CO 80305

³California State University, San Bernardino, San Bernardino, CA 92407

⁴NASA Langley Research Center, Hampton, VA 23681

⁵Pacific Northwest National Laboratory, Richland, WA 99352

⁶NASA Ames Research Center, Moffett Field, CA 94035

⁷Bay Area Environmental Research Institute, Sonoma, CA 95476

⁸University of Oslo, Oslo, Norway

⁹NASA Goddard Space Flight Center (GSFC), Greenbelt, MD 20771

Aerosol absorption optical depth (AAOD), as monitored by ground-based AERONET sites, is essential for estimating radiative forcing from absorbing aerosols in global models, but few validation studies comparing *in situ* aerosol observations and ground-based AAOD exist. Globally, AAOD derived from emission-based models is scaled by as much as 6x for consistency with AERONET measurements. Systematic, repeated vertical profiles measured during the 2016 Korea-United States Air Quality (KORUS-AQ) campaign in South Korea near Seoul provided significant temporal coverage of vertically resolved aerosol properties in a single location (Figure 1). The NOAA Humidified Dual Single Particle Soot Photometer (HD-SP2) monitored black carbon (BC) mass, size distributions, mixing state, and hygroscopicity of BC containing aerosols. Significant variability in vertically resolved BC concentrations and microphysics was observed due to varying meteorological conditions and source regions. Along with bulk aerosol size distributions and optical properties and on-board sky radiance measurements, AAOD derived from measurements is compared with AAOD measured at co-located AERONET sites to evaluate closure between *in situ* and ground-based observations. These measurements revealed absorption by internally-mixed BC can explain the majority of absorption over South Korea (at 660 nm).

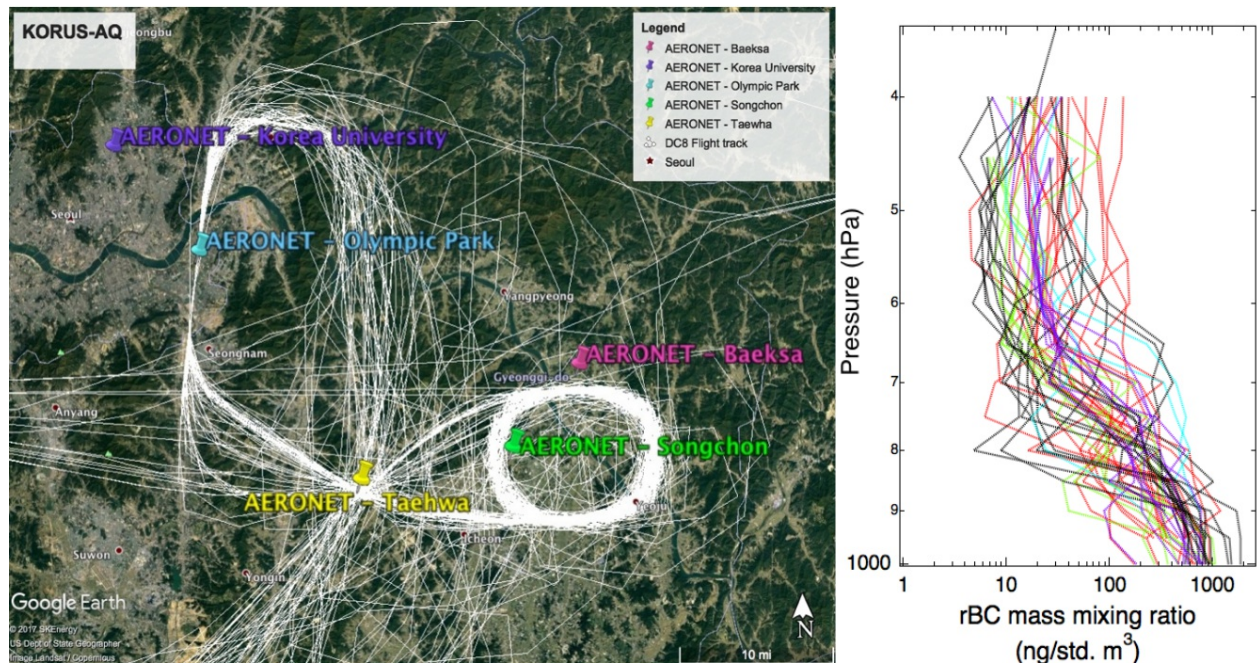


Figure 1. KORUS-AQ flight path over the Seoul Metropolitan Area, with locations of AERONET ground sites (left) and BC vertical profiles (right). Multiple spirals over Taehwa Research Forest (~30 km SE of Seoul) provided 48 *in situ* vertical profiles over approximately 6 weeks in May and June, 2016. Vertically resolved rBC mass in 50 hPa bins is shown for individual vertical profiles measured over Taehwa; colors indicate observations made during periods dominated by different synoptic scale meteorology.

NOAA Global Radiation Group Participation in International Comparisons Offering Traceable Calibration to World Solar Radiation Standards

E. Hall^{1,2}, P. Disterhoft^{1,2}, K.O. Lantz^{1,2}, C.N. Long^{1,2}, A. McComiskey², J. Wendell² and C. Wilson^{1,2}

¹Cooperative Institute for Research in Environmental Sciences (CIRES), University of Colorado, Boulder, CO 80309; 303-497-4264, E-mail: emiel.hall@noaa.gov

²NOAA Earth System Research Laboratory, Global Monitoring Division (GMD), Boulder, CO 80305

The ESRL/GMD Global Radiation Group (G-Rad) strives to collect high-quality data of the Earth's surface and atmospheric radiation budgets. Data collection requires accurate calibration of field instruments that are traceable to international standards. The G-Rad group regularly participates in international comparisons in order to calibrate our standard instruments against the accepted world standards. With our standards, we are able to perform calibrations of broadband shortwave and longwave sensors as well as broadband ultraviolet (UV) and narrowband filter radiometers.

In 2015, we participated in the Twelfth World Meteorological Organization (WMO) International Pyrheliometer Comparison (IPC-XII) hosted at the Physikalisch-Meteorologisches Observatorium Davos (PMOD). Comparing our standard active cavity pyrheliometers to the World Radiations Reference (WRR) allows us to obtain a new scale factor for our standards, which we use to perform traceable calibrations for our field instruments. We also attend the annual National Renewable Energy Laboratory (NREL) National Pyrheliometer Comparison (NPC) to check that our WRR correction factor has not changed since the last IPC.

In 2015 G-Rad also participated in the Fourth WMO Filter Radiometer Comparison (FRC) hosted by PMOD. Similar to the IPC, the FRC allows instruments to be compared to the World Optical Depth Research and Calibration Centre (WORCC) reference group for aerosol optical depth. Participation in this comparison provides us with traceable field instruments that can be used for air quality and climate studies.

In 2017, as a WMO regional UV calibration center, G-Rad sent a UV broadband instrument to participate in the second International UV Filter Radiometer Comparison (UVC), hosted at PMOD, in order to obtain traceable calibrations against the standards at the World Calibrations Center for UV (WCCUV).

The G-Rad group is committed to maintaining a high standard for calibration of our instrumentation. We will continue our participation in these inter-comparisons as well as introducing new experiments to further our understanding of the calibration process. Two such experiments that G-Rad led in 2018 are outlined here.

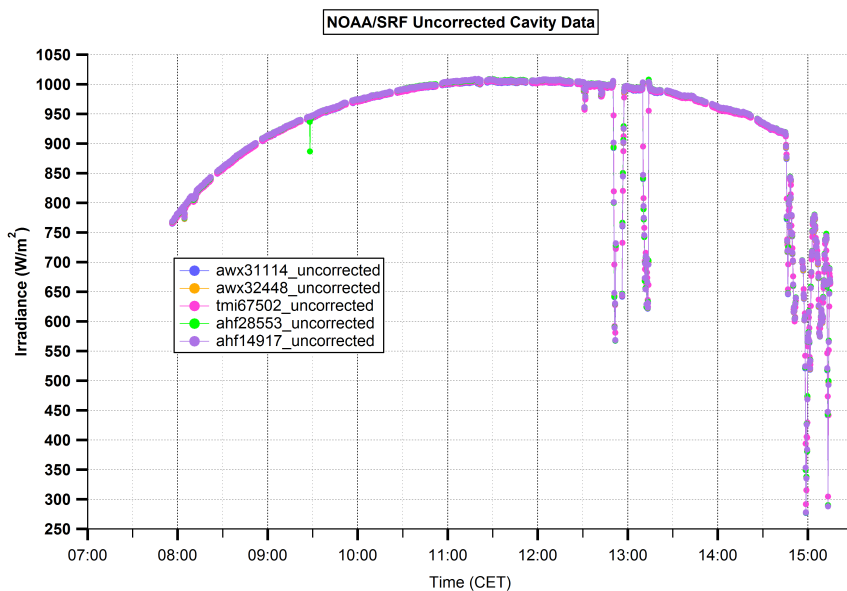


Figure 1. Irradiance data collected from the G-Rad standard cavity group during a mostly clear day at the 2015 WMO International Pyrheliometer Comparison (IPC-XII).

Variability of UV at Sites Equipped with NIWA Spectrometer Systems for 20 Years or More

R. McKenzie¹, M. Kotkamp¹, B. Liley¹ and P. Disterhoft^{2,3}

¹National Institute of Water and Atmospheric Research (NIWA), Wellington, New Zealand; +64-3-440-0429, E-mail: richard.mckenzie@niwa.co.nz

²Cooperative Institute for Research in Environmental Sciences (CIRES), University of Colorado, Boulder, CO 80309; 303-497-6355, E-mail: patrick.disterhoft@noaa.gov

³NOAA Earth System Research Laboratory, Global Monitoring Division (GMD), Boulder, CO 80305

For over 20 years, ESRL/GMD has worked with New Zealand's National Institute of Water & Atmospheric Research (NIWA) to provide high-quality measurements of ultraviolet (UV) spectral irradiance at the high-altitude Mauna Loa Observatory (MLO), Hawaii (19.5°N, altitude 3.4 km) and at Boulder, CO (40°N, 1.7 km). These data sets complement the long-term measurements that have been undertaken since 1990 from NIWA's clean-air observatory at Lauder, New Zealand (45°S, 0.3km). Data from all three sites meet the exacting standards of the Network for the Detection of Atmospheric Composition Change (NDACC). The largest peak UV index (UVI) values are seen at MLO, where there is also a small seasonal variability. Despite its lower altitude and higher latitude, UVI values in summer at Lauder are similar to those at Boulder. However, winter UVI values are lower at Lauder, where in June/July they are less than 10% of those in December/January. Measurements are compared with model calculations for clear skies to determine the effects of clouds, and to compare measured and calculated trends. The model calculations agree well with measurements at Lauder. However, at MLO they are smaller than measurements, due to the effects of underlying clouds that increase the surface albedo. And at Boulder they are larger than measurements due to the effect of aerosol extinctions. After corrections are applied to the model calculations take account of these effects at MLO and Boulder, each site shows a bi-modal distribution of cloud effects, with a primary peak near cloud transmission 1.0 corresponding to clear-sky conditions, and a secondary peak (small for MLO) near cloud transmission 0.5 that corresponds to observations when the solar disk is covered. Radiative enhancements by clouds are typically less than 20%, and show only a weak wavelength dependence, with slightly larger effects at longer wavelengths. Because of the success of the Montreal Protocol on protection of the ozone layer, long term changes in ozone have been small since these UV measurements began, and any long-term changes in noon-time UVI are within the year-to-year variability due to cloud effects.

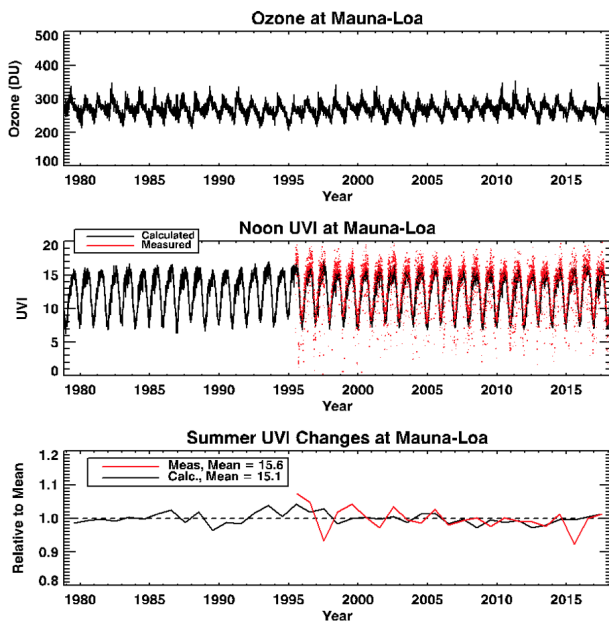


Figure 1. Time series at Mauna Loa Observatory of: ozone (top panel), measured peak daily UVI near noon and calculated UVI for solar noon (middle panel), and measured & calculated UVI trends in summer (bottom panel).

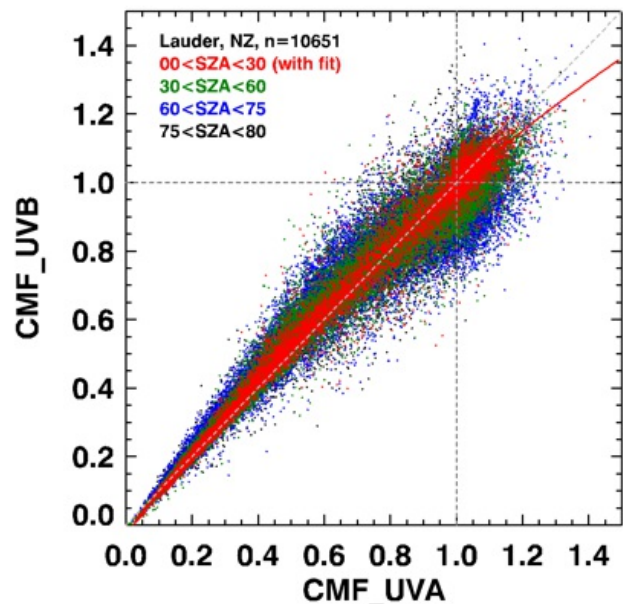


Figure 2. Cloud Effects: The left plot compares cloud modification factors (CMFs) in the UVB and UVA regions for Mauna Loa Observatory.

Improvements in the Brewer Mark IV Spectrophotometer Ultraviolet AOD Retrievals

P. Disterhoft^{1,2} and S. Stierle^{1,2}

¹Cooperative Institute for Research in Environmental Sciences (CIRES), University of Colorado, Boulder, CO 80309; 303-497-6355, E-mail: patrick.disterhoft@noaa.gov

²NOAA Earth System Research Laboratory, Global Monitoring Division (GMD), Boulder, CO 80305

The ultraviolet (UV) portion of the solar spectrum accounts for 8-10% of the total radiation budget reaching the surface of the earth. It is important to measure the aerosol optical depth (AOD) in this region of the spectrum as it contributes to the total radiative forcing. The NEUBrew network operates two Mark IV Brewer spectrophotometers, #131 and #137 in a special day-long schedule, taking only direct-sun spectral irradiance measurements from 290 to 363 nanometers at 0.5 nm increments. The two Brewers are separated by 15 kilometers between the Table Mt. Test Facility (TMTF) (#131) and the roof of the David Skaggs Research Center (#137), Boulder, Colorado. At the TMTF there is a collocated AERONET CIMEL, #705. The Brewer Mark IV and CIMEL have overlapping measurements at 340 nm which allows for direct comparison between the retrievals. Comparison between the two Brewers and the CIMEL retrievals are made and an approximation of their relative calibration offset is determined. A handheld Microtops AOD sunphotometer is used as a reference device to determine any relative difference between the Brewers. From the retrieved aerosol optical depths we compare the Angstrom exponent determined from an Angstrom plot to that calculated directly from the data. The calculated Angstrom exponent value is used to extrapolate to both lower and higher wavelength AOD values measured by the Brewer to determine the quality of the Angstrom method in the UV across the Brewer's spectral range. The Langley method is used to determine the extraterrestrial constant (ETC) calibration factor, using only days where the AOD and total column ozone are stable.

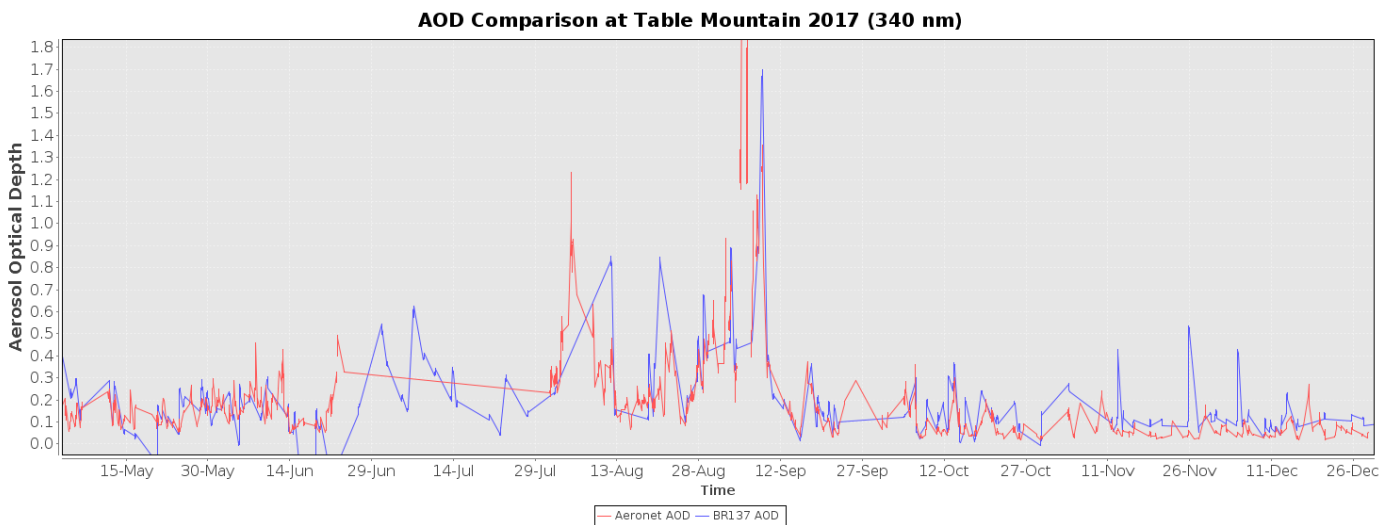


Figure 1. A preliminary comparison of Brewer 131 (Table Mt., Colorado) to the collocated AERONET CIMEL #705 AOD's at 340 nm is plotted. It shows good agreement between the two instruments. The chart also reveals a dramatic increase in the optical depth retrieved from both instruments in the summer of 2017 and is most likely due to the fires in the western U.S.

Shipboard Tilt Corrections for More Accurate Broadband Radiation Data

C. Long^{1,2}, J. Wendell², M. Reynolds³ and H. Powers⁴

¹Cooperative Institute for Research in Environmental Sciences (CIRES), University of Colorado, Boulder, CO 80309; 303-497-6056, E-mail: chuck.long@noaa.gov

²NOAA Earth System Research Laboratory, Global Monitoring Division (GMD), Boulder, CO 80305

³Remote Measurements & Research Co., Seattle, WA 98122

⁴Los Alamos National Laboratory, Los Alamos, NM 87545

Tilt from horizontal on moving platforms can result in substantial downwelling shortwave (SW) and longwave (LW) errors. In collaboration with the Department of Energy Atmospheric Radiation Measurement (ARM) Program ship-board radiation packages (ShipRad) have been developed similar to that collaboratively designed for the ARM Aerial Facility G-1 aircraft. The ShipRad set of instruments provides all the information that is needed to apply the correction for tilt from horizontal orientation developed by Long et al. (2010) to the downwelling SW measurements, as well as screen the longwave measurements for data likely contaminated by too large tilt. Three ShipRad systems were assembled, affording one each on the starboard and port sides of the ship, and one spare system in case of failures. The three systems were subsequently tested including determining the angular offsets of each radiometer from that system's navigation "level" at NOAA in Boulder, CO. Having one system on each side of the ship allows for mitigation of instrument shadowing by ship structure and other obstructions. This poster will present information on the systems and tilt correction method, plus examples from their maiden deployment as part of the Measurements of Aerosols, Radiation, and Clouds over the Southern Ocean (MARCUS) campaign.

Example of tilt correction, Dec. 14, 2017:

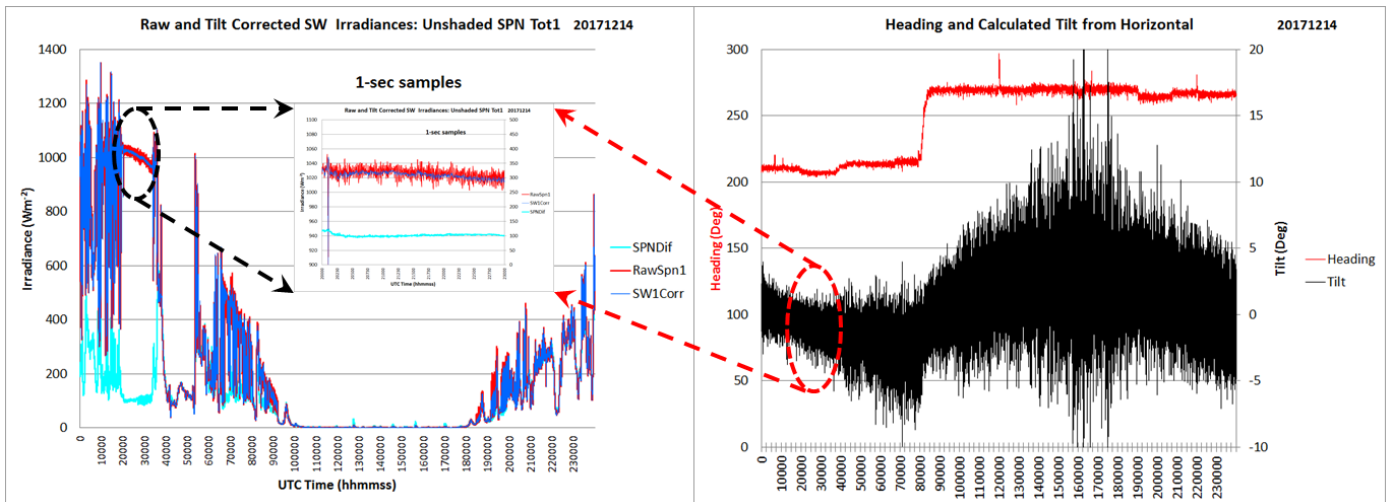


Figure 1. A brief nearly clear-sky period (dashed circle) shows the effectiveness of the preliminary tilt correction. As the zoom plot shows, even without refined detector angular offset from navigation correction, the noise in the 1-second samples is decreased from a spread of 30–40 Wm^{-2} to only a few Wm^{-2} . This despite the rapidly-changing tilt from horizontal (black) shown in the right hand plot.

Validation of the Stratospheric Aerosol and Gas Experiment-III (SAGE-III) Aerosol Data Product

T.N. Knepp^{1,2}, M. Roell², D. Flittner², L. Thomason², J.R. Moore^{1,2}, B. Anderson², E. Winstead¹ and T. Leblanc³

¹Science Systems and Applications, Inc. (SSAI), Lanham, MD 20706; 757-864-5558, E-mail: travis.n.knepp@nasa.gov

²NASA Langley Research Center, Hampton, VA 23681

³NASA Jet Propulsion Laboratory, California Institute of Technology, Pasadena, CA 91109

The third generation of the Stratospheric Aerosol and Gas Experiment (SAGE-III) was launched in February 2017 and subsequently docked with the International Space Station (ISS). SAGE-III performs solar and lunar occultation observations as the ISS experiences sunrise/moonrise and sunset/moonset events. SAGE-III reports aerosol extinction at nine channels (384, 448, 520, 601, 755, 870, 1020, 1555 nm) with vertical resolution of 0.5 km (0–40 km), and nominal baseline of 5% uncertainty. Aerosol validation will be carried out by intercomparisons with a variety of techniques (e.g. lidar, occultation, optical particle counters) from a variety of platforms (e.g. ground-based, balloon-borne, satellite). The data presented in this poster represent preliminary validation results and a discussion of future requirements.

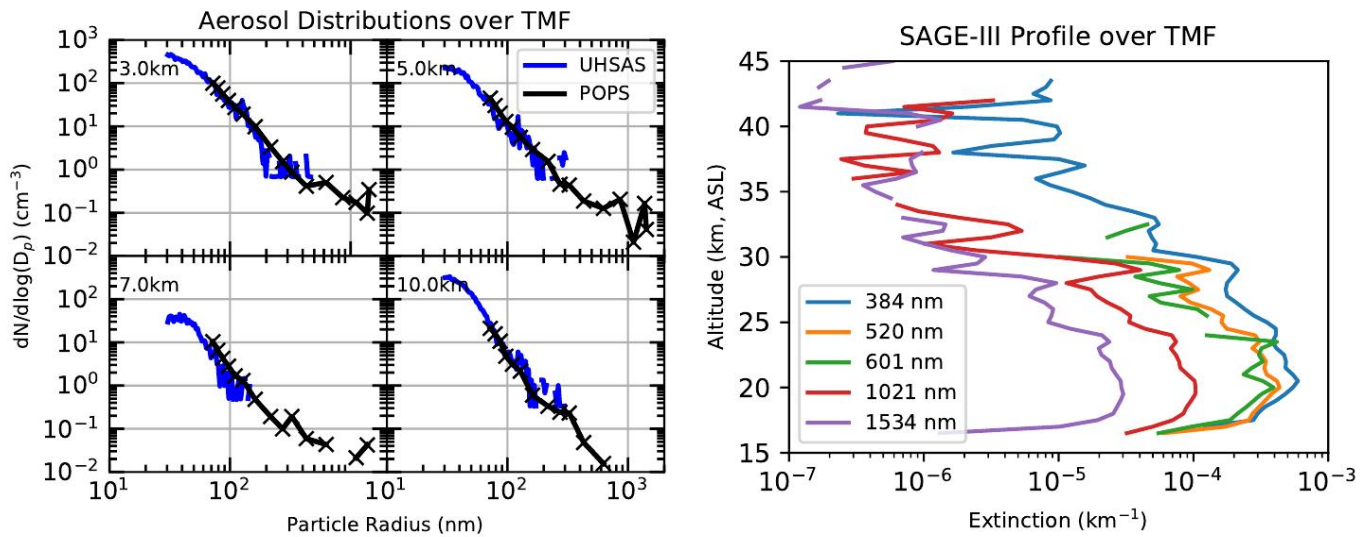


Figure 1. Aerosol data collected over Table Mountain Facility, CA. **Left panel:** aerosol size distributions from data collected on sonde (POPS) and DC8 (UHSAS) platforms. **Right panel:** aerosol extinction profiles for five wavelengths collected by the SAGE-III instrument.

Validation of the Stratospheric Aerosol and Gas Experiment III on the International Space Station (SAGE III/ISS) Science Data Ozone Product: Preliminary Results

S. Kizer^{1,2}, M. Roell², D. Flittner², L. Thomason², T. Knepp^{1,2}, J.R. Moore^{1,2}, K. Leavor^{1,2}, D. Hurst^{3,4}, E. Hall^{3,4}, A. Jordan^{3,4}, P. Cullis^{3,4}, B. Johnson⁴ and R. Querel⁵

¹Science Systems and Applications, Inc. (SSAI), Lanham, MD 20706; 757-864-8358, E-mail: susan.h.kizer@nasa.gov

²NASA Langley Research Center, Hampton, VA 23681

³Cooperative Institute for Research in Environmental Sciences (CIRES), University of Colorado, Boulder, CO 80309

⁴NOAA Earth System Research Laboratory, Global Monitoring Division (GMD), Boulder, CO 80305

⁵National Institute of Water and Atmospheric Research (NIWA), Wellington, New Zealand

The Stratospheric Aerosol and Gas Experiment III (SAGE III) instrument, installed on the International Space Station (ISS), is the most recently launched of four SAGE instruments. The SAGE III/ISS is a solar and lunar occultation instrument, scanning the light from the sun and moon, through the Earth's atmosphere at the limb, or edge, of the planet. It was launched in February 2017, almost 38 years from the day that the first instrument, SAGE I, was launched. It continues a legacy of long-term ozone, water vapor, and aerosol profile measurements and extends SAGE's lengthy record of monitoring ozone trends. The SAGE III/ISS ozone science data products have recently been released; solar in October 2017, and lunar in January 2018. This poster shows the preliminary validation results of comparing SAGE III/ISS ozone vertical profiles with those of ESRL/GMD and NIWA ozonesondes, of the Atmospheric Chemistry Experiment (ACE), of the Optical Spectrograph and InfraRed Imager System (OSIRIS), and of other SAGE III/ISS coincident overpasses.

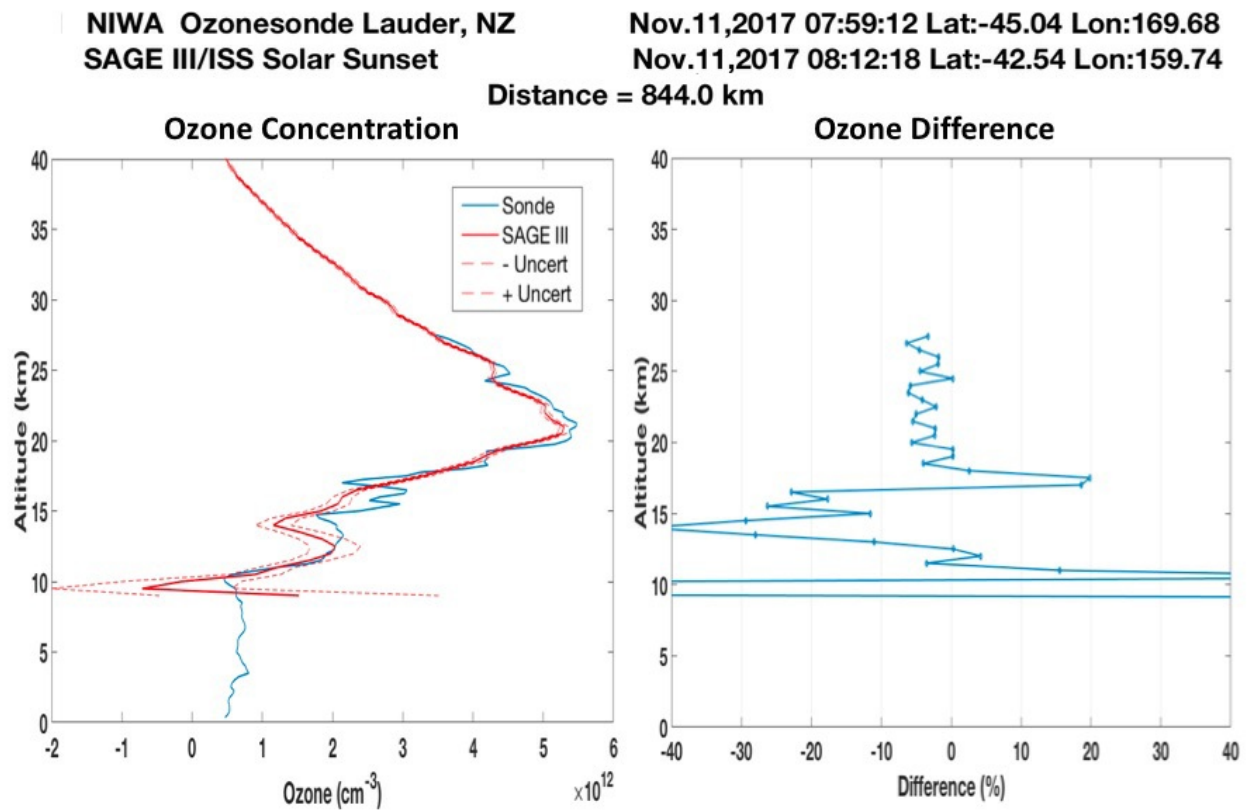


Figure 1. SAGE III/ISS and NIWA ozonesonde ozone profile comparison.

Overview and Selected Results from the NOAA Federated Aerosol Network

P. Sheridan¹, D. Hageman^{2,1} and B. Andrews^{2,1}

¹NOAA Earth System Research Laboratory, Global Monitoring Division (GMD), Boulder, CO 80305; 303-497-6672, E-mail: patrick.sheridan@noaa.gov

²Cooperative Institute for Research in Environmental Sciences (CIRES), University of Colorado, Boulder, CO 80309

ESRL/GMD maintains Atmospheric Baseline Observatories to monitor the atmospheric background levels of trace gases and aerosols. Measurements at these remote sites permit us to determine to what extent the global backgrounds are changing over time. Since aerosols are perturbed near the sources, these Observatories are in prime locations to assess baseline changes to the atmospheric aerosol. In order to better understand anthropogenic aerosol radiative forcing and its effects on climate, and to reduce the uncertainties associated with extrapolating relatively few discrete observations up to regional or global scales, many more stations in different climatological regions were needed. To accomplish this ESRL/GMD has over the past two decades significantly expanded its network of stations to include locations that are at times influenced by anthropogenic emissions. This long-term strategy permits estimates of how much of the aerosol radiative forcing at these locations is caused by human activities and sheds light on whether changes in policy can influence the effects of these aerosols. It is not realistic for ESRL/GMD to fund the operation of monitoring stations all over the world. The primary way we have been able to expand the network to include another major anthropogenic aerosol source region (Southeast Asia), the region considered the bellwether of global climate change (the Arctic), and other perturbed areas is to foster collaborations with interested science organizations and universities in the U.S. and around the world. The collaborations we have developed present advantages for all parties, and the aerosol data collected are directly comparable with those from other stations in the network. This presentation describes this collaborative global surface aerosol monitoring network (the NOAA Federated Aerosol Network) and shows some results from these collaborations.

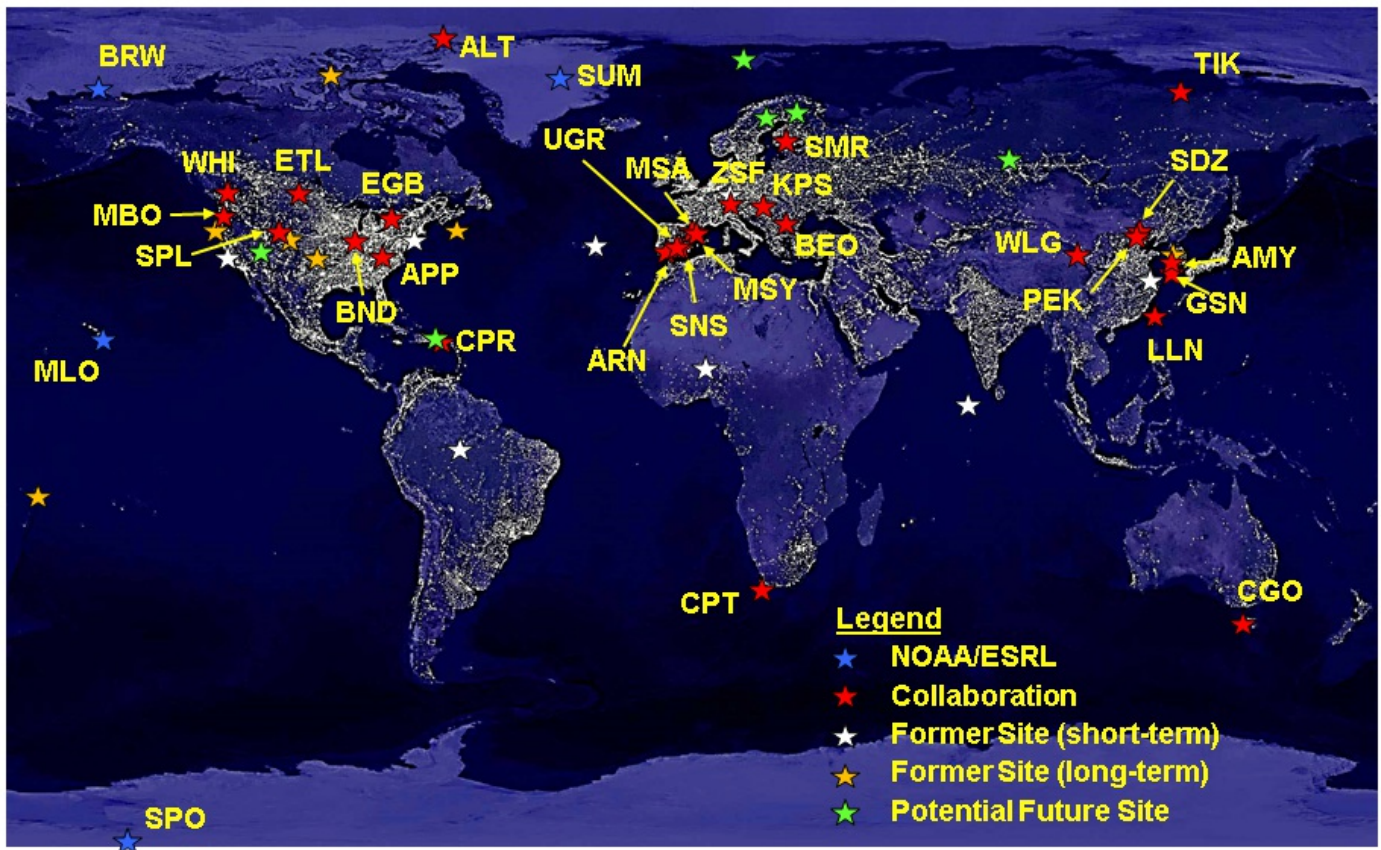


Figure 1. The NOAA Federated Aerosol Network in April 2018.

Relating Chemical and Optical Aerosol Properties at Mauna Loa Observatory

K. Sun^{1,2}, E. Andrews^{3,4}, N.P. Hyslop⁵ and P. Sheridan⁴

¹Science and Technology Corporation, Boulder, CO 80305; 303-497-6210, E-mail: katy.sun@noaa.gov

²Monarch High School, Louisville, CO 80027

³Cooperative Institute for Research in Environmental Sciences (CIRES), University of Colorado, Boulder, CO 80309

⁴NOAA Earth System Research Laboratory, Global Monitoring Division (GMD), Boulder, CO 80305

⁵University of California at Davis, Air Quality Research Center, Davis, CA 95616

This paper studies the connection between *in situ* aerosol optical properties and their elemental composition at the ESRL/GMD Mauna Loa Observatory (MLO). The data analyzed come from two independent data sets that were collected at MLO between 1992-2010. These types of co-located measurements enable the identification of the aerosol composition (and, thus, potential sources) responsible for observed changes in the aerosol optical properties. The first set of data, sampled by the Interagency Monitoring of Protected Visual Environments (IMPROVE) program, consists of total mass and chemical element mass concentrations of particulate matter with diameters less than 2.5 micrometers (PM_{2.5}). The second data set contains aerosol optical and number concentration data from ESRL/GMD long-term measurements at MLO. The chemical and optical data sets were merged together for this analysis.

At MLO, PM_{2.5} mass and sulfur have the strongest correlations with aerosol scattering while bromine and potassium are most strongly correlated with aerosol absorption. Elements with strong correlations in the all-hours data are also strong in the night-only data. However, the correlation coefficients (R²) are higher for the all-hours data. Correlations between derived optical parameters, such as single-scattering albedo and the scattering Angstrom coefficient were very weak. The next step is use the results to explain observed aerosol properties in terms of possible sources, not just during the springtime dust season but at other times of year as well.

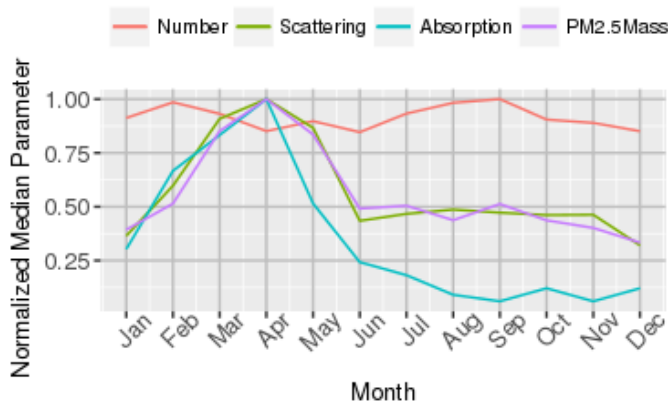


Figure 1. This figure shows monthly cycles of aerosol number concentration, aerosol scattering, aerosol absorption, and PM2.5 mass concentration.

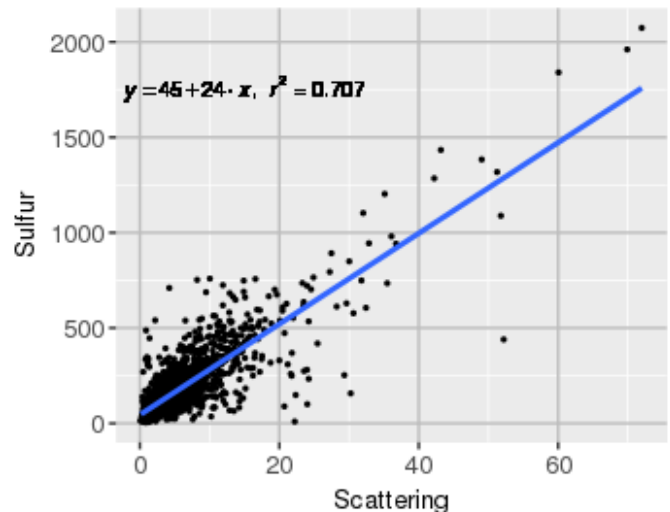


Figure 2. This figure depicts relationship between aerosol scattering and elemental sulfur mass concentration. Both plots are for all-hours data.

Reconciling Evapotranspiration Partitioning Models with Evidence of Anomalously Low Isotopic Fractionation during Evaporation in Semi-arid Landscapes

A. Kaushik^{1,2}, D. Noone^{3,1}, M. Berkelhammer⁴ and M. O'Neill^{5,6}

¹Cooperative Institute for Research in Environmental Sciences (CIRES), University of Colorado, Boulder, CO 80309; 631-681-9067, E-mail: aleya.kaushik@colorado.edu

²University of Colorado, Department of Atmospheric and Oceanic Sciences, Boulder, CO 80309

³Oregon State University, College of Earth, Ocean and Atmospheric Sciences, Corvallis, OR 97331

⁴Department of Earth and Environmental Sciences, University of Illinois at Chicago, Chicago, Illinois 60607, U.S.

⁵Formerly at Cooperative Institute for Research in Environmental Sciences (CIRES), University of Colorado, Boulder, CO 80309

⁶Formerly at NOAA Earth System Research Laboratory, Global Monitoring Division (GMD), Boulder, CO 80305

Partitioning land surface latent heat flux into evaporation (E) and transpiration (T) remains challenging despite a basic understanding of the underlying mechanisms. Water isotopologues are useful tracers for separating evaporation and transpiration contributions because E and T have distinct isotopic ratios. Here the isotope-based partitioning method is used at a semi-arid grassland tall-tower site in Colorado. Results suggest that under certain conditions evaporation cannot be isotopically distinguished from transpiration without modifying existing partitioning techniques. Over a 4-year period, profiles of stable oxygen and hydrogen isotope ratios of water vapor were measured from the surface to 300 m and soil water down to 1 m along with standard meteorological fluxes. Using these data, it was found that rainfall, equilibration, surface water vapor exchange, and sub-surface vapor diffusion all contribute to the isotopic composition of evapotranspiration (ET). Applying the standard isotopic approach to find the transpiration portion of ET (i.e., T/ET), a significant discrepancy is found compared with a method to constrain T/ET based on gross primary productivity (GPP). By evaluating kinetic effects associated with soil evaporation and vapor diffusion, a significant proportion (58-84%) of evaporation following precipitation is found to be non-fractionating. This is possible when water from discrete soil layers is nearly completely evaporated as soil dries. The isotope ratio of non-fractionating evaporative flux is indistinguishable from the isotope ratio of transpiration, and may therefore explain the overestimation of T/ET from traditional “two-stream” partitioning methods. Accounting for weaker fractionation during evaporation reconciles isotope-based partitioning T/ET estimates with the GPP method.

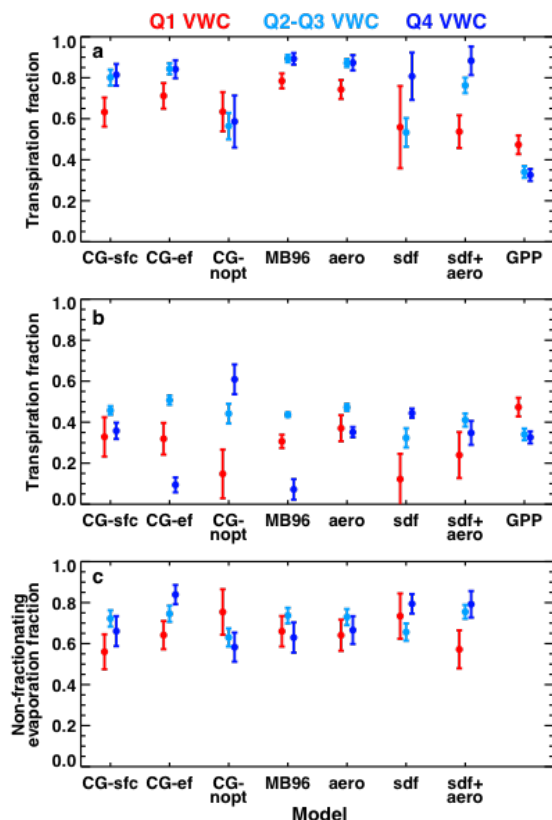


Figure 1. (a) Transpiration fraction calculated for seven different model tests for lowest quartile (Q1), intermediate quartiles (Q2-Q3) and highest quartile (Q4) of total volumetric water content in the top 15 cm of the soil column, compared to GPP method, (b) Transpiration fraction for same seven model tests including a non-fractionating evaporation component, (c) Non-fractionating evaporation fraction. Note that the fractionating evaporation fraction (not plotted here) is simply 1 minus the non-fractionating evaporation fraction plotted in (c). The GPP method predicts a transpiration fraction of 0.38 ± 0.08 , while the average of all models shown here is 0.67 ± 0.08 for (a) and 0.43 ± 0.03 for (b) where non-fractionating evaporation is included in the calculation. Non-fractionating evaporation in (c) makes up 58-84 % of the total evaporation under wet (Q4) conditions, and 56-75 % of the total evaporation under dry (Q1) conditions.

Spatial Variations of Soil Temperature and its Environmental Controls across Eurasian Continent

K. Wang¹ and T. Zhang²

¹Institute of Arctic and Alpine Research (INSTAAR), University of Colorado, Boulder, CO 80309; 303-359-4726, E-mail: Kang.Wang@colorado.edu

²Lanzhou University, College of Earth and Environmental Sciences, Lanzhou, Gansu, China

Subsurface soil thermal status is a comprehensive indicator of energy, mass, and biogeochemical exchanges in the atmosphere-ground interaction. It plays an important role in the terrestrial carbon cycle, hydrological processes, and infrastructure, and varies in a complex environment. This study represents a continental-scale analysis of the soil temperature and its climatic and environmental controls across the Eurasian continent. It provides a comprehensive picture of soil temperature over the 20-year baseline period of 1981-2000 and investigates the potential correlations between soil temperature and environmental factors, including air temperature, snow cover, vegetation, and soils. Mean annual soil temperature (MAST) ranges from -13.3 to 26.5 °C with an average of 7.5 °C across the Eurasian continent. Spatial variations of latitude and elevation could explain 82% of the variations of the MAST. MAST declines 0.5 °C with an increase of 1 degree in latitude and 0.3 °C with an increase of 100 m in elevation. The difference between air and soil temperature (ΔAT) is positive at almost sites and 3.5 ± 2.1 °C over the Eurasian continent as a whole. High ΔAT is mainly found at central and eastern Siberia, which could be > 8 °C. ΔAT has a strong nonlinear correlation to mean annual air temperature (MAAT) and the correlation becomes weak when MAAT is higher than ~ 5 °C. MAAT and snow cover index explain 71% of the variation in ΔAT .

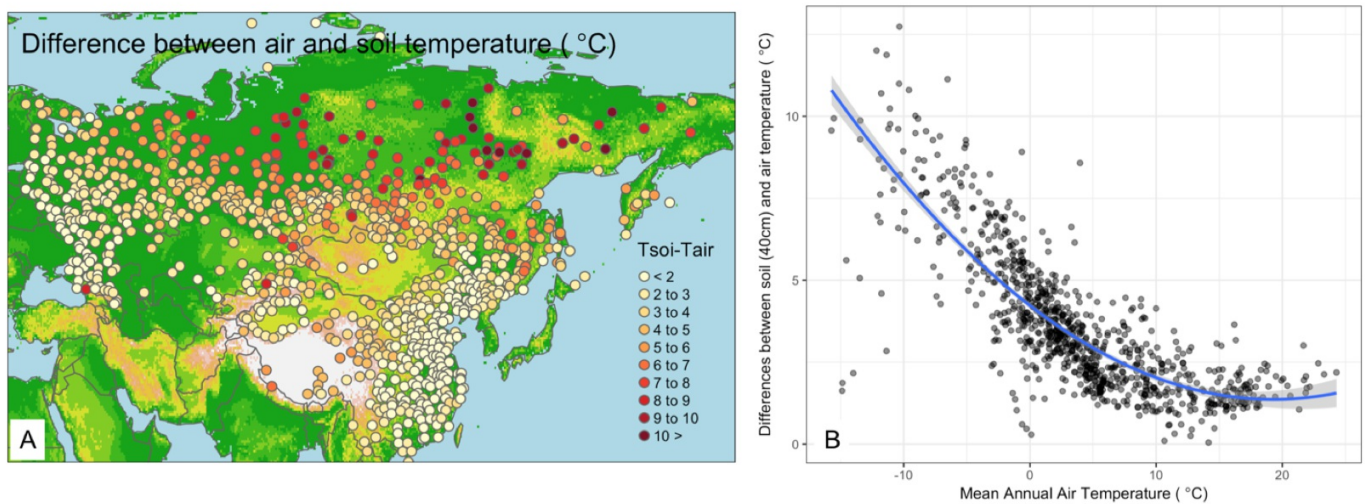


Figure 1. A) Differences between long-term mean air temperature and soil temperature at 40 cm (1981-2000) (i.e., ΔAT) across the Eurasian continent; B) relationship between ΔAT (the difference between air and soil temperatures) and long-term mean annual air temperature.

A Lamina-based Approach for Interpreting Variability in Ozonesonde Vertical Profiles

K. Minschwaner¹, G. Manney^{2,1}, I. Petropavlovskikh^{3,4}, B. Johnson⁴ and A. Jordan^{3,4}

¹New Mexico Institute of Mining and Technology, Socorro, NM 87801; 575-835-5226, E-mail: kenneth.minschwaner@nmt.edu

²NorthWest Research Associates, Boulder, CO 80301

³Cooperative Institute for Research in Environmental Sciences (CIRES), University of Colorado, Boulder, CO 80309

⁴NOAA Earth System Research Laboratory, Global Monitoring Division (GMD), Boulder, CO 80305

An improved understanding of ozone variability in the upper troposphere/lower stratosphere (UTLS) is critical for evaluating the impact of ozone transport on regional air quality and assessing ozone radiative forcing of climate. Ozonesonde measurements can play a key role in characterizing day-to-day, seasonal, and long-term changes in UTLS ozone at a given location, but interpretation of these changes is complicated by possible influences from a wide range of chemical and dynamical processes. A major component of the variability in ozonesonde vertical profiles is associated with laminar features (0.2 to ~2 km thickness) that can be traced to dynamical or chemical phenomena occurring far from the measurement site. We use an analysis package (RIO SOL - Robust Identification of Observed Signatures of Ozone Laminae) applied to the ESRL/GMD ozonesonde dataset from Boulder, Colorado. Laminae statistics from RIO SOL include the distributions of widths and amplitudes, frequencies of occurrence as functions of altitude, and classification of ozone features associated with gravity wave activity (Figure 1). The generating mechanisms associated with non-gravity wave laminae are examined using parcel back-trajectories tagged to UTLS ozone features identified by RIO SOL.

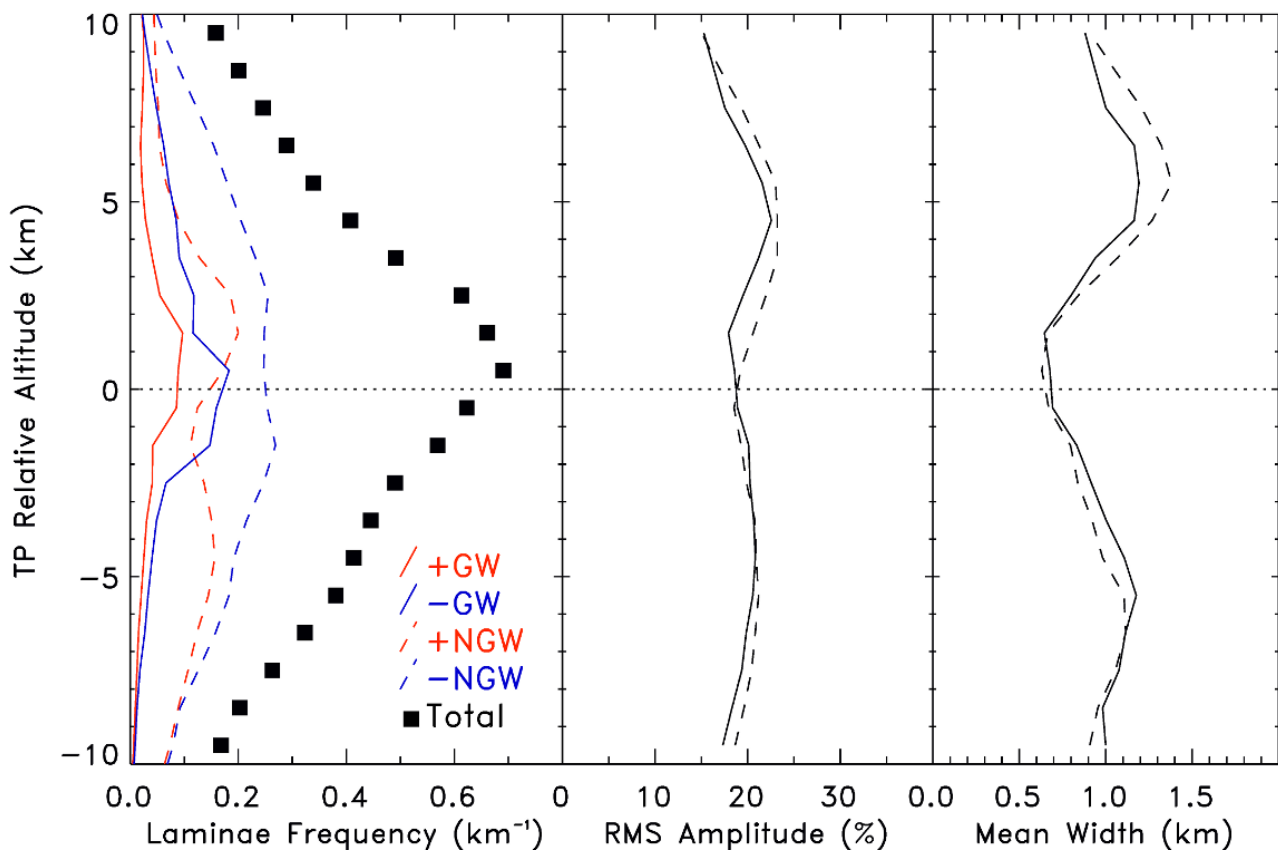


Figure 1. Vertical profiles of ozone laminae characteristics in altitude coordinates relative to the WMO tropopause (TP). Left panel shows laminae frequency as the number of laminae detected per sounding within 1-km wide altitude bins. Black squares are for all laminae types and signs. Solid lines show frequencies of gravity wave (GW) laminae, dashed lines indicate non-gravity wave (NGW) laminae, and red and blue indicate positive and negative anomalies, respectively. The middle and right panels show vertical profiles of laminae mean amplitudes and mean widths, respectively.

Analysis of Ozone Trends from NOAA's Newly Homogenized Ozonesonde Data Record

P. Cullis^{1,2}

¹Cooperative Institute for Research in Environmental Sciences (CIRES), University of Colorado, Boulder, CO 80309; 303-497-6674, E-mail: Patrick.Cullis@noaa.gov

²NOAA Earth System Research Laboratory, Global Monitoring Division (GMD), Boulder, CO 80305

Recently outlined in the paper (Sterling et al. 2017), the ESRL/GMD ozonesonde vertical profiles have now been standardized across historical instrumentation, solution recipe, and background currents. Using this new version of the data, altitude binned plots are created showing ozone mixing ratio for each year for five primary sites: Boulder, South Pole, Hilo, Trinidad Head, and American Samoa. Trends at different altitudes are looked at.

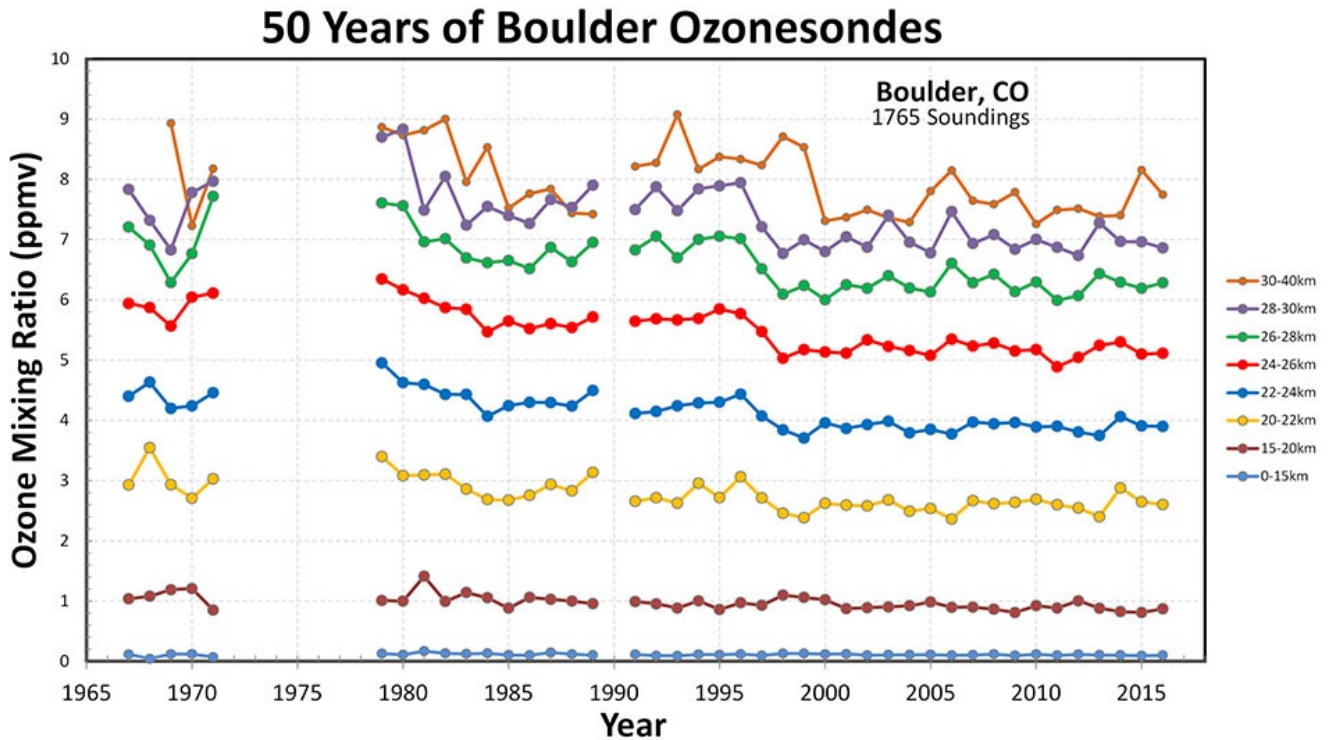


Figure 1. Annual ozone mixing ratio values from the Boulder ozonesonde record.

Stratospheric Temperature Corrections and Improvement of Total Column Ozone Records in the NOAA Dobson Ozone Spectrophotometer Network

G. McConville^{1,2}, K. Miyagawa³, I. Petropavlovskikh^{1,2} and A. McClure-Begley^{1,2}

¹Cooperative Institute for Research in Environmental Sciences (CIRES), University of Colorado, Boulder, CO 80309; 303-497-3989, E-mail: glen.mcconville@noaa.gov

²NOAA Earth System Research Laboratory, Global Monitoring Division (GMD), Boulder, CO 80305

³Guest Scientist at NOAA Earth System Research Laboratory, Global Monitoring Division (GMD), Boulder, CO 80305

The Dobson Spectrophotometer network for monitoring of long-term stratospheric ozone was established in the early 1960s and currently includes 16 stations. The network record has been reprocessed with updated quality control software (Evans et al. 2017). The official algorithm for ozone retrieval from Dobson measurements includes static absorption coefficients derived using Bass and Paur (1985) ozone cross-sections. We estimated the impact of using different ozone absorption coefficients (Brion–Daumont–Malicet [DBM] and Institute of Experimental Physics [IUP]) and derived temperature corrections based on climatology from McPeters and Labow (2011).

In this study, we investigate the impact of temperature corrections on the reduction of seasonal biases found between Dobson (ADDS) and satellite (Aura Microwave Limb Sounder [MLS], Aura Ozone Monitoring Instrument (OMI), Suomi National Polar-orbiting Partnership Ozone-Mapping Profile Suite [Suomi NPP OMPS], and Solar Backscatter Ultraviolet Merged Ozone Data [SBUV MOD]) observations selected for the station overpass criteria. We achieve 2% reduction in seasonal biases and overall improvement in long-term agreement between the ESRL/GMD Dobson network and satellite total ozone records.

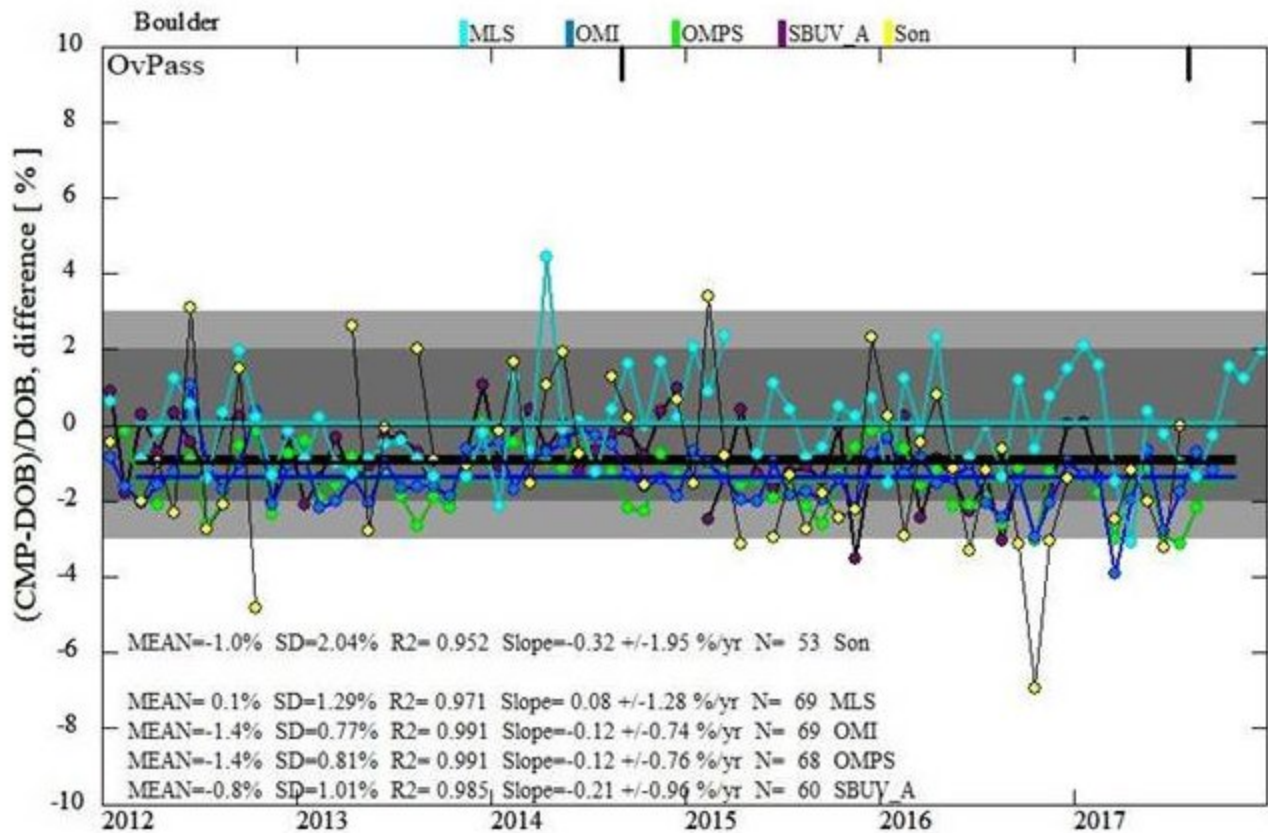


Figure 1. Difference of the total column ozone with Dobson (ADDS matched), overpass satellites (MLS, OMI, OMPS, SBUV), and ozonesonde.

Uncertainty Improvement Optimized using the GMI Model for Umkehr Ozone Profile Retrieval

K. Miyagawa¹, I. Petropavlovskikh^{2,3}, G. McConville^{2,3}, A. McClure-Begley^{2,3} and B. Noiro^{2,3}

¹Guest Scientist at NOAA Earth System Research Laboratory, Global Monitoring Division (GMD), Boulder, CO 80305; 303-497-6279, E-mail: miyagawa.koji@noaa.gov

²Cooperative Institute for Research in Environmental Sciences (CIRES), University of Colorado, Boulder, CO 80309

³NOAA Earth System Research Laboratory, Global Monitoring Division (GMD), Boulder, CO 80305

The Umkehr measurements archived at the WMO World Ozone and UV Data Center in Toronto, Canada represent the longest ozone profile data record in existence. Understanding and reducing systematic errors in the Umkehr ozone profile retrievals is important for detection of drifts in satellites and other ground-based ozone measuring records. The standardized stray light correction (SLC) developed for Dobson Umkehr ozone profiles reduces biases with respect to the long-term satellite records in the upper stratosphere. However, the bias increases in the mid-stratosphere and low-stratosphere. Furthermore, optical characteristics of each Dobson instrument are different, thus the instrument-specific biases are not corrected and can appear as drifts (or step changes) in the long-term records.

In this study, we use NASA Global Modeling Initiative (GMI) model hourly vertical ozone profile data to determine relative biases for each instrument that comprises the station long-term record. The new value for SLC is optimized relative to the reference GMI profiles. It is then tested in the operational processing software to detect the reduction of the biases and verify the removal of the instrumental biases from the station ozone record. ESRL/GMD Dobson Umkehr historical records are re-processed. We will present the results of updated Umkehr records from several ESRL/GMD stations and show comparisons against complimentary ozone profiles for alternative measuring systems (satellites and ozonesonde, etc.) co-located at the Dobson station.

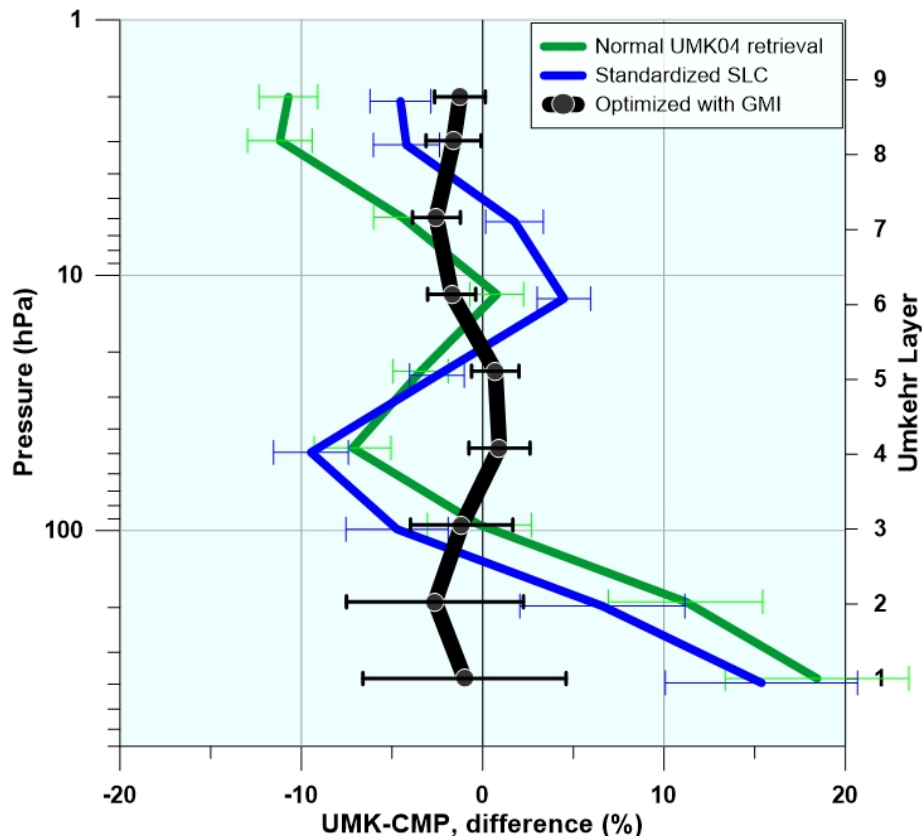


Figure 1. Mean difference of Umkehr ozone profiles is shown for three versions of the retrieval is shown. Reference is the mean of satellites (Microwave Limb Sounder [MLS], Ozone Mapping Profiler Suite [OMPS], OMPS Limb Profiler [OMPS_LP], Stratospheric Aerosol and Gas Experiment II [SAGEII], Solar Backscatter Ultraviolet Instrument [SBUV], GMI Modern-Era Retrospective analysis for Research and Applications, Version 2 [GMI_Merra2]) and Ozonesonde records. The error bar shows standard error. Umkehr ozone retrieved from the Dobson #61 measurements in Boulder between 1982 and 2017.

An Evaluation of C₁-C₃ Hydrochlorofluorocarbon (HCFC) Metrics: Lifetimes, Ozone Depletion Potentials, Radiative Efficiencies, Global Warming and Global Temperature Potentials

J. Burkholder¹, D.K. Papanastasiou^{2,1}, A. Beltrone³ and P. Marshall⁴

¹NOAA Earth System Research Laboratory, Chemical Sciences Division (CSD), Boulder, CO 80305; 303-497-3252, E-mail: James.B.Burkholder@noaa.gov

²Cooperative Institute for Research in Environmental Sciences (CIRES), University of Colorado, Boulder, CO 80309

³University of North Texas, Denton, TX 76203

⁴University of North Texas, Department of Chemistry, Denton, TX 76203

Hydrochlorofluorocarbons (HCFCs) have been used as chlorofluorocarbon (CFC) substitutes in a number of applications. Although HCFCs have lower ozone depletion potentials (ODPs) compared to CFCs, they are potent greenhouse gases. The twenty-eighth meeting of the parties to the Montreal Protocol on Substances that Deplete the Ozone Layer (Kigali 2016) included a list of 274 HCFCs to be controlled under the Montreal Protocol. However, from this list, only 15 of the HCFCs have values for their atmospheric lifetime, ODP, global warming potential (GWP), and global temperature potential (GTP) that are based on fundamental experimental studies.

Here, we present a comprehensive evaluation of the atmospheric lifetimes, ODPs, radiative efficiencies (REs), GWPs, and GTPs for all 274 HCFCs to be covered under the Montreal Protocol. In the absence of direct laboratory studies, atmospheric lifetimes were estimated based on HCFC reactivity with hydroxyl (OH) radicals and singlet oxygen (O(¹D)), as well as their removal by ultraviolet (UV) photolysis using structure activity relationships and reactivity trends. ODP values are based on the semi-empirical approach. Radiative efficiencies were estimated, based on infrared spectra calculated using theoretical electronic structure methods. GWPs and GTPs were calculated using our estimated atmospheric lifetimes and REs.

This study provides a consistent set of HCFC metrics in support of the Montreal Protocol. We emphasize that accurate metrics for a specific HCFC, if desired, require direct fundamental laboratory studies to better define the OH reactivity and infrared absorption spectrum of the compound of interest.

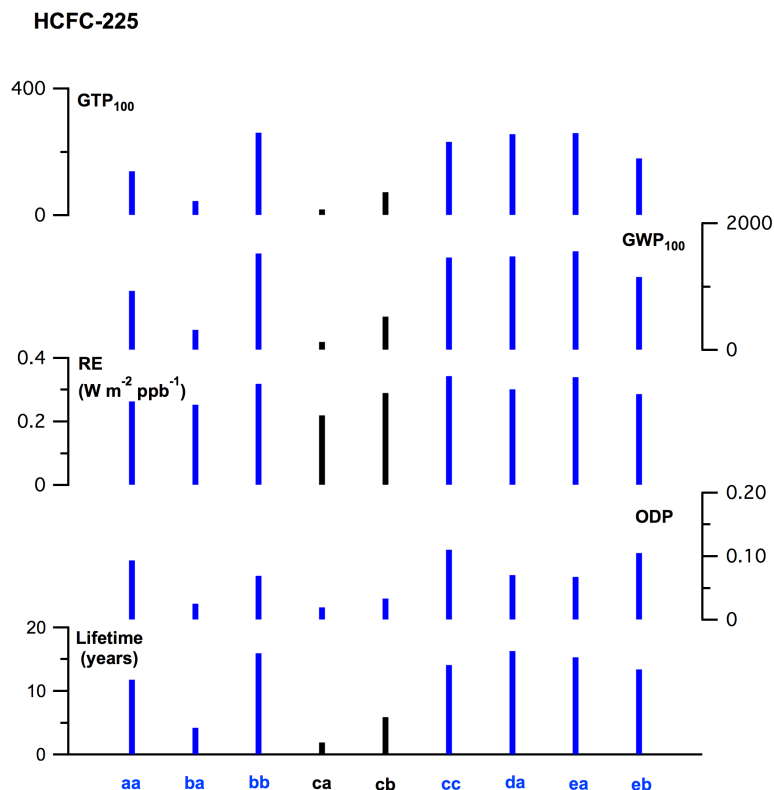


Figure 1. HCFC-225 example of isomer metric dependence. Isomers in blue values were calculated in this study, while isomers in black were derived from available experimental data.

Chloroform Emissions Estimated with the CarbonTracker-Lagrange North American Regional Inversion Framework

G. Dutton¹, S.A. Montzka¹, A.E. Andrews¹, B.R. Miller^{2,1}, C. Sweeney¹, C. Siso^{2,1}, M.J. Crotwell^{2,1} and J.W. Elkins¹

¹NOAA Earth System Research Laboratory, Global Monitoring Division (GMD), Boulder, CO 80305; 303-497-6086, E-mail: geoff.dutton@noaa.gov

²Cooperative Institute for Research in Environmental Sciences (CIRES), University of Colorado, Boulder, CO 80309

Chloroform or trichloromethane (CHCl_3) is the second largest source of natural atmospheric chlorine after methyl chloride (CH_3Cl). More than half of CHCl_3 global emissions are from natural sources such as soils and biomass burning the remaining anthropogenic sources include paper production and water treatment processes. ESRL/GMD has been measuring this gas for about two decades via *in situ* and flask grab samples at the surface and aboard aircraft. During this time, zonal and global averages have shown an increase in the atmospheric abundance (about two parts-per-trillion or 20%) along with a sizeable inter-hemispheric difference indicating predominant northern hemispheric sources. The ESRL/GMD Barrow Atmospheric Baseline Observatory (BRW), located at Utqiagvik, Alaska, is ideally situated to observe changes in the Arctic where previous studies have detected CHCl_3 emissions. Tundra CHCl_3 emissions are persistent throughout the summer when little or no snow cover is present, but low or no emissions when snow covered. It is unknown if soil temperature or hydrology are the dominant drivers for emissions.

This presentation makes use of high-frequency *in situ* measurements from Barrow, Alaska as well as surface and aircraft flask samples acquired at about 30 North America sites. Seasonal surface fluxes and emissions from 2010 to 2014 are estimated using a regional inverse modeling system. The CarbonTracker-Lagrange framework uses surface sensitivity footprints from Lagrangian particle dispersion models driven by a high-resolution Weather Research and Forecasting (WRF) meteorology. Preliminary results indicate tundra soils dominate emissions in the northernmost Arctic latitudes.

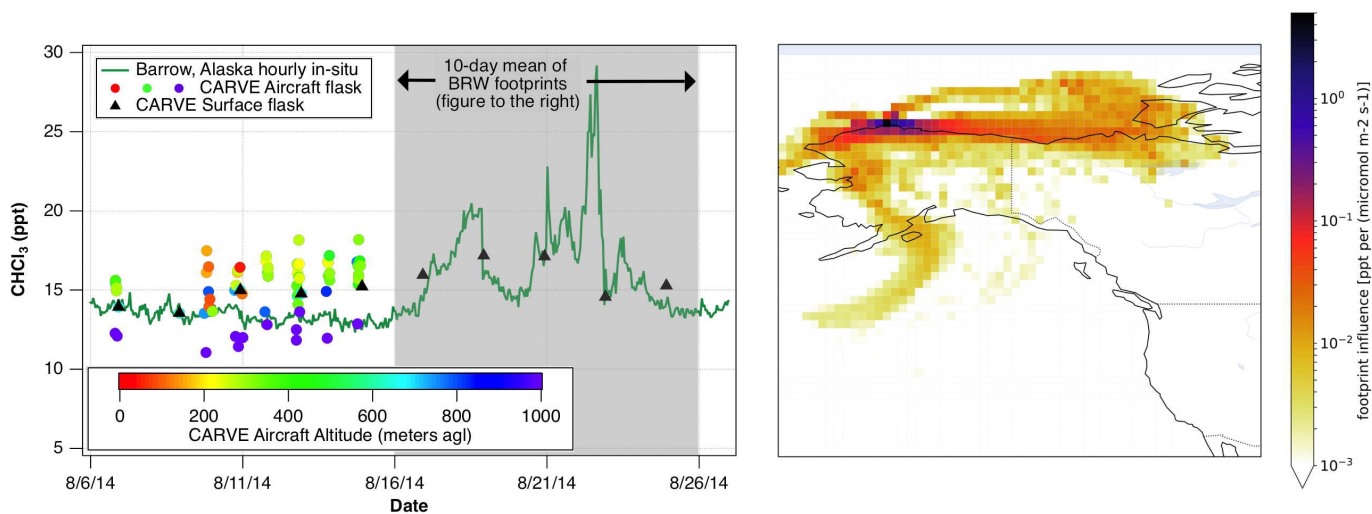


Figure 1. An example of the different measurements during mid-summer of 2014 used in the Carbon Tracker-Lagrange inversion (**left panel**). Surface flask samples collected near Fairbanks, Alaska during the Carbon in Arctic Reservoirs Vulnerability Experiment (CARVE) compare well with hourly *in situ* measurements at BRW. CARVE aircraft flask samples (filled circles) show gradients in both latitude and altitude (color bar shown). A ten-day mean footprint (**right panel**) for BRW from August 16th to the 26th show where air masses originate and their relative influence on air parcels measured. These and other ESRL/GMD data are used to model emissions in the Northern Hemisphere.

Using Observations of SF₆ to Examine Inter-annual Variations in Inter-hemispheric Exchange

B.D. Hall¹, E.J. Dlugokencky¹, D. Nance^{2,1}, D. Mondeel^{2,1}, F.L. Moore^{2,1}, E.J. Hintsa^{2,1}, G.S. Dutton^{2,1} and J.W. Elkins¹

¹NOAA Earth System Research Laboratory, Global Monitoring Division (GMD), Boulder, CO 80305; 303-497-7011, E-mail: Bradley.Hall@noaa.gov

²Cooperative Institute for Research in Environmental Sciences (CIRES), University of Colorado, Boulder, CO 80309

With a long atmospheric lifetime (~850 yr) and no known tropospheric or stratospheric loss processes, sulfur hexafluoride (SF₆) is useful as a tracer of large-scale atmospheric transport. We derive an inter-hemispheric exchange time, τ_{ex} , from surface measurements of SF₆ from two independent sampling networks and a 2-box model. The two sampling networks involve different sampling densities (12 and 38 sites, respectively) and separate analytical systems, linked to the same calibration scale. The mean exchange time derived from the lower-density network observations is ~7% higher than that derived from the higher density network from 2004-2012, and differs substantially in 2003 and 2012 (Figure 1). These differences could be related to sampling density and location, since the lower density network includes four high-altitude sites and the higher density network contains only marine boundary layer sites. Inter-annual variability in τ_{ex} shows some correlation with climate drivers (such as El Niño Southern Oscillation): higher τ_{ex} (slower exchange) during El Niño periods, and lower τ_{ex} (faster exchange) during La Niña. We will explore how differences in sampling networks influence the derived quantity, τ_{ex} .

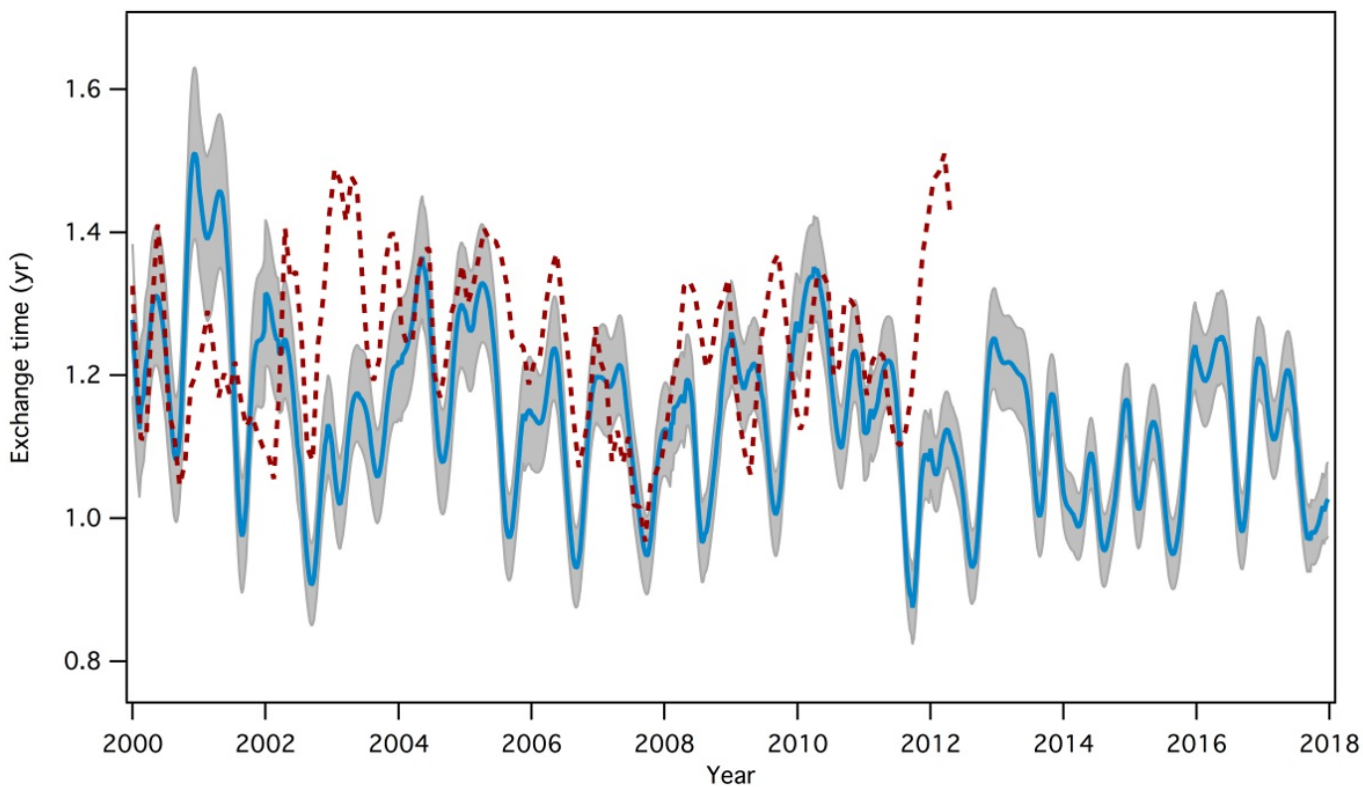


Figure 1. Inter-hemispheric exchange time derived from two independent SF₆ observing networks: 38 marine boundary layer sites (solid line with gray shading, ~1-sigma uncertainty band) and 12 sites (dashed line), assuming a source distribution of 97% Northern Hemisphere, 3% Southern Hemisphere.

Increased Propane Emissions from the United States over the Last Decade

L. Hu^{1,2}, S.A. Montzka², A.E. Andrews², B.R. Miller^{1,2}, D. Helmig³, K. Thoning², C. Sweeney², E.J. Dlugokencky², L. Bruhwiler², J.B. Miller², S. Lehman³, J.W. Elkins² and P.P. Tans²

¹Cooperative Institute for Research in Environmental Sciences (CIRES), University of Colorado, Boulder, CO 80309; 303-497-5238, E-mail: lei.hu@noaa.gov

²NOAA Earth System Research Laboratory, Global Monitoring Division (GMD), Boulder, CO 80305

³Institute of Arctic and Alpine Research (INSTAAR), University of Colorado, Boulder, CO 80309

Propane (C_3H_8) is the second most abundant non-methane hydrocarbon in the atmosphere. It contributes to photochemical air pollution, including ozone and aerosol formation in the troposphere. It is also commonly used as a tracer for distinguishing thermogenic from natural emissions of methane. Global atmospheric observations indicate increases of atmospheric C_3H_8 after mid-2009 that is largely due to U.S. oil and natural gas production (Helmig et al. 2016). We analyzed atmospheric C_3H_8 measurements from the continental U.S. as well as those from the remote atmosphere. Measured C_3H_8 mole fractions over the continental U.S. are up to three orders of magnitude larger than those measured in the remote Northern hemisphere, and they show a clear increasing trend, especially near oil and gas production regions. We then performed inverse modeling analyses of C_3H_8 with and without consideration of the photochemical losses of C_3H_8 to reaction with OH. Inverse-modeled emissions of C_3H_8 show most U.S. C_3H_8 emissions came from oil and gas production regions and the emission magnitude was a few times larger than reported by bottom-up emission inventories for 2008 - 2014. Derived emissions display seasonal variation that is consistent with C_3H_8 demand in the U.S. for all years between 2008 and 2014. Furthermore, derived emissions from atmospheric observations confirm an increase of U.S. C_3H_8 emissions over the 2008 to 2014 period, likely associated with increased C_3H_8 production (Figure 1).

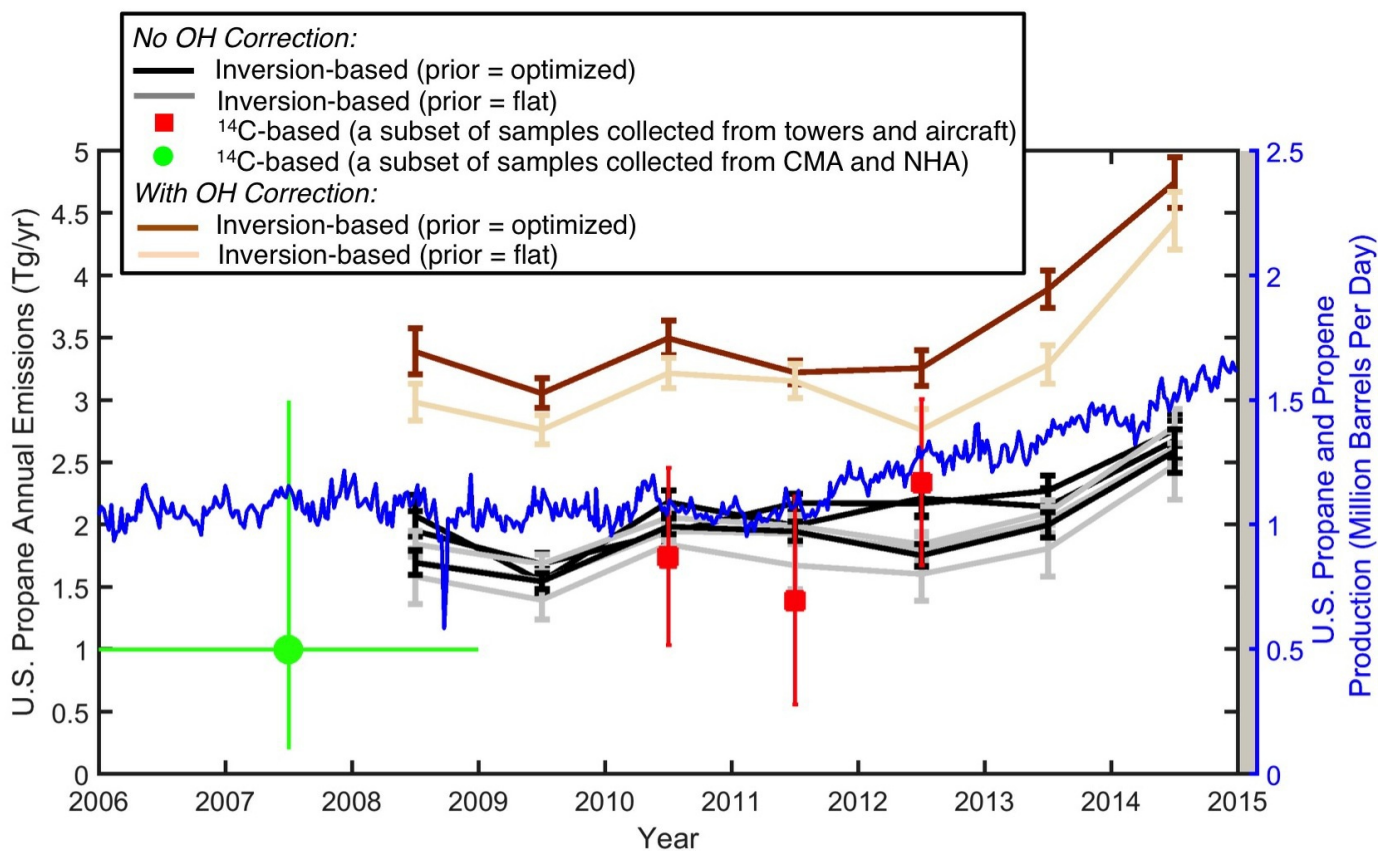


Figure 1. U.S. annual emissions of propane (the left y-axis) derived from atmospheric observations with and without considering OH chemistry. U.S. C_3H_8 and propene production is also shown in the right y-axis.

Using Carbonyl Sulfide to Explore Coastal Fog and Coast Redwood Interdependence

T.W. Hilton, M. Whelan and J.E. Campbell

University of California at Merced, Merced, CA 95343; 415-314-7478, E-mail: twhilton@ucsc.edu

Carbonyl sulfide (OCS) has received much attention as a tracer for global and continental photosynthetic carbon dioxide uptake. Here we demonstrate its utility to understand regional scale land-sea-atmosphere interactions that affect coastal fog. Lining the foggy coast of Northern California, coast redwoods (*Sequoia sempervirens*) are iconic for being the tallest living trees on Earth. Despite redwoods' widespread recognition, surprisingly little is known about the degree of interdependence between coastal redwoods and coastal fog. Are redwoods relatively primitive trees whose leaves transpire water at an unchanged rate regardless of the surrounding moisture, or are they more sophisticated, controlling their stomatal conductance in response to changing atmospheric conditions in their canopy? Here we present model simulations that demonstrate feedbacks between coastal land cover and coastal fog, showing impacts on frequency of coastal fog surprisingly far away from the redwood forests. This links the questions surrounding redwood transpiration to larger-scale regional coastal fog frequency. With coastal fog frequency expected to decline with changing climate and increasing urbanization this question gains urgency. We also present preliminary redwood canopy OCS measurements which we will use to investigate these redwood transpiration--coastal fog feedbacks.

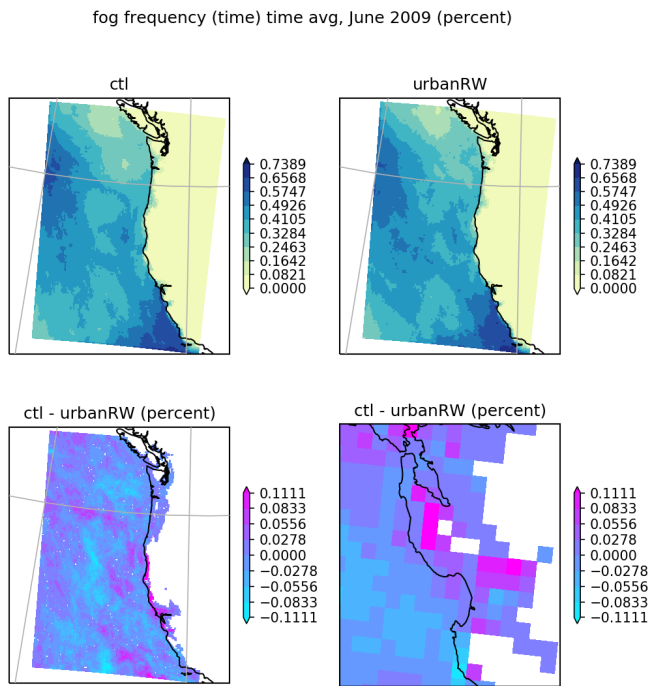


Figure 1. WRF-ARW simulated fog frequency change in urbanized redwood range experiment.



Figure 2. OCS sampling equipment deployed in redwood canopy.

NO_x Emissions from Switch Yard Locomotives Observed with the TRAX Air Quality Platform

L. Mitchell, E. Crosman, B. Fasoli, A. Jacques, J. Horel and J.C. Lin

University of Utah, Salt Lake City, UT 84112; 541-207-7204, E-mail: logan.mitchell@utah.edu

The locomotive industry plays an important role in the transport of people and products nationwide. Within locomotive rail yards, switch yard locomotives (“switchers”) are used to move freight trains around to facilitate the loading and unloading of cargo. Switchers have large diesel engines that are built to last a long time, but that also means that older diesel engines currently in operation lack modern pollution control technologies. Along Utah’s urbanized Wasatch Front the switchers are primarily older models that operate within Tier 0 or 0+ Environmental Protection Agency emission standards that have high nitrogen oxides (NO_x) emissions.

The TRAX (Utah light rail) based air quality measurement platform measures a suite of air pollutants and greenhouse gases (carbon dioxide [CO₂], methane [CH₄], ozone [O₃], fine particulate matter [PM_{2.5}]) and from June 2016-June 2017 the project was loaned a nitrogen dioxide (NO₂) analyzer to investigate the spatial patterns of NO₂ across the metropolitan area. The TRAX Green and Red lines travel adjacent to the Union Pacific rail yard in the central Salt Lake Valley and were thus fortuitously able to monitor emissions in this area. Averaged over time we observed high NO₂ concentrations, most likely due to emissions from switcher rail cars. Observations of co-located O₃ depletions due to titration provide further support for the measurements. Finally, we were able to isolate the contributions from the rail yard and the nearby I-15/I-80 interstate interchange by pairing NO₂ and CO₂ measurements.

Upgrading switcher engines to modern Tier 4 pollution control technology would reduce NO_x emissions by an estimated 90%, and would be within the range of emission reduction costs for area sources adopted by the Utah Air Quality Board. Should these upgrades occur, measurements from the TRAX air quality project could be used to observe emissions before and after these mitigation strategies to evaluate the real-world air quality improvements.

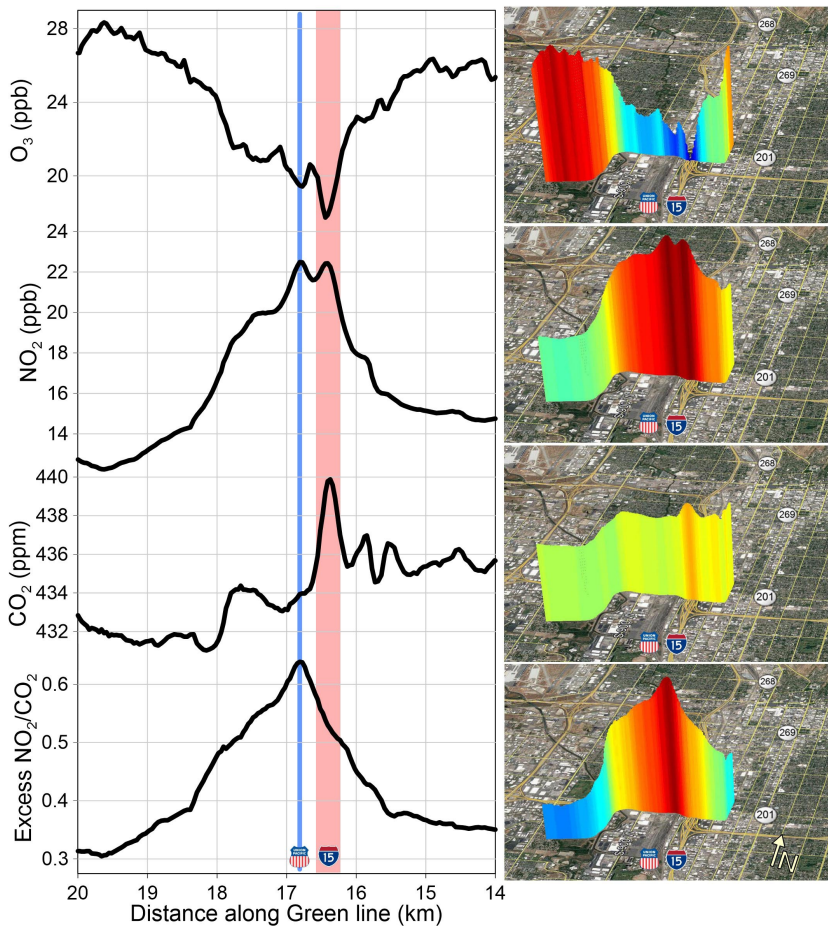


Figure 1. Relationships between species illustrating sources of NO₂ and CO₂ along a subsection of the Green TRAX line. The location of the Union Pacific rail yard and I-15 interstate highway are indicated with a blue line and red shading respectively in the left panel and with icons in both the left and right panels.

Advantages and Limitations of Measuring BTEX with a Commercial GC-PID System *In Situ*

M. Madronich^{1,2}, I. Mielke-Maday^{1,2}, P. Handley^{1,2}, J. Kofler^{1,2}, B.D. Hall², B.R. Miller^{1,2}, B. Khan³, A. Gniewek³ and G. Petron^{1,2}

¹Cooperative Institute for Research in Environmental Sciences (CIRES), University of Colorado, Boulder, CO 80309; 303-497-3264, E-mail: monica.madronich@noaa.gov

²NOAA Earth System Research Laboratory, Global Monitoring Division (GMD), Boulder, CO 80305

³Baseline Gas Analyzers & Sensors, AMETEK MOCON, Lyons, CO 80540

The performance of a commercial gas chromatograph with a photo-ionization detector (Series 9100 GC-PID, MOCON, Lyons, Colorado, U.S.A.) measuring Benzene, Toluene, Ethylbenzene and Xylenes (BTEX) was evaluated during the winter of 2017 and spring 2018. The objective of this work was to determine the accuracy and precision of the equipment to measure BTEX in field conditions. The overall goal of the project was to use this instrument near oil and gas pads to monitor BTEX ambient concentrations and use the data in a health impact study.

The equipment was operated inside a mobile laboratory that provided semi-controlled environmental conditions. The linearity response was verified by analyzing gravimetric standards made at ESRL/GMD. Figure 1 shows the regression analysis for the BTEX compounds. Results show that the equipment presents a linear response for all species within the 0.5-54 ppb range.

The instrument showed consistent results through the measurement period with the exception of certain events when temperature changed dramatically. These events affected the retention time of the compounds on the GC column.

This equipment presents advantages over other measurement techniques, one of them being its high frequency sampling (6 minutes/sample). This allowed us to measure BTEX in real-time over a large concentration range and to investigate sources of short-term variability in the vicinity of newly developed large oil and gas production pads.

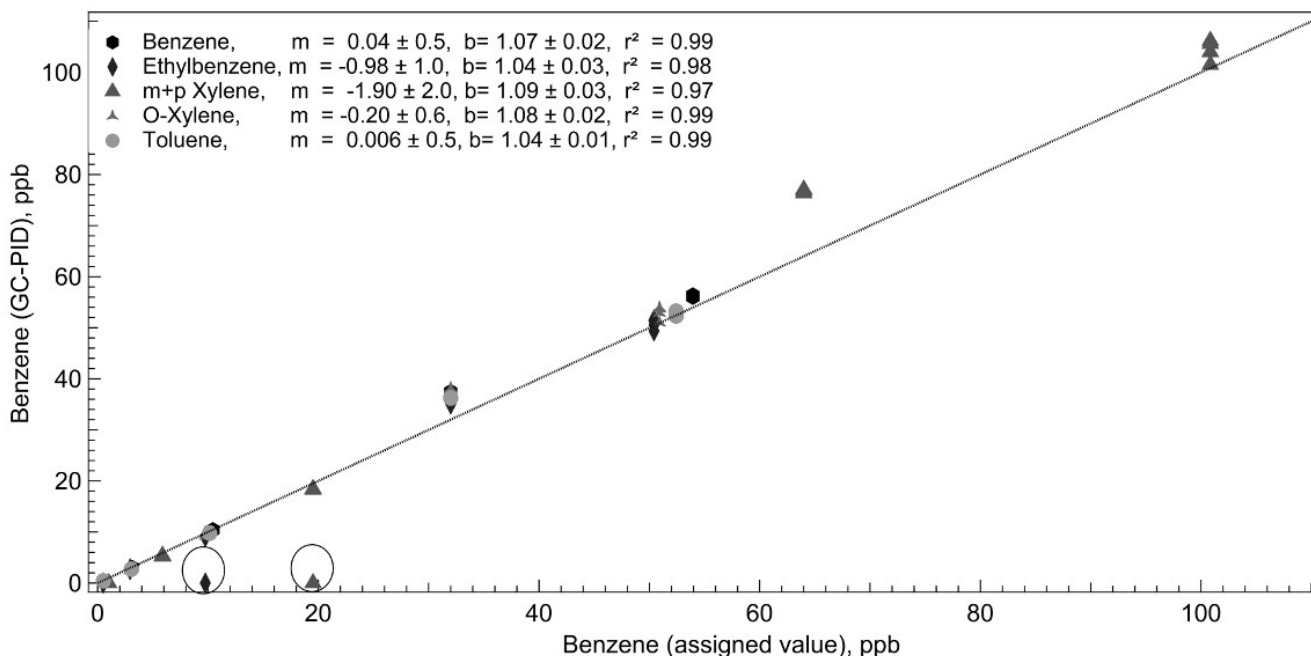


Figure 1. Regression analysis of BTEX. m and b are the correlation coefficients with $1 \pm$ standard deviation. Circles point to anomalies due to temperature fluctuations during the analysis.

One Year of AOD, Halogen Radicals, OVOCs, H₂O and NO₂ Measurements at Mauna Loa Observatory

B. Dix, T. Koenig and R. Volkamer

University of Colorado, Department of Chemistry and Biochemistry, Boulder, CO 80309; 303-735-2235, E-mail: barbara.dix@colorado.edu

The University of Colorado is conducting long-term observations of reactive trace gases, humidity, and aerosol optical depth at Mauna Loa Observatory. In particular, our measurements separate tropospheric and stratospheric bromine oxide, and nitrogen dioxide (NO₂), along with tropospheric iodine oxide, formaldehyde, glyoxal, water vapor, and other gases by means of a remote controlled state-of-the-art Multi-AXis Differential Optical Absorption Spectroscopy (MAX-DOAS) instrument. The instrument has been continuously operational since March 2017, providing a full year of measurements to investigate seasonal cycles. The instrument collects scattered light from multiple angles between zenith and horizon from two hemispheres. Using the Ring effect, i.e. the filling-in of Fraunhofer lines due to inelastic Raman scattering on air molecules, we can retrieve information on the aerosol optical density (AOD) above with high sensitivity particularly at low AOD. This is a prerequisite to quantify total trace gas columns from DOAS observations. Here we present our AOD retrieval and comparison with Aeronet data. We further discuss the seasonal cycle of the observed trace gases.

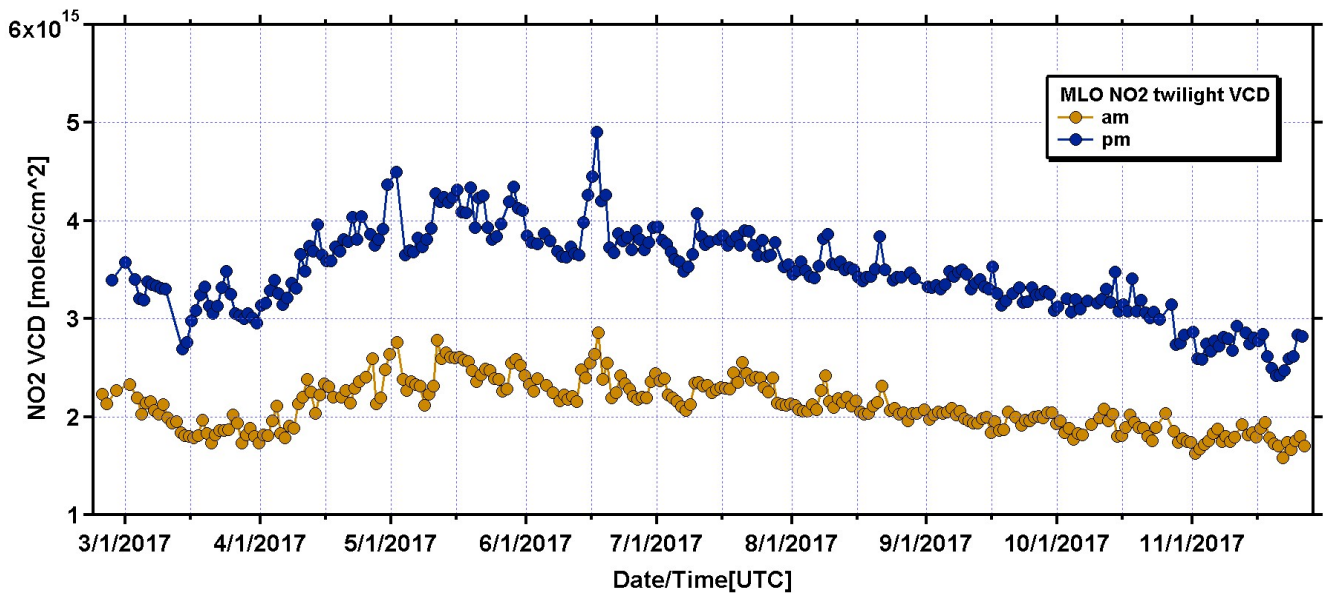


Figure 1. Stratospheric NO₂ observation.

Toward a High Degree of Freedom Full Atmosphere Retrieval of BrO Profiles from MAX-DOAS Instruments on Remote Tropical Marine Mountaintops

T. Koenig¹, B. Dix¹, F. Hendrick², M.V. Roozendael², N. Theys² and R. Volkamer¹

¹University of Colorado, Department of Chemistry and Biochemistry, Boulder, CO 80309; 303-735-2235, E-mail: theodore.koenig@colorado.edu

²Royal Belgian Institute for Space Aeronomy, Brussels, Belgium

The remote tropical troposphere is responsible for about 75% of the chemical removal of ozone (O_3) and methane (CH_4); two important greenhouse gases. Yet the atmospheric chemistry of tropospheric halogens over remote oceans is largely unconstrained in the free troposphere (FT) where natural background processes can be probed in absence of local impacts from pollution. Inorganic bromine and iodine radicals from ocean sources are responsible for about 20% of the global tropospheric ozone loss, equivalent to about 900 Tg O_x yr⁻¹ (similar to the O_x loss from hydroperoxyl). Halogens oxidize atmospheric mercury, modify aerosols, and iodine can form new particles. The Volkamer group at the University of Colorado Boulder is developing a small network of mountaintop Multiple AXis Differential Optical Absorption Spectroscopy (MAX-DOAS) instruments to probe hemispheric gradients in the remote tropical FT by long-term measurements of trace gases. Since February 2017 we have deployed MAX-DOAS instruments at two sites: 1) Mauna Loa Atmospheric Baseline Observatory (MLO) at 19.5° N, 155.6° W, at 3.4 km altitude in the northern hemisphere tropics, and 2) Maïdo Observatory (Maïdo) at 21.1° S, 55.4° E, at 2.2 km altitude in the southern hemisphere tropics. We measure the halogen oxide radicals bromine oxide (BrO) and iodine oxide (IO), small oxygenated volatile organic compounds (OVOC; e.g. formaldehyde and glyoxal), as well as total columns of O_3 , and nitrogen dioxide (NO_2), and aerosol optical depth, which can be used for satellite validation. Leveraging O_3 and NO_2 columns, and coupling photochemical change into radiative transfer we retrieve stratospheric profiles from twilight zenith measurements with additional degrees of freedom. Actively determining the reference contribution extends the degrees of freedom in tropospheric profile retrievals. Corroborating previous studies we find comparable total columns of BrO in the troposphere and stratosphere. In the troposphere we consistently find low concentrations in the lower troposphere contrasting with higher concentrations in the upper FT. We examine the implications of this trace gas distribution for development of high degree of freedom retrievals of vertical columns and atmospheric profiles aiming at up to 5 degrees of freedom.



Figure 1. A) MODIS imagery of La Réunion Island in the southwest Indian Ocean from June 11, 2017. Arcs indicate the viewing direction of the Royal Belgian Institute for Space Aeronomy (BIRA) operated MAX-DOAS in Le Port on the coast and the CU-Boulder MAX-DOAS at Maïdo Observatory at 2.16 km. B) The Maïdo Observatory. The MAX-DOAS telescope is mounted on the roof with the rest of the instrument below it. During the intensive phase other instruments will be on the roof, or use inlets extending above the roof, or horizontally from the observatory. C) The CU-Boulder MAX-DOAS telescope. The telescope can move in the vertical plane perpendicular to photo to gather profile information by probing different altitudes.

Contrasting Behavior of Inert and Photochemically Reactive Gases during the August 21, 2017, Solar Eclipse at the Boulder Reservoir

D. Helmig, B. Blanchard and J. Hueber

Institute of Arctic and Alpine Research (INSTAAR), University of Colorado, Boulder, CO 80309; 303-492-2509, E-mail: detlev.helmig@colorado.edu

The total solar eclipse on August 21, 2017 provided a rare opportunity to observe and test our understanding of atmospheric dynamics and photochemical dependency on solar irradiance. Here, we utilize observations from the continuous monitoring of both inert and photoreactive trace gases near Boulder, Colorado, for contrasting the unique dynamic and photochemical forcings on the eclipse day. The monitoring station saw a 93% solar obstruction during the peak of the eclipse. Eclipse day data are contrasted with the full month's record from this site. The loss of irradiance caused cooling of the surface air by $\sim 3^{\circ}\text{C}$, and weakened convective and turbulent mixing. This resulted in a buildup of non-reactive gases (methane, volatile organic compounds) as well as nitrogen oxides (NO , NO_2) in the surface layer. In contrast, ozone (O_3) declined by ~ 15 ppbv during the first part of the eclipse compared to median August diurnal mixing ratios. Similar O_3 signatures were observed at a series of network stations along the Northern Colorado Front Range. With the loss of irradiance, the initial ratio of $\text{NO}/(\text{NO}+\text{NO}_2)$ of ~ 0.2 dropped steadily, bottoming out at <0.01 , but rebounded to $\sim 50\%$ above average levels towards the end of the eclipse. Above average O_3 enhancements were seen in the afternoon hours following the eclipse. The contrasting behavior of reactive and non-reactive gases, and comparison with other published eclipse data, allow characterizing these responses as urban/polluted behavior.

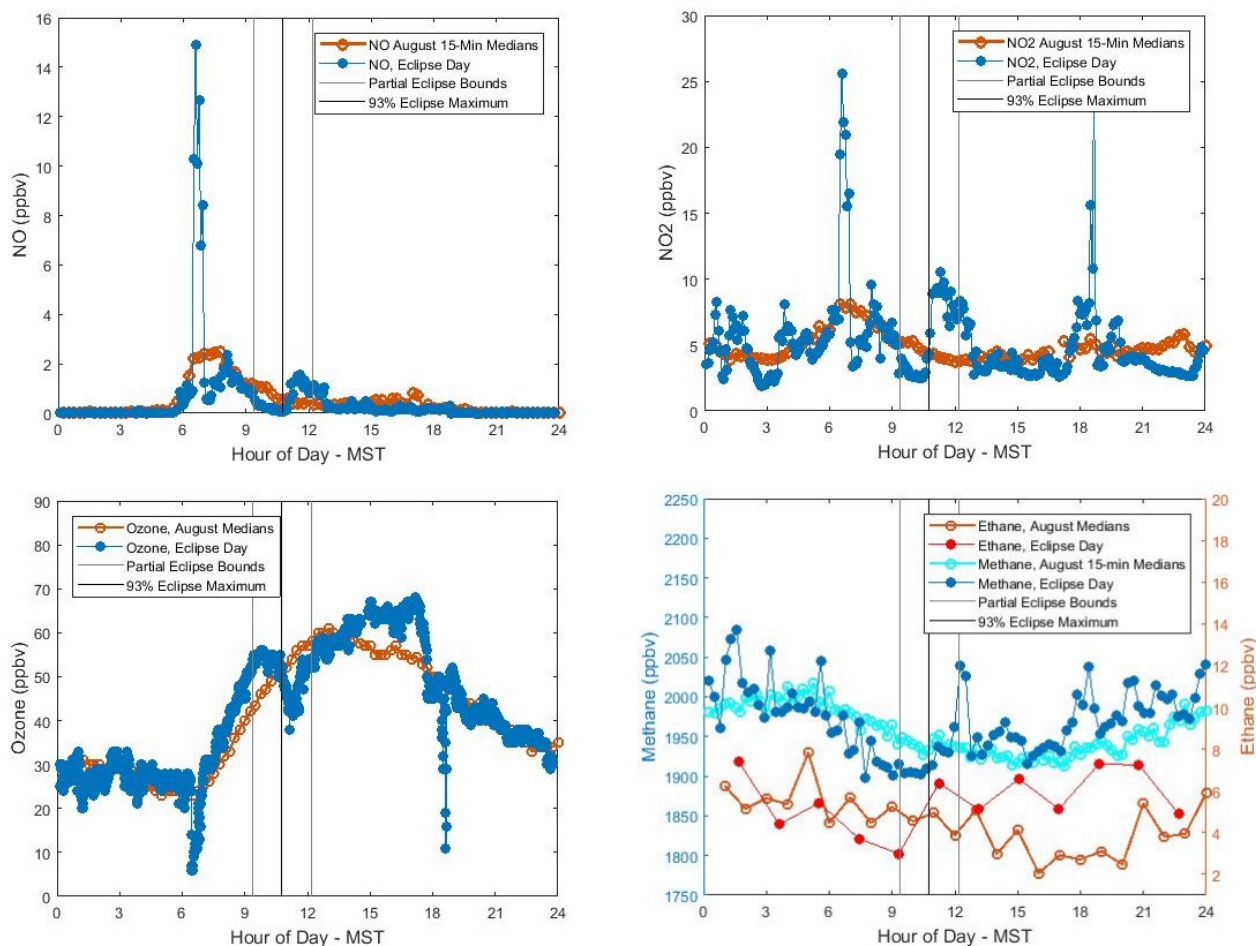


Figure 1. Diurnal cycle of trace gases on the eclipse day August 21 (filled circles) in comparison with the median diurnal cycle for August 2017 (excluding August 21) (open circles) for (a) NO (b) NO_2 , (c) ozone, (d) methane and ethane. The time window of the eclipse is indicated by the vertical grey lines (eclipse start and end), and the maxima of the eclipse is indicated by the black line.

Combining Observations and Multiple Models for an Improved Estimate of the Global Surface Ozone Distribution

K. Chang^{1,2} and O.R. Cooper^{3,4}

¹National Research Council Post-Doc, Boulder, CO 80305; 720-243-5287, E-mail: kai-lan.chang@noaa.gov

²NOAA Earth System Research Laboratory, Global Monitoring Division (GMD), Boulder, CO 80305

³Cooperative Institute for Research in Environmental Sciences (CIRES), University of Colorado, Boulder, CO 80309

⁴NOAA Earth System Research Laboratory, Chemical Sciences Division (CSD), Boulder, CO 80305

We have developed a new statistical approach for combining surface ozone observations from thousands of monitoring sites around the world with the output from multiple atmospheric chemistry models to produce a global surface ozone distribution with greater accuracy than can be provided by any individual model. The ozone observations from approximately 5,000 monitoring sites were provided by the Tropospheric Ozone Assessment Report (TOAR) surface ozone database which contains the world's largest collection of surface ozone metrics (Chang et al. 2017, Schultz et al. 2017). Output from six models were provided by the participants of the Chemistry-Climate Model Initiative (CCMI) and NASA Global Modeling and Assimilation Office (GMAO). Focus is placed on the annual maximum of the 6-month running mean of the maximum daily 8-hour average ozone value (DMA8) at each monitoring site and in each model grid cell for relevance to the long-term ozone exposure and mortality study by Turner et al (2016). This method allows us to produce a global surface ozone field that uses the TOAR observations to select the combination of global models with the greatest skill in 8 regions of the world; models with greater skill in a particular region are given higher weight, and the final model product is bias-corrected against the observations.

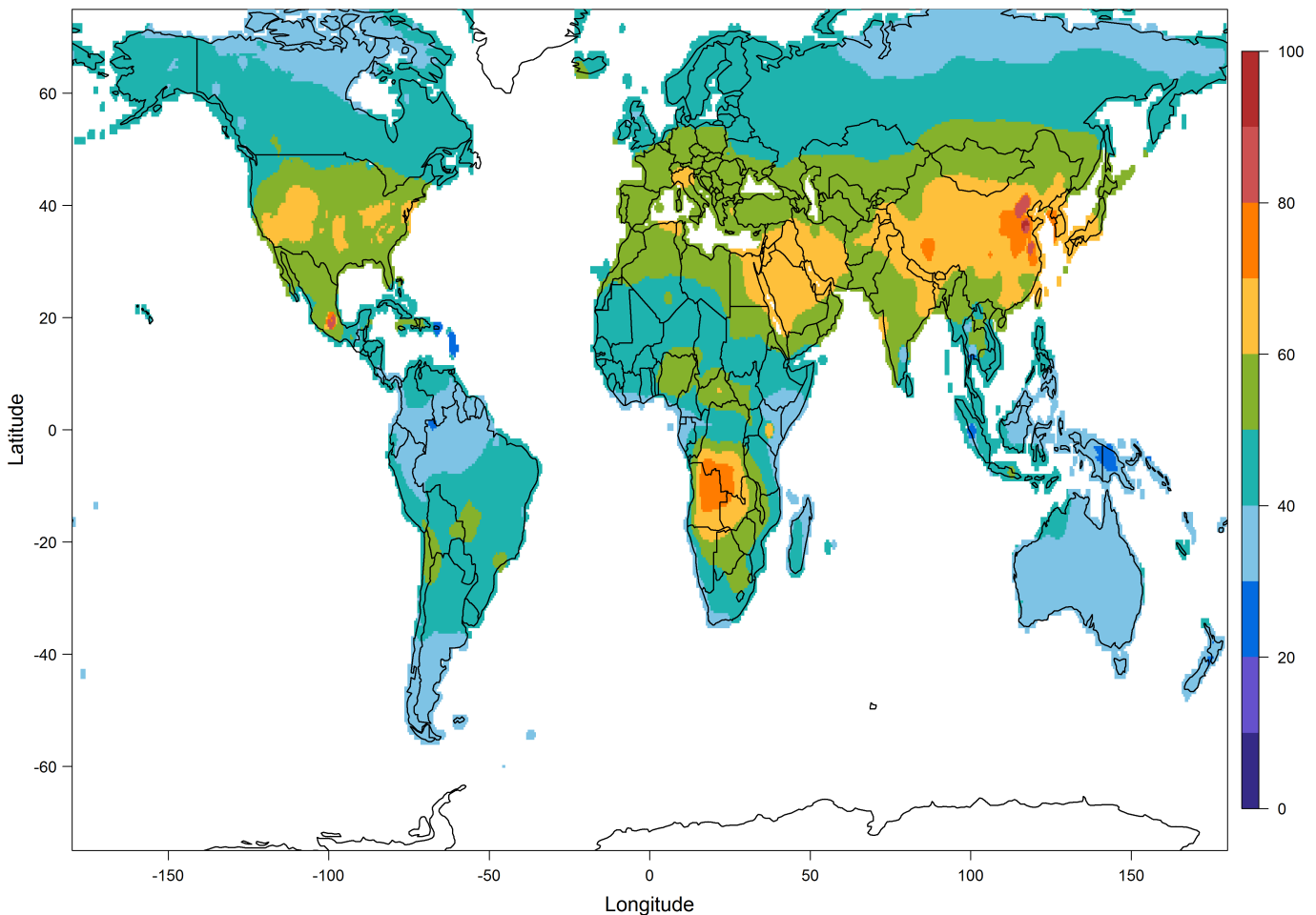


Figure 1. Fused surface ozone distribution generated from multiple models with a bias-correction by TOAR observations.

Changing Conditions in the Arctic: An Analysis of Trends in Observed Surface Ozone Conditions

A. McClure-Begley^{1,2}, S.M. Morris^{1,2}, I. Petropavlovskikh^{1,2}, T. Uttal³, O.R. Cooper^{1,4}, D. Tarasick⁵, H. Skov⁶ and S.J. Oltmans⁷

¹Cooperative Institute for Research in Environmental Sciences (CIRES), University of Colorado, Boulder, CO 80309; 303-497-6823, E-mail: audra.mcclure@noaa.gov

²NOAA Earth System Research Laboratory, Global Monitoring Division (GMD), Boulder, CO 80305

³NOAA Earth System Research Laboratory, Physical Sciences Division (PSD), Boulder, CO 80305

⁴NOAA Earth System Research Laboratory, Chemical Sciences Division (CSD), Boulder, CO 80305

⁵Air Quality Research Division, Environment and Climate Change Canada, Downsview, Ontario, Canada

⁶Aarhus University, Aarhus, Denmark

⁷Retired from NOAA Earth System Research Laboratory, Global Monitoring Division (GMD), Boulder, CO 80305

The Arctic is a region which has been experiencing rapid changes in environmental and atmospheric conditions and is likely to continue to be influenced by climate change. In order to understand the implications of drastic changes to the Arctic climate system, it is imperative to understand the expected behavior and associated impacts of different atmospheric constituents. As an important greenhouse gas, tropospheric ozone contributes to Arctic surface temperature and drives the photochemical oxidation properties of the atmosphere. Formed from the reaction of volatile organic carbons (VOC's), oxygen, and nitrogen oxides in the presence of ultraviolet (UV) radiation, ozone has an integral role in the chemical composition and behavior of the atmosphere. In addition, at high levels surface ozone has a negative impact on ecosystem functioning and public health. Surface ozone has been monitored in the Arctic since 1973 (Barrow, Alaska) and measurements have expanded spatially to the current 8 Arctic ozone measuring locations (Barrow, Alaska; Pallas, Finland; Eureka, Canada; Alert, Canada; Summit, Greenland; Tiksi, Russia; Villum Station, Greenland; and Ny-Alesund, Norway) used for this investigation. Some measurement stations, such as Barrow, show a 12% increase in observed ozone mixing ratios over the 45-year measurement period, with the dominant increases occurring during the spring months – driven by the loss of sea-ice and associated reduction in ozone depletion events and changes in transport patterns. Ozone conditions in the Arctic are strongly influenced by long-range transport of pollutants from populated regions of the northern mid-latitudes, sea-ice extent, meteorological conditions, and relative amounts of precursor species. Co-located measurements of temperature, wind direction, carbon monoxide, and aerosol composition are used in addition to climate models, back-trajectory analysis, and satellite imagery to interpret the dominant causes for observed trends in surface ozone conditions across the Arctic. The analysis of trends and seasonal distribution of ozone across the Arctic provides a valuable opportunity to investigate the spatial and temporal extent of detected trends in the region.

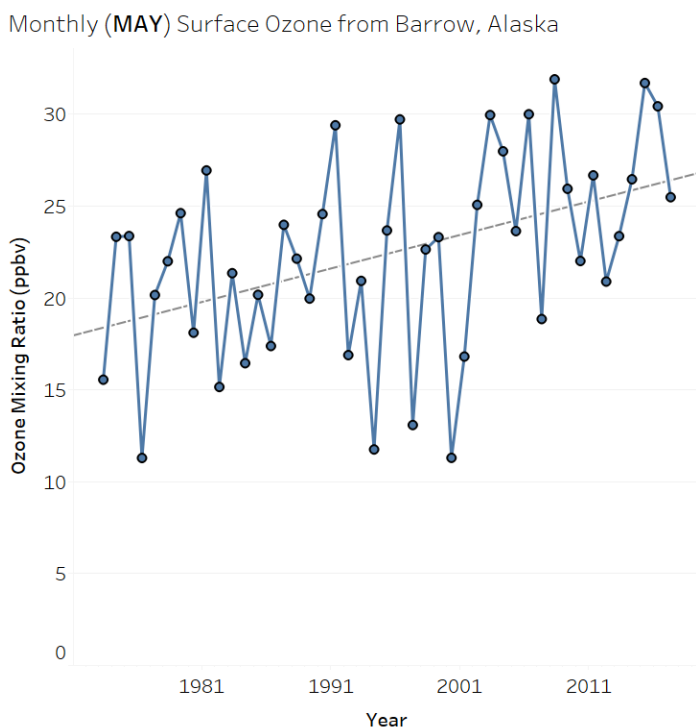


Figure 1. Yearly May (1973 – 2017) ozone mixing ratios measured at Barrow, Alaska show a positive trend in ground-level ozone conditions.

Online Inclusion of Chemical Modules Into NOAA’s Next Generation Global Prediction System (NGGPS)

L. Zhang^{1,2}, G. Grell², R. Montuoro^{1,2}, S.A. McKeen^{1,3}, R. Ahmadov^{1,2} and C. Deluca^{1,2}

¹Cooperative Institute for Research in Environmental Sciences (CIRES), University of Colorado, Boulder, CO 80309; 303-497-3956, E-mail: Kate.Zhang@noaa.gov

²NOAA Earth System Research Laboratory, Global Systems Division (GSD), Boulder, CO 80305

³NOAA Earth System Research Laboratory, Chemical Sciences Division (CSD), Boulder, CO 80305

The global Finite-Volume cubed-sphere dynamical core (FV3) developed by Geophysical Fluid Dynamics Laboratory (GFDL) was chosen by NOAA to be the Next Generation Global Prediction System (NGGPS) of the National Weather Service in the U.S. In this paper we describe the version that has been coupled with GOCART aerosol modules (FV3-GSDchem) and is now used at ESRL to provide experimental forecasts. The initial chemistry modules include simplified parameterization of sulfur/sulfate chemistry, hydrophobic and hydrophilic black and organic carbon, a 4-bin sea salt, 5-bin dust, volcanic ash, wildfires modeling using Fire Radiative Power (FRP) data from satellite observation, plume rise modeling with an online 1d cloud model. Both, the GOCART and emission modeling systems are residing within the new National Unified Operational Prediction Capability (NUOPC)-based NOAA environmental modeling system (NEMS) component, which will be initially driven by FV3. Model performance of FV3-GSDchem will be compared to Atmospheric Tomography Mission 1 (AToM-1) observations, and results from previous comparisons with FIM-Chem. Impact on numerical weather prediction will be compared to data from the 2012 South American Biomass Burning Analysis (SAMBBA) campaign.

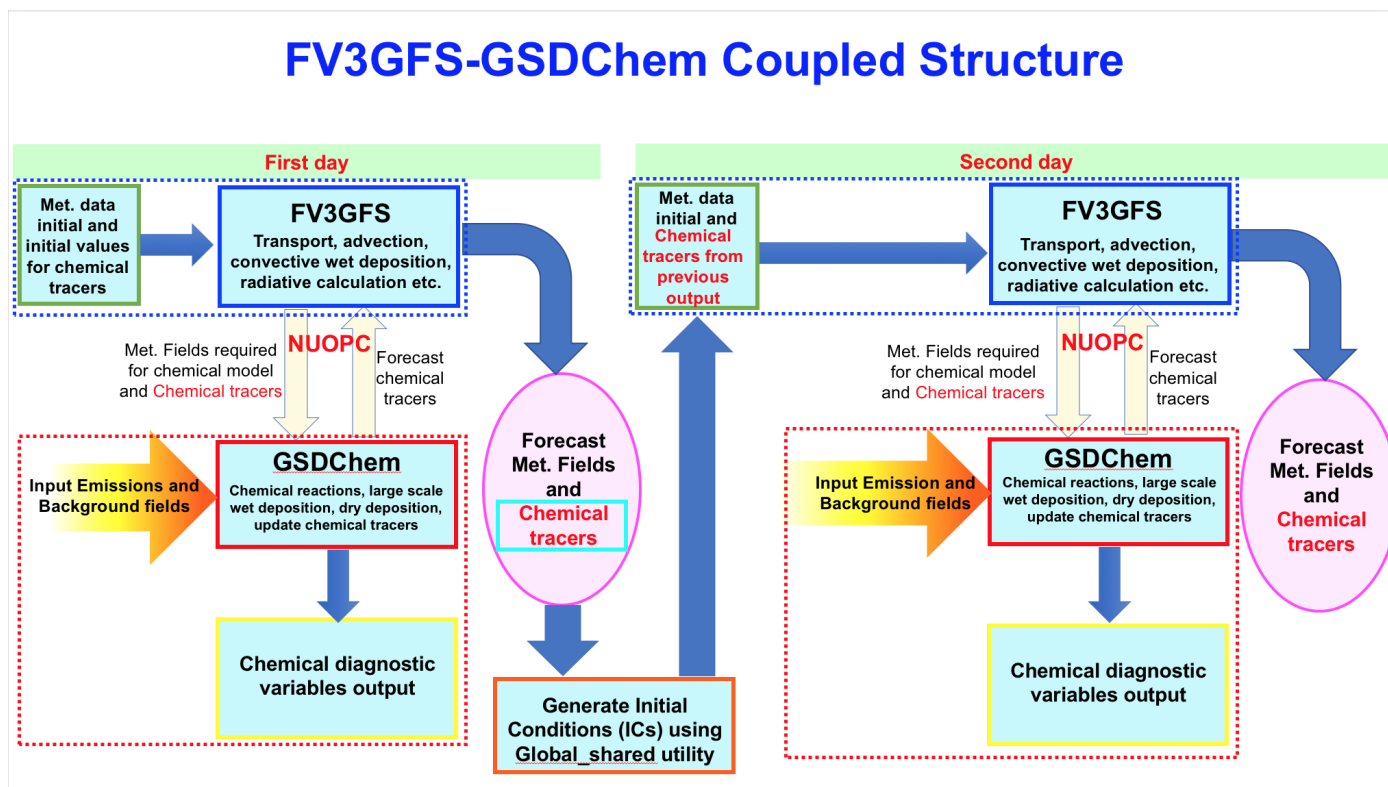


Figure 1. FV3GSF-GSDChem coupled structure.

SOS Explorer™: Interactive Visualizations for Museums and Classrooms

E. Hackathorn¹, J. Smith², J. Joyce³, J. Stewart², H. Peddicord³ and B. Russell³

¹NOAA Earth System Research Laboratory, Global Systems Division (GSD), Boulder, CO 80305; 303-497-6831, E-mail: eric.j.hackathorn@noaa.gov

²Cooperative Institute for Research in the Atmosphere (CIRA), Colorado State University, Fort Collins, CO 80521

³Cooperative Institute for Research in Environmental Sciences (CIRES), University of Colorado, Boulder, CO 80309

SOS Explorer™ (SOSx) is a flat screen version of the popular Science On a Sphere® (SOS). The software takes SOS datasets, usually only seen on a 6-foot sphere in large museum spaces and makes them more accessible. The visualizations show information provided by satellites, ground observations, and computer models. More information can be found at https://sos.noaa.gov/SOS_Explorer/

SOS Explorer™ was developed by the Informatics, Visualization, and Outreach (IVO) section of ESRL/GSD which is also the home of Science On a Sphere®. Wanting to build off of the success of SOS and expand the reach of SOS into classrooms and homes as well as museums who don't have the physical space for a full Science On a Sphere®, developers created a flat screen version of SOS called SOS Explorer™ (SOSx).

Several factors came together at the right time to lead to the development of SOSx. After field trips to see NOAA's SOS, many teachers asked how they could bring the same experience of viewing global data into their classrooms. Most of the teachers didn't have a budget for installing SOS into their schools and needed other options. A flat screen version that could be displayed on computer monitors and projectors seemed like an obvious solution.

New features include integration with the Oculus Rift virtual reality goggles, support for 360-degree content, and first person experiences.

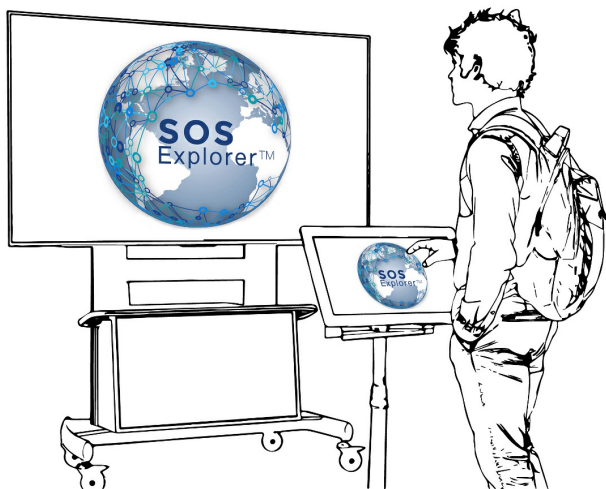
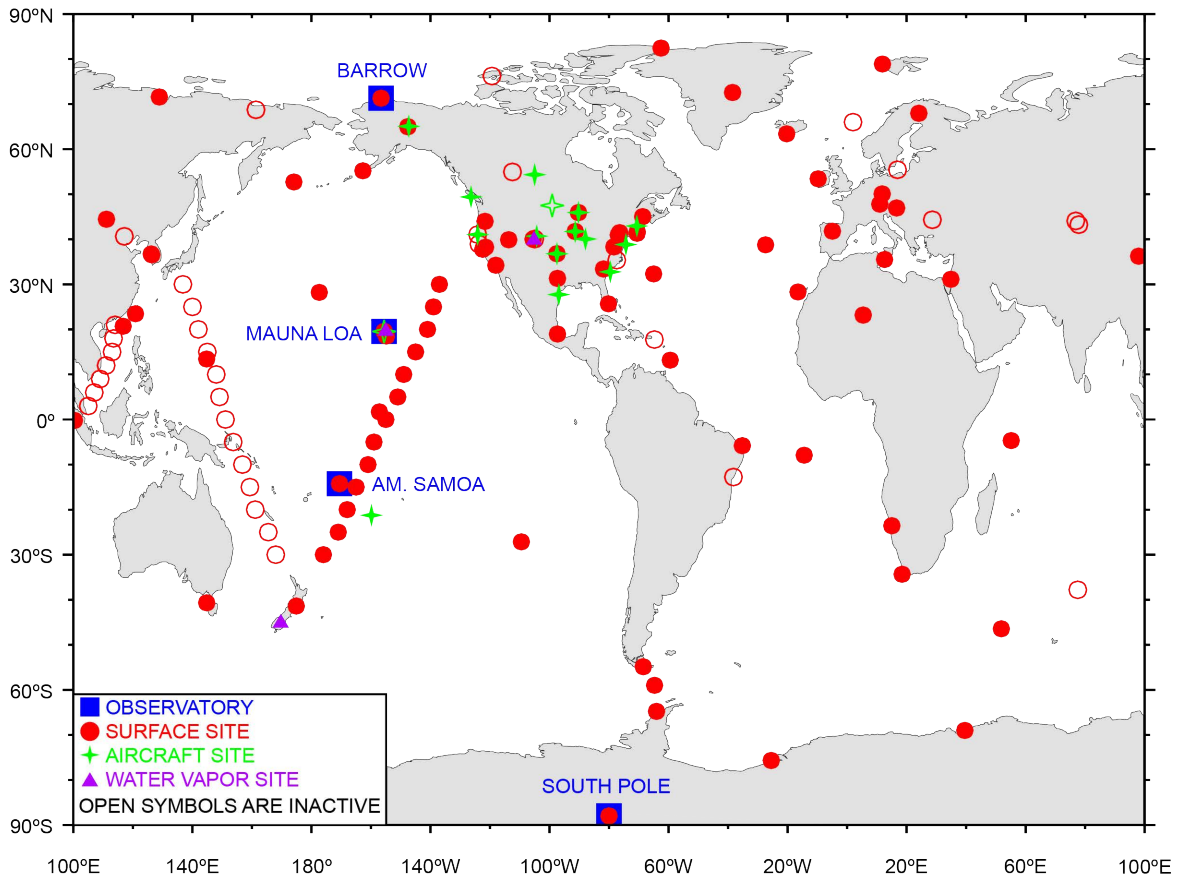


Figure 1. A visitor experimenting with SOSx.

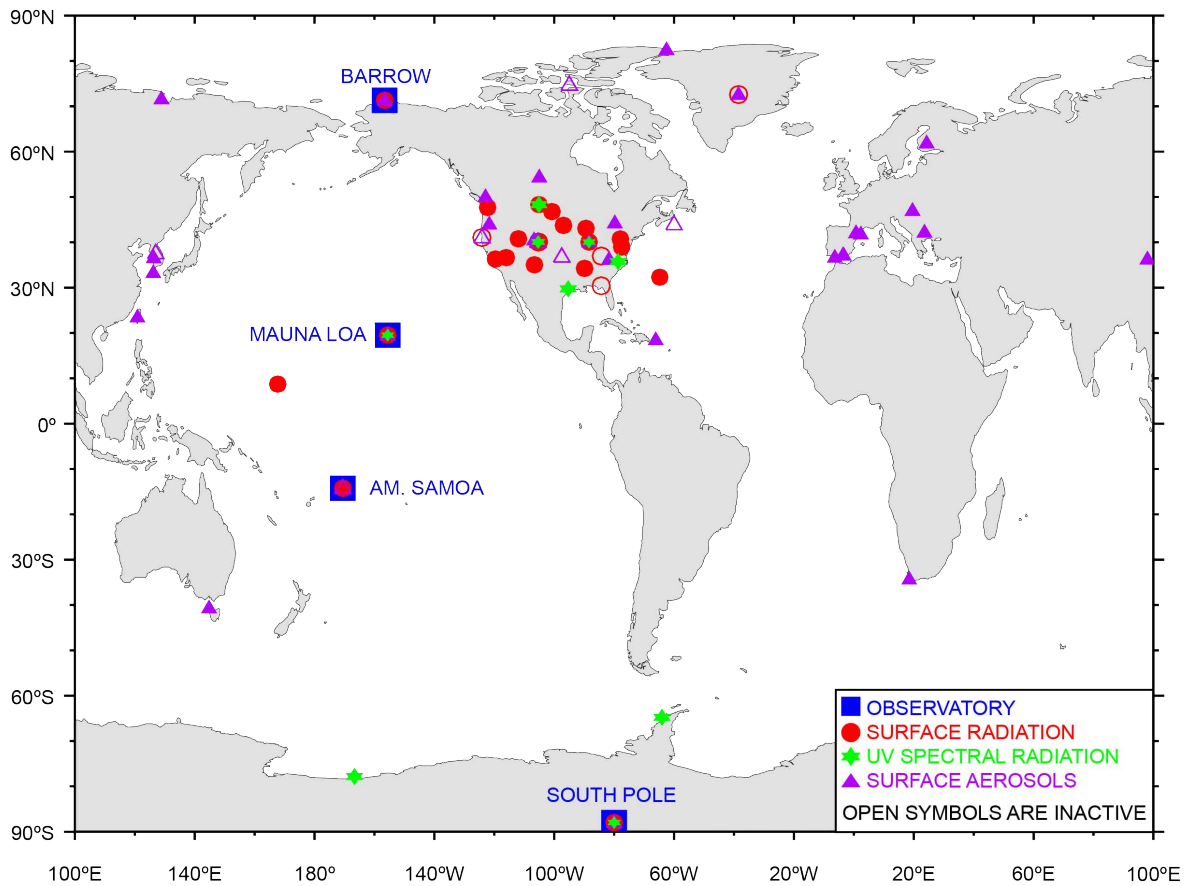


Figure 2. SOS Explorer now includes a virtual reality component bringing an immersive experience into the classroom.

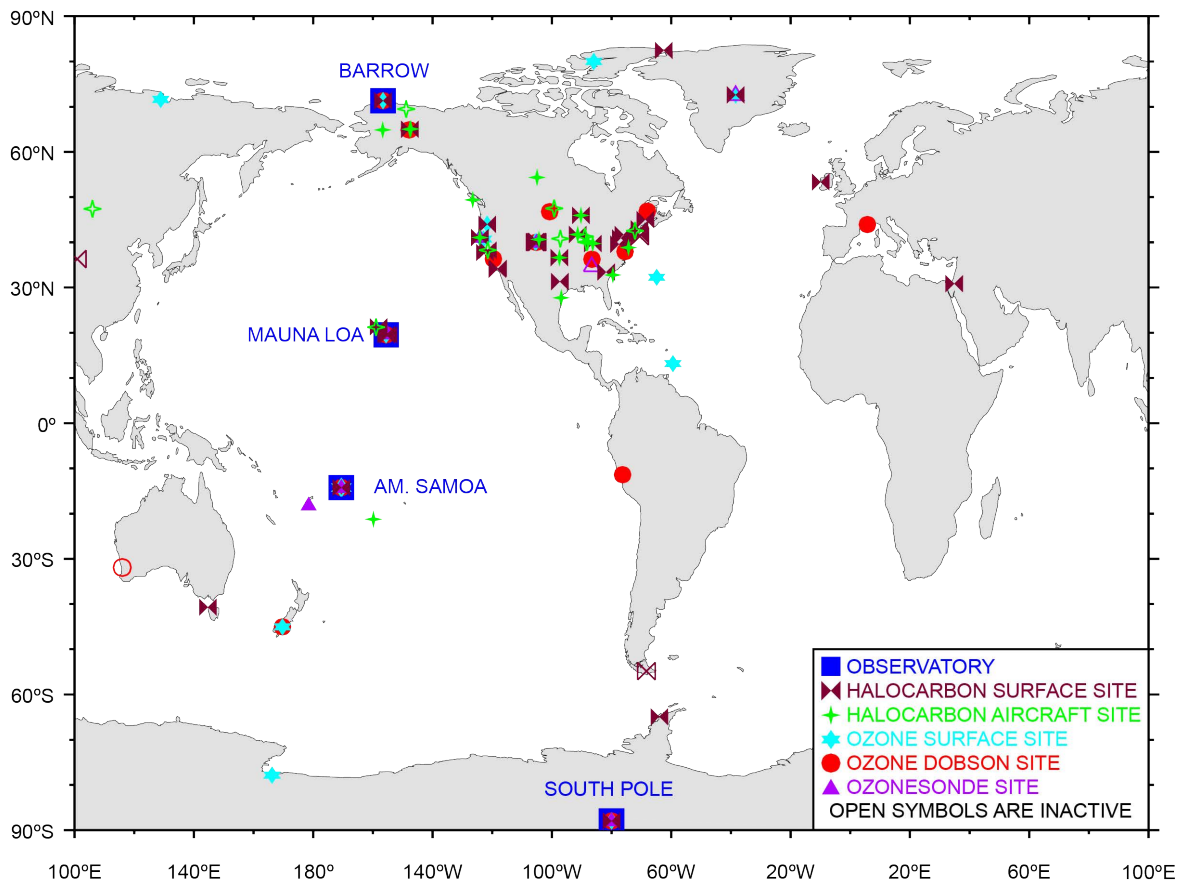
Tracking Greenhouse Gases and Understanding Carbon Cycle Feedbacks

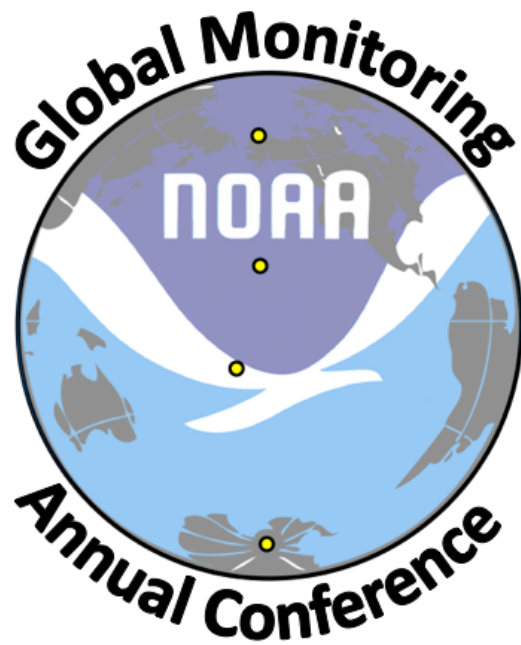


Monitoring and Understanding Changes in Surface Radiation, Clouds, and Aerosol Distributions



Guiding Recovery of Stratospheric Ozone





2018 Global Monitoring Annual Conference

